EXACTLY SOLVABLE MODELS FOR QUBITS COUPLED TO SPIN ENVIRONMENTS: DECOHERENCE AND ENTANGLEMENT

by

YAMEN HAMDOUNI

Submitted in fulfillment of the academic
requirements for the degree of
Doctor of Philosophy
in the School of Physics,
University of KwaZulu-Natal

December 2008

As the candidate's supervisor I have/have not approved this thesis/dissertation for submission.

Signed:_____ Name:_____ Date:_____

DECLARATION

I Yamen Hamdouni declare that

(i) The research reported in this thesis, except where otherwise indicated, is my original work.

(ii) This thesis has not been submitted for any degree or examination at any other university.

(iii) This thesis does not contain other persons data, pictures, graphs or other information, unless specifically acknowledged as being sourced from other persons.

(iv) This thesis does not contain other persons writing, unless specifically acknowledged as being sourced from other researchers. Where other written sources have been quoted, then:

  (a) their words have been re-written but the general information attributed to them has been referenced;

  (b) where their exact words have been used, their writing has been placed inside quotation marks, and referenced.

(v) Where I have reproduced a publication of which I am author, co-author or editor, I have indicated in detail which part of the publication was actually written by myself alone and have fully referenced such publications.

(vi) This thesis does not contain text, graphics or tables copied and pasted from the Internet, unless specifically acknowledged, and the source being detailed in the thesis and in the References sections.

Signed: 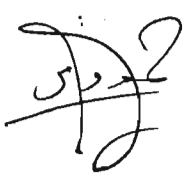

ABSTRACT

During the last decade the field of quantum information has seen considerable progress both theoretically and experimentally. The building block of this theory is the so-called qubit, the quantum counterpart of the classical bit. It turns out that spin degrees of freedom of quantum particles are among the most promising candidates for quantum information processing and computation. Thus, a deep understanding of the different processes that govern the dynamics of these objects is of fundamental importance. For instance, the decoherence process, caused the coupling of the qubits to their surrounding environment, is the main obstacle to quantum information processing: it leads them to lose their quantum coherence and thus behave classically. In addition, quantum systems exhibit correlations that have no classical counterpart. This phenomenon is called entanglement and is the vital resource for quantum teleportation and quantum computing. Decoherence and entanglement dynamics were extensively studied within the framework of the Markovian approximation using the master equation approach. However, due to the non-commuting character of quantum observables, only few models are known to be exactly solvable. Moreover, many spin systems display a strongly non-Markovian behavior. This thesis is devoted to the development of new techniques for deriving the exact dynamics of spin qubits, coupled through Heisenberg and/or Ising interactions to spin environments that have internal dynamics. The basic idea behind these techniques is to use the underlying symmetries exhibited by the Hamitonian operators of the composite systems. This allows for the study of problems related to decoherence and entanglement.

ACKNOWLEDGEMENTS

I would like to express my deepest gratitude to Prof. Francesco Petruccione, for accepting directing this thesis. I had the pleasure to be a member of his group for more than three years. I thank all the members of the QRG at the University of KwaZulu Natal, Durban, South Africa.

I thank Prof. Mark Fannes for the useful discussions we had. Special thanks go to NRF for the financial support.

LIST OF PUBLICATIONS

(i) Y. Hamdouni, M. Fannes, and F. Petruccione, Phys. Rev. B 73 (2006).

(ii) Y. Hamdouni and F. Petruccione, Phys. Rev. B 76 (2007) 174306.

(iii) Y. Hamdouni, J. Phys. A: Math. Theor. 40 (2007) 11569

(iv) Y. Hamdouni, J. Phys. A: Math. Theor. 41 (2008) 135302.

(v) Y. Hamdouni Phys. Lett. A 373 1233 (2009); arXiv:0807.3944.v2

(vi) Y. Hamdouni J. Phys. A: Math. Theor. 42 (2009) 315301; arXiv:0810.2532.v1

CONTENTS

LIST OF FIGURES

LIST OF TABLES

1. INTRODUCTION

1.1 Plan of the thesis

The thesis consists of an introduction, six research papers, and a conclusion. The reader might notice that there exists an overlap between the chapters of the thesis. Nevertheless, they are self-consistent and can be regarded as independent from each other. As a consequence, we tried to arrange them in a logical order that reflects the progress of the investigations of the problems under consideration. The presentation we adopted is standard: we start each chapter with an introduction, then we introduce the model to be studied; this is followed by a detailed presentation of the derivations of the analytical solutions we are seeking. The latter are then applied to particular initial conditions which are of interest for applications. The chapters end with a conclusion or a summary.

The introduction contains an overview of the necessary material needed for the understanding of the content of the thesis such as the principles of the theory of open quantum systems, decoherence and the entanglement. We begin the investigation in chapter 2 with the study of the dynamics of a single qubit coupled to a spin bath with internal dynamics at thermal equilibrium. The third and the fourth chapters are generalization of the first one to the case of a two-qubit system interacting with a common spin bath; much attention is given to the spin star model. Note that the third chapter can be regarded as a special case of the fourth one. In chapter 5 we analytically investigate the relationship between entanglement and quantum phase transition in the Lipkin-Meshkov-Glick model. Chapter 6 presents a discussion of the partial trace over collective spin degrees of freedom, which is of practical relevance for the study of spin baths. In chapter 7, we generalize the models of chapters 3 and 4 to the case where the qubits are interacting with separate spin star baths at infinite temperature. A short conclusion ends the thesis.

Note that each chapter contains its own bibliography. The list of references is not exhaustive; only those which have been used or are relevant for the subject under study were cited. For more details, the reader may consult review articles cited in this thesis. Note also that we have used a different representation for Pauli matrices, namely,

$$\sigma_z = \begin{pmatrix} -1 & 0 \\ 0 & 1 \end{pmatrix}, \quad \sigma_x = \begin{pmatrix} 0 & 1 \\ 1 & 0 \end{pmatrix}, \quad \sigma_y \begin{pmatrix} 0 & I \\ -I & 0 \end{pmatrix}. \tag{1.1}$$

1.2 Overview of quantum mechanics

1.2.1 Historical background

By the end of the nineteenth century, X-rays, the electron and the radioactivity were already discovered. Since then it was possible to investigate properties of atoms and molecules. The results of a number of experiments carried out at that time, revealed that classical mechanics, mainly dealing with macroscopic bodies, is unable to give an account for phenomena taking place at the microscopic level. For instance the spectral distribution of thermal radiation emitted from a black body, and the low-temperature specific heat of solids were in direct contradiction with the results of classical mechanics [1]. The seminal works of Planck on the black body radiation and Einstein on the photoelectric effect led to the discovery of the wave-corpuscule duality of radiation: the electromagnetic radiation is absorbed and emitted in discrete *quanta*, called *photons*, each carrying an amount of energy E proportional to the frequency of radiation ν, and a momentum inversely proportional to the wavelength λ, namely,

$$E = h\nu, \quad p = \frac{h}{\lambda}, \tag{1.2}$$

where h is a universal constant called Planck's constant. The wave character of electromagnetic radiation manifests itself in interference and diffraction phenomena (e.g. Young's double slit experiment), while the corpuscular one dominates in Compton scattering and the photoelectric effect.

In their experiments on the ionization potentials of gazes, Franck and Hertz established the discrete character of the atomic energy states. This led to the conclusion that the energy of atoms is quantized. The narrow lines observed in atomic emission and absorption spectra can be explained by the fact that any photon emitted by the atom carries an amount of energy equal to the difference between the permitted values E_i of atomic energies [1, 2, 3]:

$$h\nu_{ij} = |E_i - E_j|, \tag{1.3}$$

Bohr and Sommerfeld proposed a semi-classical explanation of the quantization of atomic level, by introducing the concept of electronic orbitals, and were able to come out with empirical quantization rules.

In 1922 Stern and Gerlach discovered that the component of the angular momentum of electrons, along the direction of the applied magnetic field, can take on only certain discrete values. Later, the study of the diffraction of electrons and neutrons by Davison, Germer, and Thomson showed that interference patterns can be obtained for such particles. This confirms the hypothesis of de Broglie, in which a material particle is assigned a wave length λ and a frequency ν related to its momentum p and its energy E by

$$\lambda = \frac{h}{p}, \quad E = h\nu. \tag{1.4}$$

The analogy between these relations and those corresponding to photons is clear. The contributions cited above marked the birth of quantum mechanics, the fundamental theory of atomic and molecular phenomena.

It is worth mentioning that the pattern characterizing the diffraction of monochromatic light observed in Young's experiment is due to the fact that the intensity of light at each point on the screen is proportional to the square of the amplitude of the total electric field, that is, the sum of the electric fields corresponding to each slit. The interference term, which depends on the phase difference between the fields, is responsible of the appearance of interference fringes. In fact a deep analysis of the double-slit experiment shows that, in order to give an account for the interference, one has to renounce some classical notions, central in Newtonian mechanics, such as the concept of particle trajectory (Heisenberg uncertainty principle), and to question the concept of measurement at the microscopic level. For instance the impossibility of determining through which slit the photon has passed in Young's experiment implies that quantum mechanics is essentially a probabilistic theory (see bellow).

1.2.2 State vectors, operators, and the statistical interpretation of quantum mechanics

As a result of de Broglie's hypothesis, confirmed by the diffraction experiments of Davisson and Germer, it has been postulated that the state of a material particle of mass m, subject to a potential energy $V(|\vec{r}|, t)$, can be described by means of an auxiliary complex-valued wave function, say $\psi(\vec{r}, t)$, which satisfies a differential equation containing a second derivative with respect to the position $\vec{r}$ and a first derivative with respect to time t. This equation is known as Schrödinger's equation, which reads [2]:

$$i\hbar \frac{\partial \psi(\vec{r}, t)}{\partial t} = -\frac{\hbar^2}{2m} \frac{\partial^2 \psi(\vec{r}, t)}{\partial \vec{r}^2} + V(|\vec{r}|, t)\psi(\vec{r}, t), \tag{1.5}$$

where $\hbar = h/2\pi$.

One of the most important consequences of the linearity of the Schrödinger equation resides in the so-called *superposition principle*. Roughly speaking, the above principle states that the wave function is defined up to an arbitrary constant, and that a system which can be described by the wave functions ψ_1 and ψ_2, can also be described by the wave function ψ, given by the linear combination

$$\psi = c_1\psi_1 + c_2\psi_2, \tag{1.6}$$

where c_1 and c_2 are complex coefficients.

Mathematically, one says that the wave functions belong to an abstract complex linear vector space $\mathcal{H}$, called Hilbert space, whose elements are termed state vectors. This space is equipped with a *scalar product* and a *norm*. The latter has a very important interpretation in quantum mechanics. For instance the square of the modulus of the wave function $\psi(\vec{r},t)$ multiplied by the infinitesimal volume $d\vec{r}$ represents the probability of finding the particle, at time t, in the volume $d\vec{r}$ around the point defined by $\vec{r}$.

The comparison between the classical energy equation and the Schrödinger equation suggests the representation of the momentum and the energy of a free particle by linear differential operators acting on the wave functions, namely,

$$\vec{p} \rightarrow -i\hbar\vec{\nabla}, \qquad E \rightarrow i\hbar\frac{\partial}{\partial t}. \tag{1.7}$$

This association is known as the *correspondence principle*.

In general, measurable physical quantities such as position, energy, angular momentum,...etc, are represented within the theory of quantum mechanics by linear Hermitian operators acting in the Hilbert space corresponding to the physical system. By operator one means a mathematical object (more precisely a mapping) which acts on state vectors of the Hilbert space, to yield other state vectors belonging to the same (or different) Hilbert space. For finite dimensional Hilbert spaces, operators can be represented by matrices, written in the basis of the space.

From here on we shall adopt Dirac's braket notation for state vectors and assume that the Hilbert space is finite dimensional. Within this notation, the scalar product of two state vectors $|\psi\rangle$ and $|\phi\rangle$ is denoted by $\langle\psi|\phi\rangle$. The action of the operator A on the state vector $|\psi\rangle$ is denoted by $A|\psi\rangle$. The notation $\langle\psi|A|\phi\rangle$ means the scalar product of the state vectors $|\psi\rangle$ and $A|\phi\rangle$. In particular, the quantity $\langle\psi|A|\psi\rangle$ is called the expectation value of the operator A with respect to the state vector $|\psi\rangle$

If $\{\psi_n\rangle\}_{n=1,\ldots,d}$ is an orthonormal basis for the d-dimensional Hilbert space $\mathcal{H}$, then

every state vector $|\Phi\rangle \in \mathcal{H}$ can be decomposed as

$$|\Phi\rangle = \sum_{n=1}^{d} c_n |\psi_n\rangle, \tag{1.8}$$

where the c_n are some constant coefficients satisfying $\sum_n |c_n|^2 = 1$. Furthermore, the following decomposition applies for the operator A:

$$A = \sum_{n=1}^{d} \sum_{m=1}^{d} \langle\psi_n|A|\psi_m\rangle |\psi_n\rangle\langle\psi_m|. \tag{1.9}$$

This actually follows from the closure relation

$$\sum_{n=1}^{d} |\psi_n\rangle\langle\psi_n| = \mathbb{I}, \tag{1.10}$$

where $\mathbb{I}$ designates the unit matrix in $\mathcal{H}$.

By definition, a state vector $|\psi_n\rangle$ is an eigenvector of the linear operator A if there exists a complex number λ_n such that

$$A|\psi_n\rangle = \lambda_n |\psi_n\rangle. \tag{1.11}$$

We say that λ_n is the eigenvalue associated with the eigenvector $|\psi_n\rangle$. If we denote by $\mathcal{A}$ the matrix representation of the operator A, i.e., the matrix whose elements $\mathcal{A}_{nm}$ are given by $\langle\psi_n|A|\psi_m\rangle$, then the eigenvalues λ_n of A can be determined from the characteristic equation

$$\det(\mathcal{A} - \lambda_n \mathcal{I}) = 0. \tag{1.12}$$

Note that it may happen that more than one eigenvector correspond to the same eigenvalue λ_n. In this case we say that λ_n is degenerate with a multiplicity or degeneracy equal to dimension of the subspace spanned by its eigenvectors.

Let us briefly summarize the main properties of Hermitian operators. We say that the linear operator A is Hermitian if it satisfies

$$\langle\psi|A|\phi\rangle = \langle\phi|A|\psi\rangle^*, \tag{1.13}$$

where the asterisk designates the complex conjugation. In matrix language, the above condition implies that A is equal to the complex conjugate of its transpose, that is, $A = (A^t)^* = A^\dagger$. It follows that all the diagonal elements of a Hermitian operator, and in particular all of its eigenvalues, are always real. Furthermore, it can be shown that if λ_n is an eigenvalue of A, corresponding to eigenket $|\psi_n\rangle$, then it is also eigenvalue of $A^\dagger$ associated with the eigenbra $\langle\psi_n|$.

Suppose that λ_n ($|\psi_n\rangle$) and λ_m ($|\psi_m\rangle$), $m \neq n$, are two eigenvalues (eigenvectors) of the Hermitian operator A. Then, since the eigenvalues are real, we can write $\langle\psi_n|A|\psi_m\rangle = \lambda_n\langle\psi_n|\psi_m\rangle = \lambda_m\langle\psi_n|\psi_m\rangle$. It immediately follows that $\langle\psi_n|\psi_m\rangle = 0$, meaning that the eigenvectors of a Hermitian operator corresponding to two different eigenvalues are orthogonal. Furthermore, with an appropriate choice of the eigenvectors within each eigenspace, we can in principle construct a basis for the Hilbert space. In this case the Hermitian operator A is said to be an observable.

According to the postulates of quantum mechanics, the possible outcomes of the measurement of a physical observable should be one of its *eigenvalues*. The Hermiticity condition ensures that all the eigenvalues are real. When a measurement of a physical quantity on the system in the state $|\Phi\rangle$ is carried out, giving the outcome λ_n, the state of the system, immediately after the measurement, is given by the normalized projection of $|\Phi\rangle$ onto the subspace corresponding to the outcome, that is [2],

$$|\Phi\rangle \Rightarrow \frac{1}{\sqrt{\sum_{i=1}^{g_n} |\langle\psi_n^i|\Phi\rangle|^2}} \sum_i^{g_n} \langle\psi_n^i|\Phi\rangle|\psi_n^i\rangle, \tag{1.14}$$

where g_n is the degeneracy of λ_n. The probability $P(\lambda_n)$ of finding the eigenvalue λ_n is given by

$$P(\lambda_n) = \frac{1}{|\langle\Phi|\Phi\rangle|^2} \sum_{i=1}^{g_n} |\langle\psi_n^i|\Phi\rangle|^2. \tag{1.15}$$

The Hermitian linear operator corresponding to the energy of a quantum system is called the Hamiltonian of the system; it is the quantum analog of Hamilton's function of classical mechanics. If we denote by H the Hamiltonian operator, then the Schrödinger equation can be written as ($\hbar = 1$)

$$i\partial\psi/\partial t = H\psi. \tag{1.16}$$

Thus the outcome of the measurement of the energy of a quantum system is one of the eigenvalues of the Hamiltonian H.

The algebra of linear operators in Hilbert space is similar to the algebra of $N \times N$ matrices. In particular, operators do not necessarily commute with each other. In other words, if A and B are two linear operators, then in general $AB \neq BA$. The commutator of A and B is written $[A, B]_-$, and is defined by

$$[A, B]_- = AB - BA. \tag{1.17}$$

When $[A, B]_- = 0$, i.e. when A and B commute with each other, one can construct an orthonormal basis of eigenvectors common to the above operators. In this basis A and B can be simultaneously diagonalized.

1.2.3 The density operator

The complete description of a quantum system through (pure) state vectors corresponds to situations where a full knowledge of all the independent physical parameters necessary to assign a state vector to the system is possible [3]. When this is not case, we say that the system is in a mixed state. The mathematical tool that enables the description of quantum systems in such sates is known as the density operator, or the density matrix.

Before giving a precise definition for the density operator, it should be noted that the statistical interpretation of quantum mechanics, presented in the preceding section, is based on the concept of statistical ensembles. These are collections of large numbers of identically prepared quantum systems. A mixed state can be regarded as an incoherent mixture of M pure states $|\Phi_i\rangle$ corresponding to some statistical ensembles $\mathcal{E}_i$, each of which is characterized by a statistical weight $0 \leq w_i \leq 1$ [4]. The average of any physical observable A on the system is given by

$$\langle A \rangle = \sum_{i=1}^{M} w_i \langle \Phi_i | A | \Phi_i \rangle. \tag{1.18}$$

Obviously, we have

$$\sum_{i=1}^{M} w_i = 1. \tag{1.19}$$

It is easily verified that equation (1.18) can be rewritten in terms of the operator

$$\rho = \sum_{i=1}^{M} w_i |\Phi_i\rangle\langle\Phi_i| \tag{1.20}$$

as

$$\langle A \rangle = \mathrm{tr}\{A\rho\}, \tag{1.21}$$

where tr denotes the trace over the Hilbert space $\mathcal{H}$ of the system, namely,

$$\mathrm{tr}A = \sum_{j=1} \langle \phi_j | A | \phi_j \rangle, \tag{1.22}$$

where $\{\phi_j\}$ is an orthonormal basis for the space $\mathcal{H}$.

The quantity ρ introduced in equation (1.20) is known as the density matrix; it fully characterizes the state of the system, and satisfies a number of properties which we summarize here:

- ρ is positive ($\rho \geq 0$) and is Hermitian ($\rho = \rho^\dagger$)
- $\mathrm{tr}\rho = 1$
- $\mathrm{tr}\rho^2 \leq 1$, the equality being satisfied only for pure states, i.e. when $\rho = |\psi\rangle\langle\psi|$
- The convex sum $\sum_i \lambda_i \rho_i$ of the density matrices ρ_i, where $0 < \lambda_i < 1$ and $\sum_i \lambda_i = 1$, is also a density matrix. Furthermore, a pure state $|\psi\rangle\langle\psi|$ cannot be decomposed as a nontrivial convex sum of density matrices.

1.2.4 Dynamics of closed quantum systems

In the absence of any external perturbation, the dynamics of closed quantum systems is completely causal. This follows from the fact that the evolution in time of the system's state vector $|\psi(t)\rangle$ is governed by the Schrödinger equation

$$i\frac{d|\psi(t)\rangle}{dt} = H(t)|\psi(t)\rangle, \tag{1.23}$$

where $H(t)$ denotes the Hamiltonian operator of the system, and Planck's constant is set to one.

In the case of a conservative system, that is, when the Hamiltonian is explicitly independent of time ($\partial H/\partial t = 0$), the Schrödinger equation (1.23) can be formally integrated, to yield

$$|\psi(t)\rangle = \mathbb{U}(t, t_0)|\psi(t_0)\rangle, \tag{1.24}$$

where

$$\mathbb{U}(t, t_0) = \exp\Big[-iH(t - t_0)\Big] \tag{1.25}$$

is known as the time evolution operator. The latter can be expanded in a power series as follows:

$$\mathbb{U}(t, t_0) = \sum_{n=0}^{\infty}(-iH)^n\frac{(t - t_0)^n}{n!}. \tag{1.26}$$

From equation (1.25), one can see that the time evolution operator is unitary, that is,

$$\mathbb{U}^\dagger(t, t_0) = \mathbb{U}^{-1}(t, t_0) = \mathbb{U}(t_0, t), \tag{1.27}$$

and it satisfies the equation

$$i\frac{d\mathbb{U}(t, t_0)}{dt} = H\mathbb{U}(t, t_0), \tag{1.28}$$

subject to the initial condition $\mathbb{U}(t_0, t_0) = \mathbb{I}$. Here $\mathbb{I}$ denotes the unity operator in the Hilbert space associated with the system.

If we take the Hermitian conjugate of the Schrödinger equation (1.23)we obtain

$$\langle\psi(t)| = \langle\psi(t_0)|\mathbb{U}^\dagger(t,t_0). \tag{1.29}$$

It follows that the time development of the density matrix $\rho(t)$, corresponding to the pure state $|\psi(t)\rangle$, is given by

$$\rho(t) = \mathbb{U}(t,t_0)\rho(t_0)\mathbb{U}^\dagger(t,t_0). \tag{1.30}$$

Using equation (1.28), one can show that $\rho(t)$ satisfies the von Neumann equation

$$\dot{\rho}(t) = -i[H,\rho(t)]. \tag{1.31}$$

The latter can be rewritten in terms of the Liouville operator $\mathcal{L}$ as

$$\dot{\rho}(t) = -i\mathcal{L}(\rho). \tag{1.32}$$

The solution of this equation can be formally expressed as

$$\rho(t) = \exp[-i\mathcal{L}(t-t_0)]\rho(t_0). \tag{1.33}$$

When the Hamiltonian operator is time dependent, it is still possible to find an operator $\mathbb{U}(t,t_0)$, such that the state of the system at any moment t is given by $\mathbb{U}(t,t_0)|\psi(t_0)\rangle$. This operator satisfies an equation similar to (1.28), except that the total derivative with respect to time is replaced by a partial derivative.

1.3 Open quantum systems

The concept of closed quantum systems is an idealization, since, in practice, one cannot perfectly isolate them from the remainder of the universe. Realistic quantum systems are in general parts of larger ones, and thus are subject to the influence of the surrounding through, in general, uncontrollable coupling interactions. Furthermore, measurement operations affect to some extent the state of the systems of interest. This leads to the conclusion that quantum systems should be regarded as open [4]. Generally speaking, the mutual interactions between the subparts of a quantum system generate quantum correlations that have no classical counterparts. The density matrix formalism provides a convenient description for the states of open quantum systems, enabling the study of these correlations.

1.3.1 Composite quantum systems, the partial trace, and the reduced density matrix

When a quantum system possesses more than one degree of freedom, we postulate that its Hilbert space is given by the tensor product of the Hilbert spaces corresponding to each degree of freedom. This applies to single particles with various degrees of freedom as well as to systems composed of multiple parts. The choice of a tensor product structure for the composite Hilbert space is justified by the agreement between theoretical predictions and experimental results. A typical example is the state of the electron in the atom: its Hilbert space is given by the tensor product of the Hilbert space corresponding to the orbital degrees of freedom and that associated with its intrinsic angular momentum or spin.

For simplicity let us consider the case of a quantum system C composed of two (possibly interacting) subsystems A and B described by the Hilbert spaces $\mathcal{H}_A$ and $\mathcal{H}_B$, respectively. The Hilbert space corresponding to the compound system is given by

$$\mathcal{H}_C = \mathcal{H}_A \otimes \mathcal{H}_B. \tag{1.34}$$

Let $\{|\phi_A^i\rangle\}$ and $\{|\phi_B^j\rangle\}$ denote orthonormal bases for $\mathcal{H}_A$ and $\mathcal{H}_B$, respectively. Then the state vectors $|\phi_A^i\rangle \otimes |\phi_A^i\rangle$ form an orthonormal basis for the Hilbert space $\mathcal{H}_C$. Any state vector $|\Psi\rangle \in \mathcal{H}_C$ can be decomposed as

$$|\Psi\rangle = \sum_{ij} \alpha_{ij} |\phi_A^i\rangle \otimes |\phi_B^j\rangle. \tag{1.35}$$

It follows that the dimension of the Hilbert space $\mathcal{H}_C$ is given by the product of the dimensions corresponding to the spaces $\mathcal{H}_A$ and $\mathcal{H}_B$, that is, $\dim\mathcal{H}_C = \dim\mathcal{H}_A.\dim\mathcal{H}_B$.

The tensor product of two linear operators L_A and L_B defined on the the Hilbert spaces $\mathcal{H}_A$ and $\mathcal{H}_B$, respectively, is a linear operator on $\mathcal{H}_C$, written $L_A \otimes L_B$, whose action is defined by

$$(L_A \otimes L_B)|\phi_A^i\rangle \otimes |\phi_B^j\rangle = (L_A|\phi_A^i\rangle) \otimes (L_B|\phi_B^j\rangle). \tag{1.36}$$

Let us denote by $\mathbb{I}_A$ and $\mathbb{I}_B$ the identity operators in $\mathcal{H}_A$ and $\mathcal{H}_B$. Then the operators

$$L_{AC} = L_A \otimes \mathbb{I}_B, \qquad L_{BC} = \mathbb{I}_A \otimes L_B \tag{1.37}$$

can be regarded as an extension of L_A and L_B to the Hilbert space $\mathcal{H}_C$. Using (1.36), it can be shown that

$$\begin{aligned} L_{AC}.L_{BC} &= (L_A \otimes \mathbb{I}_B).(\mathbb{I}_A \otimes L_B) \\ &= (L_A.\mathbb{I}_A) \otimes (\mathbb{I}_B.L_B) \\ &= L_A \otimes L_B = L_{BC}.L_{AC}. \end{aligned} \tag{1.38}$$

This implies that L_{AC} and L_{BC} commute with each other.

On the other hand, the elimination of the degrees of freedom corresponding to one subsystem can be achieved using a *partial trace* with respect to the basis state vectors associated with its Hilbert space. For instance, if X_C is a linear operator on $\mathcal{H}_C$, then

$$X_A = \sum_i \langle \phi_B^i | X_C | \phi_B^i \rangle \tag{1.39}$$

is an operator defined on the Hilbert space $\mathcal{H}_A$, and we write

$$X_A = \mathrm{tr}_B X_C. \tag{1.40}$$

Reduced density matrix

If the density matrix of the compound system ρ_C is known, then tracing out the degrees of freedom of the subsystem B yields an operator

$$\rho_A = \mathrm{tr}_B\{\rho_C\} \tag{1.41}$$

satisfying all the properties of density matrices. In fact ρ_A fully characterizes the state of the subsystem A; this is the reason for which it is called the *reduced density matrix*. For instance, the mean value of the observable L_A is given by

$$\begin{aligned} \langle L_A \rangle &= \mathrm{tr}\{(L_A \otimes \mathbb{I}_B)\rho_C\} \\ &= \mathrm{tr}_A\{\mathrm{tr}_B[(L_A \otimes I_B)\rho_C]\} \\ &= \mathrm{tr}_A\{L_A \rho_A\}. \end{aligned} \tag{1.42}$$

Suppose now that the subsystems A and B are uncorrelated and do not interact with each other. Hence the density matrix of the composite system is simply given by the tensor product of the density matrices corresponding to its subsystems, that is,

$$\rho_C = \rho_A \otimes \rho_B. \tag{1.43}$$

It follows that the mean value of the operator $L_A \otimes L_B$ is equal to the product of the mean values of the operators L_A and L_B evaluated with respect to the states ρ_A and ρ_B, respectively. This can be expressed as

$$\begin{aligned} \langle L_A \otimes L_B \rangle &= \mathrm{tr}\{(L_A \otimes L_B)\rho_C\} \\ &= \mathrm{tr}_A\{L_A \rho_A\}.\mathrm{tr}_B\{L_B \rho_B\} \\ &= \langle L_A \rangle . \langle L_B \rangle. \end{aligned} \tag{1.44}$$

We shall not go through all properties of the reduced density matrix. We only present the following obvious results:

$$\mathrm{tr}\rho_C = \mathrm{tr}_A\{\mathrm{tr}_B\rho_C\} = \mathrm{tr}_B\{\mathrm{tr}_A\rho_C\} = 1, \tag{1.45}$$

$$\mathrm{tr}_B\left\{\frac{d\rho_C}{dt}\right\} = \frac{d}{dt}\mathrm{tr}_B\{\rho_C\} = \frac{d\rho_A}{dt}, \tag{1.46}$$

which will be used later.

1.3.2 Dynamics of open quantum systems

We again restrict ourselves to the case of a system C composed of two subsystems A and B, described by the Hamiltonian operators H_A and H_B, respectively. The case of larger numbers of subsystems follows straightforwardly. If we denote by H_{AB} the Hamiltonian operator describing the interaction between the subsystems, then the total Hamiltonian reads:

$$H_C = H_A \otimes \mathbb{I}_B + \mathbb{I}_A \otimes H_B + H_{AB}. \tag{1.47}$$

We are interested in the case where the total system can be regarded as closed. This implies that the Liouville-von Neumann equation applies to the density matrix ρ_C, namely,

$$\frac{d\rho_C}{dt} = -i[H_C, \rho_C]. \tag{1.48}$$

Tracing out the degrees of freedom corresponding to the Hilbert space $\mathcal{H}_B$ yields

$$\frac{d\rho_A}{dt} = -i[H_A, \rho_A] - i\mathrm{tr}_B[H_{AB}, \rho_C]. \tag{1.49}$$

Clearly, when $H_{AB} \equiv 0$, we recover the Liouville-von Neumann equation for the density matrix ρ_A.

The interaction picture

When the Hamiltonian of a quantum system is the sum of a time-independent (free) term H_0, and an interaction term V, which may depend on time, then a convenient description of the dynamics may be achieved within the interaction picture. The latter is intermediate between the Schrödinger and the Heisenberg pictures, in the sense that in this picture both state vectors and operators evolve in time.

To begin we note that state vectors in the interaction picture are related to those in the Schrödinger picture by

$$|\psi^I(t)\rangle = \mathbb{U}_0^\dagger(t, t_0)|\psi(t)\rangle, \tag{1.50}$$

where,

$$\mathbb{U}_0(t) = \exp[-iH_0(t - t_0)]. \tag{1.51}$$

For the sake of simplicity, we assume that $t_0 = 0$ and we set $\mathbb{U}_0(t,0) = \mathbb{U}_0(t)$, such that $\mathbb{U}_0(0) = \mathbb{I}$. Deriving both sides of (1.50) with respect to time yields

$$\begin{aligned}\frac{\partial|\psi^I(t)\rangle}{\partial t} &= \frac{\partial\mathbb{U}_0^\dagger(t)}{\partial t}|\psi(t)\rangle + \mathbb{U}_0^\dagger(t)\frac{\partial|\psi(t)\rangle}{\partial t} \\ &= iH_0\mathbb{U}_0^\dagger(t)|\psi(t)\rangle - i\mathbb{U}_0^\dagger(t)(H_0+V)|\psi(t)\rangle \\ &= -i\mathbb{U}_0^\dagger(t)V|\psi(t)\rangle. \end{aligned}\tag{1.52}$$

Consequently, using equation (1.50), we obtain

$$i\frac{\partial|\psi^I(t)\rangle}{\partial t} = V^I(t)|\psi^I(t)\rangle, \tag{1.53}$$

where

$$V^I(t) = \mathbb{U}_0^\dagger(t)V\mathbb{U}_0(t). \tag{1.54}$$

In general, the rule for transforming an operator L, written in the Schrödinger picture, to the interaction picture is given by

$$L \to L^I(t) = \mathbb{U}_0^\dagger(t)L\mathbb{U}_0(t). \tag{1.55}$$

Clearly, when $t = 0$ then $|\psi^I(0)\rangle = |\psi(0)\rangle$ and $L^I(0) = L$.

Second-order master equation, Born and Markov approximations

Let us now apply the above results to the density matrix ρ corresponding to the composite system $C = A + B$ (from here on we omit the subscript C for convenience). To do so we set $H_0 = H_A \otimes \mathbb{I}_B + \mathbb{I}_A \otimes H_B$, and $H_{AB} = V$. In the interaction picture $\rho^I(t)$ and $V^I(t)$ are given by

$$\rho^I(t) = \mathbb{U}_0^\dagger(t)\rho(t)\mathbb{U}_0(t), \tag{1.56}$$

$$V^I(t) = \mathbb{U}_0^\dagger(t)V\mathbb{U}_0(t). \tag{1.57}$$

Consequently,

$$\begin{aligned}\frac{d\rho^I(t)}{dt} &= iH_0\mathbb{U}_0^\dagger\rho(t)\mathbb{U}_0(t) + \mathbb{U}_0^\dagger(t)\frac{d\rho(t)}{dt}\mathbb{U}_0(t) - i\mathbb{U}_0^\dagger(t)\rho(t)H_0\mathbb{U}_0(t) \\ &= i[H_0,\rho^I(t)] + \mathbb{U}_0^\dagger(t)\frac{d\rho(t)}{dt}\mathbb{U}_0(t) \\ &= i[H_0,\rho^I(t)] - i\mathbb{U}_0^\dagger(t)[H_0+V,\rho(t)]\mathbb{U}_0(t). \end{aligned}\tag{1.58}$$

It immediately follows that

$$\frac{d\rho^I(t)}{dt} = -i[V^I(t), \rho^I(t)]. \tag{1.59}$$

The latter equation can be put into the following integral form:

$$\rho^I(t) = \rho(0) - i\int_0^t [V^I(s), \rho^I(s)]ds. \tag{1.60}$$

Combining equations (1.60) and (1.59), yields the following integro-differential equation for $\rho^I(t)$:

$$\frac{d\rho^I(t)}{dt} = -i[V^I(t), \rho(0)] - \int_0^t [V^I(t), [V^I(s), \rho^I(s)]]ds. \tag{1.61}$$

The reduced density matrix describing the subsystem A, which we denote here by $\rho_A^I(t)$, is obtained by tracing out the degrees of freedom of the subsystem B, that is,

$$\frac{d\rho_A^I(t)}{dt} = -i\mathrm{tr}_B[V^I(t), \rho(0)] - \int_0^t \mathrm{tr}_B[V^I(t), [V^I(s), \rho^I(s)]]ds. \tag{1.62}$$

In most cases, solving the above equations exactly is not possible. However, it turns out that introducing some approximations may lead to exact analytical solutions. For instance, in the case of a subsystem A, weakly coupled to a very large environment B, it is reasonable to assume that the state of the latter is not considerably affected by the interaction. In other words, we assume that the density matrix factorizes into

$$\rho^I(t) = \rho_A^I(t) \otimes \rho_B. \tag{1.63}$$

This is known as Born approximation, under which equation (1.62) becomes

$$\frac{d\rho_A^I(t)}{dt} = -i\mathrm{tr}_B[V^I(t), \rho_A(0) \otimes \rho_B] - \int_0^t \mathrm{tr}_B[V^I(t), [V^I(s), \rho_A^I(s) \otimes \rho_B]]ds. \tag{1.64}$$

If we further replace $\rho_A^I(s)$ in (1.64) by $\rho_A^I(t)$, we obtain the following time-local integro-differential equation:

$$\frac{d\rho_A^I(t)}{dt} = -i\mathrm{tr}_B[V^I(t), \rho_A(0) \otimes \rho_B] - \int_0^t \mathrm{tr}_B[V^I(t), [V^I(s), \rho_A^I(t) \otimes \rho_B]]ds. \tag{1.65}$$

The Markov approximation is valid for the environments in which the time scales characterizing the decay of their correlation functions are much shorter that those describing the development of the state of the subsystem. In this case one replaces the variable s in equation (1.65) by $t - s$, such that s runs from 0 to ∞, that is,

$$\frac{d\rho_A^I(t)}{dt} = -i\mathrm{tr}_B[V^I(t), \rho_A(0) \otimes \rho_B] - \int_0^\infty \mathrm{tr}_B[V^I(t), [V^I(t-s), \rho_A^I(t) \otimes \rho_B]]ds. \tag{1.66}$$

This constitutes the second-order Markovian master equation. Very often, especially in quantum optics [5], the latter equation leads to an exponential decay of the reduced density matrix.

1.3.3 Decoherence

We have already mentioned that quantum mechanics is a theory for the infinitely small, in the sense that it describes the behaviour of the constituents of matter such as atoms and electrons. However, if one attempts to describe macroscopic bodies using the laws of quantum mechanics many problems immediately arise, in particular, the fact that the superposition principle cannot be observed for macroscopic bodies. Hence the need for a description of the transition from the quantum world to the classical world naturally emerges.

It has been recognized that the process responsible for this transition is the decoherence, which, in its simplest form, refers to the destruction of quantum interferences (coherences) characterizing quantum systems. The decoherence has attracted much attention since Schrödinger published his famous papers [6, 7]. We note here that Bohr went further and suggested to consider this phenomenon as an axiom for quantum mechanics.

In the 1980s Zurek, among others, extensively investigated the decoherence and came to the conclusion that this process can be regarded as a consequence of the axioms of quantum mechanics, in contrast to what Bohr suggested. His arguments are based on the fact that the decoherence is the result of the interaction of quantum systems with their environments [8, 10, 11, 12, 13]. The latter are responsible of the dynamical destruction of quantum interferences, leading coherent superpositions of pure states to evolve into mixed states. In the course of this process, the environment becomes correlated (entangled) with the system, and hence acquires information about it. This leads to a reduction of the set of accessible states to the system, and generates some kind of quantum noise due to the loss of information to the environment. This process selects a class of robust states (pointer states) which persist in the course of time, and hence correspond to what we observe classically.

All what has been said above can be better understood by investigating a simple illustrative model, in which the interaction Hamiltonian reads [4]

$$H_I = \sum_n |n\rangle\langle n| \otimes B_n, \tag{1.67}$$

Here the state vectors $|n\rangle$ form an orthonormal basis for the Hilbert space of the system, and B_n are environmental operators. We further assume that the free Hamiltonian H_0 commutes with the operators $|n\rangle\langle n|$ and B_n. In this case the mean energy of the system is conserved. Hence the evolution in time of any initially uncorrelated state

$$|\Psi(0)\rangle = \sum_n c_n |n\rangle \otimes |\phi\rangle \tag{1.68}$$

is given by

$$|\Psi(t)\rangle = \sum_n c_n |n\rangle \otimes |\phi_n(t)\rangle, \tag{1.69}$$

where

$$|\phi_n(t)\rangle = e^{-iB_n t}|\phi\rangle. \tag{1.70}$$

It follows that the reduced density matrix describing the state of the system is given by

$$\rho(t) = \mathrm{tr}_B|\Psi(t)\rangle\langle\Psi(t)| = \sum_{mn} c_n c_m^* |n\rangle\langle m|\langle\phi_m(t)|\phi_n(t)\rangle. \tag{1.71}$$

Consequently, the diagonal elements of the reduced density matrix are unchanged, while the off-diagonal ones are multiplied by the overlap between the environmental states. At this stage it is convenient to introduce the decoherence function by

$$\Gamma_{mn} = \ln|\langle\phi_m(t)|\phi_n(t)\rangle|. \tag{1.72}$$

Note that since $|\langle\phi_m(t)|\phi_n(t)\rangle| \leq 1$, then $\Gamma_{mn} \leq 0$. Moreover, the time-dependence of the decoherence function depends on the initial state and the nature of the environment. In general, the irreversible character of the dynamics leads to a rapid increase of the decoherence function Γ_{mn} corresponding to the off-diagonal element ρ_{mn}. In the case where the environmental operators $B_n(t)$ are such that the off-diagonal elements vanish after some time scale τ_D, which we call the decoherence time, that is

$$\Gamma_{m\neq n} \to 0, \quad t >> \tau_D, \tag{1.73}$$

then the reduced density matrix becomes an incoherent superposition of the states $|n\rangle$:

$$\rho \to \sum_n |c_n|^2 |n\rangle\langle n|. \tag{1.74}$$

Hence the coherences of the density matrix in the basis $|n\rangle$ have vanished due to the coupling to the environment. This local destruction of the coherences makes them inaccessible to any observer. It is clear from equation (1.74) that the reduced density matrix becomes diagonal in the set of basis state vectors $|n\rangle$. The latter is known as the preferred basis.

Measures for the decoherence

We have seen that the main effect of decoherence consists in transforming pure states into mixed states. Thus a measure of the degree of mixing may also be a good measure for the decoherence. Recall that for any density matrix ρ, we have $\mathrm{tr}\rho^2 \leq 1$; the equality holds for pure states. The quantity

$$P = \mathrm{tr}\rho^2 \tag{1.75}$$

is thus a good candidate for a measure for decoherence; it is usually called the *purity* of the state ρ. In a d-dimensional Hilbert space, the smallest value of P corresponds to the maximally mixed state $\rho_m = \frac{1}{d}\mathbb{I}$. In fact it is more convenient to quantify the decoherence using the quantity $D = 1 - P$ instead of the purity itself. The latter quantity is maximum for ρ_m and vanishes for pure states:

$$0 \leq D \leq 1 - \frac{1}{d}. \tag{1.76}$$

Sometimes it is desirable to quantify the distance between two density matrices, say ρ and $\tilde{\rho}$. The measure enabling the fulfillment of such a task is called the *fidelity*, which we denote by F. It is defined through the trace as follows:

$$F = \mathrm{tr}\{\rho\tilde{\rho}\}. \tag{1.77}$$

It can be shown that $0 \leq F \leq 1$. The fidelity is also used as a measure of decoherence.

1.4 Entanglement

1.4.1 The EPR paradox

Entanglement refers to quantum correlations that exist between multipartite systems even when these are spatially separated from each other. Consider for instance the state vector

$$|\psi\rangle = \frac{1}{2}\Big(|a_1\rangle \otimes |b_1\rangle + |a_2\rangle \otimes |b_2\rangle\Big), \tag{1.78}$$

of the bipartite system $C = A + B$, where a_i and b_i denote, respectively, the degrees of freedom of the systems A and B. The above state exhibits strong correlations between the subsystems: if we measure separately the state of each part, we can find with a probability $\frac{1}{2}$ the system A in the state $|a_1\rangle$ and B in the state $|b_1\rangle$, or with the same probability the system A in the state $|a_2\rangle$ and B in the state $|b_2\rangle$. In other words, if we measure the state of one of the systems, we can deduce with certainty the result of the measurement on the second one.

Einstein, Podolsky and Rosen were the first to point out the apparent paradoxical character of entanglement [14]. They used the latter to show how quantum mechanics would contrast a realistic local theory of nature. According to EPR, quantum mechanics cannot be the ultimate theory of physical phenomena because of its fundamental indeterminism. Their arguments can be summarized as follows: There is an element of reality associated with the degree of freedom b, since without disturbing the system B, we can determine

with certitude the outcome of the measurement of b. Worse, following EPR, the analysis shows that it may be possible to simultaneously measure two quantities associated with non-commuting observables such as the x and z components of the spin of the electron.

From the point of view of quantum mechanics, the systems A and B, taken separately, are not in a well defined state. What really matters is the state of the compound system. The EPR reasoning can be applied only to separable states for which a measurement on one part does not provide any information on the state of the other one, and hence there is no paradox.

The work of Bell provided a direct tool for testing the validity of quantum mechanics [15, 16]. He assigned to each EPR pair a *hidden variable* inaccessible by the observer, which ensures that the new presumed theory is local, in accordance with what Einstein was looking for. He derived some inequalities (Bell's inequalities), describing the constraints on the prediction of this theory. The results of subsequent experimental verifications proved the violation of Bell's inequalities [17]. In fact the former were in good agreement with what quantum mechanics predicted. This led to the conclusion that there cannot exist an alternative local theory for quantum mechanics.

The above discussion shows the important role played by entanglement in the development of the theory of quantum mechanics [18]. As we shall see bellow, it is also of great practical significance in the field of quantum information.

1.4.2 Measures of entanglement

Entanglement is considered as a fundamental resource for nature in the same level as energy and entropy [19]. Thus, it is important to quantify it using measures that enable one to know to what extent the state of a quantum system is entangled. Generally speaking, the state ρ of a bipartite system $A + B$ is said to be entangled (or not separable) if it cannot be written as a tensor product of pure states of its subsystems, or as a statistical mixture of tensor product (uncorrelated) states, that is [20],

$$\rho \neq \sum_k c_k \rho_A^k \otimes \rho_B^k. \tag{1.79}$$

A state which is not untangled is said to be separable.

Recall that any normalized state vector $|\psi_{AB}\rangle \in \mathcal{H}_A \otimes \mathcal{H}_B$ can be written in the form of a Schmidt decomposition

$$|\psi_{AB}\rangle = \sum_{j=1}^{\chi} \sqrt{p_j} |\phi_A^j\rangle \otimes |\varphi_B^j\rangle, \qquad \chi \leq \min(\dim \mathcal{H}_A, \dim \mathcal{H}_B), \tag{1.80}$$

where $\{|\phi_A^j\rangle\}$ and $\{|\varphi_B^j\rangle\}$ are, respectively, the orthonormalized eigenvectors of the reduced density matrices $\rho_A = \mathrm{tr}_B(|\psi_{AB}\rangle\langle\psi_{AB}|)$ and $\rho_B = \mathrm{tr}_A(|\psi_{AB}\rangle\langle\psi_{AB}|)$. The p_j can be shown to be common eigenvalues of the latter reduced density matrices. The upper limit χ of the sum in (1.80) is called the Schmidt number. Hence, if $\chi = 1$ then the state is separable, i.e., not entangled.

It turns out that, very often, the task of finding a decomposition for a given density matrix is computationally very hard. As a consequence, one should look for practical measures which enable the quantification of entanglement with a lower computational effort. Let us first remark that, generally speaking, an entanglement measure E is, by definition, a functional from the space of density matrices on the Hilbert space to the set of positive real numbers which satisfies the following requirements [21, 22, 23]:

- $E(\rho) = 0$ if and only if ρ is separable.
- $E(\rho) = 1$ for maximally entangled states.
- $E(\Lambda\rho) \leq E(\rho)$ for any LOCC[1] operation Λ. The equality holds when the operation is strictly local.
- $E(\sum_i w_i\rho_i) \leq \sum_i w_i E(\rho_i)$ with $0 \leq w_i \leq 1$ (convexity).
- $E(\rho^{\otimes n}) = nE(\rho)$ (weak additivity).
- If ρ_n is a density matrix of n pairs such that $\lim_{n\to\infty}\langle\psi^{\otimes n}|\rho_n|\psi^{\otimes n}\rangle = 1$, then $\lim_{n\to\infty}[E(|\psi\rangle\langle\psi|^{\otimes n}) - E(\rho_n)]/n = 0$ (continuity).

Since pure states contain no classical correlation, then the von Neumann entropy of the subsystems

$$S(\rho_A) = S(\rho_B) = -\mathrm{tr}_A\{\rho_A \log_2 \rho_A\} = -\mathrm{tr}_B\{\rho_B \log_2 \rho_B\} = E(|\psi_{AB}\rangle) \tag{1.81}$$

represents a convenient measure of their entanglement. When $E(|\psi_{AB}\rangle) = 0$, then the state $|\psi_{AB}\rangle$ is separable, otherwise it is entangled. Note that, in general, if we denote by λ_i the eigenvalues of ρ, then

$$S(\rho) = -\sum_i \lambda_i \log_2 \lambda_i. \tag{1.82}$$

It follows that

$$E(|\psi_{AB}\rangle) = -\sum_{j=1}^{\chi} p_j \log_2 p_j. \tag{1.83}$$

[1] LOCC: Local Operations and Classical Communication

The above measure is usually called the entropy of entanglement.

For mixed states the situation is much more complicated. Here we only consider one measure for bipartite systems, namely, the entanglement of formation E_F [24, 25, 26]. The latter is obtained by taking the infimum on all possible averages of the entropy of entanglement with respect to the ensembles of pure states $\mathcal{E} = \{|\psi_i\rangle, w_i\}$ corresponding to the mixed state $|\psi\rangle$, that is,

$$E_F(|\psi\rangle) = \inf_{\mathcal{E}} \sum_i w_i E(|\psi_i\rangle). \tag{1.84}$$

It turns out that the entanglement of formation assumes the following form:

$$E_F = h\left(\frac{1+\sqrt{1-C(\rho)^2}}{2}\right), \tag{1.85}$$

where $h(x) = -x\log_2 x + (x-1)\log_2(1-x)$, and $C(\rho)$ is called the concurrence of the density matrix ρ. Wooters [25] proved that the explicit form of the concurrence is given by

$$C(\rho) = \max\{\sqrt{\lambda_1} - \sqrt{\lambda_2} - \sqrt{\lambda_3} - \sqrt{\lambda_4}, 0\}, \tag{1.86}$$

where $\lambda_1 \geq \lambda_2 \geq \lambda_3 \geq \lambda_4$ are the eigenvalues of the operator

$$\bar{\rho} = \rho(\sigma_y \otimes \sigma_y)\rho^*(\sigma_y \otimes \sigma_y). \tag{1.87}$$

Here σ_y is the Pauli matrix, and asterisk denotes the complex conjugation. The concurrence can itself be used as a measure of entanglement: it is equal to zero for separable states and one for maximally entangled states.

1.4.3 Entanglement and quantum critical phenomena

Quantum phase transition refers to the abrupt changes in the properties of the ground states of quantum systems when some relevant parameters vary across their critical values [27]. In contrast to classical phase transitions, the quantum ones occur only at the absolute zero temperature. One may regard quantum phase transitions as the result of quantum fluctuations inherent to many body quantum systems. As an illustration, let us consider the transverse $1D$ Ising model with N spins, whose Hamiltonian is given by

$$H = -\lambda \sum_{i=1}^{N} \sigma_x^i \sigma_x^{i+1} - \sum_{i=1}^{N} \sigma_z. \tag{1.88}$$

Here $\lambda \geq 0$ is the coupling constant, and $\sigma_\alpha^i, \alpha \equiv x, z$, denote the Pauli matrices at site i. When $\lambda \to \infty$, the ground state of H is two-fold degenerate, with either all the spins

pointing up or all pointing down along the x direction. However, when $\lambda = 0$, the ground state is such that all the spins are aligned ferromagnetically along the z direction. The magnetization, in turn, vanishes in the thermodynamic limit when $\lambda \to \infty$, and tends to one as $\lambda \to 0$. There exists a critical point λ_c at which the magnetization displays a sudden change.

It should be noted that due to the appearance of criticality, some correlations characterizing many body systems may exhibit a power decay near the critical point; they, however, decay exponentially far from the point of phase transition. This is the reason which has led many authors to investigate the relation between entanglement and quantum phase transitions. These studies revealed a genuine behaviour of entanglement as measured by the entropy and the concurrence.

1.5 *Qubits: The building blocks of quantum information*

Quantum Information (QI) is a field of current research which deals with the possible ways of using quantum mechanics to treat information, in a manner that is much more efficient compared to what classical methods do offer [19]. Let us recall that, generally speaking, Information Theory allows for the establishment of a framework for communications and information processing, and provides us with tools to quantify the information. Within this framework one can, for instance, derive bounds on the complexity and costs of storing data or sending information over a noisy channel. The unit of classical information is the *bit*. The latter can only have two possible values which are conventionally denoted by 0 and 1. The two different voltages across a transistor on a chip, the two different orientations of the magnetic domain on a disc, and the two different classical light pulses traveling down an optical fibre are examples of the realization of classical bits. Any physical object used in the treatment of information is ultimately composed of atoms, and molecules. These should, in turn, be described by the laws of quantum mechanics, the fundamental theory of atomic phenomena.

Historically, Feynman was the first to come out with the idea of using quantum mechanics to accomplish tasks inaccessible by standard classical methods [28]. He pointed out that the exponential growth of the dimension of the Hilbert space, due to the increase of the number of degrees of freedom, makes it impossible to simulate large quantum systems by classical computers. Feynmann introduced the concept of quantum computer by proposing the simulation of quantum systems by other quantum systems. This marked the birth of quantum information theory, whose building block is known as the quantum

bit or *qubit* [29]. This can be any two-level quantum system described by the Hilbert space $\mathbb{C}^2$, where $\mathbb{C}$ denotes the field of complex numbers. As opposed to the classical bit, the quantum bit posses infinite number of permitted states. This follows from the superposition principle of quantum mechanics. Indeed, if we denote by $\{|0\rangle, |1\rangle\}$ an orthonormal basis for $\mathbb{C}^2$, then the general form of the state of the qubit is given by

$$|\psi\rangle = a|0\rangle + b|1\rangle, \tag{1.89}$$

where $a, b \in \mathbb{C}$, such that $|a|^2 + |b|^2 = 1$. Taking into account this normalization condition, the above state can be recast, up to a trivial unitary constant, into the form

$$|\psi\rangle = \cos\left(\frac{\theta}{2}\right)|0\rangle + e^{i\phi}\sin\left(\frac{\theta}{2}\right)|1\rangle. \tag{1.90}$$

The variables ϕ and θ represents the polar coordinates of a point on a unit sphere called *bloch sphere.*

The two main branches of quantum information theory are quantum cryptography and quantum computing. The first one is based on the fact that any measurement carried out on a quantum system inevitably disturbs its state. Hence, encoding information in quantum systems enables high communication security. For instance the effect of a spy on the quantum channel, through which a sender and receiver are exchanging information, can be instantaneously detected by the latter. Note, also, that classical cryptography is founded on the algorithmic problem of factorizing large numbers into prime integers; this is also the case for quantum cryptography, making it tightly related to the other branch of quantum information, namely, quantum computing.

In a quantum computer, any algorithm can be regarded as a set of successive quantum operations on the qubits [19]. These can be written as a linear combination of the Pauli matrices along with the identity matrix in $\mathbb{C}^2$, namely,

$$X = \begin{pmatrix} 0 & 1 \\ 1 & 0 \end{pmatrix}, \quad Y = \begin{pmatrix} 0 & -i \\ i & 0 \end{pmatrix}, \quad Z = \begin{pmatrix} 1 & 0 \\ 0 & -1 \end{pmatrix}, \quad I = \begin{pmatrix} 1 & 0 \\ 0 & 1 \end{pmatrix}. \tag{1.91}$$

In order to be able to perform quantum computing, one should add gates that act on at least two qubits simultaneously. The most important two-qubit gate is the CNOT gate, given in the natural basis $\{|11\rangle, |10\rangle, |01\rangle, |00\rangle\}$ by:

$$CNOT = \begin{pmatrix} I & 0 \\ 0 & X \end{pmatrix}. \tag{1.92}$$

The CNOT gate together with all single qubit operations constitute a universal set of quantum gates, in the sense that any n-qubit gate can be implemented by composing operations on single qubits and CNOT gates.

There have been many proposals for the implementation of quantum computers. The most successful one is based on nuclear magnetic resonance where nuclear spin states of atoms within the molecules play the role of qubits [30, 31]. This technique is characterised by a relatively long decoherence time, which enables the realization of many elementary quantum algorithms such as that of Deutsch-Jozsa. Trapped neutral atoms were also proposed for the implementation of quantum information processing. Here the spin degrees of freedom of the electrons corresponding to the ground states of atoms play the role of qubits. The coupling between the qubits can be realized by divers mechanism, among which we mention dipole-dipole interactions [32] and cold collisions [33]. Another realization which is close to the above one consists in using trapped cooled ions instead of atoms [34]. In this case, each qubit is represented by the combination of the ground state and an excited metastable state of the ion. The coupling between qubits is mediated by collective excitations of the ions.

The rapid progress in the field of spintronics and solid state nanostructures triggered the interest on spin systems as candidates for the realization of quantum computers [35, 36]. Spin systems are very promising in the sense that they offer the possibility of integrating qubits on a large scale. Among these, we find quantum dots in which electron qubits couple to the surrounding electrons, which can be regarded as a spin bath, through hyperfine interactions. The latter can be reasonably described using Heisenberg model.

Entanglement is the main resource for quantum computing and quantum cryptography [37]. Many of the known protocols are based on entanglement (e.g., see [38]). On the other hand, decoherence is the major obstacle toward the implementation of quantum computers, since it makes quantum system to behave classically. Therefore, the study of decoherence and entanglement in many-body spin systems is of great importance, both theoretically and experimentally [39, 40, 41]. Many of the precedent studies have dealt with spin chains. This thesis focuses on the study of exactly solvable models for the dynamics of simple qubit systems interacting with the collective modes of their surrounding spin environments. The obtained results are applied to the investigation of the decoherence and entanglement evolution of the central systems.

BIBLIOGRAPHY

[1] L. I. Schiff, *Quantum Mechanics* (McGraw Hill, New York, 1949).

[2] C. Cohen-Tannoudji, B. Diu, and F. Laloë, *Quantum Mechanics* (Wiley, New York, 1977), Vol. I.

[3] L. D. Landau, and E. M. Lifschitz, *Quantum Mechanics* (Pergamon Press, Oxford, 1976).

[4] H. P. Breuer and F. Petruccione, *The Theory of Open Quantum Systems* (Oxford University Press, Oxford, 2002).

[5] C. W. Gardiner, *Quantum Noise* (Springer, Berlin, 1991).

[6] E. Schrödinger, Naturwissenschaften 23, 807 (1935).

[7] E. Schrödinger, Naturwissenschaften 23, 823 (1935)

[8] W. H. Zurek, Phys. Rev. D 24, 1516 (1981).

[9] W. H. Zurek, Phys. Rev. D 26, 1862 (1982).

[10] W. H. Zurek, Phys. Today 4410, 36 (1991).

[11] W. H. Zurek, Rev. Mod. Phys. 75, 715 (2003).

[12] D. Giulini, E. Joos, C. Kiefer *et al.*, *Decoherence and the Appearance of a Classical World in Quantum Theory* (Springer-Verlag, Berlin, Heidelberg, New York, 1996).

[13] W. H. Zurek, Progr. Theor. Phys 89, 281 (1993).

[14] A. Einstein, B. Podolsky, and N. Rosen, Phys. Rev., 47, 777 (1935).

[15] J. S. Bell, Physics, 1, 195 (1964).

[16] J. S. Bell, *Speakable and Unspeakable in Quantum Mechanics* (Cambridge University Press, Cambridge, 1987).

[17] A. Aspect, J. Dalibard, and G. Roger, Phys. Rev. Lett., 49, 1804 (1982).

[18] A. Peres, *Quantum Theory: Concepts and Methods* (Kluwer, Dordrecht, 1993).

[19] M. A. Nielsen and I. L. Chuang, *Quantum Computation and Quantum Information* (Cambridge University Press, Cambridge, 2000).

[20] R. F. Werner, Phys. Rev. A, 40, 4277 (1989).

[21] G. Vidal, Phys. Rev. Lett., 91, 147902 (2003).

[22] V. Vedral, M. B. Plenio, M. A. Rippin, and P. L. Knight, Phys. Rev. Lett., 78, 2275 (1997).

[23] M. Horodecki, P. Horodecki, and R. Horodecki, Phys. Rev. Lett., 84, 2014 (2000).

[24] S. Hill and W. K. Wootters, Phys. Rev. Lett., 78, 5022 (1997).

[25] W. K. Wootters, Phys. Rev. Lett., 80, 2245 (1998).

[26] W. K. Wootters, Quantum Inf. Comput. 1, 27 (2001).

[27] S. Sachdev *Quantum Phase Transitions* (Cambridge University Press, Cambridge, 1999).

[28] R. P. Feynman, Int. J. Theor. Phys., 21, 467 (1982).

[29] N. Gisin, G. Ribordy, W. Tittel, and H. Zbinden, Rev. Mod. Phys, 74 (2002).

[30] I. L. Chuang, L. M. K. Vandersypen, X. Zhou, D. W. Leung, and S. Lloyd, Nature, 393, 143 (1998).

[31] I. L. Chuang, N. Gershenfeld, and M. Kubinec, Phys. Rev. Lett. 80, 3408 (1998).

[32] G. K. Brennen, C. M. Caves, P. S. Jessen, and I. H. Deutsch, Phys. Rev. Lett. 82, 1060 (1999).

[33] D. Jaksch, H.-J. Briegel, J. I. Cirac, C. W. Gardiner, and P. Zoller, Phys. Rev. Lett. 82, 1975 (1999).

[34] J. I. Cirac, and P. Zoller, Phys. Rev. Lett. 74, 4091 (1995).

[35] D. Loss and D. P. DiVincenzo, Phys. Rev. A 57, 120 (1998).

[36] G. Burkard, D. Loss, and D. P. DiVincenzo, Phys. Rev. B 59, 2070 (1999).

[37] C. H. Bennett and D. P. DiVincenzo, Nature, 404, 247 (2000).

[38] P. Shor, Proceedings of the 35th Annual Symposium on Foundations of Computer Science, p. 124 (IEEE Press,California, 1994).

[39] W. Zhang, N. Konstantinidis, K. Al-Hassanieh, and V. V. Dobrovitski, J. Phys.: Condens. Matter 19, 083202 (2007).

[40] L. Amico *et al*, Rev. Mod. Phys. 80, 517 (2008).

[41] A. Hutton, S. Bose, Phys. Rev. A 69, 042312 (2004).

2. TIME EVOLUTION AND DECOHERENCE OF A SPIN-$\frac{1}{2}$ PARTICLE COUPLED TO A SPIN BATH IN THERMAL EQUILIBRIUM

2.1 Introduction

The loss of quantum coherence due to unavoidable interactions of quantum systems with the surrounding environment is known as decoherence. It represents the main obstacle to quantum computing and quantum information processing [1, 2, 3]. The environment destroys quantum interferences of the central system within time scales much shorter than those typically characterizing dissipation [4]. The unwanted effect of decoherence reduces the advantages of quantum computing methods by producing errors in their outcomes. Different strategies, such as error-correcting codes, are adopted to overcome this difficulty [5, 6, 7, 8]. Great scientific effort has been devoted to the understanding of the process of decoherence in quantum systems, mainly focused on solid state spin nanostructures. These systems seem to be the most promising candidates that can be efficiently used in quantum information processing and computation [9, 10, 11].

Several models were proposed to study decoherence of single and multi-spin systems interacting with a surrounding environment [12]. Very often, the derivation of the reduced dynamics involves complications and difficulties that can be overcome in many cases by making recourse to approximation techniques. In particular, the Markovian approximation together with the master equation approach turns out to be very useful [13, 14]. However, any approximation method is inevitably based on some assumptions which do not necessarily reflect the actual properties of the composite system. Moreover, many realistic spin systems exhibit non-Markovian behavior for which the standard derivation of the master equation ceases to be applicable. The non-Markovian dynamics of a central spin-system coupled to a spin environment has been investigated by many authors [15, 16, 17, 18, 19, 20].

In general, the course of the decoherence process depends on the intrinsic properties of the bath such as temperature, polarizations, and quantum fluctuations. At low environmental temperatures, the dominant effect arises from the contributions of localized

modes such as nuclear spins [21]. In quantum dots, the decoherence of the central spins is mainly caused by the hyperfine coupling with the surrounding nuclear spins. The effect of bath polarizations and external magnetic fields on the decoherence of electron spins in quantum dots has been investigated by Zhang *et al* [22].

In this chapter we study the dynamics of a spin-$\frac{1}{2}$ particle interacting with a large spin environment in thermal equilibrium. In section 2.2, we introduce the model Hamiltonian together with the initial states of the central spin and the environment. In section 2.3, we calculate the exact time evolution operator of the composite system and we derive the reduced density matrix of the central spin. Section 2.4 is devoted to the case of an infinite number of spins in the bath. We study the long-time behavior as well as the short-time behavior of the reduced density matrix, and we discuss the effect of the magnetic field and the bath temperature on decoherence.

2.2 The model

We consider a central spin-$\frac{1}{2}$ particle coupled to a spin bath composed of N interacting spin-$\frac{1}{2}$ particles in thermal equilibrium at temperature T. The spin operators corresponding to the central system are denoted by S_i^0 with $i = x, y, z$; those associated with the bath constituents are denoted by S_i^k, where $k = 1, 2, ..., N$ and $i = x, y, z$. We assume that the central system as well as every spin in the bath couples to all other spins through long-range anisotropic Heisenberg interactions. Moreover, an external magnetic field of controlled strength μ is locally applied to the central spin along the z direction. Under the above assumptions, the model Hamiltonian can be written as

$$H = H_S + H_{SB} + H_B, \tag{2.1}$$

where H_S and H_B are, respectively, the Hamiltonian operators of the central spin and the surrounding environment. The coupling between the open system and the bath is described by the Hamiltonian H_{SB}. Explicitly, we have

$$H_S = 2\mu S_z^0, \tag{2.2}$$

$$H_{SB} = \frac{2\gamma}{\sqrt{N}} S_z^0 \sum_{i=1}^{N} S_z^i + \frac{2\alpha}{\sqrt{N}} \Big[S_x^0 \sum_{i=1}^{N} S_x^i + S_y^0 \sum_{i=1}^{N} S_y^i \Big], \tag{2.3}$$

$$H_B = \frac{g}{N} \Big[\sum_{i \neq j}^{N} \Big(S_x^i S_x^j + S_y^i S_y^j \Big) + \Delta \sum_{i \neq j}^{N} S_z^i S_z^j \Big], \tag{2.4}$$

where γ and α are the coupling constants of the central spin to the environment, g stands for the strength of interactions of spins in the bath, and Δ is the anisotropy constant. The

coefficient 2 in front of μ, γ and α in Eqs. (2.2) and (2.3) is introduced for later convenience. Furthermore, we have rescaled the above interaction strengths with appropriate powers of the number of spins in the environment in order to ensure good thermodynamical behavior, namely, an extensive free energy. Obviously, a more realistic model would include site-dependent interactions.

Note that in the case where $\gamma = 0$, H_{SB} reduces to Heisenberg XY Hamiltonian which was recently used to model the coupling of one and two qubits to star-like environments [23, 15, 16, 17]. Moreover, when $\gamma = \alpha$ we simply have $H_{SB} = \frac{\alpha}{\sqrt{N}} \vec{S}^0 \sum_{i=1}^{N} \vec{S}^i$, which should be compared with the Hamiltonian of the hyperfine contact coupling of electron spin to the nuclear spins in quantum dot . In [24], the Hamiltonian $h_B = \sum_{i>j} g_{ij}(\vec{S}^i\vec{S}^j - 3S_z^iS_z^j)$ was used to model the intrabath dipolar coupling between nuclear spins in quantum dot. If we assume uniform coupling between nuclear spins, i.e. all the g_{ij} are the same, then the operator h_B (with rescaled coupling constant) becomes equivalent to H_B in the case where $\Delta = -2$. It should also be noted that the bath Hamiltonian H_B is very close to that of the isotropic Lipkin-Meshkov-Glick model [25, 26]. There, the magnetic field globally applied to all spins plays the role of the anisotropy present in our model. This can be better seen by applying mean field approximation to the longitudinal term of H_B.

The Hamiltonian operators H_B and H_{SB} can be rewritten in terms of the lowering and raising operators $S_\pm^i = S_x^i \pm iS_y^i$ as follows

$$H_{SB} = \frac{2\gamma}{\sqrt{N}} S_z^0 \sum_{i=1}^{N} S_z^i + \frac{\alpha}{\sqrt{N}} \Big[S_+^0 \sum_{i=1}^{N} S_-^i + S_-^0 \sum_{i=1}^{N} S_+^i \Big], \tag{2.5}$$

$$H_B = \frac{g}{2N} \Big[\sum_{i\neq j}^{N} \left(S_+^i S_-^j + S_-^i S_+^j \right) + 2\Delta \sum_{i\neq j}^{N} S_z^i S_z^j \Big]. \tag{2.6}$$

By introducing the total angular momentum of the bath $\vec{J} = \sum_{i=1}^{N} \vec{S}^i$, together with the corresponding lowering and raising operators $J_\pm$, it is possible to put the above Hamiltonian operators into the following form

$$H_{SB} = \frac{2\gamma}{\sqrt{N}} S_z^0 J_z + \frac{\alpha}{\sqrt{N}} \Big[S_+^0 J_- + S_-^0 J_+ \Big], \tag{2.7}$$

$$H_B = \frac{g}{2N} \Big[K + 2\Delta J_z^2 - \frac{(2+\Delta)N}{2} \Big]. \tag{2.8}$$

Here, J_z is the z component of the total angular momentum J, and we have introduced the operator $K = J_+J_- + J_-J_+$. From here on, we shall neglect the constant $(2+\Delta)g/4$ appearing in the expression of H_B since it has no effect on the dynamics of the system. This can be done by redefining the energy origin of the spectrum of the bath Hamiltonian.

The spin spaces corresponding to the central spin and the environment are given by $\mathbb{C}^2$ and $(\mathbb{C}^2)^{\otimes N}$, respectively. The latter space can be decomposed as a direct sum of subspaces $\mathbb{C}^{d_j}$ each of which has a dimension equal to $d_j = 2j + 1$ where $0 \leq j \leq \frac{N}{2}$ [16](we take N even), namely $(\mathbb{C}^2)^{\otimes N} = \bigoplus_{j=0}^{\frac{N}{2}} \nu(N, j)\mathbb{C}^{d_j}$. The degeneracy $\nu(N, j)$ is given by [27]

$$\nu(N, j) = \frac{2j + 1}{\frac{N}{2} + j + 1} \frac{N!}{(\frac{N}{2} - j)!(\frac{N}{2} + j)!}. \tag{2.9}$$

It is worth noting that the bath Hamiltonian can be expressed in terms of the operators J^2 and J_z as $H_B = \frac{g}{N}[J^2 + (\Delta - 1)J_z^2]$. Therefore, the operator H_B is diagonal in the standard basis of $(\mathbb{C}^2)^{\otimes N}$ formed by the common eigenvectors of J^2 and J_z which we denote by $|j, m)$ where $-j \leq m \leq j$. In this basis, the eigenvalues of the operator K are simply given by $2(j(j + 1) - m^2)$ (we set $\hbar = 1$).

2.3 Reduced dynamics of the central spin

In this section we derive the exact time evolution of the central spin for finite number of environmental spins. As usual, we introduce the time evolution operator $\mathbf{U}(t) = e^{-iHt}$ together with the total density matrix operator of the spin-bath system, $\rho_{\text{tot}}(t)$. The initial value of the latter is denoted by $\rho_{\text{tot}}(0)$. The evolution in time of the composite system is unitary; its density matrix at any moment of time is given by

$$\rho_{\text{tot}}(t) = \mathbf{U}(t)\rho_{\text{tot}}(0)\mathbf{U}^\dagger(t). \tag{2.10}$$

The reduced density matrix of the central spin can be calculated by tracing $\rho_{\text{tot}}(t)$ with respect to the environmental degrees of freedom, namely,

$$\rho(t) = \text{tr}_B\{\rho_{\text{tot}}(t)\}. \tag{2.11}$$

This can be explicitly written in terms of bath states as

$$\rho(t) = \sum_{j,m} \nu(N, j)\langle j, m|\rho_{\text{tot}}(t)|j, m\rangle. \tag{2.12}$$

In order to solve the time evolution problem (2.10), one needs to calculate the exact analytical form of $\mathbf{U}(t)$ and to specify the initial density matrix.

2.3.1 Initial conditions

Initially, the central spin is assumed to be uncorrelated with the environment. The corresponding total density matrix is given by the direct product $\rho_{\text{tot}}(0) = \rho(0) \otimes \rho_B$ where

$\rho(0)$ and ρ_B are, respectively, the initial density matrices of the central spin and the bath. In the standard basis composed of the eigenvectors $|-\rangle$ and $|+\rangle$ of the operator S_z^0, $\rho_S(0)$ takes the general form

$$\rho(0) = \begin{pmatrix} \rho_{11}^0 & \rho_{12}^0 \\ \rho_{12}^{0*} & \rho_{22}^0 \end{pmatrix}, \tag{2.13}$$

where ρ_{11} and ρ_{22} are positive real numbers which satisfy $\rho_{11} + \rho_{22} = 1$. For instance, if at $t = 0$ the central system was in the state

$$|\psi(0)\rangle = a|-\rangle + b|+\rangle, \tag{2.14}$$

where a and b are complex numbers satisfying $|a|^2+|b|^2 = 1$, then $\rho_{11}^0 = |a|^2$ and $\rho_{12}^0 = ab^*$. Alternatively, $\rho(0)$ can be expressed in terms of the components of the Bloch vector $\vec{\lambda} = (\lambda_1, \lambda_2, \lambda_3)$ as

$$\rho(0) = \frac{1}{2}\begin{pmatrix} 1 - \lambda_3(0) & \lambda_1(0) - i\lambda_2(0) \\ \lambda_1(0) + i\lambda_2(0) & 1 + \lambda_3(0) \end{pmatrix}, \tag{2.15}$$

with the condition $|\vec{\lambda}| \leq 1$; the equality holds for pure initial states. We shall use both representations of the density matrix throughout the paper.

At $t = 0$, the spin bath is taken in thermal equilibrium at finite temperature T. Its density matrix is given by the Boltzmann distribution

$$\rho_B = \frac{e^{-\beta H_B}}{Z_N}, \tag{2.16}$$

where $\beta = 1/T$ (we set $k_B = 1$), and $Z_N = \mathrm{tr}_B e^{-\beta H_B}$ is the partition function of the bath. Clearly, ρ_B is diagonal in the standard basis $\{|j, m\rangle\}$ from which it follows that [28]

$$\langle j, m|\rho_B|j, m\rangle = \frac{1}{Z_N} e^{-\frac{q\beta}{N}[j(j+1)+(\Delta-1)m^2]}, \tag{2.17}$$

and

$$Z_N = \sum_{j,m} \nu(N, j)\ e^{-\frac{q\beta}{N}[j(j+1)+(\Delta-1)m^2]}. \tag{2.18}$$

In the case of the isotropic Heisenberg model, i.e., when $\Delta = 1$, the above expression simplifies to

$$Z_N = \sum_{j} \nu(N, j)(2j + 1)\ e^{-\frac{q\beta}{N}[j(j+1)]}. \tag{2.19}$$

In the extreme case of an infinite temperature ($\beta \to 0$), the density matrix of the bath reads

$$\rho_B(T = \infty) = \frac{\mathbf{1}_B}{2^N}, \tag{2.20}$$

which corresponds to a completely unpolarized spin bath. In the previous expression $\mathbf{1}_B$ stands for the unity matrix in the bath space.

2.3.2 Time evolution operator

Let U_{ij} denote the components of the time evolution operator $\mathbf{U}$ in the basis $\{|-\rangle, |+\rangle\}$ corresponding to the central system space. To be precise, we stress that the operator $\mathbf{U}$ can be written in the basis $\{|\pm\rangle \otimes |J,m\rangle\}$ as

$$\mathbf{U} = \sum_{i,j,J,J',m,m'} U_{ij;J,J',m,m'} |e_i\rangle \otimes |J,m\rangle\langle e_j| \otimes \langle J',m'|. \tag{2.21}$$

Here the quantities $U_{ij;J,J',m,m'}$ are complex numbers and $|e_i\rangle \equiv |\pm\rangle$. The operator components U_{ij} are given by

$$U_{ij} = \sum_{J,J',m,m'} U_{ij;J,J',m,m'} |J,m\rangle\langle J',m'|. \tag{2.22}$$

Therefore, we can write

$$\mathbf{U}|-\rangle = U_{11}|-\rangle + U_{21}|+\rangle, \tag{2.23}$$

$$\mathbf{U}|+\rangle = U_{12}|-\rangle + U_{22}|+\rangle. \tag{2.24}$$

On the other hand, the operator $\mathbf{U}$ satisfies the Schrödinger equation

$$i\frac{d}{dt}\mathbf{U}|\pm\rangle = H\mathbf{U}|\pm\rangle. \tag{2.25}$$

Substituting Eq. (2.23) into Eq. (2.25) yields the following system of coupled differential equations

$$i\dot{U}_{11} = \Big[-\Big(\mu + \frac{\gamma J_z}{\sqrt{N}}\Big) + \frac{g}{2N}\Big(K + 2\Delta J_z^2\Big)\Big]U_{11} + \frac{\alpha J_+}{\sqrt{N}}U_{21}, \tag{2.26}$$

$$i\dot{U}_{21} = \frac{\alpha J_-}{\sqrt{N}}U_{11} + \Big[\Big(\mu + \frac{\gamma J_z}{\sqrt{N}}\Big) + \frac{g}{2N}\Big(K + 2\Delta J_z^2\Big)\Big]U_{21}. \tag{2.27}$$

Similarly, froms Eq. (2.24) and (2.25) we obtain

$$i\dot{U}_{22} = \Big[\Big(\mu + \frac{\gamma J_z}{\sqrt{N}}\Big) + \frac{g}{2N}\Big(K + 2\Delta J_z^2\Big)\Big]U_{22} + \frac{\alpha J_-}{\sqrt{N}}U_{12}, \tag{2.28}$$

$$i\dot{U}_{12} = \frac{\alpha J_+}{\sqrt{N}}U_{22} + \Big[-\Big(\mu + \frac{\gamma J_z}{\sqrt{N}}\Big) + \frac{g}{2N}\Big(K + 2\Delta J_z^2\Big)\Big]U_{12}. \tag{2.29}$$

Since $\mathbf{U}(0) = \mathbf{1}_2 \otimes \mathbf{1}_B$, one gets the initial conditions

$$U_{11}(0) = U_{22}(0) = \mathbf{1}_B, \quad U_{12}(0) = U_{21}(0) = 0. \tag{2.30}$$

The difficulty with solving the above set of differential equations resides in the fact that the coefficients of the operator variables U_{21} and U_{12} are not diagonal and do not commute with those of U_{11} and U_{22}. Nevertheless, as we shall see bellow, this problem can be

overcome by transforming these equations into new ones involving commuting diagonal operators. Indeed, by making use of the change of variables (see [19] for a similar method)

$$U_{11} = e^{-i[-(\mu+\frac{\gamma J_z}{\sqrt{N}})+\frac{g}{2N}(K+2\Delta J_z^2)]t}\widetilde{U}_{11}, \tag{2.31}$$

$$U_{21} = J_- e^{-i[-(\mu+\frac{\gamma J_z}{\sqrt{N}})+\frac{g}{2N}(K+2\Delta J_z^2)]t}\widetilde{U}_{21}, \tag{2.32}$$

$$U_{22} = e^{-i[(\mu+\frac{\gamma J_z}{\sqrt{N}})+\frac{g}{2N}(K+2\Delta J_z^2)]t}\widetilde{U}_{22}, \tag{2.33}$$

$$U_{12} = J_+ e^{-i[(\mu+\frac{\gamma J_z}{\sqrt{N}})+\frac{g}{2N}(K+2\Delta J_z^2)]t}\widetilde{U}_{12}, \tag{2.34}$$

and taking into account the commutation relations

$$[J_z, J_\pm] = \pm J_\pm, \quad [J_z^2, J_\pm] = \pm J_\pm(2J_z \pm 1)$$

and

$$[K, J_\pm] = \mp 2J_\pm(2J_z \pm 1), \tag{2.35}$$

we obtain

$$i\dot{\widetilde{U}}_{11} = \frac{\alpha}{\sqrt{N}} J_+ J_- \widetilde{U}_{21}, \tag{2.36}$$

$$i\dot{\widetilde{U}}_{21} = \frac{\alpha}{\sqrt{N}}\widetilde{U}_{11} + 2\left\{\mu + \left[\frac{\gamma}{\sqrt{N}} + \frac{g}{N}(1-\Delta)\right]\left(J_z - \frac{1}{2}\right)\right\}\widetilde{U}_{21}, \tag{2.37}$$

$$i\dot{\widetilde{U}}_{22} = \frac{\alpha}{\sqrt{N}} J_- J_+ \widetilde{U}_{12}, \tag{2.38}$$

$$i\dot{\widetilde{U}}_{12} = \frac{\alpha}{\sqrt{N}}\widetilde{U}_{22} - 2\left\{\mu + \left[\frac{\gamma}{\sqrt{N}} + \frac{g}{N}(1-\Delta)\right]\left(J_z + \frac{1}{2}\right)\right\}\widetilde{U}_{12}. \tag{2.39}$$

Now, the terms in front of the new operator variables $\widetilde{U}_{ij}$ are diagonal in the common eigenbasis of J^2 and J_z, whence the standard method of solving systems of differential equations can be easily applied. Combining the above relations leads to the following second order homogeneous differential equations for the operators $\widetilde{U}_{21}$ and $\widetilde{U}_{12}$

$$\ddot{\widetilde{U}}_{21} + 2i\left\{\mu + \left[\frac{\gamma}{\sqrt{N}} + \frac{g}{N}(1-\Delta)\right]\left(J_z - \frac{1}{2}\right)\right\}\dot{\widetilde{U}}_{21} + \frac{\alpha^2}{N} J_+ J_- \widetilde{U}_{21} = 0, \tag{2.40}$$

$$\ddot{\widetilde{U}}_{12} - 2i\left\{\mu + \left[\frac{\gamma}{\sqrt{N}} + \frac{g}{N}(1-\Delta)\right]\left(J_z + \frac{1}{2}\right)\right\}\dot{\widetilde{U}}_{12} + \frac{\alpha^2}{N} J_- J_+ \widetilde{U}_{12} = 0, \tag{2.41}$$

which admit the following solutions

$$\widetilde{U}_{21} = 2iC_1 e^{-iF_1 t}\sin\left(t\sqrt{M_1}\right), \tag{2.42}$$

$$\widetilde{U}_{12} = 2iC_2 e^{-iF_2 t}\sin\left(t\sqrt{M_2}\right). \tag{2.43}$$

Here, C_1 and C_2 are some diagonal operators to be determined and we have

$$F_1 = \mu + \Big[\frac{\gamma}{\sqrt{N}} + \frac{g}{N}(1-\Delta)\Big]\Big(J_z - \frac{1}{2}\Big), \tag{2.44}$$

$$M_1 = F_1^2 + \frac{\alpha^2}{N} J_+ J_-, \tag{2.45}$$

$$F_2 = -\mu - \Big[\frac{\gamma}{\sqrt{N}} + \frac{g}{N}(1-\Delta)\Big]\Big(J_z + \frac{1}{2}\Big), \tag{2.46}$$

$$M_2 = F_2^2 + \frac{\alpha^2}{N} J_- J_+. \tag{2.47}$$

Integrating the right-hand side of Eq. (2.42) gives

$$\widetilde{U}_{11} = -2C_1 e^{-iF_1 t}\frac{\sqrt{NM_1}}{\alpha}\Big[\cos\Big(t\sqrt{M_1}\Big) + \frac{iF_1}{\sqrt{M_1}}\sin\Big(t\sqrt{M_1}\Big)\Big] + C_3. \tag{2.48}$$

The constant operators C_1 and C_3 can be determined using the initial conditions (2.30) and the unitarity condition for the time evolution operator, which yield $C_1 = -\alpha/(2\sqrt{NM_1})1_B$ and $C_3 = 0$. Hence, we obtain

$$U_{11}(t) = e^{-iG_1 t}\Big[\cos\Big(t\sqrt{M_1}\Big) + \frac{iF_1}{\sqrt{M_1}}\sin\Big(t\sqrt{M_1}\Big)\Big], \tag{2.49}$$

$$U_{21}(t) = -iJ_- \frac{\alpha}{\sqrt{NM_1}} e^{-iG_1 t}\sin\Big(t\sqrt{M_1}\Big), \tag{2.50}$$

where

$$G_1 = -\frac{\gamma}{2\sqrt{N}} + \frac{g}{2N}\Big[\Big(K + 2\Delta J_z^2\Big) + 2(1-\Delta)\Big(J_z - \frac{1}{2}\Big)\Big]. \tag{2.51}$$

Following the same method, we find that

$$U_{22}(t) = e^{-iG_2 t}\Big[\cos\Big(t\sqrt{M_2}\Big) + \frac{iF_2}{\sqrt{M_2}}\sin\Big(t\sqrt{M_2}\Big)\Big], \tag{2.52}$$

$$U_{12}(t) = -iJ_+ \frac{\alpha}{\sqrt{NM_2}} e^{-iG_2 t}\sin\Big(t\sqrt{M_2}\Big), \tag{2.53}$$

where

$$G_2 = -\frac{\gamma}{2\sqrt{N}} + \frac{g}{2N}\Big[\Big(K + 2\Delta J_z^2\Big) + 2(\Delta - 1)\Big(J_z + \frac{1}{2}\Big)\Big]. \tag{2.54}$$

It is easy to see that the operators G_1 and G_2 are diagonal in the common basis of J^2 and J_z. Note also that all the operator under the square root symbol have positive eigenvalues. This is the reason for which it is permissible to safely use the usual definition of the square root function.

2.3.3 *Reduced density matrix*

Having determined the exact analytical form of the time evolution operator, we are able to calculate the reduced density matrix of the central spin. Indeed, from Eqs. (2.10)

and (2.11), and by making use of the trace properties of the lowering and raising operators $J_{\pm}$, we find that

$$\rho_{11}(t) = \frac{1}{Z_N}\Big[\rho_{11}^0 \mathrm{tr}_B\Big(e^{-\beta H_B} U_{11} U_{11}^{\star}\Big) + \rho_{22}^0 \mathrm{tr}_B\Big(e^{-\beta H_B} U_{21}^{\star} U_{12}\Big)\Big], \tag{2.55}$$

$$\rho_{12}(t) = \frac{1}{Z_N}\rho_{12}^0 \mathrm{tr}_B\Big(e^{-\beta H_B} U_{11} U_{22}^{\star}\Big). \tag{2.56}$$

Furthermore, with the help of the commutation relations (4.3.2), we can easily prove that $J_- F_1 = -F_2 J_-$ and $J_- M_1 = M_2 J_-$. Using the latter equalities, one can check that the time-dependent components of the Bloch vector are given by

$$\begin{aligned}\lambda_3(t) = -\frac{2}{Z_N}\mathrm{tr}_B\Bigg\{ & \frac{\alpha^2 J_+ J_-}{N M_1} \exp\Big[-\frac{g\beta}{2N}[K + 2\Delta J_z^2 + (1-\Delta)(2J_z - 1)]\Big] \sin^2\Big(t\sqrt{M_1}\Big) \\ & \times \sinh\Big[\frac{g\beta}{2N}(1-\Delta)(2J_z - 1)\Big]\Bigg\} + \lambda_3(0)\Bigg(1 - \frac{2}{Z_N}\mathrm{tr}_B\Big\{\Big(\frac{\alpha^2 J_+ J_-}{N M_1}\Big) \\ & \times \exp\Big[-\frac{g\beta}{2N}[K + 2\Delta J_z^2 + (1-\Delta)(2J_z - 1)]\Big] \\ & \times \sin^2\Big(t\sqrt{M_1}\Big)\cosh\Big[\frac{g\beta}{2N}(1-\Delta)(2J_z - 1)\Big]\Big\}\Bigg),\end{aligned} \tag{2.57}$$

$$\lambda_1(t) = \mathrm{tr}_B\Big\{\Big(\lambda_1(0)\cos(\Omega t) + \lambda_2(0)\sin(\Omega t)\Big)A - \Big(\lambda_1(0)\sin(\Omega t) - \lambda_2(0)\cos(\Omega t)\Big)B\Big\}, \tag{2.58}$$

$$\lambda_2(t) = -\mathrm{tr}_B\Big\{\Big(\lambda_1(0)\sin(\Omega t) - \lambda_2(0)\cos(\Omega t)\Big)A + \Big(\lambda_1(0)\cos(\Omega t) + \lambda_2(0)\sin(\Omega t)\Big)B\Big\}, \tag{2.59}$$

where

$$\Omega = \frac{2g}{N}(\Delta - 1)J_z, \tag{2.60}$$

$$A = \frac{1}{Z_N}\Big\{e^{-\frac{g\beta}{2N}[K + 2\Delta J_z^2]}\Big[\cos\Big(t\sqrt{M_1}\Big)\cos\Big(t\sqrt{M_2}\Big) + \frac{F_1 F_2}{\sqrt{M_1 M_2}}\sin\Big(t\sqrt{M_1}\Big)\sin\Big(t\sqrt{M_2}\Big)\Big]\Big\}, \tag{2.61}$$

$$B = \frac{1}{Z_N}\Big\{e^{-\frac{g\beta}{2N}[K + 2\Delta J_z^2]}\Big[\frac{F_1}{\sqrt{M_1}}\sin\Big(t\sqrt{M_1}\Big)\cos\Big(t\sqrt{M_2}\Big) - \frac{F_2}{\sqrt{M_2}}\sin\Big(t\sqrt{M_2}\Big)\cos\Big(t\sqrt{M_1}\Big)\Big]\Big\}. \tag{2.62}$$

From here on, the parameters μ and γ will be given in units of the coupling constant α. The behavior of the component $\lambda_2(t)$ does not significantly differ from the one corresponding to $\lambda_1(t)$. Throughout the remainder of the paper we shall deal with the latter component and restrict ourselves to positive values of the anisotropy constant Δ.

Depending on the nature of interactions within the bath, we can distinguish two different cases. The first one corresponds to positive values of g, i.e., antiferromagnetic

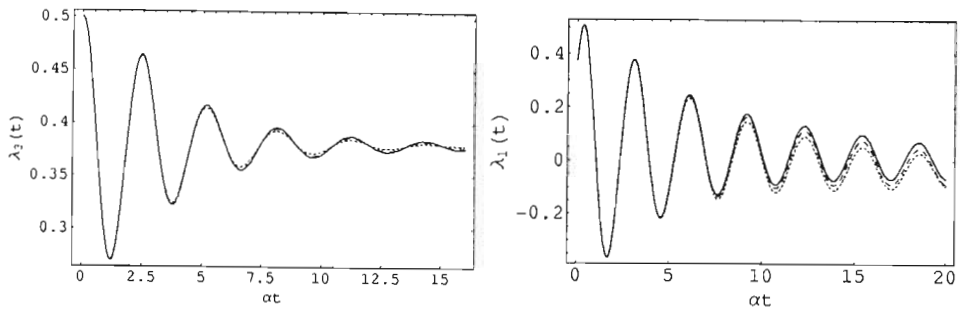

Fig. 2.1: Time evolution of the components $\lambda_3(t)$ and $\lambda_1(t)$ for different values of the number of spins in the environment: $N = 100$ (dotted lines), $N = 200$ (dashed lines), and $N = 400$ (solid lines). The other parameters are $\gamma = 0$, $g = 1$, $\beta = 0.5$, $\Delta = 0$, and $\mu = \alpha$. The initial conditions are $\lambda_3(0) = \frac{1}{2}$, $\lambda_{1,2}(0) = \frac{3}{8}$.

couplings between the constituents of the environment. In this case, as the number of spins increases, the plots saturate and a nontrivial limit exists as shown in Fig. 2.1. This will be investigated in the following section. The other case corresponds to negative values of g, i.e., ferromagnetic couplings within the bath. When $\Delta < 1$ the components of the Bloch vector exhibit in general Gaussian decay accompanied by fast damped oscillations even when the strength of the magnetic field is very weak. In contrast to $\lambda_1(t)$, the component $\lambda_3(t)$ decays faster as the number of spins increases. When the latter is small, $\lambda_3(t)$ may revive to decay again and so forth. The numerical simulation shows that the details of the time evolution of the reduced density matrix are rather complex and depend on the different values of the parameters of the model, including the number of bath spins. For example, if we set $\Delta = 0$, we observe that the oscillations are quickly suppressed with the increase of the strength of the magnetic field, or the value of the coupling constant γ. In this case, the components $\lambda_{2,3}(t)$ do not vanish at long time scales; the corresponding asymptotic values depend, however, on N in contrast to the antiferromagnetic case. For large values of the coupling constant g, the component $\lambda_1(t)$ quickly decays whereas $\lambda_3(t)$ oscillates around zero with large amplitudes (typically of the same order of magnitude as the corresponding initial value). We also notice that the frequencies of the damped oscillations increase with the increase of the number of bath spins as shown in Fig. 2.2. Roughly speaking, when $\Delta > 1$, the behavior of the components of the Bloch vector is quite similar to the antiferromagnetic counterpart. For example, when $\gamma = 0$, the components $\lambda_i(t)$ show saturation behavior with respect to the number of spins N; their asymptotic values are different from zero.

In order to explain the differences between the behavior of the reduced density matrix in the ferromagnetic and the antiferromagnetic environments, we note that in the latter

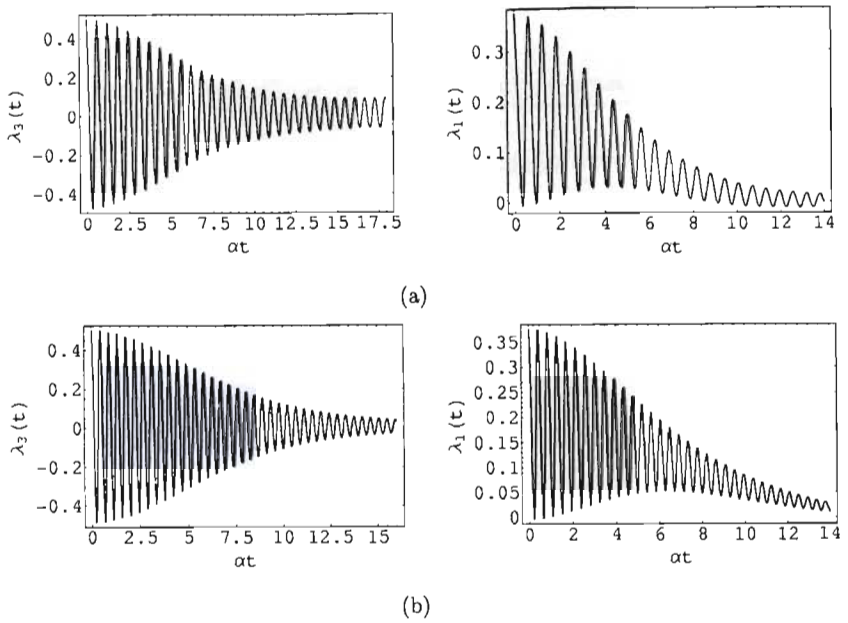

Fig. 2.2: The Gaussian decay of the Bloch vector components $\lambda_3(t)$ and $\lambda_1(t)$ in the case of ferromagnetic interactions: (a) N=100 and (b) N=200. The plot on the left of each subfigure corresponds to $\lambda_3(t)$ whereas the one on the right corresponds to $\lambda_1(t)$. The other parameters are $\gamma = 2\alpha$, $\beta = 1$, $g = -5$, $\Delta = 0.5$, $\mu = 0$, $\lambda_3(0) = \frac{1}{2}$, and $\lambda_{1,2}(0) = \frac{3}{8}$.

case, the form of interactions favors antiparallel spins. This is the reason for which the ground state of the antiferromagnetic bath, $|\Psi_G\rangle$, is equal to $|0,0\rangle$. On the contrary, ferromagnetic interactions force the spins in the bath to align along an arbitrary direction in the space. In this case $|\Psi_G\rangle$ belongs to the subspace $\mathbb{C}^{N+1}$ spanned by the state vectors $|\frac{N}{2},m\rangle$ corresponding to $j = \frac{N}{2}$. For instance, when $\Delta > 1$, the ground state of the bath turns out to be doubly degenerate, namely, $|\Psi_G\rangle = |\frac{N}{2},\pm\frac{N}{2}\rangle$. For $\Delta < 1$, we simply have $|\Psi_G\rangle = |\frac{N}{2},0\rangle$. However, when $\Delta = 1$, the ground energy of the bath is independent of the quantum number m; the degeneracy of $|\Psi_G\rangle$ is equal to $N+1$. Hence we conclude that the Hamiltonian H_B displays quantum phase transition at $\Delta = 1$. This is the reason for which the reduced dynamics depends on whether the anisotropy constant is less or greater than 1. Note that the mean value of J^2 is close to zero in the case of antiferromagnetic interactions within the spin bath in contrast with the ferromagnetic case where $\langle J^2\rangle \sim N^2$. Obviously, the central spin decoheres less if the spin bath, to which it couples, is characterized by a total angular momentum close to zero. At zero temperature, the antiferromagnetic bath occupies its ground state $|0,0\rangle$ which is an eigenvector of H_B, and satisfies $H_{SB}|\pm\rangle\otimes|0,0\rangle = 0$. Hence, the central spin remains decoupled from the bath if the initial state factorizes: the two-level system preserves its coherence regardless of the

number of environmental spins. Let us now consider the case where $\gamma = 0$ and $\Delta > 1$. At low temperatures, the total angular momentum of the ferromagnetic bath has the tendency to be directed along the z direction. Since the central spin couples to the bath through Heisenberg XY interactions ($\gamma = 0$), we end up with a situation quite similar to that where $g > 0$. The above results show that properties of the bath at zero temperature affect the behavior of the reduced dynamics when $T > 0$. At infinite temperature, the ferromagnetic and antiferromagnetic environments become completely unpolarized; the reduced dynamics displays the same behavior in both systems as N increases.

2.4 The limit $N \to \infty$

This section is devoted to the case of an infinite number of spins in the environment, i.e., the case $N \to \infty$. We investigate the effect of the bath temperature, the external magnetic field, and the anisotropy constant on the reduced density matrix of the central spin. To this end it should be noted that the trace of the operators $J_\pm/\sqrt{N}$ together with $J_z/\sqrt{N}$ is identically zero, namely,

$$\mathrm{tr}_B\Big\{\frac{J_\pm}{\sqrt{N}}\Big\} = \mathrm{tr}_B\Big\{\frac{J_z}{\sqrt{N}}\Big\} = 0. \tag{2.63}$$

A more general property of the trace of the lowering and raising operators can be expressed as

$$\lim_{N\to\infty} 2^{-N}\mathrm{tr}_B\Big\{\prod_{i=1}^{k}\Big(\frac{J_\pm J_\mp}{N}\Big)^{n_i}\Big\} = \lim_{N\to\infty} 2^{-N}\mathrm{tr}_B\Big\{\prod_{i=1}^{k}\Big(\frac{J_\pm}{\sqrt{N}}\Big)^{n_i}\Big(\frac{J_\mp}{\sqrt{N}}\Big)^{n_i}\Big\} = \frac{n!}{2^n}, \tag{2.64}$$

where $n = \sum_{i=1}^{k} n_i$ is positive integer; the exponent may be regarded as any unordered product of n_i lowering and n_i raising operators (e.g., $J_+J_+J_-J_+J_-J_-$). The trace vanishes for all the cases in which J_+ and J_- appear with different exponents. This means that $J_\pm/\sqrt{N}$ are well-behaved fluctuation operators with respect to the tracial state. Hence in the limit $N \to \infty$, the operator $J_+/\sqrt{N}$ converges to a complex random variable z with the probability density function [16]

$$z \mapsto \frac{2}{\pi} e^{-2|z|^2}. \tag{2.65}$$

Here, we wish to mention the similarity that exists between relation (2.64) and

$$4\int_0^\infty t\, dt\, t^{2n}\, e^{-2t^2} = \frac{n!}{2^n}, \tag{2.66}$$

which is a special case of $\int_0^\infty t^{2n+1}e^{-at^2}dt = \frac{n!}{2a^{n+1}}$, where $n = 0, 1, 2, ...$, and the real part of a satisfies $\mathrm{Re}(a) > 0$.

The operator $J_z/\sqrt{N}$ also converges to a real random variable m (to be differentiated from the eigenvalue m) when $N \to \infty$, with the probability density function

$$m \mapsto \sqrt{\frac{2}{\pi}}e^{-2m^2}. \tag{2.67}$$

For example, consider the operator $e^{-i\frac{2\gamma t}{\sqrt{N}}J_z}$ and let us calculate

$$\mathrm{tr}_B\Big\{e^{-i\frac{2\gamma t}{\sqrt{N}}J_z}\Big\} = \prod_{k=1}^{N}\mathrm{tr}\; e^{-i\frac{\gamma t}{\sqrt{N}}\sigma_z^k}. \tag{2.68}$$

The trace under the product in the right-hand side of the above equation can be easily evaluated as $2\cos(\frac{\gamma t}{\sqrt{N}})$. Consequently,

$$\mathrm{tr}_B\Big\{e^{-i\frac{2\gamma t}{\sqrt{N}}J_z}\Big\} = 2^N\Big[\cos\Big(\frac{\gamma t}{\sqrt{N}}\Big)\Big]^N. \tag{2.69}$$

Expanding the cosine function in a Taylor series and taking the limit $N \to \infty$ yield

$$\begin{aligned}\lim_{N\to\infty} 2^{-N}\mathrm{tr}_B\Big\{e^{-i\frac{2\gamma t}{\sqrt{N}}J_z}\Big\} &= \lim_{N\to\infty}\Big[1 - \frac{\gamma^2 t^2}{2N} + O\Big(\frac{1}{N^2}\Big)\Big]^N \\ &= e^{-\frac{\gamma^2 t^2}{2}}.\end{aligned} \tag{2.70}$$

On the other hand we have

$$\sqrt{\frac{2}{\pi}}\int_{-\infty}^{\infty} e^{-2m^2 - 2i\gamma t m}dm = e^{-\frac{\gamma^2 t^2}{2}}, \tag{2.71}$$

which is in agreement with Eq. (2.70). In particular, we can infer that

$$\lim_{N\to\infty} 2^{-N}\mathrm{tr}_B\Big(J_z/\sqrt{N}\Big)^{2n} = \frac{\Gamma(n+\frac{1}{2})}{2^n\sqrt{\pi}}, \tag{2.72}$$

where $\Gamma(z)$ is Euler gamma function. We shall use the latter results when we investigate the short-time behavior of the reduced density matrix in the case where γ is different from zero.

One can check that for large values of N,

$$\mathrm{tr}_B\Big\{\Big(\frac{J_z}{\sqrt{N}}\Big)^k\Big(\frac{J_\pm J_\mp}{N}\Big)^\ell\Big\} \approx 2^{-N}\mathrm{tr}_B\Big\{\Big(\frac{J_z}{\sqrt{N}}\Big)^k\Big\} \times \mathrm{tr}_B\Big\{\Big(\frac{J_\pm J_\mp}{N}\Big)^\ell\Big\}. \tag{2.73}$$

For odd powers of J_z, the left-hand side of the above relation vanishes as N increases; the right-hand side is always zero. Equation. (2.73) simply implies that the operators

$J_{\pm}J_{\mp}/N$ and $J_z/\sqrt{N}$ become uncorrelated under the tracial state at large values of N. Note that the above state corresponds to a bath of N independent spin-$\frac{1}{2}$ particles, i.e., the state of maximum entropy. In the limit of large number of spins such a bath has the tendency to behave as a classical stochastic system. The scaled bath operators $J_\alpha/\sqrt{N}$ (where $\alpha \equiv x, y, z$) converge to independent commuting random variables. For instance, we can easily show that the trace over the environmental degrees of freedom of the operator $\exp\Big[\frac{\epsilon t}{\sqrt{N}}\Big(a_1 J_x + a_2 J_y + a_3 J_z\Big)\Big]$, where $a_{1,2,3} \in \mathbb{C}$ and $\epsilon = \sqrt{\pm 1}$, is given by $2^N\Big[\cosh\Big(\frac{\epsilon t}{2\sqrt{N}}\sqrt{a_1^2 + a_2^2 + a_3^2}\Big)\Big]^N$. If we expand the cosh function in Taylor series and take the limit $N \to \infty$, as we did in Eq. (2.70), we end up with the result $\exp[\frac{\epsilon^2 t^2}{8}(a_1^2 + a_2^2 + a_3^2)]$. The latter can be obtained by multiple integration over three independent random variables each of which has the same probability density function as m [see Eq. (2.71)]. It follows that the random variables z and m can be treated as independent in the limit $N \to \infty$.

From the above discussion, we can conclude that

$$\lim_{N\to\infty} 2^{-N}\mathrm{tr}_B\Big\{f\Big(\frac{J_{\pm}J_{\mp}}{N}, \frac{J_z}{\sqrt{N}}\Big)\Big\} = \Big(\frac{2}{\pi}\Big)^{3/2}\int_{-\infty}^{\infty} dm \int_{\mathbb{C}} dz dz^* f(|z|^2, m)\; e^{-2(m^2+|z|^2)}, \quad (2.74)$$

at least for bounded functions $f : \mathbb{C} \times \mathbb{R} \to \mathbb{R}$. The latter relation has been numerically checked for large number of functions; the agreement between its two sides is perfect. In fact, the class of functions for which the integral in the right-hand side of Eq. (2.74) exists contains all the functions having the form $e^{-(a|z|^2+bm^2)}h(|z|^2, m)$ where h is bounded and a and b are complex numbers satisfying $\mathrm{Re}(a) > -2, \mathrm{Re}(b) > -2$. If the latter conditions are not satisfied then the integral does not converge. This is the reason for which we shall restrict ourselves to the antiferromagnetic case where g and Δ are positive.

Under the above assumptions, it is possible to evaluate the quantity

$$\bar{Z} = \lim_{N\to\infty} 2^{-N} Z_N = \Big(\frac{2}{\pi}\Big)^{3/2}\int_{-\infty}^{\infty} dm \int_{\mathbb{C}} dz dz^* e^{-(2+g\beta\Delta)m^2-(2+g\beta)|z|^2} \quad (2.75)$$

by making use of the polar coordinates (r, ϕ) where $z = re^{i\phi}$. A straightforward calculation yields

$$\bar{Z} = \frac{2\sqrt{2}}{(2+g\beta)\sqrt{2+g\beta\Delta}} \to \frac{2}{(2+g\beta)} \quad (2.76)$$

when $\Delta \to 0$. Obviously, if $g\beta = 0$ then $\bar{Z} = 1$. The agreement between the right-hand side and the left-hand side of Eq. (2.74) is illustrated in Table 2.1 where we display $2^{-N}Z_N$ at different values of N and compare it with $\bar{Z}$ for $g = 2$, $\Delta = 5$, and $\beta = 1$; the agreement is clearly very good for $N = 5000$.

Tab. 2.1: $2^{-N}Z_N$ at different values of N for $g = 2$, $\Delta = 5$ and $\beta = 1$; $\bar{Z}$=0.204124.

N	10	100	1000	5000
$2^{-N}Z_N$	0.203026	0.203997	0.204111	0.204122

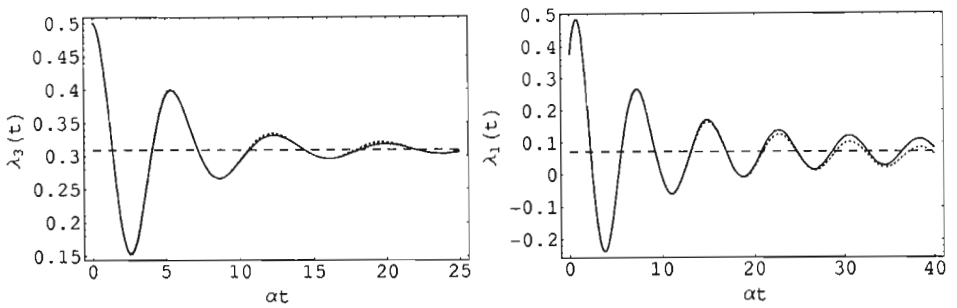

Fig. 2.3: Evolution in time of $\lambda_3(t)$ and $\lambda_1(t)$ for $N = 400$ (dotted lines), and $N \to \infty$ (solid lines); the dashed lines correspond to the asymptotic values. Other parameters are $\gamma = 0$, $g = 1$, $\beta = 5$, $\Delta = 0.5$, $\mu = 0.4\alpha$, $\lambda_3(0) = \frac{1}{2}$ and $\lambda_{1,2}(0) = \frac{3}{8}$.

Let us now focus on the general structure of Eqs. (2.57)-(2.59). Clearly, we need to evaluate terms having the general form

$$\frac{1}{Z_N}\mathrm{tr}_B\Big\{f\Big(\frac{J_\pm J_\mp}{N},\frac{J_z}{\sqrt{N}}\Big)\Big\}=\frac{2^{-N}\mathrm{tr}_B\Big\{f\Big(\frac{J_\pm J_\mp}{N},\frac{J_z}{\sqrt{N}}\Big)\Big\}}{2^{-N}Z_N}. \tag{2.77}$$

As $N \to \infty$, the previous quantity tends to

$$\langle f\rangle = \bar{Z}^{-1}4\Big(\frac{2}{\pi}\Big)^{1/2}\int_{-\infty}^{\infty} dm \int_0^{\infty} r dr f(r^2,m)\, e^{-2(m^2+r^2)}. \tag{2.78}$$

This is permissible since the functions of interest appearing in Eqs (2.57)-(2.59) fulfil all the conditions mentioned above. Note that the factor 4 in Eq. (2.78) appears after performing the integration with respect to the polar coordinate ϕ (this actually follows from the symmetry with respect to the z direction). It is also quite interesting to notice that the behavior of the central spin when $-2 < g\beta < 0$ and $-2 < g\beta\Delta < 0$ is similar to that where $g > 0$ and $\Delta > 0$ as indicated by the conditions on the convergence of the integral in Eq. (2.74).

2.4.1 *The case $\gamma = 0$*

Let us assume that the coupling constant γ is equal to zero. First of all, it should be noted that, although the operator $J_z/\sqrt{N}$ converges to a random variable, we can neglect the

contribution of J_z/N when N becomes very large. This means that in the limit $N \to \infty$, the quantities $M_{1,2}$ do not depend on the random variable m; the sinh (sin) and the cosh (cos) functions appearing in Eq. (2.57) [Eqs. (2.58)-(2.59)] should be replaced by zero and one, respectively. We only need to integrate with respect to the random variable z since the integrals with respect to m occurring in the numerator and denominator of Eq. (2.78) cancel each other. One then concludes that the anisotropy constant Δ has no effect on the dynamics of the central spin when $N \to \infty$. This is due to the fact that H_{SB} simplifies to Heisenberg XY Hamiltonian. Only transverse interactions contribute to the reduced dynamics when N is sufficiently large because $J_z/\sqrt{N}$ and K/N (or equivalently $J_\pm J_\mp/N$) become practically uncorrelated under the tracial state [see Eq.(2.73)].

Hence, in the limit of an infinite number of spins within the bath we obtain

$$\lambda_3(t) = \lambda_3(0)\Big(1 - \eta(t)\Big), \tag{2.79}$$

where

$$\eta(t) = \Big\langle 2r^2 \frac{\sin^2\Big(t\sqrt{\mu^2+r^2}\Big)}{\mu^2+r^2} \mathrm{e}^{-g\beta[r^2+\Delta m^2]} \Big\rangle. \tag{2.80}$$

Note that the time variable is now given in units of α. We show in the Appendix that the above function can be written as

$$\begin{aligned}\eta(t) = 1 - \cos\Big(2\mu t\Big) + \frac{it}{2}\sqrt{\frac{\pi}{2+g\beta}}\Big\{\mathrm{erf}\Big[\frac{\mu(g\beta+2)-it}{\sqrt{g\beta+2}}\Big] - \mathrm{erf}\Big[\frac{\mu(g\beta+2)+it}{\sqrt{g\beta+2}}\Big]\Big\} \\ \times\ e^{[(2+g\beta)\mu^2 - \frac{t^2}{2+g\beta}]} - (g\beta+2)\mu^2\, e^{(g\beta+2)\mu^2}\Gamma\Big[0,(g\beta+2)\mu^2\Big] + \mu^2(g\beta+2) \\ \times\ e^{(g\beta+2)\mu^2}\mathrm{Re}\Big\{\Gamma\Big[0,(g\beta+2)\mu^2+2\mu it\Big]\Big\} + \mu^2\mathcal{M}(t;\mu,\beta),\end{aligned} \tag{2.81}$$

where

$$\mathrm{erf}(z) = \frac{2}{\sqrt{\pi}}\int_0^z e^{-t^2}dt, \tag{2.82}$$

$$\Gamma(a,z) = \int_z^\infty t^{a-1}e^{-t}dt. \tag{2.83}$$

are, respectively, the error and the incomplete gamma functions [29]. The function $\mathcal{M}$ is given by Eq. (A.10) of the Appendix.

The remaining components of the Bloch vector are given by

$$\lambda_1(t) = \lambda_1(0)\Big[\zeta(t) + \frac{1}{2}\eta(t)\Big] + \lambda_2(0)\xi(t), \tag{2.84}$$

$$\lambda_2(t) = \lambda_2(0)\Big[\zeta(t) + \frac{1}{2}\eta(t)\Big] - \lambda_1(0)\xi(t), \tag{2.85}$$

where

$$\zeta(t) = \Big\langle\ e^{-g\beta(r^2+\Delta m^2)}\cos\Big(2t\sqrt{\mu^2+r^2}\Big)\Big\rangle$$
$$= \cos\Big(2\mu t\Big) + \frac{it}{2}\ e^{[(2+g\beta)\mu^2 - \frac{t^2}{2+g\beta}]}\sqrt{\frac{\pi}{2+g\beta}}\Big\{\mathrm{erf}\Big[\frac{\mu(g\beta+2)+it}{\sqrt{g\beta+2}}\Big] - \mathrm{erf}\Big[\frac{\mu(g\beta+2)-it}{\sqrt{g\beta+2}}\Big]\Big\}, \tag{2.86}$$

and

$$\xi(t) = \Big\langle \mu\ e^{-g\beta(r^2+\Delta m^2)}\frac{\sin\Big(2t\sqrt{\mu^2+r^2}\Big)}{\sqrt{\mu^2+r^2}}\Big\rangle$$
$$= \frac{i\mu}{2}\sqrt{\pi(2+g\beta)}\ e^{[(2+g\beta)\mu^2 - \frac{t^2}{2+g\beta}]}\Big\{\mathrm{erf}\Big[\frac{\mu(g\beta+2)-it}{\sqrt{g\beta+2}}\Big] - \mathrm{erf}\Big[\frac{\mu(g\beta+2)+it}{\sqrt{g\beta+2}}\Big]\Big\}. \tag{2.87}$$

The asymptotic behavior of the reduced density matrix can be easily determined as follows. Let us begin with the simplest functions namely, $\zeta(t)$ and $\xi(t)$. Their limits when $t \to \infty$ are equal to zero which immediately follows from the Riemann-Lebesgue lemma

$$\lim_{t\to\infty}\zeta(t) = \lim_{t\to\infty}\xi(t) = 0. \tag{2.88}$$

The same lemma can be applied to the function $\eta(t)$ after some simplifications of the integrals of interest as shown in the Appendix. Only one term survives the above approach when t goes to infinity, namely,

$$\lim_{t\to\infty}\eta(t) = 1 - \eta^{\infty}, \tag{2.89}$$

where

$$\eta^{\infty} = \mu^2(g\beta+2)\ e^{\mu^2(g\beta+2)}\Gamma\Big[0, \mu^2(g\beta+2)\Big]. \tag{2.90}$$

Hence, the asymptotic behavior of the reduced density matrix can be expressed as

$$\lim_{t\to\infty}\vec{\lambda}(t) = \vec{\lambda}_0 - \eta^{\infty}\mathcal{W}\vec{\lambda}(0) \tag{2.91}$$

with

$$\vec{\lambda}_0 = \frac{1}{2}\begin{pmatrix}\lambda_1(0)\\ \lambda_2(0)\\ 0\end{pmatrix}, \quad \mathcal{W} = \begin{pmatrix}\frac{1}{2} & 0 & 0\\ 0 & \frac{1}{2} & 0\\ 0 & 0 & -1\end{pmatrix}. \tag{2.92}$$

The evolution in time of the components $\lambda_3(t)$ and $\lambda_1(t)$ is shown in Fig. 2.3 for $N = 400$ spins in the environment, along with the corresponding infinite case and the asymptotic limits obtained in Eq. (2.91). We can see that the off-diagonal elements of the reduced density matrix show partial decoherence. At low temperature, the relevant bath states are

those with low energies (i.e., j close to zero). In this case, the central spin is weakly coupled to the bath and hence preserves most of its coherence. At high temperature, the two-level system becomes more correlated with the bath which, however, behaves as a system of independent uncoupled particles. Thus quantum fluctuations within the antiferromagnetic spin-environment reduce the effect of the decoherence of the central spin. In the following, we discuss how the bath temperature and the strength of the applied magnetic field affect the decay of the elements of the reduced density matrix.

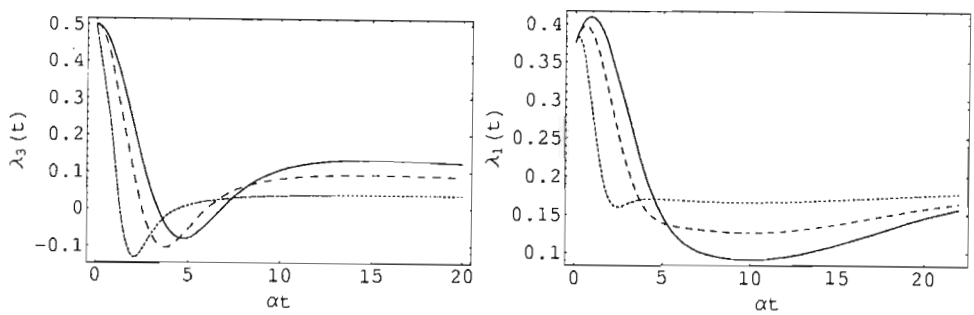

Fig. 2.4: The decay of the components$\lambda_3(t)$ and $\lambda_1(t)$ for $g = 0$ (dotted lines), $g = 5$ (dashed lines), and $g = 10$ (solid lines). Other parameters are $\beta = 1$, $\gamma = \Delta = 0$, $\mu = 0.1\alpha$, $\lambda_3(0) = \frac{1}{2}$ and $\lambda_{1,2}(0) = \frac{3}{8}$.

Clearly, if $\mu = 0$, the vector component $\lambda_3(t)$ vanishes when $t \to \infty$ regardless of the bath temperature. This means that $\rho_{11}(\infty) = \rho_{22}(\infty) = \frac{1}{2}$, which is obviously independent of the initial state of the central system. On the contrary, the off-diagonal elements tend asymptotically to half of their initial values. This follows from the fact that the temperature-dependent quantity η^{∞} is proportional to the magnetic field strength. The latter results are mainly due to the rotational symmetry of the model Hamiltonian together with the randomness of the interactions within the bath. Figure 2.4 illustrates the difference in the decoherence process between the case of a static bath ($g = 0$) and a dynamic bath ($g \neq 0$). We can see that the asymptotic value of $\lambda_1(t)$ decreases with the increase of g in contrast to $\lambda_3(t)$ which assumes larger asymptotic values when g increases. However, at short times the above components decay slower with the increase of g, implying that strong quantum correlations within the environment suppress the effect of the decoherence process [30]. As we shall see below, the decay of the reduced density matrix exhibits a reverse behavior with respect to the temperature of the bath . This can be explained by the dependence of the decoherence time constant of our model, which turns out to be equal to $\tau = \sqrt{\frac{2+g\beta}{\alpha^2}}$ as revealed by Eqs. (2.81), (2.86), and (2.87), on the product $g\beta$. Clearly, $\tau \to \infty$ as $g \to \infty$ or/and $T \to 0$, which confirms the above

statements.

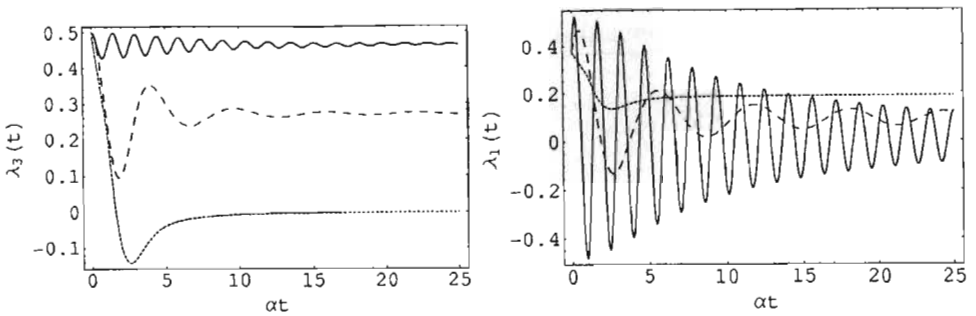

Fig. 2.5: Dependence of $\lambda_3(t)$ and $\lambda_1(t)$ on the strength of the magnetic field in the case $N \to \infty$: $\mu = 0$ (dotted lines), $\mu = 0.5\alpha$ (dashed lines), and $\mu = 2\alpha$ (solid lines). The parameters are $\gamma = 0$, $g\beta = 2$, $\lambda_3(0) = \frac{1}{2}$ and $\lambda_{1,2}(0) = \frac{3}{8}$.

Figure 2.5 illustrates the dependence of the components of the Bloch vector on the strength of the magnetic field. We can see that $\lambda_1(t)$ decays with the increase of μ whereas $\lambda_3(t)$ approaches its initial value. Indeed, by making use of the following asymptotic expression of the incomplete gamma function [29]

$$\Gamma(a,z) \sim z^{a-1}\, e^{-z}\Big[1 + \frac{a-1}{z} + \frac{(a-1)(a-2)}{z^2} + ...\Big], \tag{2.93}$$

when $z \to \infty$ in $|\arg z| < 3\pi/2$, we obtain

$$\lim_{\mu,\beta\to\infty} \eta^{\infty} = 1. \tag{2.94}$$

Therefore, if the ratio μ/α is infinitely big then the off-diagonal elements of the reduced density matrix tend asymptotically to zero; the diagonal ones assume their initial values. The above results can be explained by the fact that the effect of the bath on the dynamics of the central spin can be neglected when μ is very large compared to α. The evolution in time is thus governed by the free Hamiltonian H_S which does not affect the diagonal elements of the reduced density matrix. The off-diagonal elements, however, show periodic oscillations; the vanishing asymptotic values obtained from Eqs. (2.89) and (2.94) will never be reached since the decoherence time constant is infinite ($\alpha \to 0$).

From Fig. 2.6 it can be seen that the bath temperature has a reverse effect on the decay of the reduced density matrix elements. The components $\lambda_3(t)$ and $\lambda_1(t)$ decay faster with the increase of T. Furthermore, we can see that the diagonal elements assume larger asymptotic values in contrast with the off-diagonal ones. In the limit of zero temperature, the asymptotic behavior is identical to the one corresponding to $\mu \to \infty$, see Eq. (2.91). Indeed, at zero temperature the bath and the central spin evolve independently from each

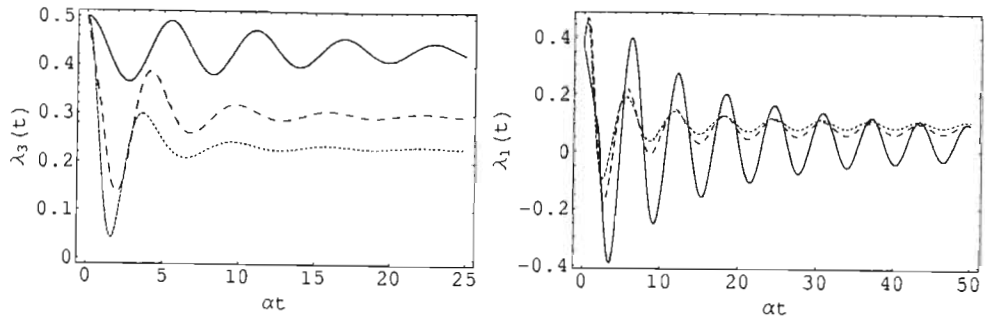

Fig. 2.6: Dependence of $\lambda_3(t)$ and $\lambda_1(t)$ on the bath temperature in the case $N \to \infty$: $\beta = 0$ (dotted lines), $\beta = 1$ (dashed lines), and $\beta = 10$ (solid lines). The parameters are $\gamma = 0$, $g = 2$, $\mu = 0.5\alpha$, $\lambda_3(0) = \frac{1}{2}$ and $\lambda_{1,2}(0) = \frac{3}{8}$.

other as we already mentioned in the previous section. Once again, we find that the dynamics of the central spin is governed by the free Hamiltonian H_S which preserves the coherence of the central system.

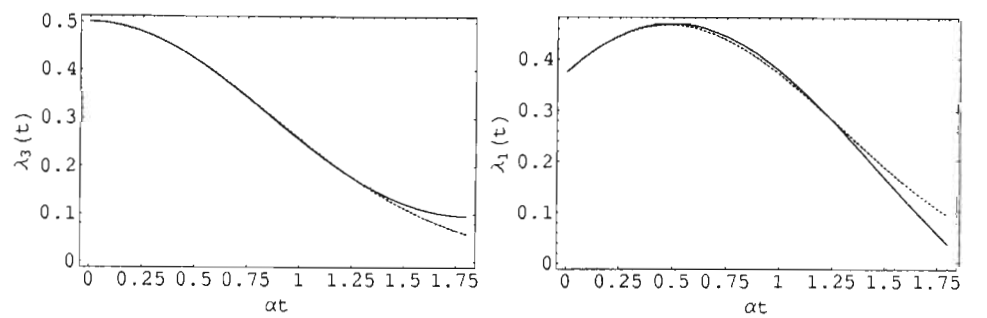

Fig. 2.7: The short-time behavior of $\lambda_3(t)$ and $\lambda_1(t)$ in the case $N \to \infty$. The solid lines correspond to the exact solutions, the dotted lines denote the approximations (2.95-2.96). Here, $\gamma = 0$, $g\beta = 1$, $\mu = 0.5\alpha$, $\lambda_3(0) = \frac{1}{2}$ and $\lambda_{1,2}(0) = \frac{3}{8}$.

Let us now discuss the short-time behavior of the reduced dynamics. The aim here is to find simple analytical expressions which describe the variation of the reduced density matrix at short time scales. It is clear from the expressions of the functions $\eta(t)$, $\zeta(t)$, and $\xi(t)$ that the term of interest which describes the decay of the Bloch vector components is given by $e^{-\frac{t^2}{(g\beta+2)}}$. We shall look for functions of the form $e^{-\frac{t^2}{(g\beta+2)}}g(t)$ where $g(t)$ is some complex-valued function of the time. In the case of the off-diagonal elements, the ansatz $g(t) = e^{2i\mu t}$ can be justified by the competition of two processes, namely, oscillations due to the external magnetic field and damping due to the coupling with the environment. In the limiting case where the magnetic field is absent, it is found that for small values of the time, the decay is purely Gaussian. On the other hand if we assume that there is no coupling between the bath and the central spin, i.e., $\alpha = 0$, then the dynamics is governed

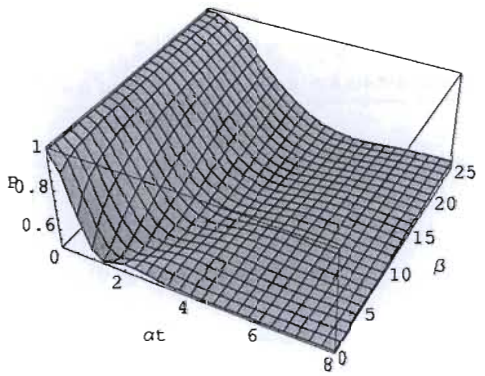

Fig. 2.8: Purity evolution for different values of the bath temperature in the case $N \to \infty$ with $\gamma = 0$, $g = 1$ and $\mu = 0$. The initial conditions are $\lambda_3(0) = \sqrt{\frac{7}{8}}$, $\lambda_{1,2}(0) = \frac{1}{4}$.

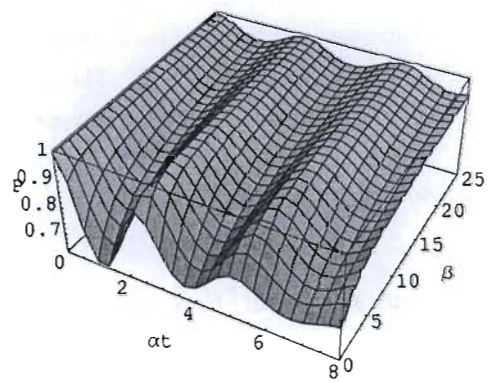

Fig. 2.9: Evolution in time of the purity for different values of the bath temperature in the case $N \to \infty$ with $\gamma = 0$, $g = 1$, and $\mu = \alpha$.

by the external magnetic field. The component $\lambda_3(t)$ is not affected by the magnetic field even when there is no coupling between the spin and the bath. It is shown in [15] that this component decays two times faster than the other ones. Consequently, the short-time behavior of the reduced density matrix can be described by

$$\frac{\lambda_3(t)}{\lambda_3(0)} \approx \exp\Big(-\frac{2t^2}{2+g\beta}\Big), \tag{2.95}$$

$$\frac{\lambda_1(t) - i\lambda_2(t)}{\lambda_1(0) - i\lambda_2(0)} \approx \exp\Big(-\frac{t^2}{2+g\beta} + 2i\mu t\Big). \tag{2.96}$$

In Fig. 2.7, the short-time behavior of the Bloch vector components $\lambda_3(t)$ and $\lambda_1(t)$ is shown together with the approximations (2.95) and (2.96); these are in good agreement with the exact solutions.

There exist many measures that allow for the quantification of the degree of the decoherence due to the interaction with an environment. In this work we use the measure

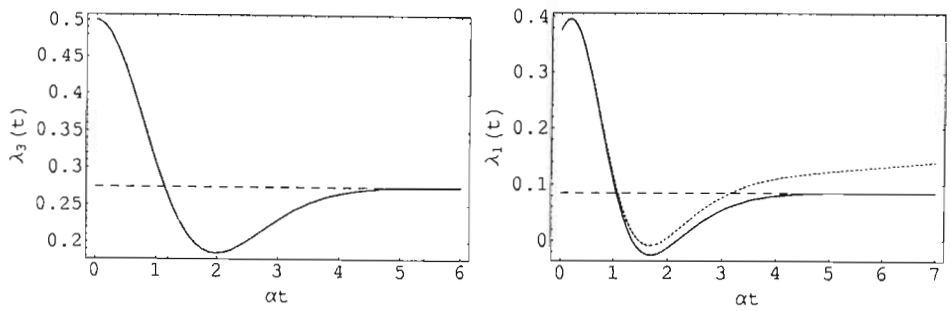

Fig. 2.10: Evolution of $\lambda_3(t)$ and $\lambda_1(t)$ for $N = 600$ (dotted lines) and $N \to \infty$ (solid lines). The dashed lines correspond to the asymptotic values. Here, $\gamma = 2\alpha$, $g = 1$, $\beta = 1.5$, $\Delta = 1$, $\mu = 0.3\alpha$, $\lambda_3(0) = \frac{1}{2}$, and $\lambda_{1,2}(0) = \frac{3}{8}$. The plots corresponding to $\lambda_3(t)$ are almost identical, the latter component saturates with respect to N faster than $\lambda_1(t)$.

$D(t) = 1 - P(t)$, where

$$P(t) = \mathrm{tr}\{\rho(t)^2\} \tag{2.97}$$

is the purity of the central system. Note that in the previous expression the trace is performed over the degrees of freedom of the central spin. The purity takes its maximum value 1 at pure states; its minimum value, 1/2, corresponds to the fully mixed state $\rho = \mathbf{1}_2/2$. In our case, the purity can be expressed in terms of the Bloch vector components as

$$P(t) = \frac{1}{2}\Big[1 + \lambda_1(t)^2 + \lambda_2(t)^2 + \lambda_3(t)^2\Big]. \tag{2.98}$$

The above expression shows that the decay of the purity in the short-time regime described by Eqs. (2.95)-(2.96) is Gaussian which reflects the non-Markovian character of the dynamics. The decay process is slowed down by decreasing the temperature of the bath and/or applying a magnetic field of sufficient strength as illustrated in Figs. 2.8 and 2.9. When $t \to \infty$, the central spin shows partial decoherence; if $\mu = 0$, then the asymptotic value of the purity is independent of the bath temperature as expected (see Fig. 2.8).

2.4.2 *The case $\gamma \neq 0$*

The time dependence of the Bloch vector components when the constant γ is different from zero can be obtained with the same method used in the previous subsection. Since $\gamma \neq 0$, the quantities $M_{1,2}$ are m-dependent which means that the effect of the anisotropy constant has to be taken into account. When $\gamma \neq 0$, we need to perform double integration with respect to the real variables r and m as shown in Eq. (2.74). By making use of the Riemann-Lebesgue lemma, it is possible to find the following asymptotic expression for

the function $\eta(t)$ obtained by replacing μ by $\mu + \gamma m$ in Eq. (2.80)(see Fig. 2.10)

$$\lim_{t\to\infty}\eta(t) = 1 - \frac{1}{\sqrt{\pi}}(2+g\beta)\sqrt{2+g\beta\Delta}\int_{-\infty}^{\infty}(\mu+\gamma m)^2\, e^{(\mu+\gamma m)^2(g\beta+2)-(2+g\beta\Delta)m^2} \times\Gamma\Big[0,(\mu+\gamma m)^2(2+g\beta)\Big]dm. \quad (2.99)$$

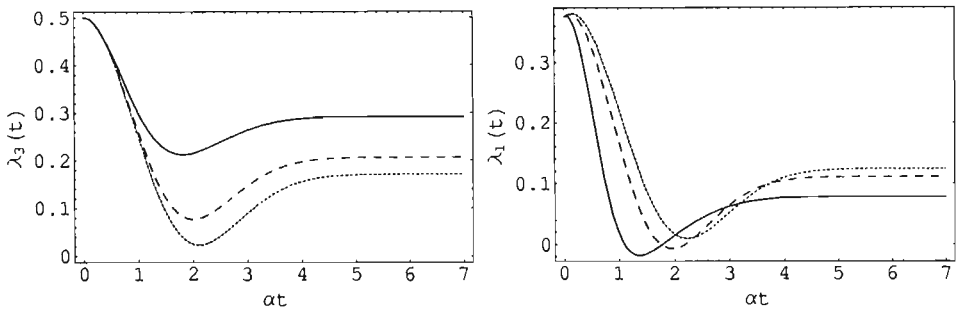

Fig. 2.11: Dependence of $\lambda_3(t)$ and $\lambda_1(t)$ on the anisotropy constant in the case $N \to \infty$: $\Delta = 0$ (solid lines), $\Delta = 5$ (dashed lines), and $\Delta = 10$ (dotted lines). Here, $\gamma = 2\alpha$, $g\beta = 1$, $\mu = 0.1\alpha$, $\lambda_3(0) = \frac{1}{2}$ and $\lambda_{1,2}(0) = \frac{3}{8}$.

Obviously, the functions $\zeta(t)$ and $\xi(t)$ tend to zero when $t \to \infty$. Hence, even if we set $\mu = 0$, the asymptotic state is still temperature dependent. Nevertheless, the dependence of the Bloch vector components on the bath temperature is quite similar to the one corresponding to $\gamma = 0$. The influence of the magnetic field on the dynamics of the central spin is appreciable only when its strength is sufficiently large; this can be seen from the absence of oscillations in the components $\lambda_1(t)$ and $\lambda_3(t)$ displayed in Figure 2.10. Figure. 2.11 shows that the off-diagonal elements decay slower and assume larger asymptotic values when the anisotropy constant Δ increases. The opposite situation holds for the component $\lambda_3(t)$, that is, when Δ decreases the latter component assumes larger asymptotic limits.

At short times the diagonal elements of the reduced density matrix do not depend on Δ in contrast with the off-diagonal ones. In the case of the Heisenberg XY model, i.e., when $\Delta = 0$, the short-time behavior of the Bloch vector components can be determined with the same procedure used in the case where $\gamma = 0$. The main difference here is that the contribution of the interaction $V = \frac{\gamma}{\sqrt{N}}S_z^0 J_z$ has to be taken into account. Using the result we obtained in Eq. (2.70), we can describe the short-time behavior of the reduced

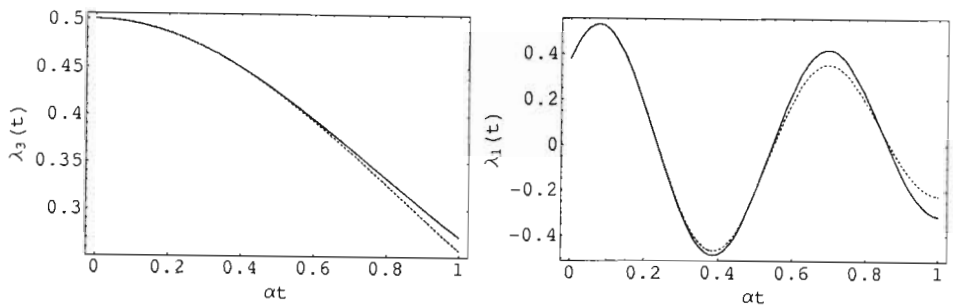

Fig. 2.12: The short-time behavior of $\lambda_3(t)$ and $\lambda_1(t)$ in the case $N \to \infty$. The solid lines correspond to the exact solutions, the the dotted lines denote the approximations (2.100-2.101). The parameters are $\gamma = 1\alpha$, $\Delta = 0$, $g\beta = 1$ and $\mu = 5\alpha$. The initial conditions are the same as in Fig.2.11.

density matrix by (see Fig. 2.12)

$$\frac{\lambda_3(t)}{\lambda_3(0)} \approx \exp\Big(-\frac{2t^2}{2+g\beta}\Big), \tag{2.100}$$

$$\frac{\lambda_1(t) - i\lambda_2(t)}{\lambda_1(0) - i\lambda_2(0)} \approx \exp\Big(-\frac{t^2}{2+g\beta} - \frac{\gamma^2 t^2}{2} + 2i\mu t\Big). \tag{2.101}$$

For $\Delta \neq 0$, the situation is much more complicated; here we only discuss the special case where $\mu = \alpha = 0$ and $\Delta >> 1$. The last condition implies that the transverse term of H_B can be neglected compared to the longitudinal one. Under the above assumption, H_B simplifies to $g\Delta/NS_z^2$ and thus all interactions are of Ising type. Therefore, the operators H_{SB} and H_B commute with each other which means that the diagonal elements are not affected by the coupling to the environment. The coherence of the central spin can be calculated as usual. Taking the limit of an infinite number of spins and using the probability density function corresponding to the random variable m, we find that the off-diagonal elements decay according to the Gaussian law $\exp\Big(-\frac{\gamma^2 t^2}{2+g\beta\Delta}\Big)$. Hence the larger the anisotropy constant, the slower the decay of the off-diagonal elements, which explains the behavior at short times of $\lambda_1(t)$ displayed in Fig. 2.11. More details about the case of Ising couplings can be found in [31]. To end our discussion about the short-time behavior, it should be noted that the deviation of the short-time expressions (2.96) and (2.101) from the exact solutions depends on the value of the strength of the magnetic field. For small values of μ, the above relations are valid at relatively large intervals of time. However, as μ increases, the domains of time for which the above approximations are valid become shorter.

The variation in time of the purity in this case differs from the one corresponding to $\gamma = 0$ by the suppression of the damped oscillations caused by the external magnetic field

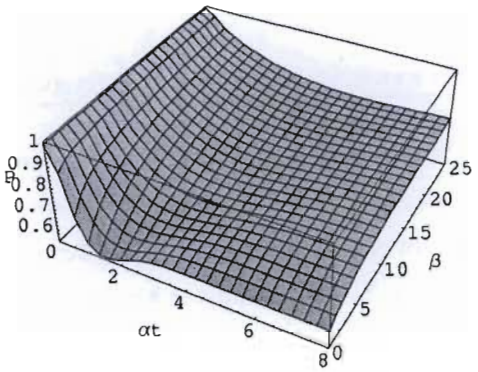

Fig. 2.13: Purity evolution for different values of the bath temperature in the case $N \to \infty$ with $\gamma = 2\alpha$, $\Delta = 1$, $g = 1$, and $\mu = \alpha$. The initial conditions are $\lambda_3(0) = \sqrt{\frac{7}{8}}$, $\lambda_{1,2}(0) = \frac{1}{4}$.

as shown in Fig 2.13. This is mainly due to the interaction described by the Hamiltonian V. Consequently, the central spin decoheres less when γ is equal to zero. The above result was expected because the longitudinal coupling vanishes: the central spin is less correlated to the environment and thus the destructive effect of the environment on the coherence of the two-level system is less appreciable. Indeed, the decoherence time constant is found to be inversely proportional to γ, namely, $\tau = \frac{1}{\alpha}\sqrt{\frac{4+2g\beta}{2+\gamma^2(2+g\beta)}}$. This simply implies that $\tau \to 0$ as $\gamma \to \infty$.

2.5 *Conclusion*

In conclusion we have investigated the dynamics of a spin-$\frac{1}{2}$ particle, subjected to the effect of a locally applied external magnetic field, and coupled to anisotropic Heisenberg spin environment in thermal equilibrium. The reduced density matrix was analytically derived for finite number of spins in the environment and arbitrary values of the interaction strengths. The evolution in time of the central spin depends on the nature of interactions within the bath. In the case of ferromagnetic environment, the decay of the Bloch vector components is Gaussian accompanied by fast damped oscillations. In the antiferromagnetic case, the components of the bloch vector saturate with respect to the number of environmental spins and display partial decoherence. We showed that the partial trace over the degrees of freedom of the bath can be calculated using the convergence of the rescaled bath operators to normal independent Gaussian random variables. This allowed us to study the case of an infinite number of environmental spins, and to analytically derive the asymptotic behavior of the components of the Bloch vector. The above limit represents a good approximation for the cases with finite number of spins ($N \sim 100$). At

short time scales, the decay of the off-diagonal elements is found to be Gaussian with a decoherence time constant given by $\tau = \sqrt{\frac{2+g\beta}{\alpha^2}}$ ($\gamma = 0$). This result is mainly due to the non-Markovian nature of the dynamics, which in turn follows from the time independence of the bath correlation functions and the symmetry of the bath Hamiltonian. Also, it has be shown that the effect of low bath temperatures on the decoherence of the central spin is similar to that of strongly applied magnetic fields and large bath anisotropy. The results obtained in this work are valid for any number of spins in the environment and arbitrary values of the strength of the external magnetic field and the bath temperature. They are in good agreement with those of [22] where the authors studied decoherence of electron spins in quantum dots. The model can be generalized to the case of two or more interacting qubits where questions related to the decoherence and the entanglement can be investigated.

BIBLIOGRAPHY

[1] W. H. Zurek, Phys. Today **44**(10), 36 (1991)

[2] D. P. DiVincenzo and D. Loss, J. Magn. Magn. Matter. **200**, 202 (1999).

[3] W. H. Zurek, Rev. Mod. Phys. **75**, 715 (2003).

[4] H. P. Breuer and F. Petruccione, *The Theory of Open Quantum Systems* (Oxford University Press, Oxford, 2002).

[5] P. W. Shor, Phys. Rev. A **52**, R2493 (1995).

[6] J. H. Reina, L. Quiroga, and N. F. Johnson, Phys. Rev. A **65**, 032326 (2002).

[7] D. Gottesman, Phys. Rev. A **54**, 1862 (1996).

[8] A. M. Steane, Phys. Rev. Lett. **77**, 793 (1996).

[9] D. Loss and D. P. DiVincenzo Phys. Rev. A **57**, 120 (1998).

[10] G. Burkard, D. Loss, and D. P. DiVincenzo, Phys. Rev. B **59**, 2070 (1999).

[11] M. A. Nielsen and I. L. Chuang, *Quantum Computation and Quantum Information* (Cambridge University Press, Cambridge, 2000).

[12] W. Zhang, N. Konstantinidis, K. Al-Hassanieh, and V. V. Dobrovitski, J. Phys.: Condens. Matter **19** 083202 (2007).

[13] C. W. Gardiner, *Quantum Noise* (Springer, Berlin, 1991).

[14] D. F. Walls and G. J. Milburn,*Quantum Optics* (Springer-Verlag, Berlin, 1995).

[15] H. P. Breuer, D. Burgarth, and F. Petruccione, Phys. Rev. B **70**, 045323 (2004).

[16] Y. Hamdouni, M. Fannes, and F. Petruccione, Phys. Rev. B **73**, 245323 (2006).

[17] Z. Huang, G. Sadiek, and S. Kais, J. Chem. Phys. **124**, 144513 (2006).

[18] D. D. Bhaktavatsala Rao, V. Ravishankar, and V. Subrahmanyam, Phys. Rev. A **74**, 022301 (2006).

[19] X. Z. Yuan, H. S. Goan, and K. D. Zhu, Phys. Rev. B **75**, 045331 (2007).

[20] E. Ferraro, H.P. Breuer, A. Napoli, M. A. Jivulescu, and A. Messinal Phys. Rev. B **78**, 064309 (2008)

[21] N. V. Prokof'ev and P. C. E. Stamp, Rep. Prog. Phys. **63** 669 (2000).

[22] W. Zhang, V. V. Dobrovitski, K. A. Al-Hassanieh, E. Dagotto, and B. N. Harmon, Phys. Rev. B **74**, 205313 (2006).

[23] A. Hutton and S. Bose, Phys. Rev. A **69**, 042312 (2004).

[24] W. Zhang, V. V. Dobrovitski, L. F. Santos, L. Viola, and B. N. Harmon, cond-mat/0703453v1.

[25] H. J. Lipkin, N. Meshkov, and A. J. Glick, Nucl. Phys. **62**, 188 (1965).

[26] S. Dusuel and J. Vidal, Phys. Rev. Lett. **93** 237204 (2004).

[27] W. Von Waldenfels, *Séminaire de probabilité (Starsburg)*, (Springer-Verlag, Berlin, 1990) tome 24, p.349-356.

[28] X. Wang and K. Mølmer, Eur. Phys. J. D, **18** 385 (2002).

[29] M. Danos and J. Rafelski, *Pocketbook of Mathematical Functions* (Harri Deutsch, Frankfurt, 1984).

[30] L. Tessieri and J. Wilkie, J. Phys. A **36** 12305 (2003).

[31] H. Krovi, O. Oreshkov, M Ryazonov, and D. Lidar, *e-print* arXiv:0707.2096.

3. EXACT DYNAMICS OF A TWO-QUBIT SYSTEM IN A SPIN STAR ENVIRONMENT

3.1 Introduction

Multi-qubit systems are of great importance in many fields of quantum technology. Experimental and theoretical evidences, accumulated during the last few years, indicate that they exhibit interesting properties that make them central subjects in quantum information processing and quantum computation [1, 2]. The inherent dissipation and decoherence phenomena due to the interaction with a surrounding environment with many degrees of freedom, unfortunately, limit their usefulness.

Recently, questions related to entanglement and decoherence of some multi-qubit systems have been investigated. Mainly, attention was focused on thermal entanglement, i.e., entanglement induced by the interaction of the multi-qubit system with an environment at thermal equilibrium. Usually, these approaches are within the framework of a master equation for the reduced density matrix of the central system and within the Markovian approximation. The main assumption is that the characteristic times of the interacting systems are much longer than those of the environment [3]. The Markovian dynamics is known to be widely applicable in quantum optics and in the study of quantum noise [4].

Several investigations have shown that dynamics of multi-qubit systems shows strong non-Markovian behavior. Therefore, one has to seek new approaches in order to study them. The Ising and Transverse Ising model were first applied to the description of the reduced dynamics of one-qubit and two-qubit systems under a symmetry broken environment in thermal equilibrium where phase transitions occur [6, 5, 7]. Later, another model was proposed [8] in which the central system is immersed in an environment composed of N spin $\frac{1}{2}$ particles arranged in a star structure. In Ref. [9] the exact solution of the dynamics of one-qubit system in spin star configuration was found assuming a Heisenberg XY interaction. In this model, the spin bath was in an unpolarized infinite temperature state.

The present chapter provides an extension of the above model to the dynamics of

a two-qubit system coupled to a spin star environment. The model is exactly solvable because of the symmetry of the structure under consideration. As mentioned in Ref. [9], this may represent a method to investigate the validity of approximation techniques and numerical methods applied to the non-Markovian dynamics.

The chapter is organized as follows. In Section 3.2 we give a detailed description of the model. In Section 3.3 we derive the exact dynamics of the reduced system. In Section 3.4 we study the case of an infinite number of environmental spins, we determine the correlation functions, and we study the long-time behavior of the density matrix of the central system. We end the chapter with a brief conclusion regarding decoherence and evolution of entanglement of the two-qubit system.

3.2 The model

We consider a system of two non-interacting qubits coupled to a set of N independent spin $\frac{1}{2}$ particles (the environment). We restrict ourselves to the case of a spin star configuration; this is a structure in which the two-qubit system is surrounded by the N spin $\frac{1}{2}$ particles located on the surface of a sphere. The central qubits as well as the environment are multipartite systems living in spaces given by two-fold and N-fold tensor products of the local two dimensional spin spaces corresponding to the individual particles. From an open quantum system point of view the central system is considered as an open system coupled to an environment with a large number of degrees of freedom.

The nature of the coupling between the qubits and the environment is, in general, complicated and depends on the details of the interaction. Nevertheless, some symmetry properties characterizing the spin star configuration lead to an enormous simplification of the model. Indeed, under some conditions [8], the structure under consideration is invariant with respect to the exchange of any two outer spins. Moreover, the spin star configuration is a rotationally invariant system which is the direct result of the isotropy of the environment. More details about SO(3)-invariant spin systems can be found in [14].

3.2.1 The qubits

Let us first consider the general case of a bipartite system **S** composed of two particles with spins j_1 and j_2. The space $\mathbb{C}^s$ of the composite system is given by the tensor product

$$\mathbb{C}^s = \mathbb{C}^{d_1} \otimes \mathbb{C}^{d_2}. \tag{3.1}$$

Here, $d_i = 2j_i + 1$ denotes the dimension of the space $\mathbb{C}^{d_i}$ corresponding to the particle with spin j_i. The total angular momentum of the global system is defined by

$$\hat{J} = \hat{J}_1 \otimes \mathbb{I} + \mathbb{I} \otimes \hat{J}_2, \tag{3.2}$$

where $\hat{J}_1$ and $\hat{J}_2$ are the angular momentum operators of the individual particles and $\mathbb{I}$ denotes the unit matrices on $\mathbb{C}^{d_1}$ and $\mathbb{C}^{d_2}$.

The standard basis in the space $\mathbb{C}^{d_i}$ is composed of the eigenvectors of the operator $\hat{J}_{iz}$ with eigenvalues $m_i = -j_i, -j_i + 1, \ldots, j_i$ with $i = 1, 2$. We denote the vectors of this basis by $|j_i, m_i\rangle$ to stress that on this space $\hat{J}_i^2 = j_i(j_i + 1)\mathbb{I}$.

The composite system admits, now, two equivalent orthonormal bases. The first one is formed by the common eigenvectors $|j_1, j_2, m_1, m_2\rangle$ of the set of operators $\{\hat{J}_1^2, \hat{J}_2^2, \hat{J}_{1z}, \hat{J}_{2z}\}$, they are given by the tensor products

$$|j_1, j_2, m_1, m_2\rangle = |j_1, m_1\rangle \otimes |j_2, m_2\rangle. \tag{3.3}$$

The second one is a standard basis constructed from the simultaneous eigenstates of the square of the total angular momentum operator $\hat{J}^2$ and its projection along the z-axis $\hat{J}_z$, namely $\{|j, m >\}$ with $|j_1 - j_2| \leq j \leq j_1 + j_2$ and $-j \leq m \leq j$. As usual, we introduce the lowering and the raising operators $\hat{J}_\pm = \hat{J}_x \pm i\hat{J}_y$. The action of these operators on a vector $|j, m\rangle$ belonging to the standard basis of the total space is given by ($\hbar = 1$)

$$\begin{aligned} \hat{J}^2|j, m\rangle &= j(j+1)|j, m\rangle, \\ \hat{J}_z|j, m\rangle &= m|j, m\rangle, \\ \hat{J}_\pm|j, m\rangle &= \sqrt{j(j+1) - m(m \pm 1)}|j, m \pm 1\rangle. \end{aligned} \tag{3.4}$$

In the special case of two spin $\frac{1}{2}$ particles, the total angular momentum j takes on either the value one or zero. One possible basis in the four-dimensional space $\mathbb{C}^2 \otimes \mathbb{C}^2$ consists of the state vectors $\{|++\rangle, |+-\rangle, |-+\rangle, |--\rangle\}$ which correspond to the different mutual orientations of the two spin vectors with respect to the z direction. The connection with the standard basis $\{|jm\rangle\}$ of the composite system leads with an appropriate choice of the phase to

$$\begin{aligned} |1, 1\rangle &= |++\rangle, \\ |1, 0\rangle &= \frac{1}{\sqrt{2}}(|+-\rangle + |-+\rangle), \\ |1, -1\rangle &= |--\rangle, \\ |0, 0\rangle &= \frac{1}{\sqrt{2}}(|+-\rangle - |-+\rangle). \end{aligned} \tag{3.5}$$

The picture is equivalent to the decomposition of the two-qubit space $\mathbb{C}^2 \otimes \mathbb{C}^2$ into a direct sum of the spaces $\mathbb{C}$ and $\mathbb{C}^3$ corresponding to spin 0 (antisymmetric vectors) and spin 1 (symmetric vectors) respectively [13]

$$\mathbb{C}^2 \otimes \mathbb{C}^2 = \mathbb{C} \oplus \mathbb{C}^3. \tag{3.6}$$

3.2.2 The environment

The above approach can be easily generalized to an arbitrary number of outer spins. In particular, the total angular momentum operator of the spin environment is simply given by the sum of the individual spin $\frac{1}{2}$ vectors. The environment space $(\mathbb{C}^2)^{\otimes N}$ is equal to a direct sum of subspaces $\mathbb{C}^{d_j}$ where $0 \leq j \leq \frac{N}{2}$ (We assume that N is even). Due to the different possible orientations of the single spins [19], the angular momentum j will have a degeneracy $\nu(N, j)$. We denote this formally as

$$(\mathbb{C}^2)^{\otimes N} = \bigoplus_{j=0}^{\frac{N}{2}} \nu(N, j)\, \mathbb{C}^{d_j}. \tag{3.7}$$

The degeneracy $\nu(N, j)$ is given by [5]

$$\nu(j, N) = \binom{N}{N/2 - j} - \binom{N}{N/2 - j - 1} \text{ with } \binom{N}{-1} = 0. \tag{3.8}$$

Obviously, the following equality holds

$$\sum_{j=0}^{\frac{N}{2}} \nu(j, N)(2j + 1) = 2^N. \tag{3.9}$$

3.2.3 The Hamiltonian

We assume that the two qubits do not interact with each other. Moreover, we will neglect any kind of interactions between the constituents of the environment, the main contribution to the total Hamiltonian comes from the interaction between the central qubits and the environment. The strength of the interaction is supposed to be the same for any two interacting particles; this insures the symmetry with respect to permutations of the outer spins. The qubits are coupled to the environment via Heisenberg XY interactions whose Hamiltonian is given by

$$H = \alpha[(\sigma_+^1 + \sigma_+^2) \otimes J_- + (\sigma_-^1 + \sigma_-^2) \otimes J_+], \tag{3.10}$$

where α denotes the strength of the interaction. In this expression, σ_1 and σ_2 are Pauli matrices associated with each of the central qubits and $J_\pm$ denote the raising and lowering operators of the environment which consists of N spin$-1/2$ particles.

It is easily seen that the action of H on any state vector of the form $|00\rangle \otimes |\Phi_B\rangle$ always gives a vanishing result. Taking into account this fact and the symmetry of the problem, it is sufficient to consider only the space $\mathbb{C}^3 \otimes (\mathbb{C}^2)^{\otimes N}$. The subspace $\mathbb{C}^3$ is spanned by the vectors $|1,-1\rangle$, $|1,0\rangle$ and $|1,1\rangle$. In this basis the lowering and raising operators admit the following representation:

$$\sigma_+ = \begin{pmatrix} 0 & 0 & 0 \\ 1 & 0 & 0 \\ 0 & 1 & 0 \end{pmatrix} \qquad \text{and} \qquad \sigma_- = \begin{pmatrix} 0 & 1 & 0 \\ 0 & 0 & 1 \\ 0 & 0 & 0 \end{pmatrix}. \tag{3.11}$$

Therefore, the Hamiltonian H can be written as

$$H = \alpha \begin{pmatrix} 0 & J_+ & 0 \\ J_- & 0 & J_+ \\ 0 & J_- & 0 \end{pmatrix}. \tag{3.12}$$

One can easily prove by induction that powers of H are given by

$$H^{2n} = \alpha^{2n} \begin{pmatrix} J_+ K^{n-1} J_- & 0 & J_+ K^{n-1} J_+ \\ 0 & K^n & 0 \\ J_- K^{n-1} J_- & 0 & J_- K^{n-1} J_+ \end{pmatrix}, \tag{3.13}$$

$$H^{2n+1} = \alpha^{2n+1} \begin{pmatrix} 0 & J_+ K^n & 0 \\ K^n J_- & 0 & K^n J_+ \\ 0 & J_- K^n & 0 \end{pmatrix}. \tag{3.14}$$

Here K denotes the anti-commutator of the operators J_+ and J_-, that is

$$K = J_+ J_- + J_- J_+ = 2(J^2 - J_z^2). \tag{3.15}$$

Note that K is diagonal in the standard basis of $(\mathbb{C}^2)^{\otimes N}$ with eigenvalues $2(j(j+1) - m^2)$; it satisfies the following commutation relations:

$$\begin{aligned} [K, J^2] &= [K, J_z] = 0, \\ [K, J_- J_+] &= [K, J_+ J_-] = 0. \end{aligned} \tag{3.16}$$

Equations (3.13) and (3.14) allow us to explicitly write out any function of the Hamiltonian restricted to $\mathbb{C}^3 \otimes (\mathbb{C}^2)^{\otimes N}$. In particular, the explicit form of the time evolution

operator $U(t) = \exp(-iHt)$ reads

$$U(t) = \begin{pmatrix} 1 + J_+ \frac{\cos(\alpha t\sqrt{K})-1}{K} J_- & -iJ_+ \frac{\sin(\alpha t\sqrt{K})}{\sqrt{K}} & J_+ \frac{\cos(\alpha t\sqrt{K})-1}{K} J_+ \\ -i\frac{\sin(\alpha t\sqrt{K})}{\sqrt{K}} J_- & \cos(\alpha t\sqrt{K}) & -i\frac{\sin(\alpha t\sqrt{K})}{\sqrt{K}} J_+ \\ J_- \frac{\cos(\alpha t\sqrt{K})-1}{K} J_- & -iJ_- \frac{\sin(\alpha t\sqrt{K})}{\sqrt{K}} & 1 + J_- \frac{\cos(\alpha t\sqrt{K})-1}{K} J_+ \end{pmatrix}. \tag{3.17}$$

3.3 Exact reduced dynamics

The state of the composite system is completely characterized by the total density matrix $\rho(t)$ whose evolution in time is given by

$$\rho(t) = U(t)\rho(0)U^\dagger(t). \tag{3.18}$$

Here $U(t)$ is the time evolution operator and $\rho(0)$ denotes the initial density matrix in the space $\mathbb{C}^3 \otimes (\mathbb{C}^2)^{\otimes N}$. For time-independent Hamiltonians, the operator $U(t)$ takes the simple form

$$U(t) = \exp(-iHt) \tag{3.19}$$

and we could use the expression (3.17).

Alternatively, one can use the Liouville superoperator $\mathcal{L}$ to describe the evolution of the total density matrix $\rho(t)$ [3]:

$$\mathcal{L}\rho(t) = -i[H, \rho(t)]. \tag{3.20}$$

This leads to the von Neumann differential equation,

$$\frac{d}{dt}\rho(t) = \mathcal{L}\rho(t), \tag{3.21}$$

whose integral form is

$$\rho(t) = \exp(\mathcal{L}t)\rho(0). \tag{3.22}$$

Tracing over the environmental degrees of freedom in the space $(\mathbb{C}^2)^{\otimes N}$, enables us to determine the dynamics of the reduced system density matrix, that is,

$$\rho_S(t) = \mathrm{tr}_B\{\rho(t)\}. \tag{3.23}$$

We have used the letters B and S to denote the environment (bath) and the qubits (system). Both descriptions of the dynamics are of course completely equivalent. The difference just consists in a regrouping of terms. We only use the Liouville operator to obtain a more concise description of the dynamics in (3.34) and (3.35).

3.3.1 Initial conditions

We assume that the initial condition factorizes into the uncorrelated tensor product state

$$\rho(0) = \rho_S(0) \otimes \rho_B(0), \tag{3.24}$$

where $\rho_S(0)$ and $\rho_B(0)$ are the initial density matrices describing the local state of the qubits and the environment, respectively. The matrices $\rho_S(0)$ and $\rho_B(0)$ are self-adjoint, positive and have trace one.

Any state vector of the qubits can be written as

$$|\psi\rangle = \beta|--\rangle + \gamma_+|+-\rangle + \gamma_-|-+\rangle + \delta|++\rangle, \tag{3.25}$$

where β, $\gamma_\pm$, and δ are complex numbers satisfying $|\beta|^2 + |\gamma_+|^2 + |\gamma_-|^2 + |\delta|^2 = 1$. Using the relations (3.5) it is possible to rewrite $|\psi\rangle$ in the standard basis of $\mathbb{C} \oplus \mathbb{C}^3$ as

$$|\psi\rangle = \beta|1,-1\rangle + \gamma|1,0\rangle + \delta|1,1\rangle + \gamma'|0,0\rangle, \tag{3.26}$$

where $\gamma = (\gamma_+ + \gamma_-)/\sqrt{2}$ and $\gamma' = (\gamma_+ - \gamma_-)/\sqrt{2}$. Thus the initial density matrix corresponding to the pure state vector $|\psi\rangle$ reads as follows

$$\rho_S(0) = \begin{pmatrix} |\beta|^2 & \beta\gamma^* & \beta\delta^* & \beta\gamma'^* \\ \gamma\beta^* & |\gamma|^2 & \gamma\delta^* & \gamma\gamma'^* \\ \delta\beta^* & \delta\gamma^* & |\delta|^2 & \delta\gamma'^* \\ \gamma'\beta^* & \gamma'\gamma^* & \gamma'\delta^* & |\gamma'|^2 \end{pmatrix}. \tag{3.27}$$

Here z^* denotes the complex conjugate of z.

Once again, because of the symmetry of the problem and the degeneracy of the anti-symmetric state vector $|0,0\rangle$, our task is reduced to the study of the dynamics of a spin-one particle in the space $\mathbb{C}^3$. Without loss of generality, we represent the initial reduced system density matrix restricted to this subspace by

$$\rho_S(0) = \begin{pmatrix} \rho_{11}^0 & \rho_{12}^0 & \rho_{13}^0 \\ \rho_{12}^{0*} & \rho_{22}^0 & \rho_{23}^0 \\ \rho_{13}^{0*} & \rho_{23}^{0*} & \rho_{33}^0 \end{pmatrix}. \tag{3.28}$$

Obviously, one has to keep in mind that the actual normalization condition for the initial density matrix of the qubits reads $\sum_{i=1}^4 \rho_{ii}^0 = 1$, where $\rho_{44}^0 = |\gamma'|^2$. Although our attention is focused on the subspace $\mathbb{C}^3$, we will investigate in parallel the evolution in time of the remaining density matrix elements.

Let us now take a look at the initial condition of the environment. It is well known that the density matrix characterizing a bath in thermal equilibrium at temperature T is given by $\rho_B(0) = (e^{-H_B/k_BT})/Z$ where H_B is the Hamiltonian of the environment, k_B is the Boltzmann constant and $Z = \mathrm{tr}_B\, e^{-H_B/k_BT}$ is the partition function. In our model, we assume that the environment is initially in a state of infinite temperature with corresponding density matrix

$$\rho_B(0) = 2^{-N}\mathbb{I}_B, \tag{3.29}$$

where $\mathbb{I}_B$ denotes the unity operator in the environment space.

3.3.2 Reduced system dynamics

The time-dependent reduced density matrix is obtained by taking the partial trace over the environmental degrees of freedom

$$\rho_S(t) = \mathrm{tr}_B\left\{\exp(-iHt)\rho_S(0)\otimes\rho_B(0)\exp(iHt)\right\} \tag{3.30}$$

$$= \mathrm{tr}_B\left\{\exp(\mathcal{L}t)\rho_S(0)\otimes\rho_B(0)\right\}. \tag{3.31}$$

Expanding the exponential function (3.31) in a Taylor series gives

$$\rho_S(t) = \sum_{k=1}^{\infty}\frac{t^k}{k!}\mathrm{tr}_B\left\{\mathcal{L}^k\rho_S(0)\otimes 2^{-N}\mathbb{I}_B\right\}. \tag{3.32}$$

In the above equation, powers of the Liouville operator appear. In order to evaluate them we expand the unitary evolution operators in (3.30) to obtain

$$\mathcal{L}^n\rho = i^n\sum_{\ell=0}^{n}(-1)^\ell\binom{\ell}{n}H^\ell\rho H^{n-\ell}. \tag{3.33}$$

For odd n's, one gets always an extra lowering or raising operator under the trace, implying that

$$\mathrm{tr}_B\{\mathcal{L}^{2n+1}\rho_S(0)\otimes 2^{-N}\mathbb{I}_B\} = 0. \tag{3.34}$$

In fact, this holds for any number of central spins. This immediately follows from the expression (3.17) for the unitary evolution operator of the full system.

With the help of the trace properties one can find that for non zero n

$$\mathrm{tr}_B\{\mathcal{L}^{2n}\rho_S(0)\otimes 2^{-N}\mathbb{I}_B\} = \sum_{k=1}^{n-1}\binom{2n}{2k}\mathcal{S}^{2n}_{2k} - \sum_{k=0}^{n-1}\binom{2n}{2k+1}\mathcal{S}^{2n}_{2k+1} + \mathcal{F}^{2n}, \tag{3.35}$$

where

$$\mathcal{S}_{2k}^{2n} = (-\alpha)^n \begin{pmatrix} (\rho_{11}^0 - \rho_{33}^0)R_{n-2} + \rho_{33}P_n & \rho_{12}^0 Q_k^n & \rho_{13}^0 O_k^n \\ \rho_{12}^{0*} Q_{n-k}^n & \rho_{22}^0 F_n & \rho_{23}^0 Q_{k+1}^n \\ \rho_{13}^{0*} O_{n-k}^n & \rho_{23}^{0*} Q_{n-k+1}^n & M_n \end{pmatrix}, \tag{3.36}$$

$$M_n = -(\rho_{11}^0 - \rho_{33}^0)R_{n-2} + \rho_{33}^0 F_n + (\rho_{11}^0 - 2\rho_{33}^0)P_n, \tag{3.37}$$

$$\mathcal{S}_{2k+1}^{2n} = (-\alpha)^n \begin{pmatrix} \rho_{22}^0 P_n & \rho_{23}^0 Q_{k+1}^n & 0 \\ \rho_{23}^{0*} Q_{n-k}^n & (\rho_{11}^0 - \rho_{33}^0)P_n + \rho_{33}^0 F_n & \rho_{12}^0 Q_{k+1}^n \\ 0 & \rho_{12}^{0*} Q_{n-k}^n & \rho_{22}^0 (F_n - P_n) \end{pmatrix}, \tag{3.38}$$

and

$$\mathcal{F}^{2n} = (-\alpha)^n \begin{pmatrix} 2\rho_{11}^0 P_n & \rho_{12}^0 (F_n + P_n) & \rho_{13}^0 F_n \\ \rho_{12}^{0*} (F_n + P_n) & 2\rho_{22}^0 F_n & \rho_{23}^0 (2F_n - P_n) \\ \rho_{13}^0 F_n & \rho_{23}^{0*} (2F_n - P_n) & 2\rho_{33}^0 (F_n - P_n) \end{pmatrix}. \tag{3.39}$$

Here we have introduced the environmental correlation functions

$$R_n = 2^{-N} \mathrm{tr}_B\{(J_- J_+)^2 K^{n-2}\}, \tag{3.40}$$

$$Q_k^n = 2^{-N} \mathrm{tr}_B\{J_+ K^{k-1} J_- K^{n-k}\}, \tag{3.41}$$

$$O_k^n = 2^{-N} \mathrm{tr}_B\{J_+ J_+ K^{k-1} J_- J_- K^{n-k-1}\}, \tag{3.42}$$

$$P_n = 2^{-N} \mathrm{tr}_B\{J_- J_+ K^{n-1}\}, \tag{3.43}$$

$$F_n = 2^{-N} \mathrm{tr}_B\{K^n\}. \tag{3.44}$$

Notice that the above correlation functions are independent for small N, they were obtained with the help of the commutation relations (3.16) with which we could derive simple expressions relating them. Nevertheless, the number of independent functions still remains large since the operator K does not commute with any polynomial of the lowering and raising operators $J_\pm$. Besides this fact, one can see that there exists some similarity among these correlation functions as it is the case between R_n and O_k^n on one hand and P_n and Q_k^n on the other hand.

By substitution into equation (3.32) one finds the explicit form of the various matrix elements of $\rho_S(t)$. One can check that the diagonal elements are given by

$$\rho_{11}(t) = \rho_{11}^0(1 + 2g(t)) + (\rho_{11}^0 - \rho_{33}^0)f(t) + \rho_{33}^0 e(t) + \rho_{22}^0 h(t), \tag{3.45}$$

$$\rho_{22}(t) = \rho_{22}^0 + (\rho_{11}^0 - \rho_{33}^0)h(t) + (\rho_{33}^0 - \rho_{22}^0)\ell(t), \tag{3.46}$$

and

$$\rho_{33}(t) = \rho_{33}^0(1-2g(t)) - (\rho_{11}^0 - \rho_{33}^0)f(t) - \rho_{22}^0 h(t) + (\rho_{11}^0 - 2\rho_{33}^0)e(t) + (\rho_{22}^0 - \rho_{33}^0)\ell(t). \tag{3.47}$$

The off-diagonal elements read

$$\rho_{12}(t) = \rho_{12}^0[\widetilde{\ell}(t) + \widetilde{e}_1(t)] + \rho_{23}^0\widetilde{h}(t), \tag{3.48}$$

$$\rho_{13}(t) = \rho_{13}^0[\widetilde{\ell}(t) + \widetilde{f}(t)], \tag{3.49}$$

$$\rho_{23}(t) = \rho_{23}^0[\widetilde{\ell}(t) + \widetilde{e}_2(t)] + \rho_{12}^0\widetilde{h}(t), \tag{3.50}$$

$$\rho_{21}(t) = \rho_{12}^*(t), \tag{3.51}$$

$$\rho_{31}(t) = \rho_{13}^*(t), \tag{3.52}$$

$$\rho_{32}(t) = \rho_{23}^*(t). \tag{3.53}$$

Here we have introduced the functions

$$f(t) = 2^{-N}\mathrm{tr}_B\Big\{J_-J_+\frac{\cos(\alpha t\sqrt{K})-1}{K}\Big\}^2, \tag{3.54}$$

$$g(t) = 2^{-N}\mathrm{tr}_B\Big\{J_-J_+\frac{\cos(\alpha t\sqrt{K})-1}{K}\Big\}, \tag{3.55}$$

$$h(t) = 2^{-N}\mathrm{tr}_B\Big\{J_-J_+\frac{\sin^2(\alpha t\sqrt{K})}{K}\Big\}, \tag{3.56}$$

$$e(t) = 2^{-N}\mathrm{tr}_B\Big\{J_-J_+\frac{(\cos(\alpha t\sqrt{K})-1)^2}{K}\Big\}, \tag{3.57}$$

$$\ell(t) = 2^{-N}\mathrm{tr}_B\Big\{\sin^2(\alpha t\sqrt{K})\Big\}, \tag{3.58}$$

$$\widetilde{\ell}(t) = 2^{-N}\mathrm{tr}_B\Big\{\cos(\alpha t\sqrt{K})\Big\}. \tag{3.59}$$

The remaining functions are quite different in their analytical form from those listed above. They are given explicitly by

$$\widetilde{f}(t) = 2^{-N}\mathrm{tr}_B\Big\{J_-^2\frac{\cos(\alpha t\sqrt{K})-1}{K}J_+^2\frac{\cos(\alpha t\sqrt{K})-1}{K}\Big\} \tag{3.60}$$

$$\widetilde{e}_1(t) = 2^{-N}\mathrm{tr}_B\Big\{J_+\frac{\cos(\alpha t\sqrt{K})-1}{K}J_-\cos(\alpha t\sqrt{K})\Big\}, \tag{3.61}$$

$$\widetilde{e}_2(t) = 2^{-N}\mathrm{tr}_B\Big\{J_-\frac{\cos(\alpha t\sqrt{K})-1}{K}J_+\cos(\alpha t\sqrt{K})\Big\}, \tag{3.62}$$

$$\widetilde{h}(t) = 2^{-N}\mathrm{tr}_B\Big\{J_+\frac{\sin(\alpha t\sqrt{K})}{\sqrt{K}}J_-\frac{\sin(\alpha t\sqrt{K})}{\sqrt{K}}\Big\}. \tag{3.63}$$

One has to be careful when dividing by the operator K since its eigenvalue corresponding to $j = 0$ vanishes. To overcome this difficulty, it is sufficient to write the quantity

under the trace sign in the normal order, that is, to first apply the lowering operator J_- on the state $|0,0\rangle$ which leads obviously to zero.

In fact, the function $e(t)$ can be expressed in terms of $g(t)$ and $h(t)$. We will leave it in this form in order to maintain its symmetry with the functions $\widetilde{e}_1(t)$ and $\widetilde{e}_2(t)$. Altogether, we need a set of nine real-valued functions to describe the reduced system dynamics in $\mathbb{C}^3$. In the special case of one-qubit dynamics [9] the number of independent functions is significantly reduced to two because of the rotational invariance of the star configuration.

When the conditions $\rho_{11}^0 = \rho_{33}^0$ and $\rho_{22}^0 \neq 0$ are satisfied (one can, e.g., set $\beta = \delta$ in Eq. (3.26)), the diagonal elements take the relatively simple form

$$\frac{\rho_{11}(t)}{\rho_{11}^0} = 1 + (\xi - 1)h(t), \tag{3.64}$$

$$\frac{\rho_{22}(t)}{\rho_{22}^0} = 1 + \Big(\frac{1-\xi}{\xi}\Big)\ell(t), \tag{3.65}$$

$$\frac{\rho_{33}(t)}{\rho_{33}^0} = 1 + (\xi - 1)(\ell(t) - h(t)). \tag{3.66}$$

where the parameter ξ is given by ρ_{22}^0/ρ_{11}^0.

It is not difficult to check that the solutions (3.45)–(3.47) as well as (3.64)–(3.66) ensure that the trace is preserved, that is, $\sum_{i=1}^3 \rho_{ii}(t) = \sum_{i=1}^3 \rho_{ii}^0$. This actually results from the fact that the time evolution operator $U(t)$ is unitary and hence trace preserving. It is worth noting that the density matrix element ρ_{44} does not evolve in time, the time evolution operator is reduced to 1 in the space $\mathbb{C}$. This is due to the symmetry of the Hamiltonian H. The subspace $\mathbb{C}$ is said to be decoherence free which was expected because of the degeneracy in energy of the antisymmetric state vector $|00\rangle$. Moreover, the density matrix elements ρ_{i4}, $i = 1, 2, 3$ evolve according to

$$\rho_{i4}(t) = 2^{-N} \sum_{k=1}^{3} \mathrm{tr}_B\{U_{ik}(t)\}\, \rho_{k4}^0, \tag{3.67}$$

since $U_{i4}(t)$ is equal to δ_{i4}. The last relation shows that the off-diagonal elements behave like the components of a three dimensional state vector. Taking into account the fact that the partial trace of any off-diagonal element of $U(t)$ is zero, it is not difficult to find that

$$\begin{pmatrix} \rho_{14}(t) \\ \rho_{24}(t) \\ \rho_{34}(t) \end{pmatrix} = \begin{pmatrix} \rho_{14}^0(1 + g(t)) \\ \rho_{24}^0 \widetilde{\ell}(t) \\ \rho_{34}^0(1 + g(t)) \end{pmatrix}. \tag{3.68}$$

Notice that the set of functions (3.54)–(3.63) can be rewritten in the standard basis of

the environment space $(\mathbb{C}^2)^{\otimes N}$. For example, we can write the functions $f(t)$ and $\widetilde{e}_1(t)$ as

$$f(t) = 2^{-N}\sum_{j,m}\nu(j,N)\Big\{\frac{\chi(j,m)}{\omega(j,m)}\cos(\alpha t\sqrt{\omega(j,m)})\Big\}^2, \tag{3.69}$$

$$\widetilde{e}_1(t) = 2^{-N}\sum_{j,m}\nu(j,N)\frac{\chi(j,m)}{\omega(j,m-1)}\cos[\alpha t\sqrt{\omega(j,m-1)}]\cos[\alpha t\sqrt{\omega(j,m)}], \tag{3.70}$$

where the quantities $\chi(j,m)$ and $\omega(j,m)$ are,respectively, the eigenvalues of the operators J_-J_+ and K:

$$\chi(j,m) = j(j+1) - m(m-1), \tag{3.71}$$

$$\omega(j,m) = 2\big(j(j+1) - m^2\big). \tag{3.72}$$

Taking the trace over the environment yields a superposition of weighted periodic functions with different frequencies. Roughly speaking, this means that the time-dependent density matrix elements evolve anharmonically starting from their initial values.

3.4 The limit of a large number of bath spins

In this section, we will investigate the behavior of the solution found previously when the number of the environmental spins becomes very large, that is, the limit $N \to \infty$.

To this end, let us anticipate and say that in the limit of large number of degrees of freedom, the environment has the tendency to behave as a classical system. Consequently, one can expect that the various operators related to the environment do commute at least for the case where the total angular momentum j is very large compared to the quantum number m. As we will see, this will enable us to determine the long-time behavior of the reduced system density matrix.

3.4.1 Environment correlation functions

The trace operation over the environmental degrees of freedom can be carried out by writing the lowering and raising operators in the standard basis of the environment space $\big\{\otimes_{i=1}^N|s^i\rangle\big\}$, namely,

$$J_\pm = \sum_{i=1}^N \frac{1}{2}\sigma_\pm^i, \tag{3.73}$$

where $\sigma_z^i|s^i\rangle = (-1)^{s^i}|s^i\rangle$. With help of the formula

$$K^n = \sum_{\ell=0}^n \binom{n}{\ell}(J_+J_-)^{n-\ell}(J_-J_+)^\ell, \tag{3.74}$$

the problem is reduced to the calculation of terms having the following general structure

$$\mathcal{A}_n = \mathrm{tr}_B\Big\{\prod_{i_1,i_2}^{n} J_{\kappa_{i_1}} J_{\kappa_{i_2}}\Big\} = \mathrm{tr}_B\Big\{\prod_{i_1,i_2}^{n}\sum_{j_1,j_2}^{N} \sigma_{\kappa_{i_1}}^{j_1}\sigma_{\kappa_{i_2}}^{j_2}\Big\}, \tag{3.75}$$

where the index κ indicates the nature of the operator, raising or lowering. The main restriction here is that the lowering and raising operators J_- and J_+ must appear the same number of times under the trace in order to insure that the result is not zero. In general, $\mathcal{A}_n$ leads to a polynomial of order n in the environment spins number N. The main contribution to such quantities comes from terms having the maximum number of indices labeling the operators σ_{κ_i}. This is due to the fact that these terms are characterized by the largest combinatorial weight and hence yield the largest exponent in N.

It is shown in [9] that

$$\mathrm{tr}_B\big\{(J_+J_-)^n\big\} \sim \mathrm{tr}_B\big\{(J_+J_-)^{n-\ell}(J_-J_+)^{\ell}\big\} \approx \frac{2^N N^n n!}{2^n}. \tag{3.76}$$

With the help of the last relation, it is easy to compute the environment correlation functions for the two-qubit case. For example we have for R_n

$$R_n = 2^{-N}\mathrm{tr}_B\Big\{\sum_{\ell=0}^{n-2}\binom{n-2}{\ell}(J_+J_-)^{n-\ell-2}(J_-J_+)^{2+\ell}\Big\} \approx \sum_{\ell=0}^{n-2}\binom{n-2}{\ell}\frac{N^n n!}{2^n}, \tag{3.77}$$

and thus

$$R_n \approx \frac{N^n n!}{4}. \tag{3.78}$$

Similarly, we find that when $N \to \infty$ then

$$O_k^n \sim R_n \approx \frac{N^n n!}{4}, \tag{3.79}$$

$$Q_k^n \sim P_n \approx \frac{N^n n!}{2}, \tag{3.80}$$

$$F_n \approx N^n n!. \tag{3.81}$$

The above method does not apply for correlation functions where at least one of the upper or lower indices is zero. In these cases the operator K appears in the denominator of the correlation functions and hence the expansion (3.75) is no longer applicable. One alternative way to determine them is by writing the trace in the eigenbasis of J_z and J^2. The point here is to write down the trace over the environment in the joint standard basis of J^2 and J_z; this gives

$$\mathrm{tr}_B\Big(\frac{J_-J_+}{K}\Big)^2 = \sum_{j,m}\nu(j,N)\frac{(j(j+1)-m(m+1))^2}{4(j(j+1)-m^2)^2}. \tag{3.82}$$

This equation can be rewritten as

$$\mathrm{tr}_B\Big(\frac{J_-J_+}{K}\Big)^2 = \frac{1}{4}\sum_{j,m}\nu(j,N)\Big\{1+\frac{m^2}{\big(j(j+1)-m^2\big)^2}\Big\}, \tag{3.83}$$

where we have used the fact that

$$\sum_{j,m}\nu(j,N)\frac{m}{j(j+1)-m^2} = 0. \tag{3.84}$$

Taking into account the relation $\sum_{j,m}\nu(j,N) = 2^N$, we find

$$R_0 = \frac{1}{4}+\Omega_N \quad \text{and} \quad \Omega_N = 2^{-N}\sum_{j,m}\frac{m^2}{4(j(j+1)-m^2)^2}. \tag{3.85}$$

Similarly, we have

$$\mathrm{tr}_B\Big\{\frac{(J_-J_+)^2}{K}\Big\} = \frac{1}{2}\sum_{j,m}\nu(j,N)\Big\{j(j+1)-m^2+\frac{m^2}{(j(j+1)-m^2)}\Big\}. \tag{3.86}$$

With the help of Eq. (3.84), we find

$$\mathrm{tr}_B\Big\{\frac{(J_-J_+)^2}{K}\Big\} = \frac{1}{2}\mathrm{tr}_B\{J_-J_+\}+\frac{1}{2}\sum_{j,m}\nu(j,N)\frac{m^2}{j(j+1)-m^2}. \tag{3.87}$$

Then,

$$R_1 = \frac{N}{2}+\Gamma_N$$

and

$$\Gamma_N = 2^{-N}\frac{1}{2}\sum_{j,m}\nu(j,N)\frac{m^2}{j(j+1)-m^2}. \tag{3.88}$$

With the same method one can find that

$$Q_0^0 = \frac{1}{4}-\Omega_N,\ Q_0^1 = \frac{N}{2}-\Gamma_N \text{ and } P_0 = \frac{1}{2}. \tag{3.89}$$

The quantity Ω_N is very small compared to 1 and can be neglected. Under this assumption both methods lead to the same result; this is actually the same thing as assuming that $K = 2J_-J_+$. Thus the environment operators behave as if they commute when N tends to infinity, a result which confirms the statement we gave in the beginning of this section.

3.4.2 Time evolution

The dynamics of the reduced system can easily be determined in the limit $N \to \infty$ by properly rescaling the coupling constant α. The substitution of the correlation functions (3.79)–(3.81) into equations (3.36)–(3.39) yields

$$\mathrm{tr}_B\{\mathcal{L}^{2n}\rho_S(0)\otimes 2^{-N}\mathbb{I}_B\} = \{2^{n-1}A + C\}\frac{(-N)^n n!}{4}, \tag{3.90}$$

where the matrices A and C are given by

$$A = \begin{pmatrix} \rho_{11}^0 + \rho_{33}^0 - 2\rho_{22}^0 & 2(\rho_{12}^0 - \rho_{23}^0) & \rho_{13}^0 \\ 2(\rho_{12}^{0*} - \rho_{23}^{0*}) & 4\rho_{22}^0 - 2(\rho_{11}^0 + \rho_{33}^0) & 2(\rho_{23}^0 - \rho_{12}^0) \\ \rho_{13}^{0*} & 2(\rho_{23}^{0*} - \rho_{12}^{0*}) & \rho_{11}^0 + \rho_{33}^0 - 2\rho_{22}^0 \end{pmatrix}, \tag{3.91}$$

and

$$C = \begin{pmatrix} 2(\rho_{11}^0 - \rho_{33}^0) & 2\rho_{12}^0 & 2\rho_{13}^0 \\ 2\rho_{12}^{0*} & 0 & 2\rho_{23}^0 \\ 2\rho_{12}^{0*} & 2\rho_{23}^{0*} & 2(\rho_{33}^0 - \rho_{11}^0) \end{pmatrix}. \tag{3.92}$$

Inserting equation (3.90) into equation (3.32) yields a power series with terms of the general form $((\alpha t)^2 N)^k$. It is then natural to rescale the coupling constant by setting

$$\alpha \to \frac{\alpha}{\sqrt{N}}. \tag{3.93}$$

Consider for example the function $f(t)$ in (3.54). We have that

$$f(t) = 2^{-N}\mathrm{tr}_B\Big\{\Big(J_-J_+\frac{\cos(\alpha t\sqrt{K})}{K}\Big)^2 - 2\Big(\frac{J_-J_+}{K}\Big)^2\cos(\alpha t\sqrt{K}) + \Big(\frac{J_-J_+}{K}\Big)^2\Big\}. \tag{3.94}$$

The first term in the right hand side of the above equation can be written as

$$\begin{aligned} 2^{-N}\mathrm{tr}_B\Big\{\Big(\frac{J_-J_+}{K}\Big)^2\Big[\frac{1}{2} + \sum_{n=0}^{\infty}(-1)^n\frac{(2\alpha t)^{2n}}{2(2n)!}K^n\Big]\Big\} \\ = R_0 - R_1(\alpha t)^2 + \sum_{n=2}^{\infty}(-1)^n\frac{(2\alpha t)^{2n}}{2(2n)!}R_n \\ = \frac{1}{4} + \Omega_N - \Gamma_N(\alpha t)^2 + \frac{1}{4}\sum_{n=1}^{\infty}(-1)^n n!\frac{(2\alpha t\sqrt{N})^{2n}}{2(2n)!}. \end{aligned} \tag{3.95}$$

Similarly, we find

$$2^{-N}\mathrm{tr}_B\Big\{\Big(\frac{J_-J_+}{K}\Big)^2\cos(\alpha t\sqrt{K})\Big\} = \frac{1}{4} + \Omega_N - \frac{1}{2}\Gamma_N(\alpha t)^2 + \frac{1}{2}\sum_{n=1}^{\infty}(-1)^n n!\frac{(\alpha t\sqrt{N})^{2n}}{2(2n)!}. \tag{3.96}$$

It is then sufficient to rescale the coupling constant to find that when $N \to \infty$ the function $f(t)$ becomes:

$$f(t) = \widetilde{f}(t) = \frac{1}{4}\zeta(2t) - \zeta(t), \tag{3.97}$$

where

$$\zeta(t) = -\frac{\alpha t}{2} D_+(-\frac{\alpha t}{2}). \tag{3.98}$$

Here $D_+(x)$ denotes the Dawson function, also called Dawson's integral [19], which arises from the calculation of the Voigt spectral lines shape [20]. It is given by

$$D_+(x) = \mathrm{e}^{-x^2} \int_0^x \mathrm{e}^{t^2}\, dt. \tag{3.99}$$

Dawson's function is related to the imaginary error function $\mathrm{erfi}(x)$ by

$$D_+(x) = \frac{\sqrt{\pi}}{2} \mathrm{e}^{-x^2} \mathrm{erfi}(x). \tag{3.100}$$

As opposed to the ordinary error function, the imaginary one is unbounded. It is given by the following series expansion

$$\mathrm{erfi}(x) = \frac{2}{\sqrt{\pi}} \sum_{k=0}^{\infty} \frac{x^{2k+1}}{k!(2k+1)}. \tag{3.101}$$

Following the same procedure, we find that

$$g(t) = \zeta(t), \tag{3.102}$$

$$h(t) = \widetilde{h}(t) = -\frac{1}{2}\zeta(2t), \tag{3.103}$$

$$\ell(t) = -\zeta(2t), \tag{3.104}$$

$$\widetilde{\ell}(t) = 1 + 2\zeta(t), \tag{3.105}$$

$$e(t) = \frac{1}{2}\zeta(2t) - 2\zeta(t), \tag{3.106}$$

$$\widetilde{e}_{1,2}(t) = \frac{1}{2}\zeta(2t) - \zeta(t), \tag{3.107}$$

It is then sufficient to substitute the above functions into the set of equations (3.45)–(3.50) to get the new form of the density matrix elements.

Fortunately, the function $\zeta(t)$ is bounded and admits a limit when t tends to infinity. In order to determine this limit let us stress that the $J_\pm/\sqrt{N}$ are well behave fluctuation operators with respect to the tracial state on the bath. From a mathematical point of view, the above statement means that $J_+/\sqrt{N}$ converges to a complex random variable z with probability density function

$$z \to \frac{2}{\pi} \mathrm{e}^{-2|z|^2}. \tag{3.108}$$

The explicit form of the functions (3.54)–(3.63) shows that it is sufficient to calculate the expectation value of the function $\cos(\beta|z|)$ where $\beta \in \mathbb{R}$, namely

$$G(\beta) = \frac{2}{\pi}\int_{\mathbb{C}} dzdz^* \, \mathrm{e}^{-2|z|^2} \cos(\beta|z|). \tag{3.109}$$

In order to obtain the asymptotic state we need to take the limit $\beta \to \infty$, but this is straightforward by the Riemann-Lebesgue lemma and so we simply obtain

$$\lim_{\beta\to\infty} G(\beta) = 0. \tag{3.110}$$

It is easy to see that $G(\alpha t) \equiv \widetilde{\ell}(t)$, it follows that the limit of the function $\xi(t)$ is equal to $-\frac{1}{2}$. Moreover, we can show that the following relation holds for any value of the non-zero real parameter θ

$$\lim_{t\to\infty} \zeta(\theta t) = -\frac{1}{2}. \tag{3.111}$$

Therefore, as $t \to \infty$

$$f(t),\ \widetilde{f}(t) \to \frac{3}{8}, \tag{3.112}$$

$$g(t) \to -\frac{1}{2}, \tag{3.113}$$

$$h(t),\ \widetilde{h}(t) \to \frac{1}{4}, \tag{3.114}$$

$$\ell(t) \to \frac{1}{2}, \tag{3.115}$$

$$\widetilde{\ell}(t) \to 0, \tag{3.116}$$

$$e(t) \to \frac{3}{4}, \tag{3.117}$$

$$\widetilde{e}_{1,2}(t) \to \frac{1}{4}. \tag{3.118}$$

Consequently, the long-time limit of the reduced system dynamics yields the following density matrix in $\mathbb{C}\oplus\mathbb{C}^3$

$$\rho_S^\infty = \begin{pmatrix} \frac{3}{8}(\rho_{11}^0 + \rho_{33}^0 + \frac{2}{3}\rho_{22}^0) & \frac{1}{4}\rho_{12}^0 + \frac{1}{4}\rho_{23}^0 & \frac{3}{8}\rho_{13}^0 & \frac{1}{2}\rho_{14}^0 \\ \frac{1}{4}\rho_{12}^{0*} + \frac{1}{4}\rho_{23}^{0*} & \frac{1}{4}(\rho_{11}^0 + \rho_{33}^0 + 2\rho_{22}^0) & \frac{1}{4}\rho_{23}^0 + \frac{1}{4}\rho_{12}^0 & 0 \\ \frac{3}{8}\rho_{13}^{0*} & \frac{1}{4}\rho_{23}^{0*} + \frac{1}{4}\rho_{12}^{0*} & \frac{3}{8}(\rho_{11}^0 + \rho_{33}^0 + \frac{2}{3}\rho_{22}^0) & \frac{1}{2}\rho_{34}^0 \\ \frac{1}{2}\rho_{14}^{0*} & 0 & \frac{1}{2}\rho_{34}^{0*} & \rho_{44}^0 \end{pmatrix}. \tag{3.119}$$

In Figs. 3.1–3.2, we have drawn the variation of the diagonal elements $\rho_{11}(t)$ and $\rho_{22}(t)$ respectively for the pure initial state $|--\rangle$. The graphs were obtained for $N = 100$, $N = 400$ and the limit $N \to \infty$. The evolution in time of the off-diagonal element $\rho_{13}(t)$ corresponding to the maximally entangled state $\frac{1}{\sqrt{2}}(|++\rangle + |--\rangle)$ is given in Fig. 3.3. The plots show that the solution corresponding to infinite number of environment spins $N \to \infty$ is almost identical to the exact solutions up to a value of time given by $\alpha t \approx 3$ then the curves start to diverge.

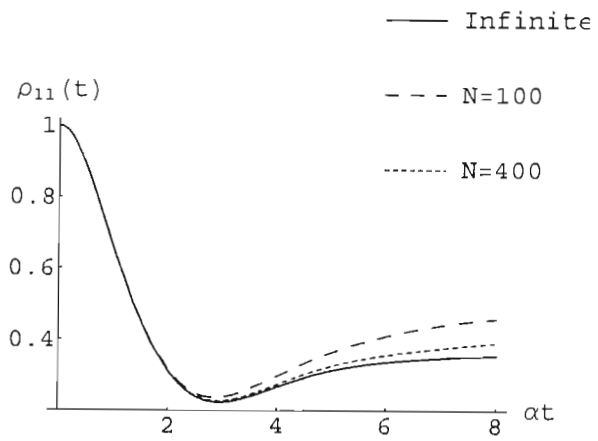

Fig. 3.1: The time evolution of the density matrix element ρ_{11}. Initial state of the two-qubit system is the pure state $|--\rangle$. The figure shows the plots obtained for $N = 100$, $N = 400$ and the limit $N \to \infty$.

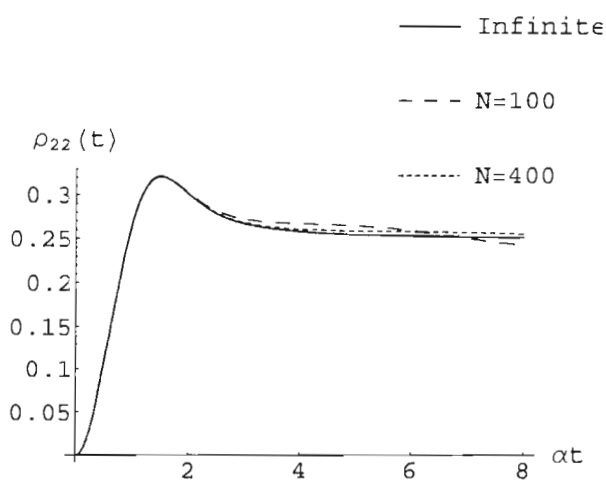

Fig. 3.2: The evolution in time of the density matrix element ρ_{22} as a function of time. The initial condition of the two-qubit system is the pure state $|--\rangle$. The figure shows the plots obtained for $N = 100$, $N = 400$ and the limit $N \to \infty$.

3.4.3 Decoherence and entanglement

From formula (3.119) we see that the off-diagonal elements show partial decoherence. Indeed, the ratio between the asymptotic and the initial values of the density matrix

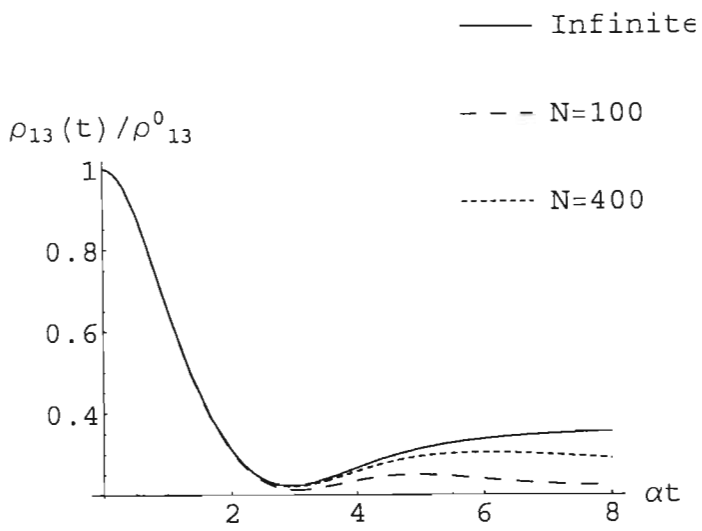

Fig. 3.3: The evolution in time of the density matrix element ρ_{13}. The initial condition of the two-qubit system is the entangled state $\frac{1}{\sqrt{2}}(|++\rangle + |--\rangle)$. The figure shows the plots obtained for $N = 100$, $N = 400$ and the limit $N \to \infty$.

element ρ_{13} is equal to $\frac{3}{8}$. The contribution to the final result of the two other off-diagonal elements, ρ_{12} and ρ_{23}, is symmetrically shared by their original values with the same weight, namely $\frac{1}{4}$. This can be seen, for example, in the case where the initial condition is the separable state $\frac{1}{\sqrt{2}}|-\rangle(|+\rangle + |-\rangle)$ or $\frac{1}{\sqrt{2}}|+\rangle(|+\rangle + |-\rangle)$. In particular, if the condition $\rho_{12}^0 = \rho_{23}^0$ is satisfied, both matrix elements relax and assume half of their initial value. Similarly, the off-diagonal elements ρ_{14} and ρ_{13} evolve asymptotically to half their original values whereas the element ρ_{24} relaxes and tends to zero.

A first look at the explicit form of the diagonal elements of the density matrix reveals that they only depend on the corresponding initial ones. Let us choose $\xi \to 1$ in relations (3.64–3.66) and assume that the remaining off-diagonal elements vanish. The resulting density matrix corresponds to the diagonal initial state $\frac{1}{3}(|1,1\rangle\langle 1,1| + |1,0\rangle\langle 1,0| + |1,-1\rangle\langle 1,-1|)$. It is not a hard task to see that this state does not change in time. Consequently, the two qubits do not feel the presence of the environment. The same result holds for the entangled antisymmetric state $|00\rangle$ which belongs to the decoherence-free subspace $\mathbb{C}$.

Because of the coupling between the central system and the environment, entanglement between the two qubits may appear. Assume for instance that the two-qubit system was

initially in a pure state, $|--\rangle$ or $|++\rangle$ for example. This corresponds to the preparation of a spin-one particle in the pure states $|1,-1\rangle$ and $|1,1\rangle$ respectively. Once the interaction is switched on, the system evolves into a mixed state.

The case where the initial condition is one of the maximally entangled states $\frac{1}{\sqrt{2}}(|+-\rangle \pm |-+\rangle)$, is quite special. Indeed, the latter are regarded as pure states for the composite system, they generally evolve into mixed states when exposed to the environment. One then asks whether the evolving state is entangled or separable.

In order to quantify the amount of entanglement created between the two qubits, we shall use the concurrence, $C(\rho)$, as a measure of entanglement for mixed states. The numerical values of the concurrence range from 0 for separable states to 1 for maximally entangled states. According to Ref. [16], $C(\rho)$ is defined as follows

$$C(\rho) = \max\{0, \sqrt{\lambda_1} - \sqrt{\lambda_2} - \sqrt{\lambda_3} - \sqrt{\lambda_4}\}. \tag{3.120}$$

$\lambda_1 \geq \lambda_2 \geq \lambda_3 \geq \lambda_4$ are the eigenvalues of the operator $\rho(V \otimes V)\rho(V \otimes V)$ where V is a linear skew-adjoint operator in $\mathbb{C} \oplus \mathbb{C}^3$ such that $VV = -\mathbb{I}$. In our case

$$V \otimes V = \begin{pmatrix} 0 & 0 & 1 & 0 \\ 0 & -1 & 0 & 0 \\ 1 & 0 & 0 & 0 \\ 0 & 0 & 0 & 1 \end{pmatrix}. \tag{3.121}$$

Here we pick out some typical results:

- The concurrence corresponding to the initial separable state $|--\rangle$ is equal to

$$C(\rho) = \max\{0, -\rho_{22}(t)\} = 0. \tag{3.122}$$

  Therefore, the two-qubit state maintains its separability during time which means that no entanglement will be produced by the interaction with the environment. For the same reason, the initial state $|++\rangle$ evolves into a separable state too. In fact, the latter result is also true for the general case of pure separable states when one of the qubits is in the state $|-\rangle$ (or $|+\rangle$) and the other one is at an angle, say θ, from the first qubit.

- If the initial state is the maximally entangled state $|\Psi\rangle = \frac{1}{\sqrt{2}}(|+-\rangle + |-+\rangle)$, then the concurrence takes the form

$$C(\rho) = \max\{0, \rho_{22}(t) - 2\sqrt{\rho_{11}(t)\rho_{33}(t)}\}. \tag{3.123}$$

The time behavior of $C(\rho)$ is shown in the plot of Fig. 3.4 where one can see that it quickly decreases and vanishes after a relatively short time. The two-qubit state is completely disentangled whence the asymptotic state becomes separable. Consequently, the coupling between the central system, initially in the maximally entangled state $|\Psi\rangle$, and the spin environment causes the qubits to lose entanglement.

- Let us now consider the maximally entangled state $|\Phi\rangle = \frac{1}{\sqrt{2}}(|--\rangle + |++\rangle)$. In this case the concurrence reads

$$C(\rho) = \max\{0, 2\rho_{13}(t) - \rho_{22}(t)\}. \tag{3.124}$$

The entanglement dynamics in this case is significantly different from the one corresponding to $|\Psi\rangle$. Indeed, the entanglement here decays from its maximum value, one, and vanishes within a certain interval of the time, then starts to increase and tends asymptotically to $C^{\infty}(\rho) = \frac{1}{8}$ as shown in Fig. 3.4. Hence, the state loses its entanglement for a short period of time in which the state is separable, entanglement between the qubits will appear again whilst the asymptotic state is partially entangled. Thus the effect of the environment is to decrease the amount of entanglement of the initial state.

The above state is a special case of the so-called Werner states; the general form of the density matrix corresponding to these states is given by

$$\rho^0 = \frac{1}{4}(1-p)\mathbb{I}_4 + p|\Phi\rangle\langle\Phi| \tag{3.125}$$

with $0 \leq p \leq 1$. One can show that the asymptotic density matrix is

$$\rho^{\infty} = \begin{pmatrix} \frac{2+p}{8} & 0 & \frac{3p}{16} & 0 \\ 0 & \frac{1}{4} & 0 & 0 \\ \frac{3p}{16} & 0 & \frac{2+p}{8} & 0 \\ 0 & 0 & 0 & \frac{1-p}{4} \end{pmatrix} \tag{3.126}$$

and has the concurrence

$$C(\rho^{\infty}) = \max\{0, \frac{5p-4}{8}\}. \tag{3.127}$$

This implies that the stationary state of the two-qubit system is entangled if $p > \frac{4}{5}$. When the last condition is satisfied the concurrence behaves in the same manner as the one associated with $|\Phi\rangle$, i.e. decreases from its initial maximum value, vanishes for certain interval of time to increase asymptotically to $C(\rho^{\infty})$. Once again, we find that the two-qubit state becomes partially entangled.

- Because of the symmetry, the concurrence corresponding to the initial states $\frac{1}{2}(|+\rangle \pm |-\rangle)(|+\rangle \pm |-\rangle)$ and $\frac{1}{\sqrt{2}}|\pm\rangle(|+\rangle \mp |-\rangle)$ is identically zero. The corresponding asymptotic states are always separable.

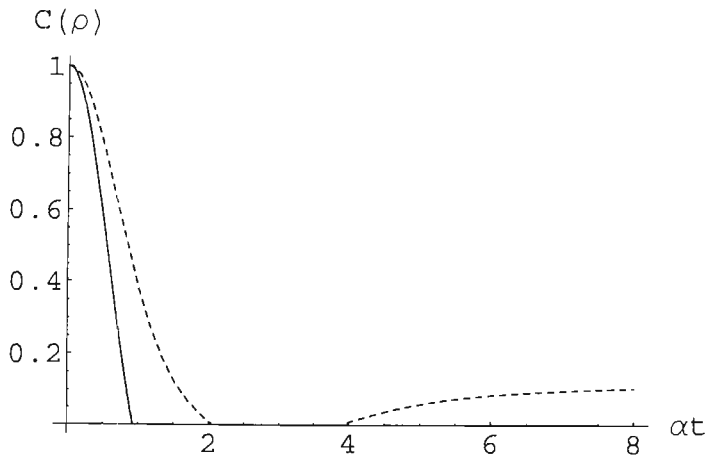

Fig. 3.4: Concurrence as a function of time for initial states $\frac{1}{\sqrt{2}}(|+-\rangle + |-+\rangle)$ (solid curve) and $\frac{1}{\sqrt{2}}(|--\rangle + |++\rangle)$ (dashed curve).

3.5 Conclusion

In this chapter, we have studied the dynamics of a two-qubit system in a spin star configuration. The Hamiltonian we chose describes a Heisenberg XY interaction. We obtained the exact analytical solution for the time evolution of the reduced system density matrix. This model can also describe the dynamics of a spin-one particle coupled to an environment. It may be used to test validity of numerical approximation techniques.

The solution which we have obtained simplifies in the limit of a large number of environmental spins. The limit is carried out by rescaling the coupling constant α. The long-time behavior of the density matrix reveals that some of the off-diagonal elements show partial decoherence. The pure entangled state $\frac{1}{\sqrt{2}}(|+-\rangle - |-+\rangle)$ of the two qubits is found to be decoherence-free, the mixed state $\frac{1}{3}(|1,-1\rangle\langle 1,-1| + |1,0\rangle\langle 1,0| + |1,1\rangle\langle 1,1|)$ written in the standard basis of a spin-one particle does not evolve in time. In these cases the central system does not feel the presence of the environment.

Any pure state of the two-qubit system evolves into a mixed state. It turns out that the environment has no effect on the separability of pure separable states. On the contrary, it

has the tendency to decrease the degree of entanglement of initially entangled states of the two-qubit system. This can be understood from the high symmetry of the XY interaction.

Many scenarios are possible regarding the extension of the model. One first step may consist of adding a suitable term to the interaction Hamiltonian and investigate the production of entanglement between the two qubits. Recently the dynamics of three qubits in a symmetry broken fermionic environment has been exactly solved [7]. This could be also investigated within the framework of the Heisenberg interaction and may be extended to more qubit cases. Because of the high symmetry of the Hamiltonian, we expect that some structure will appear when the number of central spins increases [14]. It will also be of interest to investigate the dynamics for environments that are in coherent or squeezed states.

BIBLIOGRAPHY

[1] D. Losse and D.P. DiVincenzo, Phys. Rev. A **57**, 120 (1998).

[2] J. Berezovsky, M. Ouyang, F. Meier and D.D. Awschalom, Phys. Rev. B **71**, 081309 (2005).

[3] H.P. Breuer and F. Petruccione, *The Theory of Open Quantum Systems* (Oxford University Press, Oxford, 2002).

[4] C.W. Gardiner, *Quantum Noise* (Springer, Berlin, 1991).

[5] M. Lucamarini, S. Paganelli and S. Mancini, Phys. Rev. A **67**, 062308 (2004).

[6] S. Paganelli, F. de Pasquale and S.M. Giampaolo, Phys. Rev. A **66**, 052317 (2002).

[7] X. San Ma, A. Min Wang, X. Dong Yang and H. You, J. Phys. A: Math. &Gen. **38** (2005).

[8] A. Hutton and S. Bose, Phys. Rev. A **69**, 042312 (2004).

[9] H.P. Breuer, D. Burgarth and F. Petruccione, Phys. Rev. B **70**, 045323 (2004).

[10] M.A. Nielsen and I.L. Chuang, *Quantum Computation and Quantum Information* (Cambridge University Press, Cambridge, 2000).

[11] Z. Gedik, `quant-ph/0505176v1` (2005).

[12] P. Zanardi, `quant-ph/0104114v3` (2002).

[13] C. Cohen-Tannoudji, B. Diu and F. Laloë, *Quantum Mechanics*, Vol. I and II (John Willey, New York, 1977).

[14] H.P. Breuer, Phys. Rev. A **71**, 062330 (2005).

[15] W.H. Zurek, S. Habib and I.P. Paz, Phys. Rev. A **70**, 1187 (1993).

[16] W.K. Wootters, Phys. Rev. Lett. **80**, 2245 (1998).

[17] G. Vidal, Phys. Rev. A **62**, 062315 (2000).

[18] L. Hardy, Phys. Rev. A **60**, 19121923 (1999).

[19] J. Wesemberg and K. Mølmer, Phys. Rev. A **65**, 062304 (2002).

[20] C.H. Bennett, G. Brassard, C. Crepeau, R. Jozsa, A. Peres, and W.K. Wootters, Phys. Rev. Lett. **70**, 1895 (1993).

[21] M. Danos and J. Rafelski, *Pocketbook of Mathematical Functions* (Verlag Harri Deutsch, Frankfurt, 1984).

[22] B.H. Armstrong, J. Quant. Spectrosc. Radiat. Transfer, **7**, 61-88, (1967).

4. DECOHERENCE AND ENTANGLEMENT EVOLUTION OF TWO QUBITS COUPLED THROUGH HEISENBERG INTERACTIONS TO SPIN BATH AT THERMAL EQUILIBRIUM

4.1 Introduction

Entanglement is the most intriguing feature of quantum mechanics. It is a nonlocal correlation between separate quantum mechanical systems which does not have a classical counterpart. Besides its fundamental importance in the foundation of quantum mechanics [1, 2, 3], entanglement is considered as a valuable resource for quantum communications and information processing [4, 5, 6, 7, 8, 9] since it helps speeding-up implementation of quantum algorithms and quantum communication protocols [10]. Considerable efforts, both theoretically and experimentally, have been devoted to the understanding of entanglement. Recently, intense interest was given to interacting spin systems which were proposed as candidates to achieve gate operations in solid-state quantum computation processors [11, 12]. This choice is motivated by the fact that such systems can be easily manipulated (e.g., by tunneling potentials and energy bias), and scaled up to large registers. Hence it is important to investigate entanglement generation and dynamics in spin systems.

On the other hand, quantum systems suffer decoherence because of their unwanted interactions with the surrounding environment. The decoherence process is indeed the major obstacle for quantum information processing because it directly affects quantum interferences and correlations (entanglement) of quantum systems, leading them to behave classically [13, 14, 15]. Many strategies such as error-correcting codes and decoherence free subspaces were proposed in order to protect fragile quantum information against the detrimental effect of decoherence [16, 17, 18, 19, 20, 21, 22]. A number of theoretical studies have dealt with bosonic environments for which the Markovian approximation along with the master equation approach are often used. It turns out that the main contribution to decoherence in many solid-state systems (e.g., quantum dots) arises from the coupling to localized modes like nuclear spins, which can be effectively regarded as spin baths [23]. Recently, attention was focused on the non-Markovian dynamics of multi-qubit systems

interacting with spin environments [24, 25, 26, 27, 28, 29]. In our earlier work [24], we have studied the reduced dynamics of two-qubit system coupled through Heisenberg XY interactions to spin star bath which was assumed at infinite temperature. We neglected the interaction between the central qubits. Later, Yuan *et al* [25], derived the dynamics of the two interacting qubits for particular initial states and finite bath temperature, using Holstein-Primakoff transformations expanded up to the first order with respect to the number of environmental spins. The elements of the resulting reduced density matrix were given in the thermodynamic limit by infinite series. In the following paper we derive the exact dynamics of the central qubits, for arbitrary number of environmental spins at finite bath temperature, for a particular choice of the Hamiltonian of the bath. The key ingredient in this case consists of the underlying symmetries of the model Hamiltonian which facilitate the derivation of exact analytical results.

The chapter is organized as follows. In section 4.2 we introduce the model Hamiltonian of the composite system qubits-bath. In section 4.3 after we derive the analytical form of the time evolution operator, we calculate the reduced density matrix for both finite and infinite number of spins within the environment. In section 4.4, we investigate decoherence and entanglement evolution of the two-qubit system for different initial states. We end with a short conclusion.

4.2 The Model

The system under consideration consists of a pair of interacting spin-$\frac{1}{2}$ particles (qubits) coupled to quantum bath composed of a large number of spin-$\frac{1}{2}$ particles in thermal equilibrium at temperature T. The number of environmental spins is denoted by N. The Hamiltonian of the composite system is given by the sum of three operators, namely,

$$H = H_0 + H_B + H_I. \tag{4.1}$$

H_0 describes the interaction between the central spins, it is given by the anisotropic Heisenberg Hamiltonian

$$H_0 = \Omega(\sigma_x^1\sigma_x^2 + \sigma_y^1\sigma_y^2) + \lambda\sigma_z^1\sigma_z^2, \tag{4.2}$$

where λ and Ω denote the strength of interactions, and σ_ν^i (with $\nu \equiv x, y, z$) is the ν-component of the pauli operator $\vec{\sigma}^i$associated with qubit number i. The corresponding spin-flip operators are defined by $\sigma_\pm^i = \frac{1}{2}(\sigma_x^i \pm \mathrm{i}\sigma_y^i)$.

Similarly, the environmental spins interact with each other through long-range anisotropic

Heisenberg interactions. These are described by the bath Hamiltonian

$$H_B = \frac{g}{N}\sum_{i<j}^{N}\Big(S^i_{Bx}S^j_{Bx} + S^i_{By}S^j_{By} + \Delta S^i_{Bz}S^j_{Bz}\Big), \tag{4.3}$$

where S^i_B ($i = 1, 2, ..., N$) are the spin operators of bath constituents, g is the strength of interactions and Δ is the anisotropy constant. The central spins couple to the environment through Heisenberg XY interactions, the corresponding Hamiltonian operator is given by

$$H_I = \frac{\alpha}{\sqrt{N}}\Big[(\sigma^1_x + \sigma^2_x)\sum_{i=1}^{N} S^i_{Bx} + (\sigma^1_y + \sigma^2_y)\sum_{i=1}^{N} S^i_{By}\Big]. \tag{4.4}$$

In the above equation, α designates the coupling constant of the qubits to the bath. Note that the coupling constants g and α are rescaled by, respectively, N and $\sqrt{N}$ in order to ensure good thermodynamical behavior.

By introducing the total spin operator of the environment, $\vec{J} = \frac{1}{2}\sum_{j=1}^{N}\vec{\sigma}^j$, together with the corresponding lowering and raising operators, $J_\pm = J_x \pm \mathrm{i}J_y$, it can be shown that (up to a trivial constant)

$$H_I + H_B = \frac{\alpha}{\sqrt{N}}\Big[(\sigma^1_+ + \sigma^2_+)J_- + (\sigma^1_- + \sigma^2_-)J_+\Big] + \frac{g}{2N}\Big[J^2 + (\Delta - 1)J_z^2)\Big]. \tag{4.5}$$

Clearly, the model Hamiltonian is invariant under rotations with respect to the z-direction. One can show by direct calculation that the operator $J_z + S^1_z + S^2_z$, where $S^i_z = \frac{1}{2}\sigma^i_z$, commutes with H, i.e., $[H, J_z + S^1_z + S^2_z]_- = 0$. This simply implies that the z-component of the total spin of the composite system is conserved.

The spin space corresponding to the central system is given by $\mathbb{C}^2 \otimes \mathbb{C}^2 \equiv \mathbb{C} \oplus \mathbb{C}^3$. The subspace $\mathbb{C}^3$ is spanned by the state vectors $|1,-1\rangle$, $|1,0\rangle$ and $|1,1\rangle$. These are related to the basis vectors of $\mathbb{C}^2 \otimes \mathbb{C}^2$ (called computational basis vectors) by $|1,\pm 1\rangle = |\pm,\pm\rangle$ and $|1,0\rangle = \frac{1}{\sqrt{2}}(|-+\rangle + |+-\rangle)$. The space $\mathbb{C}$ in turn is spanned by the antisymmetric maximally entangled bell state $|0,0\rangle = \frac{1}{\sqrt{2}}(|-+\rangle - |+-\rangle)$. The above equalities fully determine the unitary transformation that enable us to go from one basis to the other.

The standard basis of the bath space, $(\mathbb{C}^2)^{\otimes N}$, is composed of the joint eigenvectors of J^2 and J_z which we denote by $|j,m\rangle$, where $J^2|j,m\rangle = j(j+1)|j,m\rangle$ and $J_z|j,m\rangle = m|j,m\rangle$ (We set $\hbar = 1$, and assume N even). Note that $0 \le j \le N/2$ and $-j \le m \le j$. One can then decompose the spin space of the environment as the direct sum of subspaces $\mathbb{C}^{d_j}$ each of which has dimension $d_j = 2j + 1$, namely

$$(\mathbb{C}^2)^{\otimes N} = \bigoplus_{j=0}^{N/2} \nu(N,j)\mathbb{C}^{d_j}. \tag{4.6}$$

Here $\nu(N,j)$ is the multiplicity associated with j. In order to determine the explicit value of $\nu(N,j)$, let us introduce the subspace F_m of vectors $\vartheta \in (\mathbb{C}^2)^{\otimes N}$ satisfying $J_z\vartheta = m\vartheta$ [30]. The latter space can be decomposed as a direct sum of subspaces $E_{j,m}$ formed by the vectors $\bar{\vartheta}$ for which $J^2\bar{\vartheta} = j(j+1)\bar{\vartheta}$. Thus we simply have $F_m = \bigoplus_{j=m}^{N/2} E_{j,m}$, and $\dim(F_m) = \sum_{j=m}^{N/2} \dim(E_{j,m}) = \binom{N}{\frac{N}{2}-m}$. From the above, it immediately follows that

$$\nu(N,j) = \dim(F_j) - \dim(F_{j+1}) = \binom{N}{\frac{N}{2}-j} - \binom{N}{\frac{N}{2}-j-1}. \tag{4.7}$$

4.3 Exact time evolution

This section deals with the derivation of the exact reduced dynamics of the central qubits. The time dependence of the total density matrix describing the state of the composite system is given as usual by

$$\rho_{\text{tot}}(t) = \mathbf{U}(t)\rho_{\text{tot}}(0)\mathbf{U}^{\dagger}(t), \tag{4.8}$$

where $\mathbf{U}(t) = \exp(-\mathrm{i}Ht)$ is the time evolution operator and $\rho_{\text{tot}}(0)$ is the initial total density matrix. In the following, after we introduce the initial states of the central system and the bath, we derive the exact analytical form of $\mathbf{U}(t)$, then we calculate the time-dependent reduced density matrix $\rho(t)$ for both finite and infinite number of environmental spins.

4.3.1 Initial conditions

At $t = 0$ the central two-qubit system is assumed to be decoupled from the environment. This means that $\rho_{\text{tot}}(0)$ factorizes into the following direct product

$$\rho_{\text{tot}}(0) = \rho(0) \otimes \rho_B(0), \tag{4.9}$$

where $\rho(0)$ and $\rho_B(0)$ are, respectively, the initial density matrices corresponding to the two-qubit system and the environment.

Initially, the spin environment is taken in thermal equilibrium at finite temperature T. The density matrix $\rho_B(0)$ is simply given by the Boltzmann distribution

$$\rho_B(0) = \frac{1}{Z_N}\, \mathrm{e}^{-\frac{g\beta}{2N}[J^2+(\Delta-1)J_z^2]}, \tag{4.10}$$

where $Z_N = \mathrm{tr}_B\left\{\mathrm{e}^{-\frac{g\beta}{2N}[J^2+(\Delta-1)J_z^2]}\right\}$ is the partition function corresponding to the spin bath and $\beta = \frac{1}{T}$ is the inverse temperature. Note that the Boltzmann constant is set to

one, i.e. $k_B = 1$. The partition function Z_N can be expressed as [31]

$$Z_N = \sum_{j=0}^{N/2} \nu(N,j) \sum_{m=-j}^{j} \mathrm{e}^{-\frac{g\beta}{2N}[j(j+1)+(\Delta-1)m^2]}. \tag{4.11}$$

In particular, we have $\lim_{\beta\to\infty} \rho_B(0) = 2^{-N}\mathbb{I}_N$, where $\mathbb{I}_N$ stands for the unity matrix in the bath space.

Let us now assume that at $t = 0$ the two-qubit system is prepared in the normalized state $|\Psi(0)\rangle = \sum_i a_i|\xi_i\rangle$, where $|\xi_i\rangle \in \{|1,-1\rangle, |1,0\rangle, |1,1\rangle, |0,0\rangle\}$ and $\sum_i |a_i|^2 = 1$. Therefore, the initial density matrix of the central spins can be written in the standard basis of $\mathbb{C}\oplus\mathbb{C}^3$ as

$$\rho(0) = \sum_{ij} \rho^0_{ij}|\xi_i\rangle\langle\xi_j|, \quad \rho^0_{ij} = a_i a_j^*, \ \sum_{i=1}^{4} \rho^0_{ii} = 1. \tag{4.12}$$

The time-dependent density matrix $\rho(t)$ is calculated by performing the trace with respect to the environmental degrees of freedom, i.e. $\rho(t) = \mathrm{tr}_B\{\rho_{\mathrm{tot}}(t)\}$. This can be rewritten in terms of the common eigenvectors of J^2 and J_z as follows

$$\rho(t) = \sum_{k,\ell} \rho^0_{k\ell} \sum_{j=0}^{N/2} \nu(N,j) \sum_{m=-j}^{j} \langle jm|\mathbf{U}(t)|\xi_k\rangle \rho_B(0) \langle\xi_\ell|\mathbf{U}^\dagger(t)|jm\rangle. \tag{4.13}$$

4.3.2 Time evolution operator

Before we proceed with the determination of the reduced dynamics, it should be noted that the evolution in time of the central qubits depends on the nature of interactions between the spins in the environment. In the case of single central spin it is found that for antiferromagnetic interactions within the bath, the effect of the anisotropy constant Δ can be neglected when the number of environmental spins becomes sufficiently large (typically of the order of 100) [29]. The above result is independent of the number of central qubits as long as their coupling to the bath does not include interactions of the form $\sigma_z^i \otimes J_z$. Hence, it is sufficient to investigate the isotropic case which exhibits the advantage of making our model exactly solvable. This is mainly due to the fact that $[H_B, H_I] = 0$ when $\Delta = 1$, implying that the time evolution operator reduces to $\exp\{-\mathrm{i}(H_0 + H_I)\}$.

It is worth mentioning that due to symmetry, states belonging to $\mathbb{C}^3$ and $\mathbb{C}$ never mix; they evolve independently from each other without leaving the subspaces to which they belong. Thus we can write the model Hamiltonian as the direct sum of two operators living in the above subspaces. Indeed, the Hamiltonian operators H_0 and H_I can be written in

$\mathbb{C}^3 \otimes (\mathbb{C}^2)^{\otimes N}$ (up to a trivial constant for H_0) as

$$H_0 = \begin{pmatrix} \epsilon & 0 & 0 \\ 0 & -\epsilon & 0 \\ 0 & 0 & \epsilon \end{pmatrix} \otimes \mathbb{I}_N, \; H_I = \frac{\alpha}{\sqrt{N}} \begin{pmatrix} 0 & J_+ & 0 \\ J_- & 0 & J_+ \\ 0 & J_- & 0 \end{pmatrix}, \tag{4.14}$$

where $\epsilon = \lambda - \Omega$. Similarly, in the subspace $\mathbb{C} \otimes (\mathbb{C}^2)^{\otimes N}$ we can rewrite the free Hamiltonian as $H_0 = -\kappa \mathbb{I}_N$, where $\kappa = 3\Omega + \lambda$. Since the action of the interaction Hamiltonian vanishes in this subspace, it immediately follows that $H^n = (-\kappa)^n$. Furthermore, it can be shown that in $\mathbb{C}^3 \otimes (\mathbb{C}^2)^{\otimes N}$ the operator H_0 anticommutes with H_I, i.e., $[H_0, H_I]_+ = 0$ and $H^2 = H_I^2 + \epsilon^2$. We have shown in [24] that in $\mathbb{C}^3 \otimes (\mathbb{C}^2)^{\otimes N}$, powers of H_I are given by

$$H_I^{2n} = \left(\frac{\alpha}{\sqrt{N}}\right)^{2n} \begin{pmatrix} J_+ K^{n-1} J_- & 0 & J_+ K^{n-1} J_+ \\ 0 & K^n & 0 \\ J_- K^{n-1} J_- & 0 & J_- K^{n-1} J_+ \end{pmatrix}, \tag{4.15}$$

$$H_I^{2n+1} = \left(\frac{\alpha}{\sqrt{N}}\right)^{2n+1} \begin{pmatrix} 0 & J_+ K^n & 0 \\ K^n J_- & 0 & K^n J_+ \\ 0 & J_- K^n & 0 \end{pmatrix}, \tag{4.16}$$

where $K = J_+ J_- + J_- J_+ = 2(J^2 - J_z^2)$. Using the above relations it is possible to derive general expressions for even and odd powers of $H = H_0 + H_I$.

As an example, let us calculate H_{11}^{2n}. We have for $n \geq 1$

$$H^{2n} = \sum_{k=0}^{n} H_I^{2k} \epsilon^{2(n-k)} \binom{n}{k}. \tag{4.17}$$

Therefore,

$$\begin{aligned} H_{11}^{2n} &= \epsilon^{2n} + J_+ \sum_{\ell=1}^{n} \tilde{\alpha}^{2\ell} K^{\ell-1} \epsilon^{2(n-\ell)} \binom{n}{\ell} J_- \\ &= \epsilon^{2n} + J_+ \Big[\sum_{\ell=0}^{n} \frac{\tilde{\alpha}^{2\ell}}{K} K^{\ell} \epsilon^{2(n-\ell)} \binom{n}{\ell} - \frac{\epsilon^{2n}}{K} \Big] J_- \\ &= \epsilon^{2n} + J_+ \frac{(\epsilon^2 + \tilde{\alpha}^2 K)^n - \epsilon^{2n}}{K} J_-, \end{aligned} \tag{4.18}$$

where we have introduced $\tilde{\alpha} = \alpha/\sqrt{N}$ for ease of notation. Using the same method we get

$$H^{2n} = \begin{pmatrix} \epsilon^{2n} + J_+ \frac{(\epsilon^2 + \tilde{\alpha}^2 K)^n - \epsilon^{2n}}{K} J_- & 0 & J_+ \frac{(\epsilon^2 + \tilde{\alpha}^2 K)^n - \epsilon^{2n}}{K} J_+ \\ 0 & (\epsilon^2 + \tilde{\alpha}^2 K)^n & 0 \\ J_- \frac{(\epsilon^2 + \tilde{\alpha}^2 K)^n - \epsilon^{2n}}{K} J_- & 0 & \epsilon^{2n} + J_- \frac{(\epsilon^2 + \tilde{\alpha}^2 K)^n - \epsilon^{2n}}{K} J_+ \end{pmatrix}, \tag{4.19}$$

$$H^{2n+1} = \begin{pmatrix} \epsilon^{2n+1} + \epsilon J_+ \frac{(\epsilon^2+\tilde{\alpha}^2K)^n - \epsilon^{2n}}{K} J_- & \tilde{\alpha} J_+ (\epsilon^2 + \tilde{\alpha}^2 K)^n & \epsilon J_+ \frac{(\epsilon^2+\tilde{\alpha}^2K)^n - \epsilon^{2n}}{K} J_+ \\ \tilde{\alpha}(\epsilon^2 + \tilde{\alpha}K)^n J_- & -\epsilon(\epsilon^2 + \tilde{\alpha}^2 K)^n & \tilde{\alpha}(\epsilon^2 + \tilde{\alpha}^2 K)^n J_+ \\ \epsilon J_- \frac{(\epsilon^2+\tilde{\alpha}^2K)^n - \epsilon^{2n}}{K} J_- & \tilde{\alpha} J_- (\epsilon^2 + \tilde{\alpha}^2 K)^n & \epsilon^{2n+1} + \epsilon J_- \frac{(\epsilon^2+\tilde{\alpha}^2K)^n - \epsilon^{2n}}{K} J_+ \end{pmatrix} \quad (4.20)$$

Now we have all the ingredients that enable us to derive the explicit form of the time evolution operator. Indeed, expanding $\mathbf{U}(t)$ in power series and using equations (4.19) and (4.20) we find that the matrix elements of the time evolution operator in the space $\mathbb{C}^3 \oplus \mathbb{C}$ are given by

$$U_{11}(t) = \exp(-\mathrm{i}\epsilon t) + J_+ \Big[\frac{\cos(tM) - \cos(\epsilon t)}{K} - \mathrm{i} \frac{\epsilon \sin(tM) - M \sin(\epsilon t)}{KM} \Big] J_-, \quad (4.21)$$

$$U_{12}(t) = -\mathrm{i}\tilde{\alpha} J_+ \frac{\sin(tM)}{M}, \quad (4.22)$$

$$U_{13}(t) = J_+ \Big[\frac{\cos(tM) - \cos(\epsilon t)}{K} - \mathrm{i} \frac{\epsilon \sin(tM) - M \sin(\epsilon t)}{KM} \Big] J_+, \quad (4.23)$$

$$U_{22}(t) = \cos(tM) + \mathrm{i}\epsilon \frac{\sin(tM)}{M}, \quad (4.24)$$

$$U_{23}(t) = -\mathrm{i}\tilde{\alpha} \frac{\sin(tM)}{M} J_+, \quad (4.25)$$

$$U_{33}(t) = \exp(-\mathrm{i}\epsilon t) + J_- \Big[\frac{\cos(tM) - \cos(\epsilon t)}{K} - \mathrm{i} \frac{\epsilon \sin(tM) - M \sin(\epsilon t)}{KM} \Big] J_+, \quad (4.26)$$

$$U_{14}(t) = U_{24}(t) = U_{34}(t) = 0, \quad (4.27)$$

$$U_{44}(t) = \exp(\mathrm{i}\kappa t), \quad (4.28)$$

where we have introduced the operator $M = \sqrt{\epsilon^2 + \alpha^2 K/N}$. The remaining matrix elements can be found by simply taking the transpose (not the hermitian conjugate) of those listed above. Taking into account the trace properties of the lowering and raising operators, it can be shown by virtue of equation (4.13) that the elements of the reduced density matrix can be written as

$$\rho_{11}(t) = \mathrm{tr}_B \Big\{ \rho_B(0) \Big[\rho_{11}^0 U_{11}(t) U_{11}^\dagger(t) + \rho_{22}^0 U_{12}(t) U_{12}^\dagger(t) + \rho_{33}^0 U_{13}(t) U_{13}^\dagger(t) \Big] \Big\}, \quad (4.29)$$

$$\rho_{12}(t) = \mathrm{tr}_B \Big\{ \rho_B(0) \Big[\rho_{12}^0 U_{11}(t) U_{22}^\dagger(t) + \rho_{23}^0 U_{12}(t) U_{23}^\dagger(t) \Big] \Big\}, \quad (4.30)$$

$$\rho_{13}(t) = \mathrm{tr}_B \Big\{ \rho_B(0) \Big[\rho_{13}^0 U_{11}(t) U_{33}^\dagger(t) \Big] \Big\}, \quad (4.31)$$

$$\rho_{14}(t) = \mathrm{tr}_B \Big\{ \rho_B(0) \Big[\rho_{14}^0 U_{11}(t) U_{44}^\dagger(t) \Big] \Big\}, \quad (4.32)$$

$$\rho_{22}(t) = \mathrm{tr}_B \Big\{ \rho_B(0) \Big[\rho_{11}^0 U_{21}(t) U_{21}^\dagger(t) + \rho_{22}^0 U_{22}(t) U_{22}^\dagger(t) + \rho_{33}^0 U_{23}(t) U_{23}^\dagger(t) \Big] \Big\}, \quad (4.33)$$

$$\rho_{23}(t) = \mathrm{tr}_B \Big\{ \rho_B(0) \Big[\rho_{12}^0 U_{21}(t) U_{32}^\dagger(t) + \rho_{23}^0 U_{22}(t) U_{33}^\dagger(t) \Big] \Big\}, \quad (4.34)$$

$$\rho_{24}(t) = \mathrm{tr}_B \Big\{ \rho_B(0) \Big[\rho_{24}^0 U_{22}(t) U_{44}^\dagger(t) \Big] \Big\}, \quad (4.35)$$

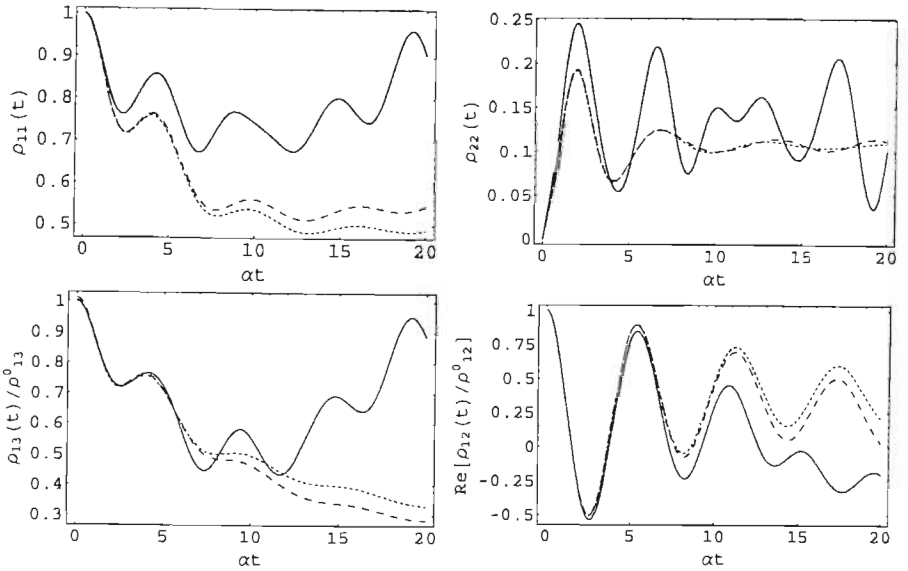

Fig. 4.1: Evolution in time of some elements of the reduced density matrix for different values of environmental spins: $N = 10$ (solid lines), $N = 100$ (dashed lines), and $N = 300$ (dotted lines). The initial state corresponding to $\rho_{11}(t)$ and $\rho_{22}(t)$ is the product state $|--\rangle$. Here we have set $\rho^0_{12} = \rho^0_{23}$. The parameters are $\epsilon = \alpha$ and $g\beta = 10$.

$$\rho_{33}(t) = \mathrm{tr}_B\Big\{\rho_B(0)\Big[\rho^0_{11}U_{31}(t)U^\dagger_{31}(t) + \rho^0_{22}U_{32}(t)U^\dagger_{32}(t) + \rho^0_{33}U_{33}(t)U^\dagger_{33}(t)\Big]\Big\}, \quad (4.36)$$

$$\rho_{34}(t) = \mathrm{tr}_B\Big\{\rho_B(0)\Big[\rho^0_{34}U_{33}(t)U^\dagger_{44}(t)\Big]\Big\}, \quad (4.37)$$

$$\rho_{44}(t) = \rho^0_{44}. \quad (4.38)$$

The remaining matrix elements are obtained by taking the complex conjugate of those listed above.

Figure 4.1 illustrates the time dependence of some elements of the reduced density matrix for different values of the number of spins in the environment. We can see that the curves corresponding to each matrix element get more and more closer from each other as the number of bath spins increases. If we let N to take sufficiently large values ($N \sim 100$), then the curves saturate with respect to N and become almost identical. In the next subsection we study the case in which $N \to \infty$. All the results regarding decoherence and entanglement evolution will be studied in this limit.

4.3.3 *Infinite number of spins in the bath*

In order to study the limit of an infinite number of environmental spins it should be stressed that the operators $J_\pm$ as well as J_z are traceless in the standard basis formed

by the common eigenvectors of J^2 and J_z. Moreover, the scaled lowering and raising operators $J_\pm/\sqrt{N}$ are well behaved fluctuation operators with respect to the tracial state on the bath, and satisfy

$$\lim_{N\to\infty} 2^{-N}\mathrm{tr}_B\Big\{\prod_{i=1}^{k}\Big(\frac{J_\pm J_\mp}{N}\Big)^{n_i}\Big\}=\lim_{N\to\infty} 2^{-N}\mathrm{tr}_B\Big\{\prod_{i=1}^{k}\Big(\frac{J_\pm}{\sqrt{N}}\Big)^{n_i}\Big(\frac{J_\mp}{\sqrt{N}}\Big)^{n_i}\Big\}=\frac{n!}{2^n},$$

where $n=\sum_{i=1}^{k} n_i$ and $n_i\in\mathbb{N}$. This follows from the fact that [24, 27]

$$\mathrm{tr}_B\{(J_+J_-)^n\}\approx\frac{2^N N^n n!}{2^n}. \tag{4.39}$$

Thus , $J_+/\sqrt{N}$ converges to a normal complex random variable, z, with the probability density function [24]

$$z\mapsto\frac{2}{\pi}\mathrm{e}^{-2|z|^2}. \tag{4.40}$$

In particular, we can infer that

$$\lim_{N\to\infty} 2^{-N}\mathrm{tr}_B\Big\{f\Big(\frac{J_\pm J_\mp}{N}\Big)\Big\}=\frac{2}{\pi}\int_{\mathbb{C}} f(|z|^2)\mathrm{e}^{-2|z|^2}\mathrm{d}z\mathrm{d}z^* \tag{4.41}$$

provided that the integral converges. This is typically the case for the functions $\mathrm{e}^{-ar^2}h(r^2)$ where $|h(r^2)|<\infty$, $r\in\mathbb{R}$ and $\mathrm{Re}(a)>-2$. Similarly, the operator $J_z/\sqrt{N}$ converges to a normal real random variable, τ, with probability density function

$$\tau\mapsto\sqrt{\frac{2}{\pi}}\mathrm{e}^{-2\tau^2}. \tag{4.42}$$

In this case a similar equation to (4.41) can be obtained by replacing $J_\pm/\sqrt{N}$ and $|z|$ by $J_z/\sqrt{N}$ and τ, respectively. We have already mentioned that for antiferromagnetic interactions within the bath, isotropic and anisotropic Heisenberg Hamiltonian operators with $\Delta\geq 0$ are completely equivalent when $N\to\infty$. Let us explain this a little bit. One can see that $\rho_B(0)$ always appears between two matrix elements of $\mathbf{U}(t)$. If we exchange the order of $\rho_B(t)$ with one of the above matrix elements, which is possible using simple commutation relations, we end up with extra operators of the form J_z/N. These can be indeed neglected when $N\to\infty$. Then using the cyclic property of the trace, it is possible to transform any function $\Upsilon_{ijk\ell}=U_{ij}U^\dagger_{k\ell}$ inside the trace sign into a function which depends on $\frac{J_\pm J_\mp}{N}$. Hence for all $\Delta\geq 0$

$$\begin{aligned}\langle\Upsilon_{ijk\ell}\rangle &= \lim_{N\to\infty}\frac{1}{\mathrm{tr}_B\Big\{\mathrm{e}^{\frac{-g\beta}{2N}[J^2+(\Delta-1)J_z^2]}\Big\}}\mathrm{tr}_B\Big\{\mathrm{e}^{\frac{-g\beta}{2N}[J^2+(\Delta-1)J_z^2]}\Upsilon_{ijk\ell}\Big(\frac{J_\pm J_\mp}{N}\Big)\Big\}\\ &= \frac{\int_{\mathbb{R}}\int_{\mathbb{C}}\exp\{-(2+g\beta/2)|z|^2-(2+g\beta\Delta/2)\tau^2\}\Upsilon_{ijk\ell}(|z|^2)\mathrm{d}\tau\mathrm{d}z\mathrm{d}z^*}{\int_{\mathbb{R}}\int_{\mathbb{C}}\exp\{-(2+g\beta/2)|z|^2-(2+g\beta\Delta/2)\tau^2\}\mathrm{d}\tau\mathrm{d}z\mathrm{d}z^*}\\ &= \frac{\int_0^\infty \mathrm{e}^{-(2+g\beta/2)r^2}\Upsilon_{ijk\ell}(r^2)r\mathrm{d}r}{\int_0^\infty \mathrm{e}^{-(2+g\beta/2)r^2}r\mathrm{d}r}=(4+g\beta)\int_0^\infty \mathrm{e}^{-(2+g\beta/2)r^2}\Upsilon_{ijk\ell}(r^2)r\mathrm{d}r\end{aligned} \tag{4.43}$$

where we have used polar coordinates (r,ϕ) to simplify the integrals with respect to the complex variable $z = re^{i\phi}$. Clearly the latter expression is independent of Δ. Using the above result we find that

$$\begin{aligned}
\langle U_{11}U_{11}^\dagger\rangle &= \langle U_{11}U_{33}^\dagger\rangle = \langle U_{33}U_{33}^\dagger\rangle \\
&= \frac{1}{4}\Big[\frac{3}{2} + \frac{1}{2}f(2t) + 2\cos(\epsilon t)f(t) + g(t) + 2\sin(\epsilon t)\ell(t)\Big], && (4.44)\\
\langle U_{12}U_{12}^\dagger\rangle &= \langle U_{12}U_{23}^\dagger\rangle = \langle U_{23}U_{23}^\dagger\rangle = \langle U_{32}U_{32}^\dagger\rangle = h(t), && (4.45)\\
\langle U_{13}U_{13}^\dagger\rangle &= \frac{1}{4}\Big[\frac{3}{2} + \frac{1}{2}f(2t) - 2\cos(\epsilon t)f(t) + g(t) - 2\sin(\epsilon t)\ell(t)\Big], && (4.46)\\
\langle U_{11}U_{22}^\dagger\rangle &= \frac{1}{2}\Big[\frac{1}{2} + \frac{1}{2}f(2t) - g(t) - i\ell(2t) + e^{-i\epsilon t}\Big(f(t) - i\ell(t)\Big)\Big], && (4.47)\\
\langle U_{22}U_{22}^\dagger\rangle &= \frac{1}{2}\Big[1 + f(2t) + 2g(t)\Big], && (4.48)\\
\langle U_{22}U_{33}^\dagger\rangle &= \frac{1}{2}\Big[\frac{1}{2} + \frac{1}{2}f(2t) - g(t) + i\ell(2t) + e^{i\epsilon t}\Big(f(t) + i\ell(t)\Big)\Big], && (4.49)\\
\langle U_{11}\rangle &= \langle U_{33}\rangle = \frac{1}{2}\Big[f(t) - i\ell(t) + e^{-i\epsilon t}\Big], && (4.50)\\
\langle U_{22}\rangle &= f(t) + i\ell(t). && (4.51)
\end{aligned}$$

Here we have introduced the functions

$$\begin{aligned}
f(t) &= \Big\langle \cos\Big(t\sqrt{\epsilon^2+2r^2}\Big)\Big\rangle, \qquad g(t) = \Big\langle \epsilon^2 \frac{\sin^2\Big(t\sqrt{\epsilon^2+2r^2}\Big)}{\epsilon^2+2r^2}\Big\rangle,\\
h(t) &= \Big\langle r^2 \frac{\sin^2\Big(t\sqrt{\epsilon^2+2r^2}\Big)}{\epsilon^2+2r^2}\Big\rangle, \quad \ell(t) = \Big\langle \epsilon \frac{\sin\Big(t\sqrt{\epsilon^2+2r^2}\Big)}{\sqrt{\epsilon^2+2r^2}}\Big\rangle, \qquad (4.52)
\end{aligned}$$

where ϵ and t are, respectively, given in units of α^{-1} and α. Let us derive for example the explicit expression of $\ell(t)$. We have

$$\begin{aligned}
\ell(t) &= \epsilon(4+g\beta)\int_0^\infty e^{-(2+g\beta/2)r^2}\frac{\sin\Big(t\sqrt{\epsilon^2+2r^2}\Big)}{\sqrt{\epsilon^2+2r^2}} r dr\\
&= \frac{\epsilon}{2}(4+g\beta)\, e^{\frac{\epsilon^2}{4}(4+g\beta)}\int_\epsilon^\infty d\eta\, e^{-\frac{\eta^2}{4}(4+g\beta)}\sin(\eta t), \qquad (4.53)
\end{aligned}$$

where we have made the change of variable $\eta^2 = \epsilon^2 + 2r^2$. The above expression can be further simplified to

$$\ell(t) = \epsilon(4+g\beta)\ \exp\Big[\frac{\epsilon^2}{4}(4+g\beta) - \frac{t^2}{4+g\beta}\Big]\mathrm{Im}\Big\{\int_a^\infty e^{-\delta^2}\mathrm{d}\delta\Big\}, \qquad (4.54)$$

where $\delta = \frac{\eta}{2}\sqrt{4+g\beta} - i\frac{t}{\sqrt{4+g\beta}}$, $a = \frac{\epsilon}{2}\sqrt{4+g\beta} - i\frac{t}{\sqrt{4+g\beta}}$, and $\mathrm{Im}(x)$ stands for the imaginary part of x. The latter integral is nothing but the complementary error function [32], which

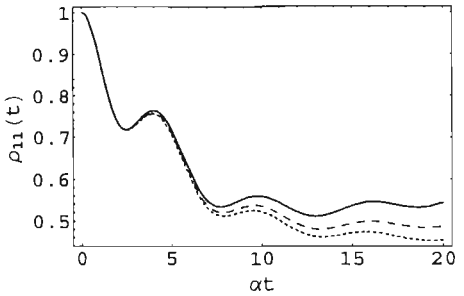

Fig. 4.2: Comparison between the behaviour of $\rho_{11}(t)$ obtained for finite and infinite number of environmental spins: $N = 100$ (solid line), $N = 300$ (dashed line), and $N \to \infty$ (dotted line). The initial state is $|--\rangle$ with $\epsilon = \alpha$ and $g\beta = 10$.

can be transformed into a sum of two ordinary error functions and we simply get

$$\ell(t) = \frac{i\sqrt{\pi}\epsilon}{4}\sqrt{4+g\beta}\exp\Big[\frac{\epsilon^2}{4}(4+g\beta)-\frac{t^2}{4+g\beta}\Big] \times\Big\{\mathrm{erf}\Big[\frac{\epsilon/2(4+g\beta)-it}{\sqrt{4+g\beta}}\Big]-\mathrm{erf}\Big[\frac{\epsilon/2(4+g\beta)+it}{\sqrt{4+g\beta}}\Big]\Big\}, \tag{4.55}$$

with

$$\mathrm{erf}(z) = \frac{2}{\sqrt{\pi}}\int_0^z \mathrm{e}^{-t^2}\,\mathrm{d}t. \tag{4.56}$$

Following the same method we find that

$$f(t) = \cos(\epsilon t)+\frac{it}{2}\sqrt{\frac{\pi}{4+g\beta}}\exp\Big[\frac{\epsilon^2}{4}(4+g\beta)-\frac{t^2}{4+g\beta}\Big] \times\Big\{\mathrm{erf}\Big[\frac{\frac{\epsilon}{2}(4+g\beta)+it}{\sqrt{4+g\beta}}\Big]-\mathrm{erf}\Big[\frac{\frac{\epsilon}{2}(4+g\beta)-it}{\sqrt{4+g\beta}}\Big]\Big\}, \tag{4.57}$$

$$g(t) = \frac{\epsilon^2(4+g\beta)}{8}\,\mathrm{e}^{\frac{\epsilon^2}{4}(4+g\beta)}\Gamma\Big[0,\frac{\epsilon^2}{4}(4+g\beta)\Big]-\frac{\epsilon^2(4+g\beta)}{4}\mathrm{e}^{\frac{\epsilon^2}{4}(4+g\beta)} \times\int_\epsilon^\infty \mathrm{d}r\frac{\cos(2rt)}{r}\mathrm{e}^{-\frac{r^2}{4}(4+g\beta)}, \tag{4.58}$$

$$h(t) = \frac{1}{4}-\frac{\epsilon^2}{16}(4+g\beta)\mathrm{e}^{\frac{\epsilon^2}{4}(4+g\beta)}\Gamma\Big[0,\frac{\epsilon^2}{4}(4+g\beta)\Big]-\frac{1}{4}\cos(2\epsilon t) +\frac{it}{4}\sqrt{\frac{\pi}{4+g\beta}}\exp\Big[\frac{\epsilon^2}{4}(4+g\beta)-\frac{4t^2}{4+g\beta}\Big]\Big\{\mathrm{erf}\Big[\frac{\frac{\epsilon}{2}(4+g\beta)-2it}{\sqrt{4+g\beta}}\Big] -\mathrm{erf}\Big[\frac{\frac{\epsilon}{2}(4+g\beta)+2it}{\sqrt{4+g\beta}}\Big]\Big\}+\frac{\epsilon^2(4+g\beta)}{8}\mathrm{e}^{\frac{\epsilon^2}{4}(4+g\beta)}\int_\epsilon^\infty \mathrm{d}r\frac{\cos(2rt)}{r}\mathrm{e}^{-\frac{r^2}{4}(4+g\beta)} \tag{4.59}$$

where

$$\Gamma(a,z) = \int_z^\infty t^{a-1}\mathrm{e}^{-t}\,\mathrm{d}t \tag{4.60}$$

is the incomplete gamma function. Note that the integral in equations (4.58) and (4.59) cannot be calculated analytically, we leave it in that form.

Using the Riemann-Lebesgue lemma it is possible to find the asymptotic behaviour (i.e. when $t \to \infty$) of the above functions, namely

$$f(\infty) = \ell(\infty) = 0, \tag{4.61}$$

$$g(\infty) = \frac{\epsilon^2}{8}(4+g\beta)\, \mathrm{e}^{\frac{\epsilon^2}{4}(4+g\beta)}\Gamma\Big[0, \frac{\epsilon^2}{4}(4+g\beta)\Big], \tag{4.62}$$

$$h(\infty) = \frac{1}{4} - \frac{\epsilon^2}{16}(4+g\beta)\, \mathrm{e}^{\frac{\epsilon^2}{4}(4+g\beta)}\Gamma\Big[0, \frac{\epsilon^2}{4}(4+g\beta)\Big], \tag{4.63}$$

Furthermore, we can prove using the following asymptotic expression of the incomplete gamma function [32]

$$\Gamma(a,z) \sim z^{a-1}\mathrm{e}^{-z}\Big[1 + \frac{a-1}{z} + \frac{(a-1)(a-2)}{z^2} + ...\Big], \tag{4.64}$$

when $z \to \infty$ provided $|\arg z| < 3\pi/2$, that

$$\lim_{\beta,\epsilon\to\infty} g(\infty) = \frac{1}{2}, \quad \lim_{\beta,\epsilon\to\infty} h(\infty) = 0. \tag{4.65}$$

The latter results will be used below to study decoherence and entanglement of the central qubits. In figure 4.2 we have displayed the evolution in time of $\rho_{11}(t)$ corresponding to the state $|--\rangle$ for different vales of N including the limit $N \to \infty$.

4.3.4 Second-order master equation

The second order master equation can be derived in the interaction picture by noting that

$$\tilde{\rho}_{\mathrm{tot}}(t) = \rho(0)\otimes\rho_B(0) - \mathrm{i}\int_0^t [\tilde{H}_I(s), \tilde{\rho}_{\mathrm{tot}}(s)]\mathrm{d}s, \tag{4.66}$$

where $\tilde{A}(t) = \mathrm{e}^{\mathrm{i}H_0 t}A(t)\mathrm{e}^{-\mathrm{i}H_0 t}$. It is easy to see that

$$\mathrm{tr}_B\Big\{[\tilde{H}_I(t), \rho(0)\otimes\rho_B(0)]\Big\} = 0. \tag{4.67}$$

Then under Born approximation, one can show that the second order master equation yields the following set of integro-differential equations

$$\dot{\tilde{\rho}}_{11}(t) = -2\alpha^2 R \int_0^t \cos[2\epsilon(t-s)]\Big[\tilde{\rho}_{11}(s) - \tilde{\rho}_{22}(s)\Big]\, \mathrm{d}s, \tag{4.68}$$

$$\dot{\tilde{\rho}}_{12}(t) = -\alpha^2 R \int_0^t \Big[3\mathrm{e}^{2\mathrm{i}\epsilon(t-s)}\tilde{\rho}_{12}(s) - 2\mathrm{e}^{2\mathrm{i}\epsilon(t+s)}\tilde{\rho}_{23}(s)\Big]\, \mathrm{d}s, \tag{4.69}$$

$$\dot{\tilde{\rho}}_{13}(t) = -2\alpha^2 R \int_0^t \cos[2\epsilon(t-s)]\tilde{\rho}_{13}(s)\, \mathrm{d}s, \tag{4.70}$$

$$\dot{\tilde{\rho}}_{22}(t) = -2\alpha^2 R \int_0^t \cos[2\epsilon(t-s)]\Big[2\tilde{\rho}_{22}(s) - \tilde{\rho}_{11}(s) - \tilde{\rho}_{33}(s)\Big]\, \mathrm{d}s, \tag{4.71}$$

$$\dot{\tilde{\rho}}_{23}(t) = -\alpha^2 R \int_0^t \Big[3\mathrm{e}^{2\mathrm{i}\epsilon(s-t)}\tilde{\rho}_{23}(s) - 2\mathrm{e}^{-2\mathrm{i}\epsilon(s+t)}\tilde{\rho}_{12}(s)\Big]\, \mathrm{d}s, \tag{4.72}$$

$$\dot{\tilde{\rho}}_{33}(t) = -2\alpha^2 R \int_0^t \cos[2\epsilon(t-s)]\Big[\tilde{\rho}_{33}(s) - \tilde{\rho}_{22}(s)\Big]\, \mathrm{d}s, \tag{4.73}$$

$$\dot{\tilde{\rho}}_{14}(t) = -\alpha^2 R \int_0^t \mathrm{e}^{2\mathrm{i}\epsilon(t-s)}\tilde{\rho}_{14}(s)\, \mathrm{d}s, \tag{4.74}$$

$$\dot{\tilde{\rho}}_{24}(t) = -2\alpha^2 R \int_0^t \mathrm{e}^{-2\mathrm{i}\epsilon(t-s)}\tilde{\rho}_{24}(s)\, \mathrm{d}s, \tag{4.75}$$

$$\dot{\tilde{\rho}}_{34}(t) = -\alpha^2 R \int_0^t \mathrm{e}^{2\mathrm{i}\epsilon(t-s)}\tilde{\rho}_{34}(s)\, \mathrm{d}s, \tag{4.76}$$

$$\dot{\tilde{\rho}}_{44}(t) = 0, \tag{4.77}$$

where the correlation function is given by $R = \mathrm{tr}_B\Big\{\frac{J_+J_-}{N}\rho_B(0)\Big\} = \mathrm{tr}_B\Big\{\frac{J_-J_+}{N}\rho_B(0)\Big\}$. In the limit $N \to \infty$, we find that $R = \frac{2}{4+g\beta}$. Clearly, $\dot{\tilde{\rho}}_{11}(t) + \dot{\tilde{\rho}}_{22}(t) + \dot{\tilde{\rho}}_{33}(t) = 0$, as it should be because $\tilde{\rho}_{44}(t) = \rho_{44}(t) = \rho_{44}(0)$. The time-local master equation can be obtained by replacing the matrix elements $\tilde{\rho}_{ij}(s)$ in equations (4.68-4.77) by $\tilde{\rho}_{ij}(t)$. The integration of the resulting first order differential equations yields solutions involving the exponential function. For example when $\epsilon = 0$, we find that

$$\rho_{13}(t) = \rho_{13}(0)\exp\Big[-\frac{2\alpha^2 t^2}{4+g\beta}\Big]. \tag{4.78}$$

This solution is valid only at short intervals of time, it quickly diverges from the exact solution as t increases. Nevertheless, we can see that the Gaussian behaviour is clearly reproduced. It should be noted that the form of the master equation presented in the paper where this chapter has been published are somewhat wrong. All matrix elements within the integrand are, in fact, written in the Schrödinger picture, while the left-hand side is written in the interaction picture. We shall not solve the above equations since we shall encounter similar ones in chapter 6, where we obtained analytical solutions for the time-local master equation.

4.4 Decoherence and entanglement evolution

From equation (4.38), we can see that the maximally entangled state $|0,0\rangle$ does not evolve in time. The corresponding one-dimensional subspace $\mathbb{C}$ is thus decoherence-free. Taking into account the unitarity condition of the time evolution operator $\mathbf{U}(t)\mathbf{U}^{\dagger}(t) = \mathbb{I}_4$, we find that the state $\frac{1}{3}\mathbb{I}_3$ is also decoherence-free. Hence the decoherence-free subspace of our model is of dimension two. The qubits prepared in any linear combination of the above states do not perceive the surrounding environment. On the contrary, any other pure state decoheres evolving into mixed one and hence loses partially or completely its purity.

Generally speaking, the elements of the reduced density matrix show partial decoherence. Indeed, by virtue of equations (4.61-4.63), it can be shown that the elements of the stationary density matrix $\rho(\infty)$ are given by

$$\rho_{11}(\infty) = \rho_{33}(\infty) = \frac{1}{8}\Big[(3+\Sigma)(\rho_{11}^0+\rho_{33}^0) + 2\rho_{22}^0(1-\Sigma)\Big], \tag{4.79}$$

$$\rho_{12}(\infty) = \rho_{23}(\infty) = \frac{\rho_{12}^0+\rho_{23}^0}{4}(1-\Sigma), \tag{4.80}$$

$$\frac{\rho_{13}(\infty)}{\rho_{13}^0} = \frac{3+\Sigma}{8}, \tag{4.81}$$

$$\frac{\rho_{14}(\infty)}{\rho_{14}^0} = \frac{\rho_{34}(\infty)}{\rho_{34}^0} = \frac{1}{2}\,\mathrm{e}^{-\mathrm{i}(\epsilon+\kappa)t}, \tag{4.82}$$

$$\rho_{22}(\infty) = \frac{1}{4}\Big[(1-\Sigma)(\rho_{11}^0+\rho_{33}^0) + 2\rho_{22}^0(1+\Sigma)\Big], \tag{4.83}$$

$$\rho_{24}(\infty) = 0, \tag{4.84}$$

$$\rho_{44}(\infty) = \rho_{44}^0, \tag{4.85}$$

where $\Sigma = \frac{\epsilon^2}{4}(4+g\beta)\exp[\frac{\epsilon^2}{4}(4+g\beta)]\Gamma[0, \frac{\epsilon^2}{4}(4+g\beta)]$. Note that the latter quantity satisfies $0 \leq \Sigma \leq 1$. This allows us to find upper bounds of the asymptotic values of the matrix elements $\rho_{ij}(\infty)$. For instance, if $2\rho_{22}^0 \leq \rho_{11}^0+\rho_{33}^0$ then we have $\rho_{11}(\infty) \leq \frac{1}{2}(\rho_{11}^0+\rho_{33}^0)$ and $\rho_{13}(\infty) \leq \frac{1}{2}\rho_{13}^0$. Similarly, when $2\rho_{22}^0 \geq \rho_{11}^0+\rho_{33}^0$ then $\rho_{11}(\infty) \leq \frac{1}{8}[2\rho_{22}^0 + 3(\rho_{11}^0+\rho_{33}^0)]$, and $\rho_{22}(\infty) \leq \rho_{22}^0$. The matrix elements $\rho_{14}(\infty)$ and $\rho_{34}(\infty)$ oscillate around half of their initial values with period equal to $2\pi/(\epsilon+\kappa)$. When $\epsilon = 0$, the asymptotic state is independent of the bath temperature.

4.4.1 Measures of decoherence and entanglement

Due to the decoherence process, initially pure states evolve into mixed ones. Thus it is natural to use the extent of mixing as a measure of decoherence. This task can be carried

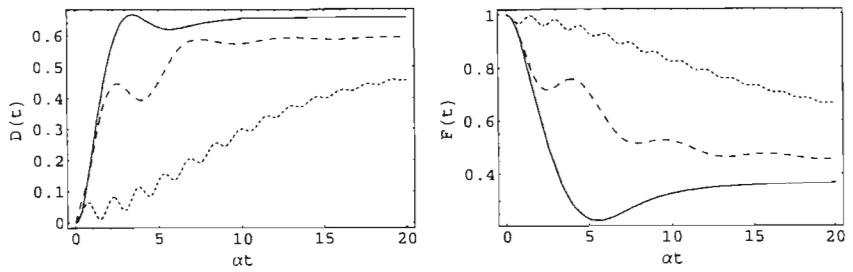

Fig. 4.3: Time evolution of the linear entropy and the fidelity in the case of the initial state $|--\rangle$ for different values of ϵ: $\epsilon = 0$ (solid lines), $\epsilon = 0.5\alpha$ (dashed lines), and $\epsilon = 2\alpha$ (dotted lines) with $g\beta = 10$.

out with the help of the quantity

$$D(t) = 1 - \mathrm{tr}\Big[\rho(t)^2\Big], \tag{4.86}$$

usually called linear entropy or idempotency. The above measure is effectively a monotonic decreasing function of the purity of the system, it vanishes for pure states and reaches its maximum value, $D_{\max} = \frac{3}{4}$, for the completely mixed state $\frac{1}{4}\mathbb{I}_4$.

Although the linear entropy quantifies the decoherence, it does not provide any other information about the state of the system. The so-called *Fidelity*, which we denote by $F(t)$, is a measure of decoherence that quantifies the deviation from the free evolution of the system, i.e., in absence of the surrounding environment [33]. Explicitly, we have

$$F(t) = \mathrm{tr}\Big[\bar{\rho}(t)\rho(t)\Big], \tag{4.87}$$

where $\bar{\rho}(t)$ describes the evolution, under the influence of the Hamiltonian operator H_0, of the central system initially prepared in the pure state $\rho(0)$, namely

$$\bar{\rho}(t) = \mathrm{e}^{-\mathrm{i}H_0 t}\rho(0)\, e^{\mathrm{i}H_0 t}, \quad \mathrm{e}^{-\mathrm{i}H_0 t} = \begin{pmatrix} \mathrm{e}^{-\mathrm{i}\epsilon t} & 0 & 0 & 0 \\ 0 & \mathrm{e}^{\mathrm{i}\epsilon t} & 0 & 0 \\ 0 & 0 & \mathrm{e}^{-\mathrm{i}\epsilon t} & 0 \\ 0 & 0 & 0 & \mathrm{e}^{\mathrm{i}\kappa t} \end{pmatrix}. \tag{4.88}$$

Note that the fidelity reaches its maximum value $F_{\max} = 1$ if and only if $\rho(t) = \bar{\rho}(t)$. Clearly, in the case of initial pure state $\rho(0) = |\Psi(0)\rangle\langle\Psi(0)|$, where $|\Psi(0)\rangle$ is eigenvector of H_0, we simply have $\bar{\rho}(t) \equiv \rho(0)$. This means that the maximum values of the fidelity indicate the revival of the initial state when the latter is eigenvector of H_0. We shall use this property when studying entanglement evolution.

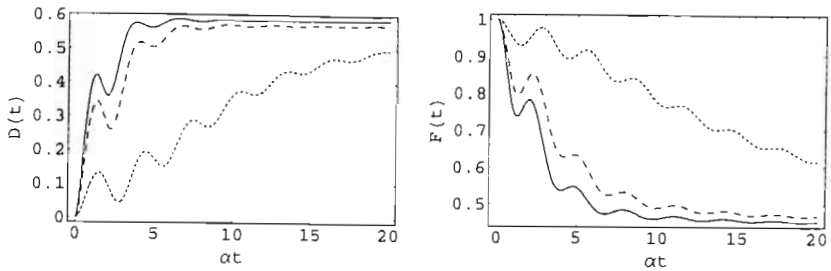

Fig. 4.4: Time evolution of the linear entropy and the fidelity in the case of the initial state $|--\rangle$ at different values of $g\beta$: $g\beta = 0$ (solid lines), $g\beta = 2$ (dashed lines), and $g\beta = 20$ (dotted lines) with $\epsilon = \alpha$.

In this work we use the concurrence as a measure of entanglement between the central qubits. Recall that the concurrence corresponding to the reduced density matrix $\rho(t)$ is defined by [34]

$$C(\rho) = \max\{\sqrt{\lambda_1} - \sqrt{\lambda_2} - \sqrt{\lambda_3} - \sqrt{\lambda_4}, 0\}, \tag{4.89}$$

where $\lambda_1, \lambda_2, \lambda_3$ and λ_4 are the eigenvalues, in descending order, of the operator

$$\varrho(t) = \rho(t)(\sigma_y \otimes \sigma_y)\rho^*(t)(\sigma_y \otimes \sigma_y) \tag{4.90}$$

written in $\mathbb{C}^2 \otimes \mathbb{C}^2$, and $\rho^*(t)$ designates the complex conjugate of the density matrix. The values of the concurrence range from zero, for unentangled states, to one for maximally entangled states. Since the concurrence is invariant under unitary transformations, we can rewrite the operator $\varrho(t)$ in the basis of the space $\mathbb{C}^3 \oplus \mathbb{C}$ as

$$\varrho(t) = \rho(t)V\rho^*(t)V, \quad V = \begin{pmatrix} 0 & 0 & 1 & 0 \\ 0 & -1 & 0 & 0 \\ 1 & 0 & 0 & 0 \\ 0 & 0 & 0 & 1 \end{pmatrix}. \tag{4.91}$$

Bellow, we investigate decoherence and entanglement dynamics for some particular initial states that are of interest for applications. Other states can be studied with exactly the same method.

4.4.2 *Results and discussion*

Case 1: $|\Psi(0)\rangle = |\mp\mp\rangle$.

Let us suppose that the two-qubit system is initially prepared in the product state $|--\rangle = |1, -1\rangle$. The corresponding time-dependent density matrix is diagonal, the idempotency

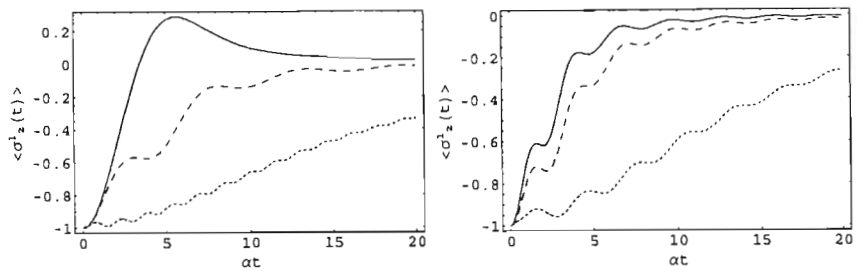

Fig. 4.5: $\langle\sigma_z^1(t)\rangle$ versus the scaled time αt for different values of ϵ and $g\beta$: i) $\epsilon = 0$ (solid line), $\epsilon = 0.5\alpha$ (dashed line), and $\epsilon = 2\alpha$ (dotted line) with $g\beta = 10$ for the figure on the left; ii) $g\beta = 0$ (solid lines), $g\beta = 2$ (dashed line), and $g\beta = 20$ (dotted line) with $\epsilon = \alpha$ for the figure on the right. The initial state is $|--\rangle$.

is then equal to $D(t) = 1 - \sum_i [\rho_{ii}(t)]^2$. Since $|--\rangle$ is eigenvector of the Hamiltonian H_0, the fidelity simplifies to $F(t) = \rho_{11}(t)$. The time dependence of the linear entropy is shown in figures 4.3 and 4.4 for different values of the interaction strength ϵ and the bath temperature T. We can see that $D(t)$ increases starting from its initial value, zero, tending asymptotically to $D(\infty)$ which can be evaluated as $(21 - 2\Sigma - 3\Sigma^2)/32$. This limit assumes larger values as the strength of interactions ϵ decreases in contrast with the bath temperature T. Therefore, in order to ensure lower linear entropy, and consequently to reduce the effect of the environment, one has to increase (decrease) the value of the ratio ϵ/α (temperature T). Thus we set $\Sigma = 1$ to find that $D_{\min}(\infty) = 0.5$. The fidelity shown in the above figures displays reverse behavior compared to that of $D(t)$; its asymptotic value turns out to be $(3 + \Sigma)/8$ from which it follows that $F_{\max}(\infty) = 0.5$. It is quite interesting to notice that $D_{\min}(\infty) + F_{\max}(\infty) = 1$.

The mean value of the operator $\sigma_z^1(t) = 2S_z^1(t)$ corresponding to the first spin is found to be

$$\langle\sigma_z^1(t)\rangle = -[\cos(\epsilon t)f(t) + \sin(\epsilon t)\ell(t)]. \tag{4.92}$$

The latter quantity decays to zero, as shown in figure 4.5, indicating that the asymptotic state of the qubit is a fully mixture of the eigenvectors $|\pm\rangle$. Moreover, we can see that $\langle\sigma_z^1(t)\rangle$ decays slower at low bath temperatures and large values of ϵ. A straightforward calculation yields the following expression of the concurrence

$$C(t) = \max\Big\{0, 2\max\Big[\sqrt{\rho_{11}(t)\rho_{33}(t)}, \rho_{22}(t)\Big] - 2\sqrt{\rho_{11}(t)\rho_{33}(t)} - \rho_{22}(t)\Big\}. \tag{4.93}$$

It turns out that $C(t) \equiv 0$ independently of the values of ϵ and the temperature T. This implies that the state of the system is always separable; neither the interaction between the central qubits nor the coupling with the bath is able to generate entanglement. All

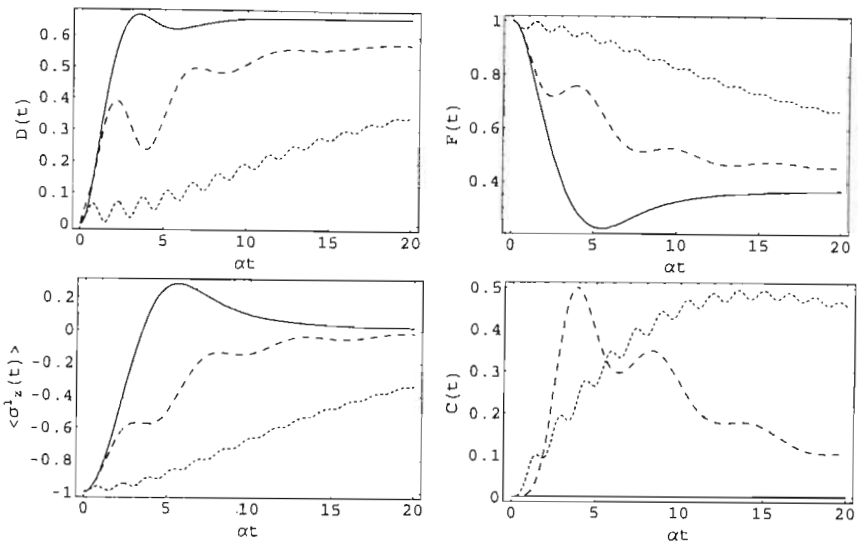

Fig. 4.6: Time dependence of $D(t)$, $F(t)$, $\langle\sigma_z^1(t)\rangle$ and $C(t)$ for different values of λ in the case of the initial state $|-+\rangle$: $\lambda = 0$ (solid lines), $\lambda = 0.5\alpha$ (dashed lines), and $\lambda = 2\alpha$ (dotted lines) with $\Omega = 0$ and $g\beta = 10$.

the above results apply for the state $|++\rangle$ as well.

$$Case2 : |\Psi(0)\rangle = |-+\rangle.$$

The state $|-+\rangle$ can be written as a combination of the states $|1,0\rangle$ and $|0,0\rangle$, namely, $|-+\rangle = \frac{1}{\sqrt{2}}(|1,0\rangle + |0,0\rangle)$. In this case the diagonal elements together with $\rho_{24}(t)$ are the only non-zero elements of the reduced density matrix. The idempotency, the fidelity and the mean value of $\sigma_z^1(t)$ are explicitly given by

$$D(t) = \frac{3}{4} - [\rho_{11}(t)]^2 - [\rho_{22}(t)]^2 - [\rho_{33}(t)]^2 - 2|\rho_{24}(t)|^2, \tag{4.94}$$

$$F(t) = \frac{1}{4}\Big\{1 + 2\rho_{22}(t) + 4\mathrm{Re}[\rho_{24}(t)e^{4i\Omega t}]\Big\}, \quad \langle\sigma_z^1(t)\rangle = -2\mathrm{Re}[\rho_{24}]. \tag{4.95}$$

The time dependence of the latter quantities is similar to that of the above case. When $\Omega = 0$, the asymptotic values of the linear entropy and the fidelity are, respectively, equal to $(21-2\Sigma-3\Sigma^2)/32$ and $(3+\Sigma)/8$. Hence we find again that $D_{\min}(\infty) = F_{\max}(\infty) = 0.5$, and $\lim_{t\to\infty}\langle\sigma_z^1(t)\rangle = 0$.

The expression of the concurrence is quite long, we will not show it here for shortness. Nevertheless, we can distinguish to different cases. The first one corresponds to $\Omega = 0$, the variation in time of the corresponding concurrence is displayed in figures 4.6 and 4.7 for different values of λ and T. We can see that entanglement between the central qubits is

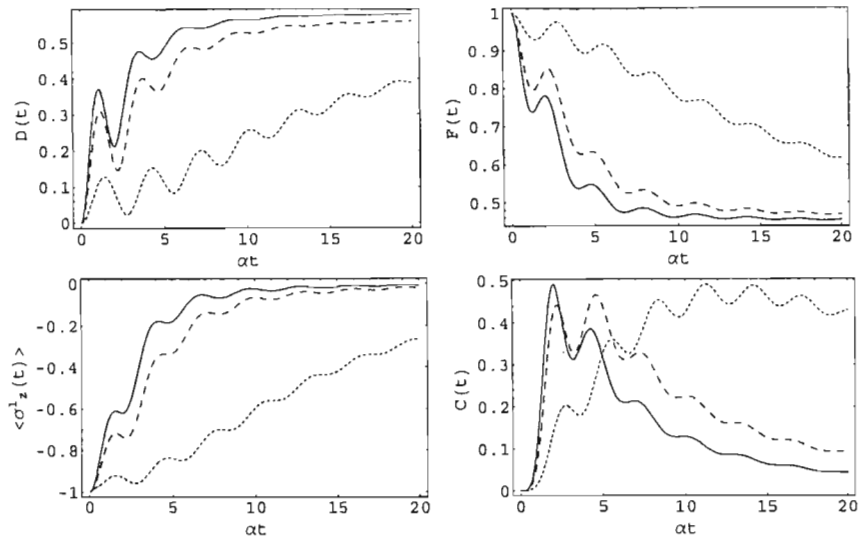

Fig. 4.7: Evolution in time of $D(t)$, $F(t)$, $\langle\sigma_z^1(t)\rangle$ and $C(t)$ at different values of $g\beta$ in the case of the initial state $|-+\rangle$: $g\beta = 0$ (solid lines), $g\beta = 2$ (dashed lines), and $g\beta = 20$ (dotted line) with $\lambda = \alpha$ and $\Omega = 0$.

generated when $\lambda \neq 0$ even though the initial state is separable. If there is no interaction between the central spins, the concurrence is always zero. We can see that the increase and the decay of the concurrence are faster at high temperatures and vice versa. Moreover, the numerical simulation shows that the concurrence never exceeds the value $C_{\max} = 0.5$: no maximally entangled states can be produced in this case. Note that $|-+\rangle$ is eigenvector of the Hamiltonian H_0, in absence of the surrounding environment, the latter state remains always separable. Roughly speaking, the interaction with the spin bath changes the state of the central system so that the action of H_0 produces, to some extent, entanglement between the qubits.

The second case corresponds to $\Omega \neq 0$. Here $|-+\rangle$ is not eigenvector of H_0, the action of the latter on this state periodically generates maximally entangled states. Hence, the effect of the environment consists of reducing the amount of the produced entanglement as shown in figure 4.8 . We can also see that the maximum values of $C(t)$ occur at instances of time for which $\langle\sigma_z^1(t)\rangle$ is equal to zero.

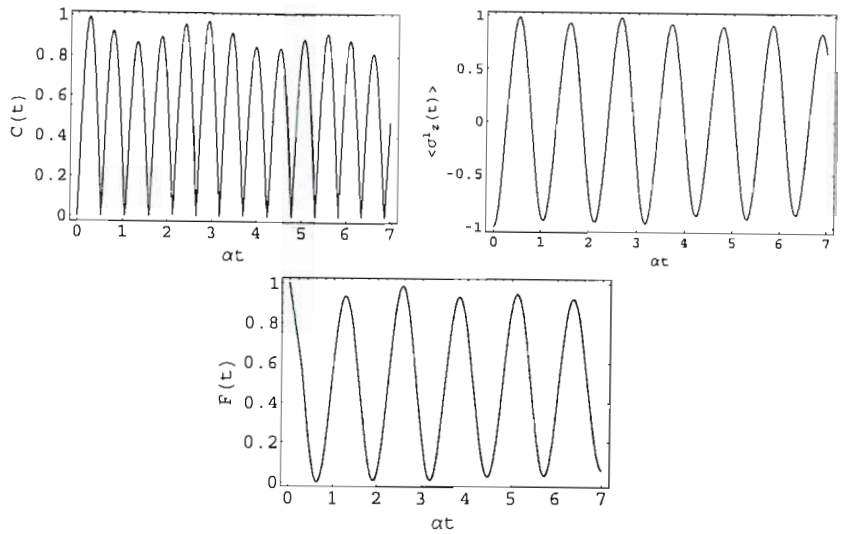

Fig. 4.8: Time dependence of $C(t)$, $\langle\sigma_z^1(t)\rangle$, and $F(t)$ in the case of the initial state $|-+\rangle$ for $\lambda = 2\alpha$, $\Omega = \alpha$ and $g\beta = 10$.

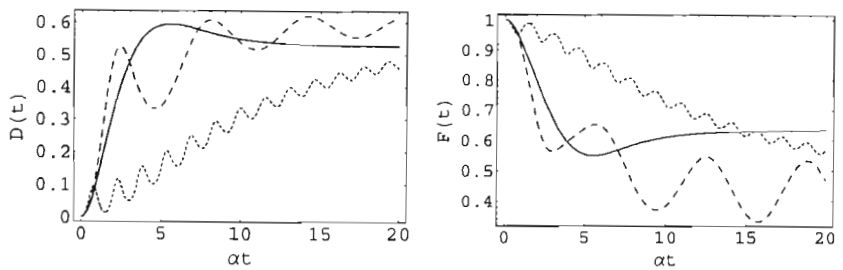

Fig. 4.9: Time dependence of $D(t)$ and $F(t)$ at different values of ϵ in the case of the initial state $\frac{1}{2}(|-\rangle + |+\rangle)^{\otimes 2}$: $\epsilon = 0$ (solid lines), $\epsilon = 0.5\alpha$ (dashed lines) and $\epsilon = 2\alpha$ (dotted lines) with $g\beta = 10$.

Case 3: $|\Psi(0)\rangle = \frac{1}{2}(|-\rangle + |+\rangle)^{\otimes 2}$.

In this case, it can be shown that

$$D(t) = 1 - [\rho_{22}(t)]^2 - 2\Big\{[\rho_{11}(t)]^2 + |\rho_{12}(t)|^2 + |\rho_{13}(t)|^2 + |\rho_{23}(t)|^2\Big\}, \quad (4.96)$$

$$F(t) = \frac{1}{4}\Big\{1 + \rho_{22}(t) + 2\mathrm{Re}[\rho_{13}(t)] + \sqrt{2}\Big[(\rho_{12}^*(t) + \rho_{23}(t))\ \mathrm{e}^{-2i\epsilon t} + \mathrm{c.c}\Big]\Big\}, \quad (4.97)$$

$$\langle\sigma_z^1(t)\rangle = 0. \quad (4.98)$$

Hence, the asymptotic value of the linear entropy is equal to $(267 + 114\Sigma - 77\Sigma^2)/256$, from which it follows that $D_{\max}(\infty) = 19/32$, $D_{min} = 167/256$. The dependence of $D(t)$ and $F(t)$ on ϵ is shown in figure 4.9; their variation with respect to T is quite similar to that of the above two cases. Since H_0 induces entanglement between the central qubits,

we conclude that the influence of the environment consists of reducing the degree of entanglement of the central system. This is shown in figure 4.10 where we have displayed the dynamics of entanglement at different values of ϵ.

$$\textit{Case4: } |\Psi(0)\rangle = \tfrac{1}{\sqrt{2}}(|-+\rangle + |+-\rangle).$$

If the initial state of the qubits is the maximally entangled state $|1,0\rangle$ then the density matrix is again diagonal. Since $|1,0\rangle$ is eigenvector of H_0, we simply get $F(t) = \rho_{22}(t)$. The mean value of $\sigma_z^1(t)$ remains always zero. The behaviour of the linear entropy and the fidelity is shown in figures 4.11 and 4.12. The asymptotic values of the above measures are given by $(5-2\Sigma-3\Sigma^2)/8$ and $(1+\Sigma)/2$, respectively. Hence, we find that $D_{\min}(\infty) = 0$ and $F_{\max}(\infty) = 1$. Note that the above values are obtained for $\epsilon, \beta \to \infty$. This implies that the state of the qubits can be protected from decohering at very low bath temperatures or when their mutual interactions are sufficiently strong.

The concurrence in this case is given by relation (4.93). We can see form figure 4.11 that for $\epsilon = 0$ the concurrence decays from its maximum value to vanish at certain value of time, the state of the two-qubit system becomes separable. This behaviour is known as entanglement sudden death which has been investigated for bosonic environments [35]. As we increase the value of the interaction strength ϵ, the concurrence approaches its initial maximum value $C_{\max} = 1$. This happens when the fidelity in turn approaches its maximum value implying that the initial state of the two-qubit system revives. For example, the asymptotic value of the concurrence turns out to be

$$C(\infty) = \Sigma. \tag{4.99}$$

Since the quantity Σ is a monotonic increasing function of both ϵ and β, and satisfies $\lim_{\epsilon,\beta\to\infty} \Sigma = 1$, we simply obtain $C_{\max}(\infty) = F_{\max}(\infty) = 1$. When $\epsilon \neq 0$ the concurrence

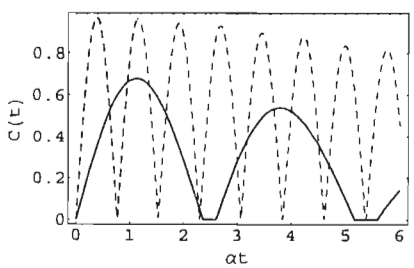

Fig. 4.10: $C(t)$ versus αt at different values of ϵ in the case of the initial state $\frac{1}{2}(|-\rangle + |+\rangle)^{\otimes 2}$: $\epsilon = 0.5$ (solid line), $\epsilon = 2\alpha$ (dashed line) with $g\beta = 10$. The concurrence corresponding to $\epsilon = 0$ is identically zero.

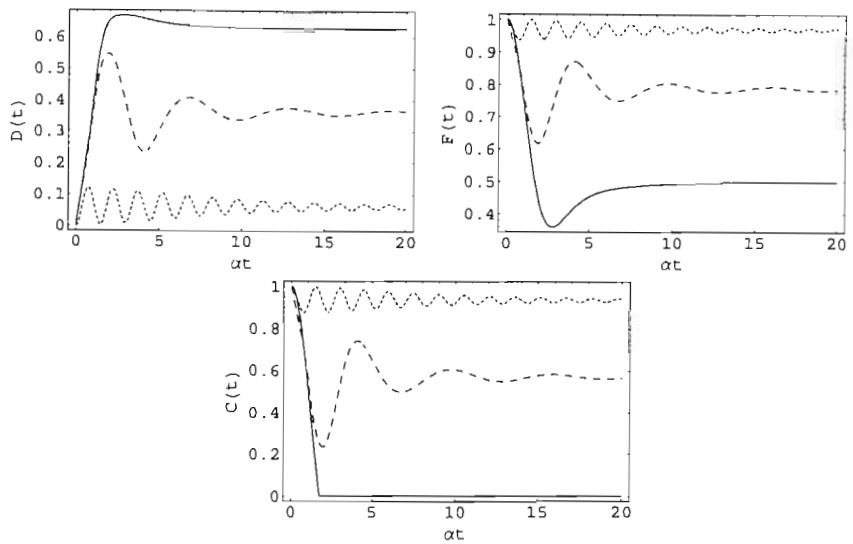

Fig. 4.11: Time dependence of $D(t)$, $F(t)$ and $C(t)$ at different values of ϵ in the case of the maximally entangled state $\frac{1}{\sqrt{2}}(|-+\rangle + |+-\rangle)$: $\epsilon = 0$ (solid lines), $\epsilon = 0.5\alpha$ (dashed lines), and $\epsilon = 2\alpha$ (dotted line) with $g\beta = 10$.

may vanish for certain interval of time then revives again to tend to its asymptotic value (4.99). If ϵ is sufficiently large, the concurrence never vanishes as displayed in figure 4.11.

Case 5: $|\Psi(0)\rangle = \frac{1}{\sqrt{2}}(|++\rangle + |--\rangle)$.

In this case, the non-zero elements of the reduced density matrix are $\rho_{11}(t)$, $\rho_{22}(t)$, $\rho_{33}(t)$ and $\rho_{13}(t)$. Consequently, the mean value of $\sigma_z^1(t)$ remains always zero. The idempotency and the fidelity are given by

$$D(t) = 1 - 2\Big([\rho_{11}(t)]^2 + [\rho_{13}(t)]^2\Big) - [\rho_{22}(t)]^2, \quad F(t) = \rho_{11}(t) + \rho_{13}(t). \tag{4.100}$$

The asymptotic values of the above measures are, respectively, given by $(75 - 14\Sigma - 13\Sigma^2)/128$ and $(9 + 3\Sigma)/16$. It follows that $D_{\min}(\infty) = 0.375$ and $F_{\max}(\infty) = 0.75$

The square roots of the eigenvalues of the matrix $\varrho(t)$ can be easily calculated; they are given explicitly by $\rho_{22}(t)$, $|\rho_{11}(t) + \rho_{13}(t)|$ and $|\rho_{11}(t) - \rho_{13}(t)|$. Hence the concurrence in this case is given by

$$\begin{aligned} C(t) = \max\Big\{0, 2\max\Big[\rho_{22}(t), |\rho_{11}(t) + \rho_{13}(t)|, |\rho_{11}(t) - \rho_{13}(t)|\Big] \\ -\rho_{22}(t) - |\rho_{11}(t) + \rho_{13}(t)| - |\rho_{11}(t) - \rho_{13}(t)|\Big\}. \end{aligned} \tag{4.101}$$

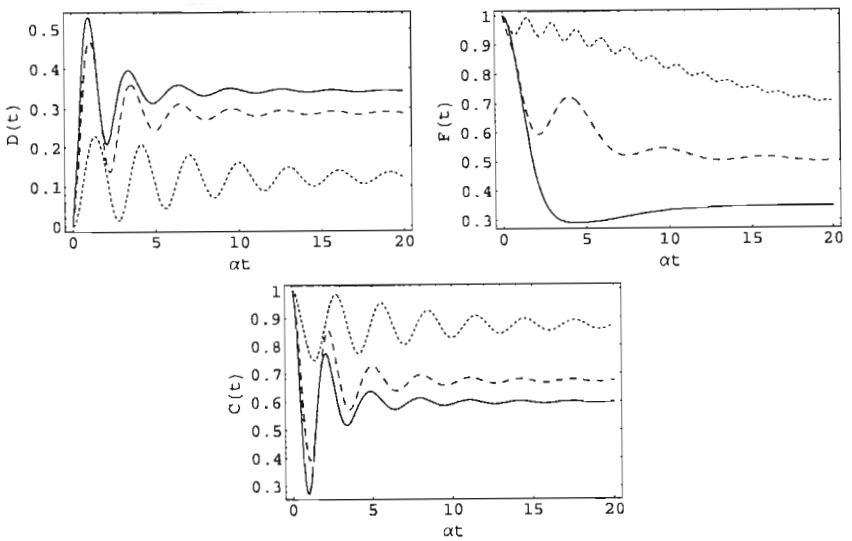

Fig. 4.12: Variation in time of $D(t)$, $F(t)$ and $C(t)$ for different values of $g\beta$ in the case of the maximally entangled state $\frac{1}{\sqrt{2}}(|-+\rangle + |+-\rangle)$: $g\beta = 0$ (solid lines), $g\beta = 2$ (dashed lines), and $g\beta = 20$ (dotted lines) with $\epsilon = \alpha$.

From figure 4.13, we can see that even when $\epsilon = 0$ the asymptotic value of the concurrence is different from zero. Indeed, by direct calculation we find

$$C(\infty) = \frac{1 + 3\Sigma}{8}, \tag{4.102}$$

implying that $0.125 \leq C(\infty) \leq 0.5$. By contrast with $|1,0\rangle$, the maximally entangled state $\frac{1}{\sqrt{2}}(|1,-1\rangle + |1,1\rangle)$ does not revive, its entanglement cannot be recovered even for large values of ϵ at very low temperatures of the bath. We also see that for noninteracting qubits, entanglement vanishes for some interval (dark period) then revives again.

case 6: Werner states.

Let us consider werner states

$$\rho_W^0 = \frac{1}{4}(1-p)\mathbb{I}_4 + p|\Phi\rangle\langle\Phi|, \tag{4.103}$$

where $|\Phi\rangle = \frac{1}{\sqrt{2}}(|--\rangle + |++\rangle)$, and $0 \leq p \leq 1$. In $\mathbb{C}^3 \oplus \mathbb{C}$ the above density matrix takes the form

$$\rho_W^0 = \begin{pmatrix} \frac{1+p}{4} & 0 & \frac{p}{2} & 0 \\ 0 & \frac{1-p}{4} & 0 & 0 \\ \frac{p}{2} & 0 & \frac{1+p}{4} & 0 \\ 0 & 0 & 0 & \frac{1-p}{4} \end{pmatrix}. \tag{4.104}$$

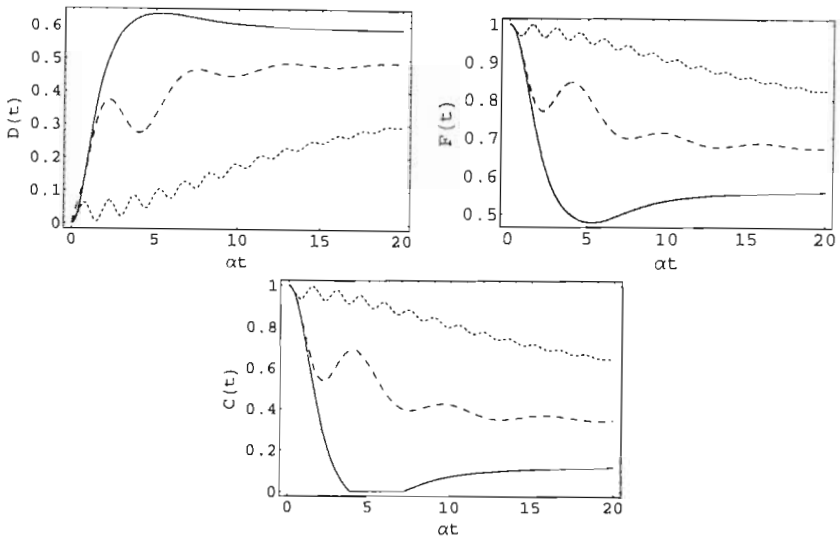

Fig. 4.13: Time dependence of $D(t)$, $F(t)$ and $C(t)$ at different values of ϵ in the case of the maximally entangled state $\frac{1}{\sqrt{2}}(|--\rangle + |++\rangle)$: $\epsilon = 0$ (solid lines), $\epsilon = 0.5\alpha$ (dashed lines), and $\epsilon = 2\alpha$ (dotted lines) with $g\beta = 10$.

The corresponding stationary density matrix is then equal to

$$\rho_W^{\infty} = \begin{pmatrix} \frac{2+p\ (1+\Sigma)}{8} & 0 & \frac{p\ (3+\Sigma)}{16} & 0 \\ 0 & \frac{1-p\ \Sigma}{4} & 0 & 0 \\ \frac{p\ (3+\Sigma)}{16} & 0 & \frac{2+p\ (1+\Sigma)}{8} & 0 \\ 0 & 0 & 0 & \frac{1-p}{4} \end{pmatrix}, \tag{4.105}$$

The maximum values of the asymptotic linear entropy and fidelity are, respectively, given by $(6-3p^2)/8$ and $(1+2p^2)/4$. The square root of the largest eigenvalue of the operator ϱ^{∞} is equal to $(4+5p+3p\Sigma)/16$, the root squared remaining ones read $(1-p)/4$, $(1-p\Sigma)/4$ and $(4+p\Sigma-p)/16$. The asymptotic value of the concurrence is then equal to

$$C(\rho_W^{\infty}) = \max\Big\{0, \frac{1}{8}[p\ (3\Sigma+5)-4]\Big\}. \tag{4.106}$$

Therefore, the two-qubit system is entangled if and only if

$$p > \frac{4}{5+3\Sigma}. \tag{4.107}$$

The minimum value of p for which the asymptotic state of the qubits is entangled is equal to 0.5 which corresponds to $\epsilon \to \infty$ and/or $T \to 0$. The behaviour of the concurrence in this case is similar to that of $|\Phi\rangle$.

To conclude our discussion we note that in [36], the fidelity of mixed state, calculated with respect to a maximally entangled state, is shown to be bounded above by $[1+C(t)]/2$.

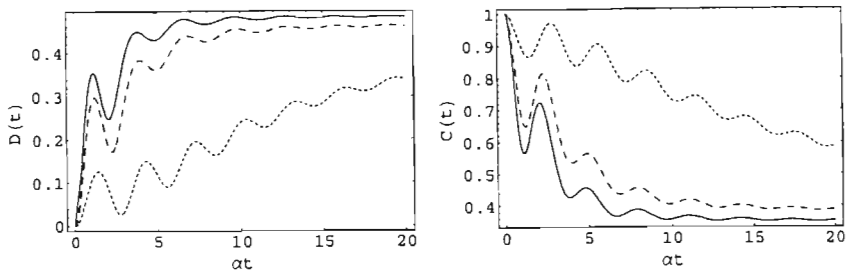

Fig. 4.14: Variation in time of $D(t)$ and $C(t)$ for different values of $g\beta$ in the case of the maximally entangled state $\frac{1}{\sqrt{2}}(|--\rangle + |++\rangle)$: $g\beta = 0$ (solid lines), $g\beta = 2$ (dashed lines), and $g\beta = 20$ (dotted lines) with $\epsilon = \alpha$.

This fully agrees with our results as can be seen in the case of the maximally entangled state $|1,0\rangle$. Indeed, when $\rho_{22}(t) \geq \rho_{11}(t)$ then $C(t) = \max[2\rho_{22}(t) - 1, 0] = \max[2F(t) - 1, 0]$. The corresponding asymptotic values do satisfy the latter condition. The above equality implies that the concurrence is equal to the negativity [36]. The critical point at which $C(t)$ vanishes corresponds to $F(t) = 0.5$ (see figure 4.11). These results also hold for $C(t)$ and $F(t)$ corresponding to the state $\frac{1}{\sqrt{2}}(|++\rangle + |--\rangle)$ at least at long times. In [37] numerical simulation was used to study entanglement dynamics of two qubits coupled to anisotropic bath. The authors found that concurrence can be produced in the case of the initial states $|\pm\pm\rangle$ if the qubits are subjected to external magnetic field. It would then be interesting to investigate this situation analytically.

4.5 Conclusion

In conclusion we have studied decoherence and entanglement dynamics of two qubit interacting with antiferromagnetic spin bath at thermal equilibrium. The time evolution operator of the composite system was analytical derived using symmetry properties of the model Hamiltonian. The reduced density matrix was calculated by performing the partial trace over the irrelevant bath degrees of freedom. In the limit of infinite number of spins in the environment, N, the lowering and raising operators corresponding to the total angular momentum, as well as its z-component, converge to normal random variables. This enabled us to calculate the partial trace when $N \to \infty$. The above limit turns out to be very good approximation for finite numbers of spins. We found that the off-diagonal elements of the reduced density matrix show partial decoherence. The decoherence-free subspace in this model is spanned by the states $|0,0\rangle\langle 0,0|$ and $\frac{1}{3}\mathbb{I}_3$. Using the linear entropy and the fidelity, we studied decoherence of the central qubits for different initial states. We

showed that the decay of the elements of the reduced density matrix is Gaussian, which is a hallmark of non-Markovian dynamics. The effect of decoherence can be reduced at low bath temperature and strong coupling between the central qubits.

Entanglement behaviour depends on the initial states of the qubits. The concurrence remains always zero when the central qubits are initially prepared in the pure product states$|\pm\pm\rangle$. These remains always separable. On the contrary, the qubits become entangled if they are prepared in the states $|\pm\mp\rangle$ or $\frac{1}{2}(|-\rangle+|+\rangle)^{\otimes 2}$. In the latter case, entanglement generation is due to mutual interactions between the central qubits. The situation is different in the case of the states $|\pm\mp\rangle$ which are eigenvectors of the free Hamiltonian when $\Omega=0$: this is an example of environment-induced entanglement. Initially entangled states lose partially or completely their entanglement. This behavior strongly depends on bath temperature and the strength of interactions between qubits. It is found that entanglement can be protected to some extent from decohering at low bath temperatures and/or strong interactions between the central qubits if they are prepared in the maximally entangled state $|1,0\rangle$. For small values of ϵ, it is found that entanglement displays sudden death. I think that the results presented here help extending the class of exactly solvable models for spin systems.

BIBLIOGRAPHY

[1] Einstein A, Podolsky B and Rosen N 1935 *Phys. Rev.* **47** 777

[2] Schrödinger E 1935 *Naturwissenschaften* **23** 807

[3] Bell J S 1964 *Physics* **1** 195

[4] Nielsen M A and Chuang I L 2000 *Quantum Computation and Quantum Information* (Cambridge: Cambridge University Press)

[5] Bennett C H and Wiesner S J 1993*Phys. Rev. Lett.* **69** 2881

[6] Bennett C H and DiVincenzo D P 2000 *Nature* **404** 247

[7] Bennett C H, Brassard G, Crépeau C, Jozsa R, Peres A and Wootters W K 1993 *Phys. Rev. Lett.* **70** 1895

[8] Bennett C H, DiVincenzo D P, Smolin J A and Wootters W K 1996 *Phys. Rev.* A **54** 3824

[9] Lloyd S 1004 *Science* **261** 1569 (1993)

[10] Ekert A and Josza R 1998 *Philos. Trans. R. Soc. Lond.* A **356** 1769

[11] Loss D and DiVincenzo D P 1998 *Phys. Rev.* A **57** 120

[12] Burkard G Loss D and DiVincenzo D P 1999 *Phys. Rev.* B **59** 2070

[13] Zurek W H 1991 *Phys. Today* **44** 36

[14] DiVincenzo D P and Loss D 2000 *J. Magn. Magn. Matter.* **200** 202

[15] Zurek W H 2003 *Rev. Mod. Phys.* **75**, 715-775

[16] Shor P W *Phys. Rev.* A **52** R2493

[17] Preskill J 1998 *Proc. R. Soc. Lond.* A **454** 385

[18] Reina J H, Quiroga L and Johnson N F 2002 *Phys. Rev.* A **65** 032326

[19] Gottesman D 1996 *Phys. Rev.* A **54** 1862

[20] Steane A M 1996*Phys. Rev. Lett.* **77** 793

[21] Lidar D A, Chuang I L and Whaley K B 1998 *Phys. Rev. Lett.***81** 2594

[22] Lidar D A, Bacon D and Whaley K B 1999 *Phys. Rev. Lett.***82** 4556

[23] Prokof'ev N V and Stamp P C E 2000 *Rep. Prog. Phys.* **63** 669

[24] Hamdouni Y, Fannes M and Petruccione F 2006 *Phys. Rev.* B **73** 245323

[25] Yuan X Z, Goan H J and Zhu K D 2007 *Phys. Rev.* B **75** 045331

[26] Huang Z, Sadiek G and Kais S 2006 *J. Chem. Phys.* **124** 144513

[27] Breuer H P, Burgarth D and Petruccione F 2004 *Phys. Rev.* B **70** 045323

[28] Bhaktavatsala Rao D D, Ravishankar V and Subrahmanyam V 2006 *Phys. Rev.* A **74** 022301

[29] Hamdouni Y and Petruccione F 2007 *Phys. Rev.* B **76** 174306

[30] Von Waldenfels W 1990 *Séminaire de probabilité (Starsburg)* tome 24 (Berlin: Springer-Verlag) pp 349-56

[31] Wang X and Mølmer K 2002 *Eur. Phys. J.* D **18** 385

[32] Danos M and Rafelski J 1984 *Pocketbook of Mathematical Functions* (Frankfurt: Verlag Harri Deutsch)

[33] Fedichkin L and Privman V 2006 v2 *Preprint* cond-mat/0610756

[34] Wootters W K 1998 *Phys. Rev. Lett.* **80** 2245

[35] Yu T and Eberly J H 2004 *Phys. Rev. Lett.* **93** 140404

[36] Verstraete F and Verschelde H 2002 *Phys. Rev.* A **66** 022307

[37] Jing J and LÜ Z 2007 *Phys. Rev.* B **75** 174425

5. NONZERO TEMPERATURE DYNAMICS NEAR QUANTUM PHASE TRANSITION IN THE ISOTROPIC LIPKIN-MESHKOV-GLICK MODEL: AN OPEN QUANTUM SYSTEM APPROACH

5.1 Introduction

Quantum Phase Transitions (QPTs) are associated with qualitative changes in the ground states of many-body quantum systems, at the absolute zero temperature, when some relevant parameters vary across their critical values [1]. Their manifestation in many experimental results on the cuprate superconductors and organic conductors stimulated much attention during the last decade. Recently, the relation between the entanglement and the quantum phase transitions has been the subject of many studies [1, 2, 3, 4, 5, 6, 7, 8, 9, 10]. The critical behaviour of the former was proposed as a tool for detecting the presence of QPTs in multi-spin systems. Most of the investigations have dealt with the zero-temperature dynamics near the critical point at which the transition occurs. However, it is believed that quantum phase transitions leave their fingerprints at temperatures close to the zero absolute. Generally speaking, at such low temperatures, the long-time collective dynamics of a quantum many-body system is investigated using the concepts of order parameters and quasiparticles which lead, however, to a semiclassical description of the dynamics [11]. Moreover, at nonzero temperatures, quantum correlations are suppressed by the thermal fluctuations: there exits a threshold temperature above which the thermal entanglement ceases to exist. Thus a deep understanding of the dynamics of multi-spin systems at low temperatures is of theoretical and experimental significance.

The Lipkin-Meshkov-Glick (LMG) model [12, 13, 14], initially introduced in nuclear physics, has found many physical applications such as the Josephson effect and the two-mode Bose-Einstein condensate [15, 16, 17]. This model was extensively used to investigate the connection between the zero-temperature entanglement and QPTs [18, 19, 20, 21, 22, 23]. The Hamiltonian of the isotropic LMG model with N spins subjected to a magnetic field of strength h is explicitly given by

$$H = \frac{g}{2N}\sum_{i<j}^{N}\left(\sigma_x^i\sigma_x^j + \sigma_y^i\sigma_y^j\right) + \frac{h}{2}\sum_{i}^{N}\sigma_z^i, \tag{5.1}$$

where g is the coupling constant and $\vec{\sigma}^i = 2\vec{S}^i$ is the Pauli operator corresponding to the particle labeled by i. The above Hamiltonian can be cast, up to an additive constant, into the form

$$H = \frac{g}{N}\left(\mathcal{J}^2 - \mathcal{J}_z^2\right) + h\mathcal{J}_z, \tag{5.2}$$

where $\vec{\mathcal{J}} = \sum_i^N \vec{S}^i$ is the total angular momentum of the multi-spin system. The standard basis of H is composed of the state vectors $|j, m\rangle$ common to $\mathcal{J}^2$ and $\mathcal{J}_z$ such that $0 \leq j \leq N/2$, and $-j \leq m \leq j$ (we set $\hbar = 1$). In the ferromagnetic case, i.e. $g < 0$, the ground state and the first exited state belong to the subspace $\mathbb{C}^{N+1}$ spanned by the eigenvectors $|N/2, m\rangle$. The model Hamiltonian displays a second order phase transition at the critical point $|h_c| = -g$. Indeed, for $|h| > |h_c|$, the ground state is unique and is equal to the fully polarized state $|N/2, -\text{sign}(h_c)N/2\rangle$ (symmetric phase), where $\text{sign}(x)$ designates the sign of x. On the contrary, in the domain $|h| < |h_c|$, the ground state depends on the coupling constant g (symmetry broken phase); its explicit form is given by $|N/2, I(\frac{hN}{2g})\rangle$, where $I(x)$ denotes the round value of x.

In this chapter, we apply the general formalism of open quantum systems to investigate the dynamics at low temperatures near the critical point of the isotropic LMG model. The idea consists of deriving the reduced density matrix of a central spin system which is coupled to a spin bath governed by the Hamiltonian (5.1). In section 5.2 we derive the one-qubit and two-qubit thermal reduced density matrix and we investigated the pairwise thermal entanglement. In section 5.3, we study the time evolution of the coherence and the entanglement of, respectively, a single and a two spin $\frac{1}{2}$ particles coupled via Heisenberg or Ising interactions to the LMG spin bath. We end the paper with a short summary.

5.2 Thermal reduced density matrix

Let $\rho_N(0)$ denote the total density matrix of the multi-spin system whose dynamics is governed by the Hamiltonian (5.1). The state of any subsystem with m spins is fully described by its reduced density matrix, obtained by eliminating the degrees of freedom corresponding to the remaining $N - m$ particles. Note that H is invariant with respect to the exchange of sites; it follows that the reduced density matrix should be independent of the choice of the central particles. In the following we assume that our multi-spin system is in thermal equilibrium at arbitrary temperature T. The corresponding total density matrix is given by the Gibbs thermal state

$$\rho_N(0) = \frac{\exp\left(-H/T\right)}{\text{tr}_N\{\exp(-H/T)\}}, \tag{5.3}$$

where the Boltzmann constant is set to one, and $Z = \mathrm{tr}_N\{\exp(-H/T)\}$ is the partition function. Here, tr_N designates the trace with respect to the full set of the eigenvectors of H. In the following we derive the reduced density matrix for both one and two central qubits. Without loss of generality we suppose that $g = -1$, and we only consider positive values of h since the spectrum of H is odd.

5.2.1 The one-particle reduced density matrix

First of all, it should be noted that the reduced density matrix can be obtained by directly calculating the mean values of the operators $\mathcal{J}^2$ and $\mathcal{J}_z$, with respect to the thermal state [24]. However, we shall proceed differently and use an other method which allows us to investigate, in a straightforward manner, the time evolution of a central qubit coupled to the isotropic LMG bath (see the next section). Furthermore, one is usually seeking new techniques that lead to exact analytical results.

Let us choose one arbitrary particle, whose spin vector operator is denoted by $\vec{S}$, and call it central spin. The remaining $N-1$ particles can be viewed as a spin bath with a total angular momentum $\vec{J}$. At this stage it is useful to decompose the total spin vector of the full system as the sum of those corresponding to the central particle and the bath, namely

$$\vec{\mathcal{J}} = \vec{S} + \vec{J}, \quad \mathcal{J}_z = S_z + J_z. \tag{5.4}$$

Then, one can easily show that the isotropic Lipkin-Meshkov-Glick Hamiltonian can be rewritten in terms of the new spin operators as

$$H = \frac{g}{N}[J^2 - J_z^2 + \frac{1}{2}] + h(J_z + S_z) + \frac{g}{N}[S_+J_- + S_-J_+], \tag{5.5}$$

where $L_\pm = L_x \pm \mathrm{i}L_y$. Hence the full system is equivalent to a central qubit coupled to a spin bath through Heisenberg XY interactions. Similarly, the spin space of the composite system, $(\mathbb{C}^2)^{\otimes N}$, can be decomposed as

$$\mathbb{C}^2 \otimes (\mathbb{C}^2)^{\otimes N-1} = \mathbb{C}^2 \otimes \Big[\bigoplus_j^{\frac{N-1}{2}} \nu(N-1,j)\mathbb{C}^{2j+1}\Big], \tag{5.6}$$

where [25]

$$\nu(N,j) = \binom{N}{\frac{N}{2}-j} - \binom{N}{\frac{N}{2}-j-1}. \tag{5.7}$$

The basis of the latter space is formed by the vectors $|k\rangle \otimes |j,m\rangle$, where $S_z|k\rangle = -\frac{(-1)^k}{2}|k\rangle$ ($k \in \{0,1\}$), $J^2|j,m\rangle = j(j+1)|j,m\rangle$, and $J_z|j,m\rangle = m|j,m\rangle$. Note that in equation (5.6), the summation over j takes into account whether N is odd or even. Also, due to

the last term in the right-hand side of equation (5.5), the Hamiltonian operator H is no longer diagonal in this new basis.

The method we adopt here is based on the fact that the operator $\varrho = Z\ \rho_N(0) = \exp[-\beta H]$ satisfies the following equation

$$\frac{\partial}{\partial\beta}\varrho = -H\varrho. \tag{5.8}$$

In the standard basis of $\mathbb{C}^2$, the above operator can be written as $\varrho = \sum_{k,\ell}\varrho_{k\ell}|k\rangle\langle\ell|$. Consequently, equations (5.8) and (5.5) yield a set of four coupled first-order differential equations, namely

$$\frac{\partial}{\partial\beta}\varrho_{11} = -\Big[\frac{g}{N}(J^2 - J_z^2 + \frac{1}{2}) + h(J_z - \frac{1}{2})\Big]\varrho_{11} - \frac{g}{N}J_+\varrho_{21}, \tag{5.9}$$

$$\frac{\partial}{\partial\beta}\varrho_{21} = -\frac{g}{N}J_-\varrho_{11} - \Big[\frac{g}{N}(J^2 - J_z^2 + \frac{1}{2}) + h(J_z + \frac{1}{2})\Big]\varrho_{21}, \tag{5.10}$$

$$\frac{\partial}{\partial\beta}\varrho_{22} = -\Big[\frac{g}{N}(J^2 - J_z^2 + \frac{1}{2}) + h(J_z + \frac{1}{2})\Big]\varrho_{22} - \frac{g}{N}J_-\varrho_{12}, \tag{5.11}$$

$$\frac{\partial}{\partial\beta}\varrho_{12} = -\frac{g}{N}J_+\varrho_{22} - \Big[\frac{g}{N}(J^2 - J_z^2 + \frac{1}{2}) + h(J_z - \frac{1}{2})\Big]\varrho_{12}. \tag{5.12}$$

The latter can be transformed into diagonal ones by introducing the following transformations [26]:

$$\varrho_{11} = \exp\Big\{-\beta\Big[\frac{g}{N}(J^2 - J_z^2 + \frac{1}{2}) + h(J_z - \frac{1}{2})\Big]\Big\}V_{11}, \tag{5.13}$$

$$\varrho_{21} = J_-\exp\Big\{-\beta\Big[\frac{g}{N}(J^2 - J_z^2 + \frac{1}{2}) + h(J_z - \frac{1}{2})\Big]\Big\}V_{21}, \tag{5.14}$$

$$\varrho_{22} = \exp\Big\{-\beta\Big[\frac{g}{N}(J^2 - J_z^2 + \frac{1}{2}) + h(J_z + \frac{1}{2})\Big]\Big\}V_{22}, \tag{5.15}$$

$$\varrho_{12} = J_+\exp\Big\{-\beta\Big[\frac{g}{N}(J^2 - J_z^2 + \frac{1}{2}) + h(J_z + \frac{1}{2})\Big]\Big\}V_{12}. \tag{5.16}$$

Using the commutation relations $[J_z, J_\pm] = \pm J_\pm$ and $[J_z^2, \pm] = \mp J_\pm(2J_z \pm 1)$, it can be shown that the operator variables V_{ij} satisfy

$$\frac{\partial}{\partial\beta}V_{11} = -\frac{g}{N}J_+J_-V_{21}, \quad \frac{\partial}{\partial\beta}V_{21} = -\frac{g}{N}V_{11} - \frac{g}{N}(2J_z - 1)V_{21}, \tag{5.17}$$

$$\frac{\partial}{\partial\beta}V_{22} = -\frac{g}{N}J_-J_+V_{12}, \quad \frac{\partial}{\partial\beta}V_{12} = -\frac{g}{N}V_{22} + \frac{g}{N}(2J_z + 1)V_{12}. \tag{5.18}$$

Combining equations (5.17) leads to the following second-order differential equation

$$\ddot{V}_{21} + 2\frac{g}{N}\Big(J_z - \frac{1}{2}\Big)\dot{V}_{21} - \Big(\frac{g}{N}\Big)^2 J_+J_-V_{21} = 0. \tag{5.19}$$

It is worth mentioning that $\lim\limits_{T\to\infty}\varrho = \lim\limits_{\beta\to 0}\varrho = \mathbb{I}_N$, where $\mathbb{I}_N$ denotes the 2^N-dimensional unit matrix. Therefore, $V_{ii}(\beta = 0) = \mathbb{I}_{N-1}$ and $V_{ij}(\beta = 0) = 0$ for $i \neq j$. Taking into

account the last conditions, it is easy to show that the general form of the solutions of equation (5.19) is given by

$$V_{21} = 2Ae^{-\frac{g\beta}{N}(J_z-\frac{1}{2})}\sinh\Big[\frac{|g|\beta}{N}\sqrt{\Big(J_z-\frac{1}{2}\Big)^2+J_+J_-}\Big], \tag{5.20}$$

where A is a yet-to-be-determined diagonal operator. It is then sufficient to integrate the right-hand side of the first equation in (5.17) to obtain the exact form of V_{11}. Taking into account the values of V_{ij} at $\beta = 0$, one can find that $A = -\sqrt{(g/N)^2[(J_z-1/2)^2+J_+J_-]}/(2g)$, and thus by virtue of the transformations (5.13)-(5.14) we obtain

$$\begin{aligned}\varrho_{11} &= e^{-\beta G_1}\Big\{\cosh\Big[\frac{|g|\beta}{N}\sqrt{\Big(J_z-\frac{1}{2}\Big)^2+J_+J_-}\Big] \\ &+\frac{\mathrm{sign}(g)\Big(J_z-\frac{1}{2}\Big)}{\sqrt{\Big(J_z-\frac{1}{2}\Big)^2+J_+J_-}}\sinh\Big[\frac{|g|\beta}{N}\sqrt{\Big(J_z-\frac{1}{2}\Big)^2+J_+J_-}\Big]\Big\}, \qquad (5.21)\\ \varrho_{21} &= \mathrm{sign}(-g)J_-e^{-\beta G_1}\frac{1}{\sqrt{\Big(J_z-\frac{1}{2}\Big)^2+J_+J_-}}\sinh\Big[\frac{|g|\beta}{N}\sqrt{\Big(J_z-\frac{1}{2}\Big)^2+J_+J_-}\Big]\Big\} \qquad (5.22)\end{aligned}$$

where $G_1 = \frac{g}{N}(J^2 - J_z^2 - 1/2) + (h + \frac{g}{N})(J_z - \frac{1}{2})$, and $\mathrm{sign}(g)$ designates the sign of the coupling constant g.

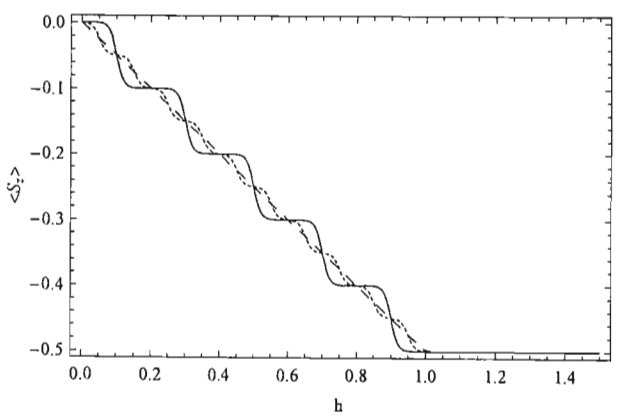

Fig. 5.1: The dependence of the mean value of S_z on the strength of the magnetic field at different values of the number of spins: $N = 10$ (solid line), $N = 20$ (dashed line), and $N = 30$ (dotted line) with $T = 0.01$.

Similarly, it can be shown that V_{12} satisfies

$$\ddot{V}_{12} - 2\frac{g}{N}\Big(J_z+\frac{1}{2}\Big)\dot{V}_{12} - \Big(\frac{g}{N}\Big)^2 J_-J_+V_{12} = 0. \tag{5.23}$$

Following the same method presented above, we find that

$$\varrho_{22} = \mathrm{e}^{-\beta G_2}\Big\{\cosh\Big[\frac{|g|\beta}{N}\sqrt{\Big(J_z+\frac{1}{2}\Big)^2+J_-J_+}\Big] + \frac{\mathrm{sign}(-g)\Big(J_z+\frac{1}{2}\Big)}{\sqrt{\Big(J_z+\frac{1}{2}\Big)^2+J_-J_+}}\sinh\Big[\frac{|g|\beta}{N}\sqrt{\Big(J_z+\frac{1}{2}\Big)^2+J_-J_+}\Big]\Big\}, \tag{5.24}$$

$$\varrho_{12} = \mathrm{sign}(-g)J_+\mathrm{e}^{-\beta G_2}\frac{1}{\sqrt{\Big(J_z+\frac{1}{2}\Big)^2+J_-J_+}}\sinh\Big[\frac{|g|\beta}{N}\sqrt{\Big(J_z+\frac{1}{2}\Big)^2+J_-J_+}\Big]\Big\}, \tag{5.25}$$

where $G_2 = \frac{g}{N}(J^2 - J_z^2 + 1/2) + (h - \frac{g}{N})(J_z + \frac{1}{2})$.

In order to obtain the reduced density matrix corresponding to the central spin-$\frac{1}{2}$ particle, we need to perform the trace in the space spanned by the common eigenvectors of J^2 and J_z. This task can be carried out with the help of the relation

$$\tilde{f} = \mathrm{tr}_{N-1}\{f(J^2, J_z)\} = \sum_{j,m}\nu(N-1,j)f[j(j+1),m], \tag{5.26}$$

where f is some function of J^2 and J_z. Since the trace of the lowering and raising operators is identically zero, we can immediately infer that the reduced density matrix is diagonal in the standard basis of $\mathbb{C}^2$, namely

$$\rho = \frac{1}{Z}\begin{pmatrix}\tilde{\varrho}_{11} & 0\\ 0 & \tilde{\varrho}_{22}\end{pmatrix}, \tag{5.27}$$

where the elements $\tilde{\varrho}_{ii}$ are calculated using equation (5.26). It follows that the mean value

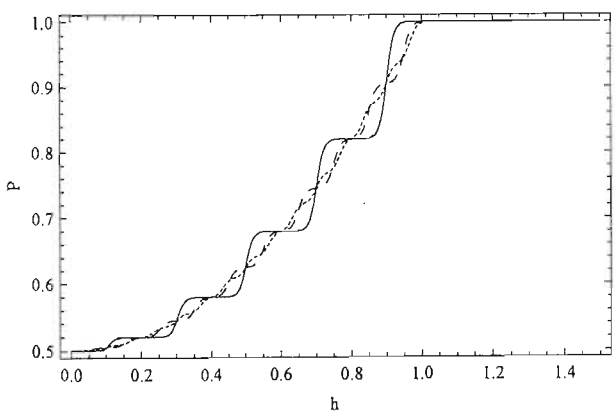

Fig. 5.2: The dependence of the mean value of the purity of the reduced density matrix on the strength of the magnetic field at different values of the number of spins: $N = 10$ (solid line), $N = 20$ (dashed line), and $N = 30$ (dotted line) with $T = 0.01$.

of S_z, the purity and the von Neumann entropy corresponding to ρ are, respectively given by $\langle S_z \rangle = \frac{1}{2Z}(\tilde{\varrho}_{22} - \tilde{\varrho}_{11})$, $P = \mathrm{tr}\rho^2 = \frac{1}{Z^2}(\tilde{\varrho}_{11}^2 + \tilde{\varrho}_{22}^2)$, and $S(\rho) = -(\tilde{\varrho}_{11}/Z)\log_2(\tilde{\varrho}_{11}/Z) - (\tilde{\varrho}_{22}/Z)\log_2(\tilde{\varrho}_{22}/Z)$.

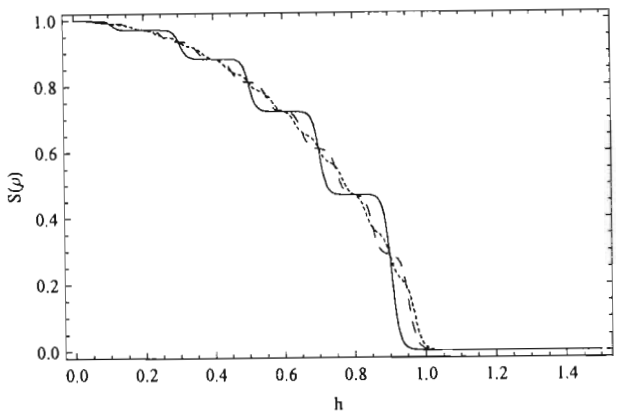

Fig. 5.3: The von Neumann entropy as a function of the strength of the magnetic field at different values of the number of spins: $N = 10$ (solid line), $N = 20$ (dashed line), and $N = 30$ (dotted line) with $T = 0.01$.

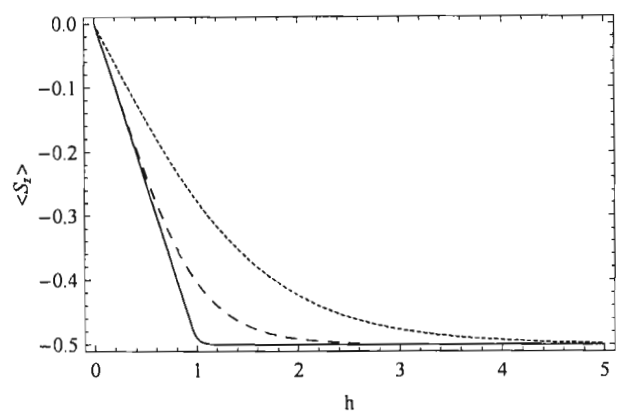

Fig. 5.4: The mean value of S_z as a function of the strength of the magnetic field at different values of the temperature: $T = 0.1$ (solid line), $T = 0.4$ (dashed line), and $T = 0.8$ (dotted line) with $N = 300$.

Figures 5.1–5.3 display the variation of the above quantities as a function of the strength of the magnetic field at different values of the number of spins. We can see that $\langle S_z \rangle$ vanishes for $h = 0$ regardless of the values of N and T. This follows from the fact that, when h is equal to zero, the operator H reduces to Heisenberg XY Hamiltonian, which is invariant under rotations with respect to the z direction. The above operator is clearly even function of J_z, which is also the case for the corresponding density matrix,

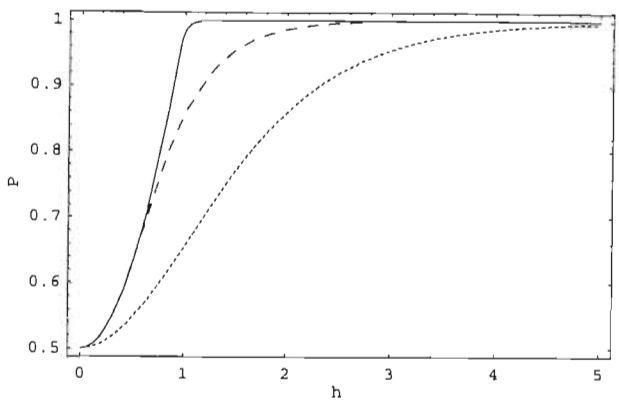

Fig. 5.5: The dependence of the purity on the strength of the magnetic field at different values of the temperature: $T = 0.1$ (solid line), $T = 0.4$ (dashed line), and $T = 0.8$ (dotted line) with $N = 300$.

$\rho_N(0)$: the thermal average of J_z is identically equal to zero.

From the above figures one can also see that, in the symmetry broken phase, starting from some value h_0 in the neighborhood of the critical point $h_c = 1$, the von Neumann entropy vanishes whereas $\langle S_z \rangle$ and P become identically equal to -1 and 1, respectively. This means that all the spins are pointing in the direction of the magnetic field. Obviously, the above quantities maintain these values in the symmetric phase since the ground state of the spin system is equal to the fully polarized state vector $|N/2, -N/2\rangle$. Furthermore, it can be seen that the variation of $\langle S_z \rangle$, P and $S(\rho)$ is accompanied in the broken phase by some kind of oscillations which become appreciable at small values of N. This can be explained by the dependence of the ground state $|N/2, -I(hN/2)\rangle$, which exhibits at low temperatures the largest statistical weight, on the strength of the magnetic field. Clearly, the quantity $I(hN/2)$ has the structure of a step function with respect to h; as T increases, the mean value of S_z slightly deviates from $-I(hN/2)/N$. A similar behaviour can also be observed for the purity and the von Neumann entropy. As we increase the number of spins and/or the temperature T, the oscillations completely disappear. Also, we observe that $h_0 \to h_c$ for $N \to \infty$ and $T \to 0$, as expected, since in this limit $I(hN/2)/N \approx h/2$. The behaviour of the above quantities at large N is shown in figures 5.4-5.6.

5.2.2 *The two-particle reduced density matrix, pairwise thermal entanglement*

Next, consider entanglement properties of the isotropic Lippkin-Meshkov-Glick model at temperatures close to the zero absolute. The relevant quantity we shall look for

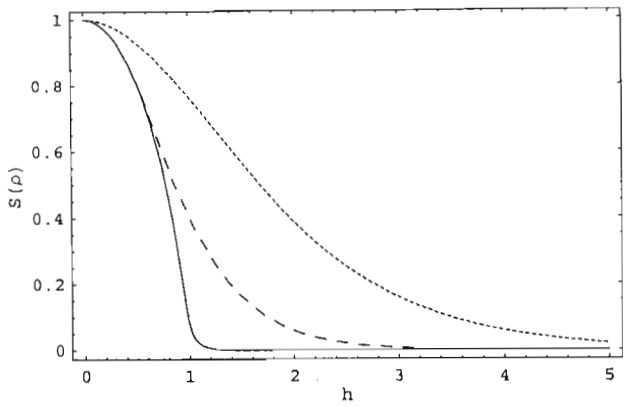

Fig. 5.6: Variation of the von Neumann entropy with the strength of the magnetic field at different values of the temperature: $T = 0.1$ (solid line), $T = 0.4$ (dashed line), and $T = 0.8$ (dotted line) with $N = 300$.

is the two-spin reduced density matrix, ρ. A knowledge of the latter enables one to quantify the pairwise thermal entanglement between the pairs of spin-$\frac{1}{2}$ particles. The simplest measure we can use is the concurrence, which is explicitly defined by $C(\rho) = \max\Big\{0, 2\max\Big[\sqrt{\lambda_i}\Big] - \sum_{i=1}^{4}\sqrt{\lambda_i}\Big\}$[27], where the λ_i are the eigenvalues of the operator $\rho(\sigma_y \otimes \sigma_y)\rho^*(\sigma_y \otimes \sigma_y)$. It is worth mentioning that due to the invariance with respect to exchange of sites, the two-spin reduced density matrix in the space $\mathbb{C}^2 \otimes \mathbb{C}^2$ takes the form

$$\rho = \begin{pmatrix} a_- & 0 & 0 & 0 \\ 0 & b & c & 0 \\ 0 & c & b & 0 \\ 0 & 0 & 0 & a_+ \end{pmatrix}, \tag{5.28}$$

where, $a_\pm$, b, and c are real numbers. The fact that c is real ensures that the reduced density matrix is diagonal in the space $\mathbb{C}^3 \oplus \mathbb{C} \equiv \mathbb{C}^2 \otimes \mathbb{C}^2$ spanned by the vectors $\{|1,-1\rangle, |1,0\rangle, |1,1\rangle, |0,0\rangle\}$[25]. The method presented in the previous subsection can also be applied here to derive the explicit form of ρ; we find that in $\mathbb{C}^3 \oplus \mathbb{C}$, the first two diagonal elements of ϱ read

$$\begin{aligned} \varrho_{11} \;=\; & \frac{2}{M^4 - M^2}\exp\Big\{-\beta\Big[\frac{g}{N}(J^2 - J_z^2 + 1) + h(J_z - 1)\Big]\Big\} \\ & \times\Big\{\Big[J_+J_- + 4(J_+J_-)^2 - 2J_z - 12J_zJ_+J_- + 10J_z^2 + 12J_+J_-J_z^2 \\ & -16J_z^3 + 8J_z^4\Big]\cosh(g\beta M/N) - M\sinh(g\beta M/N) \end{aligned}$$

$$\times\Big[3J_+J_- - 2J_z - 4J_zJ_+J_- + 6J_z^2 - 4J_z^3\Big]$$
$$+\Big[J_+J_- + 4(J_+J_-)^2 - 4J_+J_-J_z + 4J_+J_-J_z^2\Big]\mathrm{e}^{\frac{g\beta}{N}}\Big\}, \tag{5.29}$$

$$\varrho_{22} = \frac{4\mathrm{e}^{\frac{g\beta}{N}}}{M^4 - M^2}\Big\{\Big[J_+J_- + 4(J_+J_-)^2 - J_z - 8J_+J_-J_z + 4J_z^2J_+J_-$$
$$+4J_z^2(1 - J_z)\Big]\cosh(g\beta M/N) - M\sinh(g\beta M/N)\Big[J_+J_- - J_z + 2J_z^2\Big]$$
$$+\mathrm{e}^{\frac{g\beta}{N}}\Big[4J_+J_-J_z^2 + J_z^2 + 4J_z^3(J_z - 1)\Big]\Big\}$$
$$\times\exp\Big\{-\beta\Big[\frac{g}{N}(J^2 - J_z^2 + 2) + h(J_z)\Big]\Big\} \tag{5.30}$$

where $M = \sqrt{1 - 4J_z + 4J_z^2 + 4J_+J_-}$. Due to the symmetry, the explicit form of the matrix element ϱ_{33} can be obtained from the expression of ϱ_{11} by simply making the substitution $h \to -h$. Moreover, since $J_\pm|0,0\rangle \equiv 0$, then the fourth diagonal element corresponding to $\mathbb{C}$ is simply given by

$$\varrho_{44} = \exp\Big\{-\beta\Big[\frac{g}{N}(J^2 - J_z^2) + hJ_z\Big]\Big\}. \tag{5.31}$$

Then the elements of the two-spin reduced density matrix are given by

$$\rho_{ii} = \frac{1}{Z}\sum_{j,m}\nu(N-2,j)\langle j,m|\varrho_{ii}|j,m\rangle. \tag{5.32}$$

One can check their equivalence with the results of reference [24], where the elements of the density matrix (5.28) are shown to be explicitly given by

$$a_\pm = \frac{N^2 - 2N + 4\langle\mathcal{J}_z^2\rangle \pm 4(N-1)\langle\mathcal{J}_z\rangle}{4N(N-1)}, \tag{5.33}$$

$$b = \frac{N^2 - 4\langle\mathcal{J}_z^2\rangle}{4N(N-1)}, \tag{5.34}$$

$$c = \frac{\langle\mathcal{J}_+\mathcal{J}_- + \mathcal{J}_-\mathcal{J}_+\rangle - N}{2N(N-1)}, \tag{5.35}$$

where the thermal average is defined as $\langle L\rangle \equiv \mathrm{tr}_N\{L\rho_N(0)\}$.

The main aim here is to investigate the pairwise thermal entanglement in the Lipkin-Meshkov-Glick model. From figures 5.7 and 5.8, we can see that, even at nonzero temperature, the concurrence is still sensitive to the phase of the system. Clearly, the above quantity strongly depends on both the temperature and the number of spins of the system. It turns out that, at sufficiently low T (N), there exists a threshold N_0 (T_0) above which the pairwise concurrence becomes identically zero. The values of N_0 and T_0 depend, however, on the temperature and the number of spins, respectively. Moreover, the concurrence displays, in the broken phase, oscillations in the form of steps whose amplitudes increase with the increase of h. Within the latter phase, $C(\rho)$ also exhibits a peak which

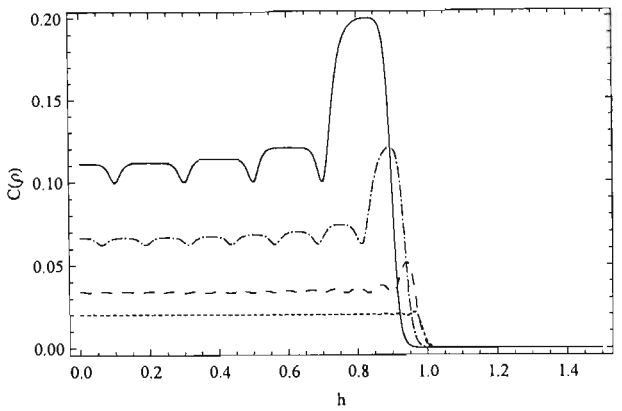

Fig. 5.7: The pairwise thermal entanglement as a function of h at different values of N: $N = 10$ (dotted line), $N = 15$ (dot dashed line), $N = 30$ (dashed line), and $N = 50$ (dotted line) with $T = 0.01$.

rapidly falls to zero in the neighborhood of the critical point h_c. At slightly higher T, we can see that the accompanying oscillations together with the peak disappear; in this case the concurrence is a monotonic decreasing function of the strength of the magnetic field. As N increases, $C(\rho)$ decreases until it becomes practically independent of h in the symmetry broken phase. For sufficiently large h, the concurrence is obviously zero since the state of the system is, to a good approximation, equal to its fully polarized ground state. Finally, note that the behaviour of the mean value of S_z, the purity and the von Neumann entropy is quite similar to that of the one-particle case.

At zero temperature, the derivative of the concurrence with respect to h is expected to display divergence at the critical point. However, for small N, even at zero temperature, the concurrence vanishes at h_0 and not at $h_c = g$. This is illustrated in figure 5.9 where the variation of $D(\rho) = \frac{dC(\rho)}{dh}$ as a function of h is shown for $N = 10$ and $T = 0.001$. Notice that the concurrence vanishes in the neighborhood of $h = 0.9$, which is exactly the value of h_0 in this particular case when $T \to 0$. It is worth mentioning that the behaviour of ground state entanglement (i.e., zero-temperature entanglement) of multi-spin systems displaying quantum phase transition can be treated within the framework of density functional theory as explained in reference [28].

5.3 Coherence and concurrence dynamics

In this section we investigate the dynamics of the central spin system, assuming that its coupling constant to the bath, which we denote by α, is different from g. The former

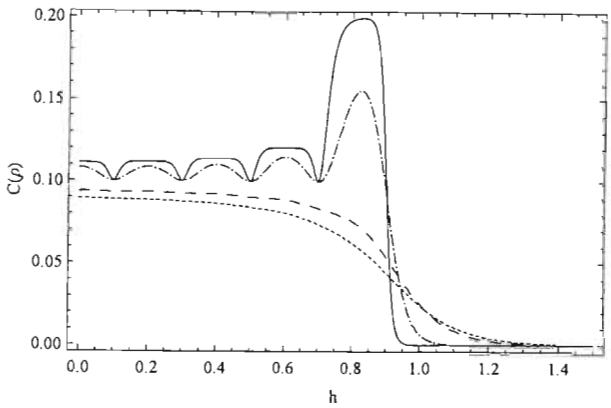

Fig. 5.8: The pairwise thermal entanglement as a function of h at different values of T: $T = 0.01$ (solide line), $T = 0.03$ (dot-dashed line), $T = 0.08$ (dashed line), and $T = 0.1$ (dotted line) with $N = 10$.

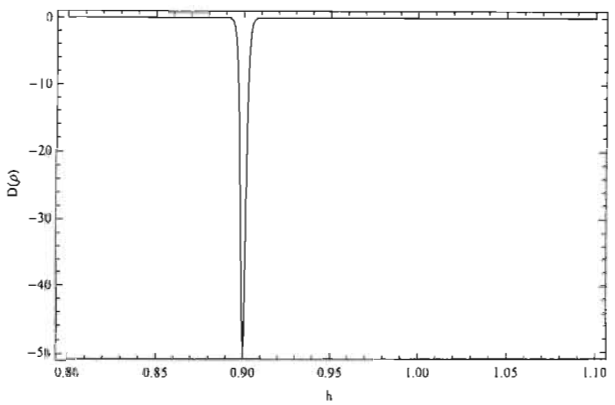

Fig. 5.9: The derivative of concurrence as a function of h for $N = 10$ and $T = 0.001$.

will be rescaled, as usual, by $\sqrt{N}$ to ensure an extensive free energy. The Hamiltonian operator describing the interaction between the two systems reads

$$H_I = \frac{\alpha}{\sqrt{N}}\left[S_+^0 J_- + S_-^0 J_+\right], \tag{5.36}$$

where $\vec{S}^0$ stands for the spin operator vector of the central system. Here we use the notation $\vec{J}$ for the total spin instead of $\vec{\mathcal{J}}$ for convenience. In order to determine the exact analytical form of the time evolution operator, $\mathbf{U}(t)$, governing the unitary dynamics of the full system, we note that it satisfies the equation [29]

$$i\frac{d\mathbf{U}(t)}{dt} = (H_0 + H_I + H)\mathbf{U}(t), \tag{5.37}$$

with $H_0 = hS_z^0$. Then the matrix elements of $\mathbf{U}(t)$ can be determined, for both one and two central spins, using the same method presented above. However, we shall not go

through the details of the calculations since it is sufficient to make the replacement

$$\beta \rightarrow \mathrm{i}\, t, \tag{5.38}$$

and to take into account the fact that the coupling constants are different. In the case of a single central spin one can find that in $\mathbb{C}^2$,

$$\begin{aligned} U_{11}(t) &= e^{-\mathrm{i}tG_1}\Big\{\cos\Big[t\sqrt{\Big(\frac{g}{N}(J_z-\frac{1}{2})\Big)^2+\frac{\alpha^2}{N}J_+J_-}\Big] \\ &+\frac{\mathrm{i}g/N\Big(J_z-\frac{1}{2}\Big)}{\sqrt{\Big(\frac{g}{N}(J_z-\frac{1}{2})\Big)^2+\frac{\alpha^2}{N}J_+J_-}}\sin\Big[t\sqrt{\Big(\frac{g}{N}(J_z-\frac{1}{2})\Big)^2+\frac{\alpha^2}{N}J_+J_-}\Big]\Big\}, \end{aligned} \tag{5.39}$$

$$\begin{aligned} U_{22}(t) &= e^{-\mathrm{i}tG_2}\Big\{\cos\Big[t\sqrt{\Big(\frac{g}{N}(J_z+\frac{1}{2})\Big)^2+\frac{\alpha^2}{N}J_-J_+}\Big] \\ &-\frac{\mathrm{i}g/N\Big(J_z+\frac{1}{2}\Big)}{\sqrt{\Big(\frac{g}{N}(J_z+\frac{1}{2})\Big)^2+\frac{\alpha^2}{N}J_-J_+}}\sin\Big[t\sqrt{\Big(\frac{g}{N}(J_z+\frac{1}{2})\Big)^2+\frac{\alpha^2}{N}J_-J_+}\Big]\Big\}, \end{aligned} \tag{5.40}$$

$$U_{12}(t) = J_+\frac{-\mathrm{i}\alpha/\sqrt{N}\mathrm{e}^{-\mathrm{i}G_2t}}{\sqrt{\Big[\frac{g}{N}(J_z+\frac{1}{2})\Big]^2+\frac{\alpha^2}{N}J_-J_+}}\sin\Big\{t\sqrt{\Big[\frac{g}{N}(J_z+\frac{1}{2})\Big]^2+\frac{\alpha^2}{N}J_-J_+}\Big\}, \tag{5.41}$$

$$U_{21}(t) = J_-\frac{-\mathrm{i}\alpha/\sqrt{N}\mathrm{e}^{-\mathrm{i}G_1t}}{\sqrt{\Big[\frac{g}{N}(J_z-\frac{1}{2})\Big]^2+\frac{\alpha^2}{N}J_+J_-}}\sin\Big\{t\sqrt{\Big[\frac{g}{N}(J_z-\frac{1}{2})\Big]^2+\frac{\alpha^2}{N}J_+J_-}\Big\}. \tag{5.42}$$

The coherence of the central system, which is assumed to be initially decoupled from the bath, is given by

$$S_-^0(t) = \frac{1}{Z}\mathrm{tr}_N\Big\{\mathbf{U}(t)\Big(S_-^0(0)\otimes \mathrm{e}^{-\beta H}\Big)\mathbf{U}^\dagger(t)\Big\} = \Phi(t)S_-^0(0), \tag{5.43}$$

where

$$\Phi(t) = \frac{1}{Z}\mathrm{tr}_N\Big[U_{11}(t)\ \mathrm{e}^{-\beta H}U_{22}^\dagger(t)\Big]. \tag{5.44}$$

In the case of the two-qubit central system, we only consider the evolution in time of the maximally entangled state $|1,0\rangle = \frac{1}{\sqrt{2}}(|01\rangle + |10\rangle)$; other cases can be treated in exactly the same manner. It can be shown that the time-dependent reduced density matrix corresponding to the above initial state is diagonal in $\mathbb{C}^3$, with the matrix elements [25] $\rho_{\ell\ell}(t) = \mathrm{tr}_N[U_{\ell 2}\rho_N(0)U_{\ell 2}^\dagger]$ where

$$U_{22}(t) = \mathrm{e}^{-\mathrm{i}t[g/N(J^2-J_z^2)+hJ_z]} \sum_{k=1}^{3} \frac{\mathrm{e}^{r_k t}}{H_k} \Big[\Big(\frac{g}{N}\Big)^2 (1-4J_z^2) + 2\mathrm{i}\frac{g}{N} r_k - r_k^2 \Big], \tag{5.45}$$

$$U_{12}(t) = -\frac{\sqrt{2}\alpha}{\sqrt{N}} J_+ \mathrm{e}^{-\mathrm{i}t[g/N(J^2-J_z^2)+hJ_z]} \sum_{k=1}^{3} \frac{\mathrm{e}^{r_k t}}{H_k} \Big[\Big(\frac{g}{N}\Big)(1-2J_z^2) + \mathrm{i}r_k \Big], \tag{5.46}$$

$$U_{32}(t) = -\frac{\sqrt{2}\alpha}{\sqrt{N}} J_- \mathrm{e}^{-\mathrm{i}t[g/N(J^2-J_z^2)+hJ_z]} \sum_{k=1}^{3} \frac{\mathrm{e}^{r_k t}}{H_k} \Big[\Big(\frac{g}{N}\Big)(1+2J_z^2) - \mathrm{i}r_k \Big]. \tag{5.47}$$

Here, $H_k = \left(\frac{g}{N}\right)^2 (1-4J_z^2) - 4\alpha^2/N(J_+J_- - J_z) + 4\mathrm{i}\frac{g}{N} r_k - 3r_k^2$; the quantities r_k are the solutions of the equation

$$r^3 - 2\mathrm{i}g/N r^2 + \Big[\Big(\frac{g}{N}\Big)^2 (4J_z^2 - 1) + 4\frac{\alpha^2}{N}(J_+J_- - J_z) \Big] r + 4\mathrm{i}\alpha^2 g/N^3 (J_z - 2J_z^2 - J_+J_-) = 0. \tag{5.48}$$

They are explicitly given by

$$r_1 = \frac{1}{3R}\Big[2\mathrm{i}Rg/N - (K - R^2)\Big], \tag{5.49}$$

$$r_2 = \frac{1}{6R}\Big[4\mathrm{i}Rg/N + (1+\mathrm{i}\sqrt{3})(K + \mathrm{i}R^2)\Big], \tag{5.50}$$

$$r_3 = \frac{1}{6R}\Big[4\mathrm{i}Rg/N + (K - R^2) - \mathrm{i}\sqrt{3}(K + R^2)\Big], \tag{5.51}$$

where

$$K = 12(\alpha^2/N)(J_+J_- - J_z) + (g/N)^2(1 + 12J_z^2), \tag{5.52}$$

and

$$R = \Big[\mathrm{i}Qg/N + \frac{1}{2}\sqrt{4K^3 - 4(g/N)^2 Q^2}\Big]^{1/3}, \tag{5.53}$$

with

$$Q = (g/N)^2(-1 + 36J_z^2) - 18\alpha^2/N[J_+J_- + J_z(-1 + 6J_z)]. \tag{5.54}$$

The concurrence corresponding to the sate $|1,0\rangle$ is simply given by [25, 30] $C(t) = \max\{0, 2\max[\rho_{22}, \sqrt{\rho_{11}\rho_{33}}] - \rho_{22} - 2\sqrt{\rho_{11}\rho_{33}}\}$. The evolution in time of both $C(t)$ and the absolute value of $\Phi(t)$ is shown in figures 5.10 and 5.11. Clearly, the behaviour of the above quantities depends on the phase of the system even though the temperature is different from zero. This actually becomes more clear as N increases in contrast to the thermal pairwise entanglement which exists only for small values of N. The change of the behaviour of the concurrence and the coherence is related to the change of the ground state of the bath at the critical point. Once again we recall that the ground state is characterized by the largest statistical weight at low temperatures, which means that any

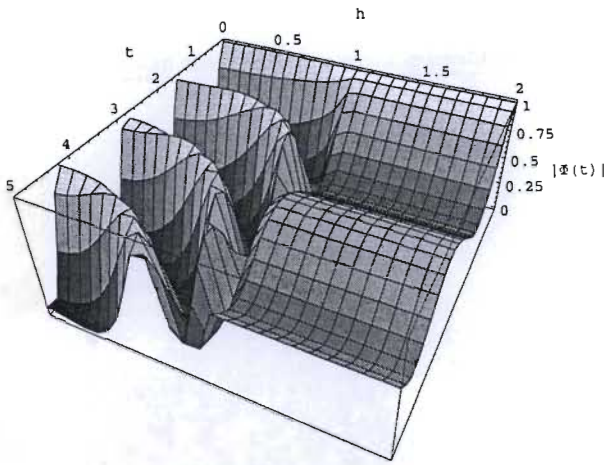

Fig. 5.10: Time dependence of $|\Phi(t)|$ for different values of h with $N = 100$ and $T = 0.01$. The time variable is given in units of α.

perturbation of the latter state affects the time evolution of the central spins. It can be checked that at high temperatures, the behaviour of the reduced density matrix is exactly the same in both phases.

So far we have only considered Heisenberg XY interactions between the central system and the bath. Let us briefly investigate the case where the couplings are of Ising type. The corresponding interaction Hamiltonian operator is given by $H_I = \frac{\lambda}{\sqrt{N}} S_z^0 J_z$, where λ is the coupling constant. One can easily see that the Lipkin-Meshkov-Glick Hamiltonian (5.1) commutes with H_I, that is $[H, H_I] = 0$. Therefore, in the case of a single central spin, the coherence is proportional to the function

$$\Lambda(t) = \frac{1}{Z} \sum_{j,m} \nu(N,j) \exp\Big\{ 2ih\ t - \beta[g/N(j(j+1) - m^2) + h\ m] + \frac{i\lambda t}{\sqrt{N}} m \Big\} \qquad (5.55)$$

whose dependence on the time and the strength of the magnetic field is illustrated in figure 5.12. This reveals that, at low temperatures, the absolute value of $\Lambda(t)$ is equal to one in the symmetric phase independently of the values of h. In the case of two central spins, the bell state $|1,0\rangle$ is found to be decoherence-free: its concurrence does not evolve in time. However, the behaviour of the concurrence corresponding to the maximally entangled state $\frac{1}{\sqrt{2}}(|1,1\rangle + |1,-1\rangle)$ is identical to that of $\Lambda(t)$, except that it decays twice faster than the above function. Once again, we find that the dynamics of the central system depends on the phase of the bath. As a final remark, note that the sudden change of the concurrence at the critical point above which it vanishes is quite similar to entanglement sudden death [31, 32]. One should not take this comparison too seriously since entanglement sudden

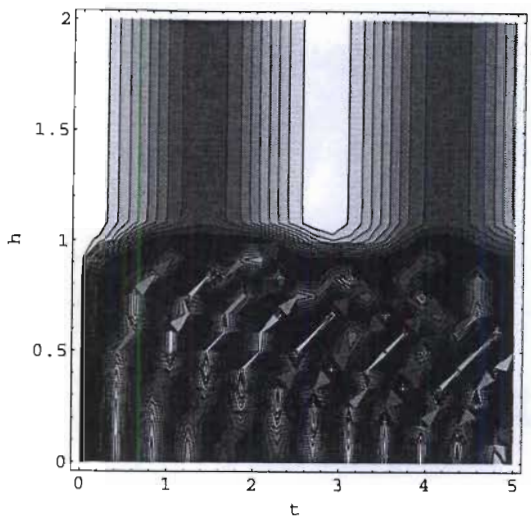

Fig. 5.11: Contour plot showing the time dependence of $C(t)$ for different values of h with $N = 100$ and $T = 0.01$. The time variable is given in units of $\alpha/\sqrt{2}$.

death corresponds to the time dependence of entanglement. In our case, however, the parameter that controls the variation of entanglement is the strength of the magnetic field, externally applied to the spin bath. What really matters is the difference in the behaviour of the dynamics in both phases rather than the vanishing of the entanglement itself.

5.4 Summary

In summary we have investigated the nonzero temperature dynamics of one and two central qubits coupled to an isotropic Lipkin-Meshkov-Glick bath near its critical point. We showed that the reduced density matrix of the central spin-system can be exactly derived using an operator technique that makes use of the underlying symmetries of the model Hamiltonian. It is found that, at sufficiently low temperatures, the dynamics is sensitive to the phase of the bath. This is simply due to the fact that the main contribution to the thermal state of the bath comes from its ground state. For small values of the number of spins, the pairwise thermal entanglement clearly signals the existence of the critical point at which the transition occurs. However, above some threshold values of both the temperature and the number of spins within the bath, the pairwise thermal entanglement ceases to exist. This turns out to be not the case when the central spin-system is not part of the bath, i.e. its coupling constant is different form those of bath spins; here we

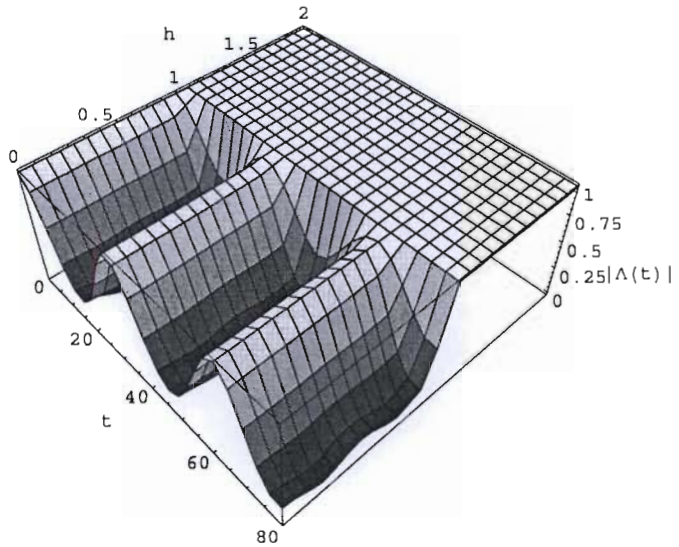

Fig. 5.12: Time dependence of $|\Lambda(t)|$ at different values of h with $N = 100$ and $T = 0.01$; the time variable is given in units of λ.

find that the differences between the behaviour of the concurrence within the two possible phases of the bath become more clear at large values of the number of spins.

BIBLIOGRAPHY

[1] Sachdev S 1999 *Quantum Phase Transitions* (Cambridge: Cambridge University Press)

[2] Osterloh A, Amico L, Falci G and Fazio R 2002 *Nature* (London) **416** 608

[3] Osborn T J and Nielson M A 2002 *Phys. Rev.*A **66** 032110

[4] Vidal G, Latorre J I, Rico E and Kitaev A 2003 *Phys. Rev. Lett.* **90** 227902

[5] Gu S J, Lin H Q and Li Y Q 2003 *Phys. Rev.* A **68** 042330

[6] Huang Z, Osendo O and Kais S 2004 *Phys. Lett.* A **322** 137

[7] Barnum H, Knill E, Ortiz G, Somma R and Viola L 2004 *Phys. Rev. Lett.* **92** 107902

[8] Alcaraz F C, Saguia A and Sarandy M S 2004 *Phys. Rev.* A **70** 032333

[9] Wu L A, Sarandy M S and Lidar D A 2004 *Phys. Rev. Lett.* **93** 250404

[10] Gu S J, Tian G S and Lin H Q 2005 *Phys. Rev.* A **71** 052322

[11] Sachdev S 2001 v2 *Preprint* cond-mat/0110161

[12] Lipkin H J, Meshkov N and Glick N 1965 *nucl. Phys.* A **62** 188

[13] Meshkov N , Glick N abd Lipkin H J 1965 *nucl. Phys.* A **62** 199

[14] Glick N, Lipkin H J and Meshkov N 1965 *nucl. Phys.* A **62** 211

[15] Botet R, Julien R and Pfeuty P 1982 *Phys. Rev. Lett.* **49**, 478

[16] Botet R and Julien R 1983 *Phys. Rev.* B **28** 3955

[17] Cirac J I, Lewenstein M, Mølmer K and Zoller P 1998 *Phys. Rev.* A **57** 1208

[18] Vidal J, Palacios G and Mosseri R 2004 *Phys. Rev.* A **69** 022107

[19] Vidal J, Mosseri R and Dukelsy J 2004 *Phys. Rev.* A **69** 054101

[20] Vidal J, Palacios G and Aslangul C 2004 *Phys. Rev.* A **70** 062304

[21] Vidal J 2006 *Phys. Rev.* A **73** 062318

[22] Chen G and Liang J-Q 2006 *New Journal of Physics* **8** 297

[23] Quant H T, Wang Z D and Sun C P 2007 *Phys. Rev.* A **76** 012104

[24] Wang X and Mølmer K 2002 *Eur. Phys. J* D **18** 385

[25] Hamdouni Y 2007 *J. Phys. A: Math. Theor.* **40** 11569

[26] Hamdouni Y and Petruccione F 2007 *Phys. Rev.* B **76** 174306

[27] Wootters W K 1998 *Phys. Rev. Lett.* **80** 2245

[28] Wu L -A, Sarandy M S, Lidar D A and Sham L J 2006 *Phys. Rev.* A **74** 052335

[29] Yuan X Z, Goan H S and Zhu K D 2007 *Phys. Rev.* B **75** 045331

[30] Hamdouni Y, Fannes M and Petruccione F 2006 *Phys. Rev.* B **73** 245323

[31] Yu T and Eberly J H 2006 *Phys. Rev. Lett.* **97** 140403

[32] Obada A S -F and Abdel-Aty M 2006 *Phys. Rev.* B **75** 195310

6. ON THE PARTIAL TRACE OVER COLLECTIVE SPIN DEGREES OF FREEDOM

6.1 Introduction

In recent years there has been an increasing interest in the description of the dynamics of small quantum systems interacting with their surrounding [1]. This was motivated by the necessity of understanding the phenomenon of decoherence in quantum systems [2, 3, 4, 5], and the attempt to build quantum devices that enable the implementation of quantum algorithms [6]. However, the main difficulty one faces in such a task consists in dealing with the large number of environmental degrees of freedom, which makes most of the proposed theoretical models impossible to be solved analytically even for finite sizes of the surrounding.

Among the promising candidates to quantum information processing and quantum computing, spin systems seem to be the most suitable for the construction of quantum gates [7, 8]. Recently, it has been shown that exact analytical solutions can be obtained for the dynamics of few central qubits coupled to spin baths of finite and infinite sizes [9, 10, 11]. There, the interaction Hamiltonians together with the baths Hamiltonians are functions of the collective spin operators of the environments. In order to derive the reduced density matrix of the central qubits, the partial trace over the environmental spin degrees of freedom was carried out within the subspaces corresponding to the different values of the total angular momentum of the surrounding.

Recall that the state space of single spin-$\frac{1}{2}$ particle is given by $\mathbb{C}^2$, where $\mathbb{C}$ denotes the field of complex numbers. The corresponding basis is formed by the eigenvectors $\{|-\rangle, |+\rangle\}$ associated with the eigenvalues $\pm\frac{1}{2}$ of the operator $S_z = \frac{1}{2}\sigma_z$, where σ_z designates the z-component of the Pauli operator $\vec{\sigma}$. In general, the state space of a system of N qubits is given by the N-fold tensor product of the state spaces of the individual particles, namely, $\mathbb{C}^{2\otimes N}$. One possible basis of the latter space consists of the state vectors $\bigotimes_i^N |\epsilon_i\rangle$, with $\epsilon_i = \pm$. These are eigenvectors of the collective spin operator J_z, where $\vec{J} = \frac{1}{2}\sum_{i=1}^N \vec{\sigma_i}$. Alternatively, one can construct new basis composed of the common eigenvectors of the

operators J^2 and J_z; we shall denote them by $|j,m\rangle$ such that $\kappa \leq j \leq N/2$ and $-j \leq m \leq j$, as imposed by the laws of addition of angular momentum in quantum mechanics [12]. In the above, $\kappa = 0$ for N even, and $\kappa = 1/2$ for N odd. Note that the scalar product of state vectors corresponding to different values of j vanishes. This means that the total space $\mathbb{C}^{2\otimes N}$ can be decomposed as the direct sum of subspaces $\mathbb{C}^{2j+1}$, that is

$$\mathbb{C}^{2\otimes N} = \bigoplus_{j=\kappa}^{\frac{N}{2}} \nu(N,j)\mathbb{C}^{2j+1}. \tag{6.1}$$

The quantity $\nu(N,j)$ is the multiplicity corresponding to the value j of the total angular momentum; its exact form reads [13]

$$\nu(N,j) = \binom{N}{N/2-j} - \binom{N}{N/2-j-1} = \frac{2j+1}{\frac{N}{2}+j+1}\frac{N!}{(\frac{N}{2}-j)!(\frac{N}{2}+j)!}. \tag{6.2}$$

Hence, given any operator $\hat{G}(\vec{J})$ on $\mathbb{C}^{2\otimes N}$, its trace can be written as

$$\text{tr } \hat{G} = \sum_{j=\kappa}^{\frac{N}{2}} \nu(N,j) \sum_{m=-j}^{j} \langle j,m|\hat{G}|j,m\rangle. \tag{6.3}$$

Following the general ideas of the theory of open quantum systems, the problem of finding a relation between the multiplicities of the subspaces $\mathbb{C}^{2\otimes N_i}$ and that of $\mathbb{C}^{2\otimes N}$, where $\sum_i N_i = N$, naturally arises. In this work we illustrate how this problem can be solved, in the case $N = N_1 + N_2$, using the invariance of the trace. The latter property will also be used to describe the dynamics of two qubits in separate spin baths.

6.2 A decomposition law for the degeneracy $\nu(N,J)$.

Let us denote by $|j_i,m_i\rangle$ the basis state vectors in the space $\mathbb{C}^{2\otimes N_i}$ $(i=1,2)$. Hence the trace of $\hat{G}(\vec{J})$ can also be expressed as

$$\text{tr}\hat{G} = \sum_{j_1=\kappa_1}^{N_1/2} \sum_{m_1=-j_1}^{j_1} \sum_{j_2=\kappa_2}^{N_2/2} \sum_{m_2=-j_2}^{j_2} \nu(N_1,j_1)\nu(N_2,j_2)\langle j_1,j_2,m_1,m_2|\hat{G}|j_1,j_2,m_1,m_2\rangle. \tag{6.4}$$

On the other hand we have [14]

$$|j_1,j_2,m_1,m_2\rangle = \sum_{J=|j_1-j_2|}^{j_1+j_2} \sum_{M=-J}^{J} (-1)^{j_1-j_2+M}\sqrt{2J+1} \times \begin{pmatrix} j_1 & j_2 & J \\ m_1 & m_2 & -M \end{pmatrix} |J,M\rangle, \tag{6.5}$$

where the quantity in matrix form denotes Wigner $3j$-symbol; obviously, the condition $m_1 + m_2 = M$ along with the triangle rule $|j_1 - j_2| \leq J \leq j_1 + j_2$ must be satisfied. By equations (6.4) and (6.5), we can write:

$$\begin{aligned}\mathrm{tr}\hat{G} = \sum_{j_1,m_1}\sum_{j_2,m_2}\nu(N_1,j_1)\nu(N_2,j_2)\sum_{J,J'=|j_1-j_2|}^{j_1+j_2}\sum_{M=-J}^{J}\sum_{M'=-J'}^{J'}(-1)^{2(j_1-j_2)+M+M'} \\ \times\sqrt{(2J+1)(2J'+1)}\begin{pmatrix} j_1 & j_2 & J \\ m_1 & m_2 & -M \end{pmatrix} \\ \times\begin{pmatrix} j_1 & j_2 & J' \\ m_1 & m_2 & -M' \end{pmatrix}\langle J',M'|\hat{G}|J,M\rangle, \end{aligned} \tag{6.6}$$

where we have used the fact that $3j$-symbols are real. The operator $\hat{G}$ is arbitrary; it can be chosen such that it satisfies $\langle J',M'|\hat{G}|J,M\rangle = \langle J,M|\hat{G}|J,M\rangle\delta_{JJ'}\delta_{MM'}$. In this case equation (6.6) reduces to

$$\begin{aligned}\mathrm{tr}\hat{G} = \sum_{j_1,m_1}\sum_{j_2,m_2}\nu(N_1,j_1)\nu(N_2,j_2)\sum_{J=|j_1-j_2|}^{j_1+j_2}\sum_{M=-J}^{J}(-1)^{2(j_1-j_2)+2M} \\ (2J+1)\left\{\begin{pmatrix} j_1 & j_2 & J \\ m_1 & m_2 & -M \end{pmatrix}\right\}^2\langle J,M|\hat{G}|J,M\rangle. \end{aligned} \tag{6.7}$$

The lower and upper limits of the sum over J in the above equation are, respectively, $|j_1 - j_2|$ and $j_1 + j_2$. For $J < |j_1 - j_2|$, or $J > j_1 + j_2$, the triple (j_1, j_2, J) does not satisfy the triangle rule and hence the corresponding Wigner $3j$-symbol vanishes. Consequently, the right-hand side of equation (6.7) will not be affected if we take $\frac{N_1+N_2}{2}$ as an upper limit, and κ as a lower limit for the sum over J such that $\kappa = 0$ for $N_1 + N_2$ even and $\kappa = 1/2$ for $N_1 + N_2$ odd. This effectively allows us to exchange the order of the sums in the above equation. Then by comparing the resulting equation with (6.3), we obtain

$$\begin{aligned}\nu(N_1+N_2,J) = \sum_{j_1,m_1}\sum_{j2,m2}\nu(N_1,j_1)\nu(N_2,j_2)(-1)^{2(j_1-j_2+J)}(2J+1) \\ \times\left\{\begin{pmatrix} j_1 & j_2 & J \\ m_1 & m_2 & -J \end{pmatrix}\right\}^2. \end{aligned} \tag{6.8}$$

Herein, we have replaced M by its maximum value J (or equivalently by $-J$ because of the symmetry) since the sum does not depend on this quantum number; once again the condition $m_1 + m_2 = J$ is implied.

Equation (6.8) can be regarded as a decomposition law for the degeneracy; many useful relations satisfied by the latter can be easily obtained from it. Let us first begin by noting that

$$\sum_{J=\kappa}^{\frac{N}{2}} \nu(N,J) = \binom{N}{\frac{N}{2}-\kappa}, \tag{6.9}$$

$$\sum_{J=\kappa}^{\frac{N}{2}} (2J+1)\nu(N,J) = 2^N. \tag{6.10}$$

The first equation can be readily proved by expanding the sum over J. The second one simply expresses the fact that the sum of the dimensions of the subspaces $\mathbb{C}^{2j+1}$ is equal to the dimension of the total state space, $\mathbb{C}^{2\otimes N}$. Furthermore, if we let J to take the value $\frac{N_1+N_2}{2}$ in equation (6.8), we obtain

$$(-1)^{N_1+N_2}(N_1+N_2+1)\sum_{j_1,m_1}\sum_{j2,m2}\nu(N_1,j_1)\nu(N_2,j_2)(-1)^{2(j_1-j_2)} \times\left\{\begin{pmatrix} j_1 & j_2 & \frac{N_1+N_2}{2} \\ m_1 & m_2 & -\frac{N_1+N_2}{2}\end{pmatrix}\right\}^2 = 1. \tag{6.11}$$

Now let us suppose that $J=0$, which is possible only when N_1 and N_2 are either both even or both odd positive integers. Here it should be noted that the denominator of the corresponding Wigner $3j$-symbol contains the product $(j_1-j_2)!(j_2-j_1)!$ [14]; but since $x! = \infty$ for $x<0$, we conclude that when $J=0$, the quantity under the sum sign in the right-hand side of equation (6.8) is nonzero only when $j_1 = j_2$. In fact one should have [12, 14]

$$\begin{pmatrix} j_1 & j_2 & 0 \\ m_1 & m_2 & 0\end{pmatrix} = (-1)^{j_1-m_1}\sqrt{\frac{1}{2j_1+1}}\delta_{j_1j_2}\delta_{-m_1m_2}. \tag{6.12}$$

By inserting the latter expression of Wigner $3j$-symbol into equation (6.8), and performing the sum over j_2 and m_2, we obtain

$$\begin{aligned}\nu(N_1+N_2,0) &= \sum_{j}^{\min\{\frac{N_1}{2},\frac{N_2}{2}\}}\sum_{m=-j}^{j}\nu(N_1,j)\nu(N_2,j)\frac{(-1)^{2(j-m)}}{2j+1} \\ &= \sum_{j}^{\min\{\frac{N_1}{2},\frac{N_2}{2}\}}\nu(N_1,j)\nu(N_2,j),\end{aligned} \tag{6.13}$$

where we have used the fact that $\sum_{m=-j}^{j}(-1)^{2m} = (-1)^{2j}(2j+1)$. It immediately follows that

$$\sum_{j}^{N/2}\nu(N,j)^2 = \frac{(2N)!}{(N+1)(N!)^2}. \tag{6.14}$$

The above procedure can be easily generalized to further decompositions of the total number of spins.

6.3 Dynamics of two qubits in separate spin baths.

As a second application, let us investigate the dynamics of two qubits coupled via ising interactions to separate spin environments of the same size, N. The total angular momentum operators of the latter are denoted by $\vec{J}$ and $\vec{\mathcal{J}}$. The full Hamiltonian of the composite system is given by

$$H = \lambda(\sigma_x^1\sigma_x^2 + \sigma_y^1\sigma_y^2) + \delta\sigma_z^1\sigma_z^2 + \frac{\gamma}{\sqrt{N}}(\sigma_z^1 J_z + \sigma_z^2 \mathcal{J}_z) + \mu(\sigma_z^1 + \sigma_z^2) + H_{B_1} + H_{B_2}. \quad (6.15)$$

Here, λ and δ are the strengths of interaction of the central qubits with each other, γ is the coupling constant to the baths, and μ is the strength of an applied magnetic field. The operators H_{B_i}, with $i = 1, 2$, denote the Hamiltonians of the spin baths. One can show that the interaction Hamiltonian describing the coupling of the central qubits to the environments is diagonal in the standard basis of $\mathbb{C}^2 \otimes \mathbb{C}^2$, namely,

$$H_I = \frac{\gamma}{\sqrt{N}}\mathrm{diag}(-\Sigma_z, -\Delta_z, \Delta_z, \Sigma_z), \quad (6.16)$$

where we have introduced the operators $\vec{\Sigma} = \vec{J} + \vec{\mathcal{J}}$ and $\vec{\Delta} = \vec{J} - \vec{\mathcal{J}}$. Then it can be shown that the model Hamiltonian is given by the direct sum of the Hamiltonian operators H_1 and H_2, where

$$H_1 = \sigma_z(2\mu + \frac{\gamma}{\sqrt{N}}\Sigma_z) + \mathbb{I}_2(H_B + \delta), \quad (6.17a)$$

$$H_2 = 2\lambda\sigma_x + \frac{\gamma}{\sqrt{N}}\sigma_z\Delta_z + \mathbb{I}_2(H_B - \delta), \quad (6.17b)$$

with $H_B = H_{B_1} + H_{B_2}$ and $\mathbb{I}_2$ is the 2×2 unit matrix. Note that the basis vectors of the subspace corresponding to H_1 are given by

$$|\downarrow\rangle \equiv |--\rangle, \quad (6.18)$$

$$|\uparrow\rangle \equiv |++\rangle; \quad (6.19)$$

those associated with H_2 are given by

$$|0\rangle \equiv |-+\rangle, \quad (6.20)$$

$$|1\rangle \equiv |+-\rangle. \quad (6.21)$$

Thus the system under consideration can be mapped onto two pseudo two-level systems $\mathbf{S}_1$ and $\mathbf{S}_2$ whose dynamics is governed by the operators H_1 and H_2, respectively. Each one

is coupled to a spin environment consisted of $2N$ spin-$\frac{1}{2}$ particles with the only exception that $\mathbf{S}_1$ and $\mathbf{S}_2$ see different compositions of the total angular momentum, namely Σ_z and Δ_z, respectively. Notice that the above pseudo systems become completely independent from each other if the initial density matrix of the qubits takes the form

$$\rho(0) = \begin{pmatrix} \rho_{11}^0 & 0 & 0 & \rho_{14}^0 \\ 0 & \rho_{22}^0 & \rho_{23}^0 & 0 \\ 0 & \rho_{32}^0 & \rho_{33}^0 & 0 \\ \rho_{41}^0 & 0 & 0 & \rho_{44}^0 \end{pmatrix}. \tag{6.22}$$

In such a case, it is sufficient to investigate the coupling of each pseudo system separately. For a reason that will become apparent bellow, we set $H_B = H_{B_1} + H_{B_2} = h(J_z - \mathcal{J}_z)$, where h is the strength of an applied magnetic field. Moreover, we assume that the baths are initially in thermal equilibrium at temperatures $T_1 = T_2 = T$ (we set $k_B = 1$); the corresponding total initial density matrix is given by

$$\rho_B(0) = \exp(-h\beta\Delta_z)/\Big[2\cosh\Big(\frac{h\beta}{2}\Big)\Big]^{2N}, \tag{6.23}$$

where $\beta = 1/T$ is the inverse temperature and $Z = \Big[2\cosh\Big(\frac{h\beta}{2}\Big)\Big]^{2N}$ is the partition function. Under the above assumptions, the contributions of the coupling constant δ can be neglected.

The dynamics of $\mathbf{S}_2$ is quite trivial since the corresponding time evolution operator is diagonal. Indeed, it is easy to show that $\rho_{11}(t) = \rho_{11}^0$ and $\rho_{44}(t) = \rho_{44}^0$. Moreover,

$$\begin{aligned} \rho_{14}(t) = Z^{-1}\rho_{14}^0 \sum_{j_1,m_1} \sum_{j_2,m_2} \nu(N,j_1)\nu(N,j_2) \\ \times \exp\{2i[2\mu + \gamma(m_1+m_2)/\sqrt{N}]t - h\beta(m_1 - m_2)\}. \end{aligned} \tag{6.24}$$

In the special case when $h = 0$ or $T \to \infty$, we can write

$$\begin{aligned} \rho_{14}(t) &= 2^{-2N}\rho_{14}^0 e^{4it\mu} \sum_{J,M} \nu(2N,J) e^{2\sqrt{2}it\gamma M/\sqrt{2N}} \\ &= \rho_{14}^0 e^{4it\mu} \cos\Big(\frac{\gamma t}{\sqrt{N}}\Big)^{2N}. \end{aligned} \tag{6.25}$$

For arbitrary values of h and T, the right-hand side of equation (6.24) can be evaluated within the computational basis; this yields

$$\rho_{14}(t)/\rho_{14}^0 = e^{4it\mu}\Big[1 + \frac{\cos^2(\gamma t/\sqrt{N}) - 1}{\cosh^2(h\beta/2)}\Big]^N. \tag{6.26}$$

Then, by expanding the cosine function in Taylor series and taking the limit $N \to \infty$, we obtain the Gaussian decay law:

$$|\frac{\rho_{14}(t)}{\rho_{14}^0}| = \exp\Big\{-\frac{\gamma^2 t^2}{\cosh^2(h\beta/2)}\Big\}. \tag{6.27}$$

This means that the decoherence time scale is given by $\tau_D = \cosh(h\beta/2)/|\gamma|$. Obviously $\tau_D \to \infty$ as $T \to 0$ or $h \to \infty$.

As a measure of entanglement, we use the concurrence defined by [15]

$$C(\rho) = \max\{0, 2\max[\sqrt{\lambda_i}] - \sum_{i=1}^{4} \sqrt{\lambda_i}\}, \tag{6.28}$$

where the quantities λ_i are the eigenvalues of the operator $\rho(\sigma_y \otimes \sigma_y)\rho^*(\sigma_y \otimes \sigma_y)$. In our case, when applied to $\rho(t)$, the above definition of the concurrence leads to the evaluation of the eigenvalues of the operator $\rho(t)\sigma_x\rho(t)^*\sigma_x$ where $\rho(t)$ is now restricted to the subspace of H_1. A straightforward calculation yields

$$C(t) = 2|\rho_{14}(t)|. \tag{6.29}$$

An example of the evolution in time of the real value of $\rho_{14}(t)$ along with the concurrence $C(t)$ corresponding to the initial state $(|--\rangle + |++\rangle)/\sqrt{2}$ is shown in Figure 6.1. We notice the revival of the concurrence in the case of finite number of spins. At short times, the curves corresponding to $N \to \infty$ coincide with those of finite N.

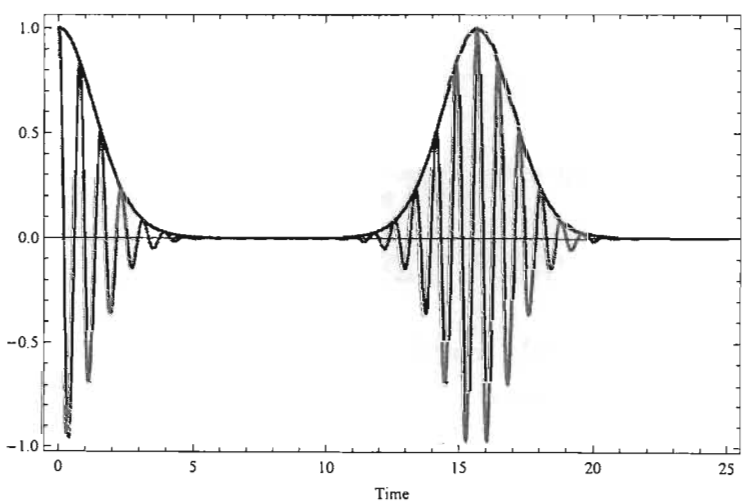

Fig. 6.1: Evolution in time of the real part of $\rho_{14}(t)/\rho_{14}^0$ (oscillating curve) and the concurrence (enveloping curve) corresponding to the initial state $(|--\rangle + |++\rangle)/\sqrt{2}$. Here, $N = 100$, $\gamma = 2$, $h\beta = 1$, and $\mu = 4$. For $t < 10$, the curves coincide with those of the limit $N \to \infty$.

It should be stressed that when the Hamiltonian of the composite spin bath is given by $H_B = h(J_z + \mathcal{J}_z) = h\Sigma_z$, then

$$\rho_{14}(t) = \rho_{14}^0 e^{4i\mu t}\Big[\cos(\gamma t/\sqrt{N}) - i\sin(\gamma t/\sqrt{N})\tanh(h\beta/2)\Big]^{2N}. \tag{6.30}$$

The existence of the sine function makes it not possible to find a relation similar to (6.27) when $N \to \infty$. However if we rescale the coupling constant γ by N instead of $\sqrt{N}$, that is [16],

$$\frac{\gamma}{\sqrt{N}} \to \frac{\gamma}{N}, \tag{6.31}$$

exact analytical expression can be derived for the case of an infinite number of spins, namely,

$$\rho_{14}(t) = \rho_{14}^0 \exp\Big\{-it[4\mu + \gamma\tanh(h\beta/2)]\Big\}. \tag{6.32}$$

Consequently the central qubits preserve their coherence, since the decoherence time scale in this case is infinite, as indicated by formula (6.32). With the new scaling of γ, the larger the number of spins to which the qubits are coupled, the less appreciable is the decoherence.

The Hamiltonian operator H_2 can be diagonalized by dealing with the operator Δ_z as a scalar. This yields the following matrix elements in $\mathbb{C}^2$:

$$U_{22}(t) = \cos\Big(t\sqrt{4\lambda^2 + \gamma^2\Delta_z^2/N}\Big) + i\frac{\gamma}{\sqrt{N}}\Delta_z\frac{\sin\Big(t\sqrt{4\lambda^2 + \gamma^2\Delta_z^2/N}\Big)}{\sqrt{4\lambda^2 + \gamma^2\Delta_z^2/N}} \tag{6.33}$$

$$U_{23}(t) = U_{32}(t) = -\frac{2i\lambda}{\sqrt{4\lambda^2 + \gamma^2\Delta_z^2/N}}\sin\Big(t\sqrt{4\lambda^2 + \gamma^2\Delta_z^2/N}\Big) \tag{6.34}$$

$$U_{33}(t) = \cos\Big(t\sqrt{4\lambda^2 + \gamma^2\Delta_z^2/N}\Big) - i\frac{\gamma}{\sqrt{N}}\Delta_z\frac{\sin\Big(t\sqrt{4\lambda^2 + \gamma^2\Delta_z^2/N}\Big)}{\sqrt{4\lambda^2 + \gamma^2\Delta_z^2/N}}, \tag{6.35}$$

Here we have omitted the contribution of $H_B = h\Delta_z$ since it simply introduces a global unitary term to the dynamics.

Let us consider the case when the qubits are initially prepared in the maximally entangled state $|\psi\rangle = \frac{1}{\sqrt{2}}(|-+\rangle + |+-\rangle)$.(the case of the singlet state displays a similar behavior.) Clearly, the density matrix $\rho(0) = |\psi\rangle\langle\psi|$ belongs to the subspace corresponding to the Hamiltonian H_2. Using the fact that $|U_{22}(t)|^2 + |U_{23}(t)|^2 = \mathbb{I}_B$, and $U_{22}(t)U_{23}^\dagger(t) + U_{23}(t)U_{33}^\dagger = 0$, it can be shown that the elements of the above density matrix evolve in time according to $\rho_{22}(t) = \frac{1}{2}[1 - g(t)]$, $\rho_{23} = \frac{1}{2}[1 - f(t)]$, where

$$g(t) = \frac{4\lambda\gamma}{[2\cosh(h\beta/2)]^{2N}}\mathrm{tr}\Big\{\frac{\Delta_z e^{-h\beta\Delta_z}}{\sqrt{N}}\frac{\sin^2\Big(t\sqrt{4\lambda^2 + \gamma^2\Delta_z^2/N}\Big)}{4\lambda^2 + \gamma^2\Delta_z^2/N}\Big\}, \tag{6.36}$$

and

$$f(t) = \frac{1}{[2\cosh(h\beta/2)]^{2N}} \mathrm{tr}\Big\{ \frac{2\gamma^2\Delta_z^2 e^{-h\beta\Delta_z}}{N} \frac{\sin^2\Big(t\sqrt{4\lambda^2+\gamma^2\Delta_z^2/N}\Big)}{4\lambda^2+\gamma^2\Delta_z^2/N} - i\frac{\gamma e^{-h\beta\Delta_z}}{\sqrt{N}}\Delta_z \frac{\sin\Big(2t\sqrt{4\lambda^2+\gamma^2\Delta_z^2/N}\Big)}{\sqrt{4\lambda^2+\gamma^2\Delta_z^2/N}} \Big\}. \tag{6.37}$$

Figures 6.2 and 6.3 display the behavior of the concurrence as a function of time for some particular values of the model parameters. We can see that for $h\beta = 1$ (i.e. at relatively high temperature) the concurrence shows damped oscillations and converges to a certain asymptotic limit which can be analytically derived, as we shall see bellow, only for $h = 0$ and/or $\beta = 0$. As $h\beta$ increases, the oscillations disappear and the concurrence converges to lower asymptotic values as shown in Figure 6.2.

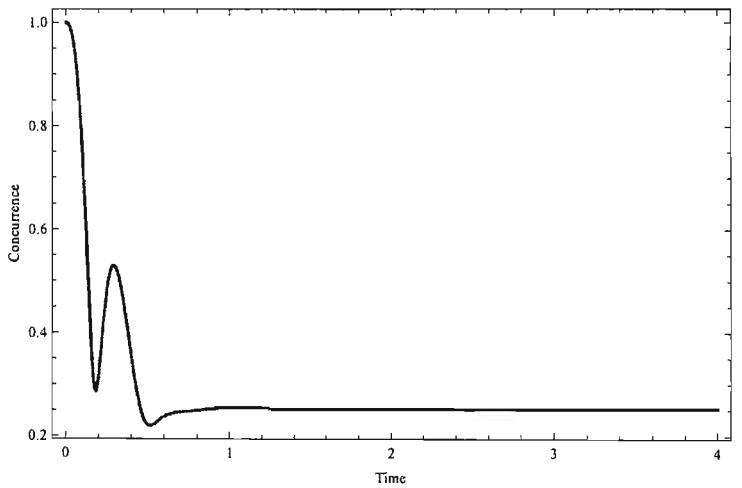

Fig. 6.2: Concurrence as a function of time in the case of the initial state $(|-+\rangle + |+-\rangle)/\sqrt{2}$ for $N = 100$, $\gamma = 4$, $h\beta = 4$, and $\lambda = 2$.

In what follows we focus our attention on the infinite temperature limit, i.e, $\beta \to 0$. In this case the reduced density matrix takes the form

$$\rho(t) = \frac{1}{2}\begin{pmatrix} 1 & 1-f(t) \\ 1-f(t) & 1 \end{pmatrix}, \tag{6.38}$$

whereas the function $f(t)$ simplifies to

$$f(t) = 2^{-2N}\mathrm{tr}\Big\{ \frac{2\gamma^2\Delta_z^2}{N} \frac{\sin^2\Big(t\sqrt{4\lambda^2+\gamma^2\Delta_z^2/N}\Big)}{4\lambda^2+\gamma^2\Delta_z^2/N} \Big\}. \tag{6.39}$$

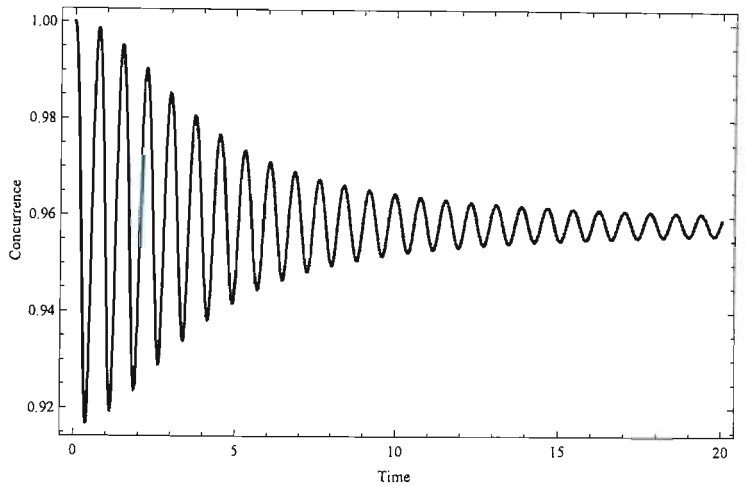

Fig. 6.3: Concurrence as a function of time in the case of the initial state $(|-+\rangle + |+-\rangle)/\sqrt{2}$ for $N = 100$, $\gamma = 1$, $h\beta = 1$, and $\lambda = 2$.

Notice that $0 \leq f(t) \leq 1$, in accordance with the general properties of density matrices in $\mathbb{C}^2$. This enables us to derive the following explicit expression for the concurrence:

$$\begin{aligned} C(t) =& \frac{1}{2}[\sqrt{f(t)^2 - 4f(t) + 4} - f(t)] \\ =& 1 - f(t). \end{aligned} \tag{6.40}$$

In the thermodynamic limit, $N \to \infty$, the function $f(t)$ can be expressed as

$$f(t) = 4\gamma^2\sqrt{\frac{2}{\pi}}\int_{-\infty}^{\infty} \frac{x^2 e^{-2x^2}}{4\lambda^2 + 2\gamma^2 x^2} \sin^2\Big(t\sqrt{4\lambda^2 + 2\gamma^2 x^2}\Big)dx. \tag{6.41}$$

Some comments are in order here: We have shown in [9] that the operator $J_z/\sqrt{N}$ converges to a real normal random variable α with the probability density function $F(\alpha) = \sqrt{2/\pi}\exp\{-2\alpha^2\}$; this is also the case for the operator $\mathcal{J}_z/\sqrt{N}$. Thus we are led to the task of finding the probability distribution function $L(\alpha)$ of the sum of two independent random variables α_1 and α_2 characterized by $F(\alpha_1)$ and $F(\alpha_2)$, respectively. (note that the probability distribution function of $a\alpha$, where a is nonzero real number, is equal to $(1/|a|)F(\alpha/a)$.) The function $L(\alpha)$ is simply given by the convolution of $F(\alpha)$ with itself, which yields $L(\alpha) = (1/\sqrt{\pi})\exp\{-\alpha^2\}$. This becomes apparent from the change of variable $\alpha \to \sqrt{2}\alpha$ carried out in equation (6.41). An other way to see that is to simply notice that $\Delta_z/(\sqrt{2N})$ converges to the random variable $\alpha \mapsto F(\alpha)$. From equation (6.41) it follows that

$$\lim_{t\to\infty} f(t) = 1 - 2\sqrt{\pi}\frac{\lambda}{\gamma}e^{4\frac{\lambda^2}{\gamma^2}}\operatorname{erfc}\Big(2\frac{\lambda}{\gamma}\Big), \tag{6.42}$$

where $\mathrm{erfc}(x)$ denotes the complementary error function. By virtue of equation (6.40), we obtain

$$C(\infty) = \lim_{t\to\infty} C(t) = 2\sqrt{\pi}\frac{\lambda}{\gamma}e^{4\frac{\lambda^2}{\gamma^2}}\mathrm{erfc}\Big(2\frac{\lambda}{\gamma}\Big). \tag{6.43}$$

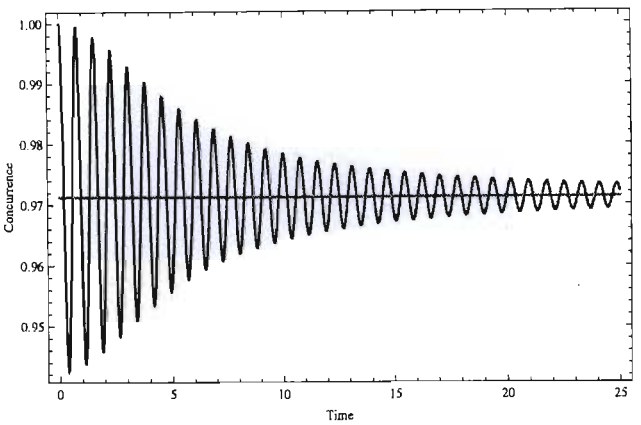

Fig. 6.4: Concurrence as a function of time in the case of the initial state $(|-+\rangle + |+-\rangle)/\sqrt{2}$ for $N = 100$ (coincides with that of the limit $N \to \infty$), $\gamma = 1$, $h\beta = 0$, and $\lambda = 2$. The straight line corresponds to the asymptotic limit.

In Figure 6.4 we have plotted the concurrence as a function of time in the limit $N \to \infty$ along with the asymptotic value given by formula (6.43). The behavior of $C(\infty)$ as a function of λ and γ is shown in Figures 6.5 and 6.6 . As one may expect, $\lim_{\lambda\to\infty} C(\infty) = 1$, and $\lim_{\gamma\to\infty} C(\infty) = 0$. This confirms the results of [10] where it is shown that strong coupling between the central qubits reduces the effect of the environment on their dynamics. Finally it is worth mentioning that due to the XY interaction between the central spins, entanglement will be generated between them when the initial state is $|\pm\mp\rangle$. However, the corresponding off-diagonal elements of the reduced density matrix vanish at long times, making the asymptotic state of the qubits unentangled.

6.4 Summary

In summary we have used the invariance of the trace to derive analytical properties of the degeneracy $\nu(N, j)$, and to describe the dynamics of two qubits embedded in separate spin baths. We have shown that when the baths have the same size, the form of the model Hamiltonian enables us to map the full dynamics onto the evolution in time of two pseudo two-level systems coupled to a spin bath whose size is twice larger than the physical ones. This allowed us to derive the limit of an infinite number of spins within the environments

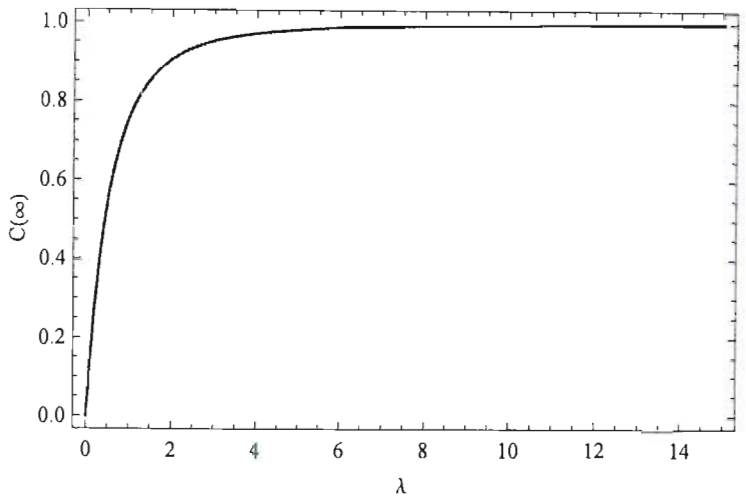

Fig. 6.5: $C(\infty)$ as a function of λ for $\gamma = 2$.

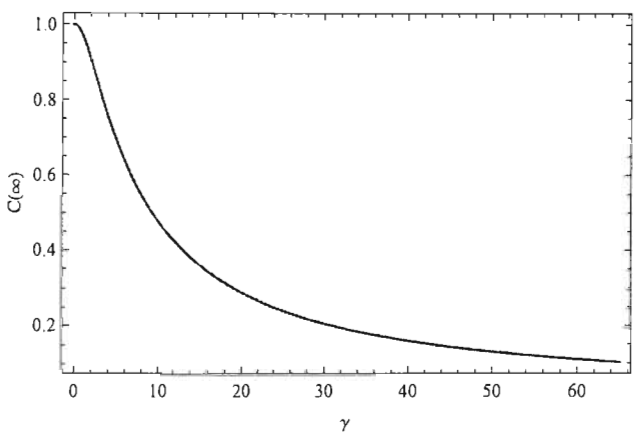

Fig. 6.6: $C(\infty)$ as a function of γ for $\lambda = 2$.

and to analytically calculate the asymptotic state. The results of this work provide more evidences regarding the role played by the mutual interactions between the central qubits in diminishing the effects of their coupling to the surrounding spin environments.

BIBLIOGRAPHY

[1] H. P. Breuer and F. Petruccione, The Theory of Open Quantum Systems, Oxford University Press, Oxford, 2002.

[2] W. H. Zurek, Phys. Today 44 (1991) No. 10, 36

[3] D. P. DiVincenzo, D. Loss, J. Magn. Magn. Matter. 200 (1999) 202 .

[4] W. H. Zurek, Rev. Mod. Phys. 75 (2003) 715-775 .

[5] W. Zhang, N. Konstantinidis, K. Al-Hassanieh, V. V. Dobrovitski, J. Phys.: Condens. Matter 19 (2007) 083202 .

[6] M. A. Nielsen, I. L. Chuang, Quantum Computation and Quantum Information, Cambridge University Press, Cambridge, 2000.

[7] D. Loss, D. P. DiVincenzo Phys. Rev. A 57 (1998) 120.

[8] G. Burkard, D. Loss, D. P. DiVincenzo , Phys. Rev. B 59 (1999) 2070.

[9] Y. Hamdouni, F. Petruccione, Phys. Rev. B 76 (2007) 174306

[10] Y. Hamdouni, M. Fannes, F. Petruccione, Pyhs. Rev. B 73 (2006) 245323; X. Z. Yuan, H. S. Goan, K. D. Zhu, Phys. Rev. B 75 (2007) 045331; Y. Hamdouni, J. Phys. A: Math. Theor. 40(2007) 11569 ; Y. Hamdouni, J. Phys. A: Math. Theor. 41 (2008) 135302.

[11] X. Wang, K. Mølmer, Eur. Phys. J. D (2002) 385.

[12] C. Cohen-Tannoudji, B. Diu, and F. Lalo, Quantum Mechanics, Wiley, New York, 1977, Vols. I and II.

[13] W. Von Waldenfels, Séminaire de probabilité (Starsburg), tome(24), pp.349-356, Springer-Verlag, Berlin, 1990.

[14] L. D. Landau, and E. M. Lifschitz, Quantum Mechanics, Pergamon Press, Oxford, 1976.

[15] W. K. Wootters Phys. Rev. Lett. 80 (1998) 2245.

[16] H. T. Quant , Z. D. Wang, C. P. Sun Phys. Rev. A 76 (2007) 012104.

7. AN EXACTLY SOLVABLE MODEL FOR THE DYNAMICS OF TWO SPIN-$\frac{1}{2}$ PARTICLES EMBEDDED IN SEPARATE SPIN STAR ENVIRONMENTS

7.1 Introduction

Exactly solvable models play a very useful role in various fields of physics. They help improving our understanding of physical processes and allow us to gain more insight into complicated phenomena that take place in nature [1]. One may recall for instance the usefulness of exactly solvable models such as the harmonic oscillator, the nuclear shell model and the Ising model, to mention but a few. From a practical point of view, exactly solvable models serve as a very convenient tool for testing the accuracy of numerical algorithms, often used in the study of problems that cannot be analytically solved due to the complexity of the systems under investigation. This is usually the case in the field of open quantum systems, where one faces the uncontrolled degrees of freedom of the environments.

Let us recall that realistic quantum systems are influenced by their surrounding through, in general, complicated coupling interactions, leading them to lose their coherences [2]. This refers to as the decoherence process, which is the main obstacle to quantum information processing [3, 4, 5]. The latter can be improved by exploiting the entanglement, i.e. the nonlocal quantum correlations that exist between quantum systems [6]. This resource has no classical analogue, and it turns out to be of great importance in quantum teleportation and quantum computing [7, 8, 9, 10, 11, 12]. It is worth mentioning that over the last years many proposals have been made for the implementation of quantum information processing. Solid state systems are very promising [13, 14] and have been the subject of many investigations. Much attention was devoted to the study of the decoherence and the entanglement of simple qubit systems that are coupled to spin environments [15, 16, 17, 18, 19]. Thus new exactly solvable models describing the dynamics of qubits within spin baths are highly welcome. Recently, the spin star configuration, initially proposed in [20], has been extensively investigated [21, 22, 23, 24, 25]. An exact treatment of the dynamics of two qubits coupled to common spin star bath via XY interactions is presented in [26, 27].

In this chapter we propose to investigate analytically the dynamics when the two qubits interact with separate spin star baths (see [28] for a similar situation) .

The chapter is organized as follows. In section 7.2 the model Hamiltonian is introduced. In section 7.3 we present a detailed derivation of the time evolution operator and we investigate the dynamics of the qubits at finite N for some particular initial conditions. In section 7.4 we study the thermodynamic limit, in which the sizes of the spin environments become infinite. Section 7.5 is devoted to the second-order master equation.

7.2 Model

The system under study consists of two two-level systems (e.g., spin-$\frac{1}{2}$ particles) each of which is embedded in its own spin star environment composed of N spins-$\frac{1}{2}$. The central particles interact with each other through a Ising interaction; the corresponding coupling constant is equal to 4δ, where the factor 4 is introduced for later convenience. We shall assume that each qubit couples to its environment via Heisenberg XY interaction whose coupling constant is α, which is, in turn, scaled by $N^{1/2}$ in order to ensure good thermodynamic behavior. The spin baths will be denoted by B_1 and B_2. The Hamiltonian for the composite system has the form

$$H = H_0 + H_{S_1B_1} + H_{S_2B_2}, \tag{7.1}$$

where

$$H_0 = 4\delta S_z^1 S_z^2, \tag{7.2}$$

and

$$H_{S_iB_i} = \frac{\alpha}{\sqrt{N}}(S_+^i \sum_{k=1}^{N} S_-^{ik} + S_-^i \sum_{k=1}^{N} S_+^{ik}), \quad (i = 1, 2). \tag{7.3}$$

Here $\vec{S^1}$ and $\vec{S^2}$ denote the spin operators corresponding to the central qubits, whereas $\vec{S^{ik}}$ denotes the spin operator corresponding to the k^{th} particle within the i^{th} environment. Introducing the total spin operators $\vec{J} = \sum_{k=1}^{N} \vec{S^{1k}}$ and $\vec{\mathcal{J}} = \sum_{k=1}^{N} \vec{S^{2k}}$ of the environments B_1 and B_2, respectively, one can rewrite the full Hamiltonian as

$$H = 4\delta S_z^1 S_z^2 + \frac{\alpha}{\sqrt{N}}(S_+^1 J_- + S_-^1 J_+ + S_+^2 \mathcal{J}_- + S_-^2 \mathcal{J}_+). \tag{7.4}$$

The dynamics of the two-qubit system is fully described by its density matrix $\rho(t)$ obtained, as usual, by tracing the time-dependent total density matrix $\rho_{\text{tot}}(t)$, describing

the composite system, with respect to the environmental degrees of freedom, namely,

$$\begin{aligned}\rho(t) &= \mathrm{tr}_{B_1+B_2}[\rho_{\mathrm{tot}}(t)] \\ &= \mathrm{tr}_{B_1+B_2}\Big[\mathbf{U}(t)\rho_{\mathrm{tot}}(0)\mathbf{U}^{\dagger}(t)\Big],\end{aligned} \tag{7.5}$$

where $\mathbf{U}(t)$ and $\rho_{\mathrm{tot}}(0)$ designate the time evolution operator and the initial total density matrix, respectively.

At $t = 0$ the central qubits are assumed to be uncoupled with the environments; the latter are assumed to be at infinite temperature. This means that the initial total density density matrix can be written as

$$\rho_{\mathrm{tot}}(0) = \rho(0) \otimes \frac{\mathbf{1}}{2^N} \otimes \frac{\mathbf{1}}{2^N}. \tag{7.6}$$

Here $\rho(0)$ is the initial density matrix of the two-qubit system, and $\mathbf{1}$ is the unit matrix on the space $\mathbb{C}^{2\otimes N}$. The former can be written as $\rho(0) = \sum_{k,\ell,} \rho^0_{k\ell}|\chi_k\rangle\langle\chi_\ell|$, with $|\chi_\ell\rangle \in \{|--\rangle, |-+\rangle, |+-\rangle, |++\rangle\}$ for $\ell = \overline{1,4}$. Similarly, we introduce the basis state vectors $|j,m\rangle$ of $\mathbb{C}^{2\otimes N}$, such that $\kappa \leq j \leq N/2$ ($\kappa = 0$ for N even and $\kappa = 1/2$ for N odd), and $-j \leq m \leq j$. The time-dependent reduced density matrix can be expressed as

$$\rho(t) = 2^{-2N} \sum_{k,\ell} \rho^0_{k\ell} \sum_{j,m} \sum_{r,s} \nu(N,j)\nu(N,r)\langle j,r,m,s|\mathbf{U}(t)|\chi_k\rangle\langle\chi_\ell|\mathbf{U}^{\dagger}(t)|j,r,m,s\rangle, \tag{7.7}$$

where $|j,r,m,s\rangle = |j,m\rangle \otimes |r,s\rangle$, and $\nu(N,j) = \binom{N}{N/2-j} - \binom{N}{N/2-j-1}$ [29]. Hence, our task reduces to finding the exact form of the matrix elements of the time evolution operator $\mathbf{U}(t) = \exp(-iHt)$ ($\hbar = 1$). This will be the subject of the next section.

7.3 Derivation of the exact form of the time evolution operator

The time evolution operator can be expanded as

$$\mathbf{U}(t) = \sum_{n=0}^{\infty} \frac{(-1)^n t^{2n}}{(2n)!}(H)^{2n} - i\sum_{n=0}^{\infty} \frac{(-1)^n t^{2n+1}}{(2n+1)!}(H)^{2n+1}. \tag{7.8}$$

In order to derive analytical expressions for even and odd powers of the total Hamiltonian H let us notice that H_0 anticommutes with $H_{S_1B_1} + H_{S_2B_2}$, that is,

$$[H_0, H_{S_1B_1} + H_{S_2B_2}]_+ = 0. \tag{7.9}$$

This can easily be shown using the following properties for spin-$\frac{1}{2}$ operators: $S_zS_\pm = \pm S_\pm$, and $S_\pm S_z = \mp S_\pm$. Moreover, it is easily seen that $H_0^{2n} \equiv \delta^{2n}$, which simply implies that for $n \geq 0$,

$$H^{2n} = \sum_{\ell=0}^{n} \binom{n}{\ell} (H_{S_1B_1} + H_{S_2B_2})^{2\ell}\delta^{2(n-\ell)}. \tag{7.10}$$

In the standard basis of $\mathbb{C}^2 \otimes \mathbb{C}^2$, it can be shown that powers of $H_{S_1B_1}$ and $H_{S_2B_2}$ are given by

$$H_{S_1B_1}^{2k} = \left(\frac{\alpha}{\sqrt{N}}\right)^{2k} \begin{pmatrix} (J_+J_-)^k & 0 & 0 & 0 \\ 0 & (J_+J_-)^k & 0 & 0 \\ 0 & 0 & (J_-J_+)^k & 0 \\ 0 & 0 & 0 & (J_-J_+)^k \end{pmatrix}, \tag{7.11}$$

$$H_{S_1B_1}^{2k+1} = \left(\frac{\alpha}{\sqrt{N}}\right)^{2k+1} \begin{pmatrix} 0 & 0 & J_+(J_-J_+)^k & 0 \\ 0 & 0 & 0 & J_+(J_-J_+)^k \\ J_-(J_+J_-)^k & 0 & 0 & 0 \\ 0 & J_-(J_+J_-)^k & 0 & 0 \end{pmatrix} \tag{7.12}$$

$$H_{S_2B_2}^{2k} = \left(\frac{\alpha}{\sqrt{N}}\right)^{2k} \begin{pmatrix} (\mathcal{J}_+\mathcal{J}_-)^k & 0 & 0 & 0 \\ 0 & (\mathcal{J}_-\mathcal{J}_+)^k & 0 & 0 \\ 0 & 0 & (\mathcal{J}_+\mathcal{J}_-)^k & 0 \\ 0 & 0 & 0 & (\mathcal{J}_-\mathcal{J}_+)^k \end{pmatrix}, \tag{7.13}$$

$$H_{S_2B_2}^{2k+1} = \left(\frac{\alpha}{\sqrt{N}}\right)^{2k+1} \begin{pmatrix} 0 & \mathcal{J}_+(\mathcal{J}_-\mathcal{J}_+)^k & 0 & 0 \\ \mathcal{J}_-(\mathcal{J}_+\mathcal{J}_-)^k & 0 & 0 & 0 \\ 0 & 0 & 0 & \mathcal{J}_+(\mathcal{J}_-\mathcal{J}_+)^k \\ 0 & 0 & \mathcal{J}_-(\mathcal{J}_+\mathcal{J}_-)^k & 0 \end{pmatrix} \tag{7.14}$$

It follows that

$$\begin{aligned} (H_{S_1B_1} + H_{S_2B_2})^{2\ell} &= \sum_{k=0}^{\ell} \binom{2\ell}{2k} H_{S_1B_1}^{2k} H_{S_2B_2}^{2(\ell-k)} + \sum_{k=0}^{\ell-1} \binom{2\ell}{2k+1} H_{S_1B_1}^{2k+1} H_{S_2B_2}^{2(\ell-k)-1} \\ &= \left(\frac{\alpha}{\sqrt{N}}\right)^{2\ell} \left[\sum_{k=0}^{\ell} \binom{2\ell}{2k} D_{\ell k} + \sum_{k=0}^{\ell-1} \binom{2\ell}{2k+1} L_{\ell k}\right]. \end{aligned} \tag{7.15}$$

where

$$\begin{aligned} D_{\ell k} = \operatorname{diag}\Big[&(J_+J_-)^k(\mathcal{J}_+\mathcal{J}_-)^{\ell-k}, (J_+J_-)^k(\mathcal{J}_-\mathcal{J}_+)^{\ell-k}, \\ &(J_-J_+)^k(\mathcal{J}_+\mathcal{J}_-)^{\ell-k}, (J_-J_+)^k(\mathcal{J}_-\mathcal{J}_+)^{\ell-k}\Big] \end{aligned} \tag{7.16}$$

and

$$\begin{aligned} L_{\ell k} = \operatorname{antidiag}\Big[&J_+\mathcal{J}_+(J_-J_+)^k(\mathcal{J}_-\mathcal{J}_+)^{\ell-k-1}, J_+\mathcal{J}_-(J_-J_+)^k(\mathcal{J}_+\mathcal{J}_-)^{\ell-k-1}, \\ &J_-\mathcal{J}_+(J_+J_-)^k(\mathcal{J}_-\mathcal{J}_+)^{\ell-k-1}, J_-\mathcal{J}_+(J_+J_-)^k(\mathcal{J}_+\mathcal{J}_-)^{\ell-k-1}\Big]. \end{aligned} \tag{7.17}$$

Using the fact that

$$\sum_{k=0}^{\ell}\binom{2\ell}{2k}x^k y^{\ell-k} = \frac{1}{2}\Big[(\sqrt{x}+\sqrt{y})^{2\ell}+(\sqrt{x}-\sqrt{y})^{2\ell}\Big], \tag{7.18}$$

$$\sum_{k=0}^{\ell-1}\binom{2\ell}{2k+1}x^k y^{\ell-k-1} = \frac{1}{2\sqrt{xy}}\Big[(\sqrt{x}+\sqrt{y})^{2\ell}-(\sqrt{x}-\sqrt{y})^{2\ell}\Big], \tag{7.19}$$

one obtains

$$(H_{S_1B_1}+H_{S_2B_2})^{2\ell} = \Big(\frac{\alpha}{\sqrt{N}}\Big)^{2\ell} \times \begin{pmatrix} F_1^+ & 0 & 0 & J_+\mathcal{J}_+\frac{F_4^-}{\sqrt{J_-J_+\mathcal{J}_-\mathcal{J}_+}} \\ 0 & F_2^+ & J_+\mathcal{J}_-\frac{F_3^-}{\sqrt{J_-J_+\mathcal{J}_+\mathcal{J}_-}} & 0 \\ 0 & J_-\mathcal{J}_+\frac{F_2^-}{\sqrt{J_+J_-\mathcal{J}_-\mathcal{J}_+}} & F_3^+ & 0 \\ J_-\mathcal{J}_-\frac{F_1^-}{\sqrt{J_+J_-\mathcal{J}_+\mathcal{J}_-}} & 0 & 0 & F_4^+ \end{pmatrix} \tag{7.20}$$

where

$$F_1^{\pm} = \frac{1}{2}\Big[\Big(\sqrt{J_+J_-}+\sqrt{\mathcal{J}_+\mathcal{J}_-}\Big)^{2\ell}\pm\Big(\sqrt{J_+J_-}-\sqrt{\mathcal{J}_+\mathcal{J}_-}\Big)^{2\ell}\Big], \tag{7.21}$$

$$F_2^{\pm} = \frac{1}{2}\Big[\Big(\sqrt{J_+J_-}+\sqrt{\mathcal{J}_-\mathcal{J}_+}\Big)^{2\ell}\pm\Big(\sqrt{J_+J_-}-\sqrt{\mathcal{J}_-\mathcal{J}_+}\Big)^{2\ell}\Big], \tag{7.22}$$

$$F_3^{\pm} = \frac{1}{2}\Big[\Big(\sqrt{J_-J_+}+\sqrt{\mathcal{J}_+\mathcal{J}_-}\Big)^{2\ell}\pm\Big(\sqrt{J_-J_+}-\sqrt{\mathcal{J}_+\mathcal{J}_-}\Big)^{2\ell}\Big], \tag{7.23}$$

$$F_4^{\pm} = \frac{1}{2}\Big[\Big(\sqrt{J_-J_+}+\sqrt{\mathcal{J}_-\mathcal{J}_+}\Big)^{2\ell}\pm\Big(\sqrt{J_-J_+}-\sqrt{\mathcal{J}_-\mathcal{J}_+}\Big)^{2\ell}\Big]. \tag{7.24}$$

Inserting equation (7.20) into equation (7.10), yields

$$H^{2n} = \frac{1}{2} \begin{pmatrix} (\mathcal{M}_1^+)^n+(\mathcal{M}_1^-)^n & 0 & 0 & J_+\mathcal{J}_+\frac{(\mathcal{M}_4^+)^n-(\mathcal{M}_4^-)^n}{\sqrt{J_-J_+\mathcal{J}_-\mathcal{J}_+}} \\ 0 & (\mathcal{M}_2^+)^n+(\mathcal{M}_2^-)^n & J_+\mathcal{J}_-\frac{(\mathcal{M}_3^+)^n-(\mathcal{M}_3^-)^n}{\sqrt{J_-J_+\mathcal{J}_+\mathcal{J}_-}} & 0 \\ 0 & J_-\mathcal{J}_+\frac{(\mathcal{M}_2^+)^n-(\mathcal{M}_2^-)^n}{\sqrt{J_+J_-\mathcal{J}_-\mathcal{J}_+}} & (\mathcal{M}_3^+)^n+(\mathcal{M}_3^-)^n & 0 \\ J_-\mathcal{J}_-\frac{(\mathcal{M}_1^+)^n-(\mathcal{M}_1^-)^n}{\sqrt{J_+J_-\mathcal{J}_+\mathcal{J}_-}} & 0 & 0 & (\mathcal{M}_4^+)^n+(\mathcal{M}_4^-)^n \end{pmatrix} \tag{7.25}$$

where

$$\mathcal{M}_1^{\pm} = \delta^2+\frac{\alpha^2}{N}\Big(\sqrt{J_+J_-}\pm\sqrt{\mathcal{J}_+\mathcal{J}_-}\Big)^2, \tag{7.26}$$

$$\mathcal{M}_2^{\pm} = \delta^2+\frac{\alpha^2}{N}\Big(\sqrt{J_+J_-}\pm\sqrt{\mathcal{J}_-\mathcal{J}_+}\Big)^2, \tag{7.27}$$

$$\mathcal{M}_3^{\pm} = \delta^2+\frac{\alpha^2}{N}\Big(\sqrt{J_-J_+}\pm\sqrt{\mathcal{J}_+\mathcal{J}_-}\Big)^2, \tag{7.28}$$

$$\mathcal{M}_4^{\pm} = \delta^2+\frac{\alpha^2}{N}\Big(\sqrt{J_-J_+}\pm\sqrt{\mathcal{J}_-\mathcal{J}_+}\Big)^2. \tag{7.29}$$

The above operators satisfy

$$\mathcal{M}^{\pm}_{1,2}J_+ = J_+\mathcal{M}^{\pm}_{3,4}, \qquad \mathcal{M}^{\pm}_{1,2}\mathcal{J}_+ = \mathcal{J}_+\mathcal{M}^{\pm}_{3,4}, \tag{7.30}$$

$$\mathcal{M}^{\pm}_{1}J_+\mathcal{J}_+ = J_+\mathcal{J}_+\mathcal{M}^{\pm}_{4}, \qquad \mathcal{M}^{\pm}_{2}J_+\mathcal{J}_- = J_+\mathcal{J}_-\mathcal{M}^{\pm}_{3}. \tag{7.31}$$

Furthermore, one can show that the matrix elements of H^{2n+1} are given by

$$(H^{2n+1})_{11} = \frac{1}{2}\delta[(\mathcal{M}^{+}_{1})^n + (\mathcal{M}^{-}_{1})^n], \tag{7.32}$$

$$(H^{2n+1})_{12} = \mathcal{J}_+\frac{\alpha}{2\sqrt{N\mathcal{J}_-\mathcal{J}_+}}[(\sqrt{\mathcal{J}_-\mathcal{J}_+} + \sqrt{J_+J_-})(\mathcal{M}^{+}_{2})^n \tag{7.33}$$

$$+ (\sqrt{\mathcal{J}_-\mathcal{J}_+} - \sqrt{J_+J_-})(\mathcal{M}^{-}_{2})^n], \tag{7.34}$$

$$(H^{2n+1})_{13} = J_+\frac{\alpha}{2\sqrt{NJ_-J_+}}[(\sqrt{\mathcal{J}_+\mathcal{J}_-} + \sqrt{J_-J_+})(\mathcal{M}^{+}_{3})^n \tag{7.35}$$

$$+ (\sqrt{J_-J_+} - \sqrt{\mathcal{J}_+\mathcal{J}_-})(\mathcal{M}^{-}_{3})^n], \tag{7.36}$$

$$(U^{2n+1})_{14} = (\delta/2)J_+\mathcal{J}_+\frac{(\mathcal{M}^{+}_{4})^n - (\mathcal{M}^{-}_{4})^n}{\sqrt{J_-J_+\mathcal{J}_-\mathcal{J}_+}}, \tag{7.37}$$

$$(H^{2n+1})_{21} = \mathcal{J}_-\frac{\alpha}{2\sqrt{N\mathcal{J}_+\mathcal{J}_-}}[(\sqrt{\mathcal{J}_+\mathcal{J}_-} + \sqrt{J_+J_-})(\mathcal{M}^{+}_{1})^n \tag{7.38}$$

$$+ (\sqrt{\mathcal{J}_+\mathcal{J}_-} - \sqrt{J_+J_-})(\mathcal{M}^{-}_{1})^n], \tag{7.39}$$

$$(H^{2n+1})_{22} = -\frac{1}{2}\delta[(\mathcal{M}^{+}_{2})^n + (\mathcal{M}^{-}_{2})^n], \tag{7.40}$$

$$(H^{2n+1})_{23} = -(\delta/2)J_+\mathcal{J}_-\frac{(\mathcal{M}^{+}_{3})^n - (\mathcal{M}^{-}_{3})^n}{\sqrt{J_-J_+\mathcal{J}_+\mathcal{J}_-}}, \tag{7.41}$$

$$(H^{2n+1})_{24} = J_+\frac{\alpha/2}{\sqrt{NJ_-J_+}}[(\sqrt{\mathcal{J}_-\mathcal{J}_+} + \sqrt{J_-J_+})(\mathcal{M}^{+}_{4})^n \tag{7.42}$$

$$+ (\sqrt{J_-J_+} - \sqrt{\mathcal{J}_-\mathcal{J}_+})(\mathcal{M}^{-}_{4})^n], \tag{7.43}$$

$$(H^{2n+1})_{31} = J_-\frac{\alpha/2}{\sqrt{NJ_+J_-}}[(\sqrt{J_+J_-} + \sqrt{\mathcal{J}_+\mathcal{J}_-})(\mathcal{M}^{+}_{1})^n \tag{7.44}$$

$$+ (\sqrt{J_+J_-} - \sqrt{\mathcal{J}_+\mathcal{J}_-})(\mathcal{M}^{-}_{1})^n], \tag{7.45}$$

$$(H^{2n+1})_{32} = -(\delta/2)J_-\mathcal{J}_+\frac{(\mathcal{M}^{+}_{2})^n - (\mathcal{M}^{-}_{1})^n}{\sqrt{J_+J_-\mathcal{J}_-\mathcal{J}_+}}, \tag{7.46}$$

$$(H^{2n+1})_{33} = -\frac{1}{2}\delta[(\mathcal{M}^{+}_{3})^n + (\mathcal{M}^{-}_{3})^n], \tag{7.47}$$

$$(H^{2n+1})_{34} = \mathcal{J}_+\frac{\alpha/2}{\sqrt{N\mathcal{J}_-\mathcal{J}_+}}[(\sqrt{\mathcal{J}_-\mathcal{J}_+} + \sqrt{J_-J_+})(\mathcal{M}^{+}_{4})^n \tag{7.48}$$

$$+ (\sqrt{\mathcal{J}_-\mathcal{J}_+} - \sqrt{J_-J_+})(\mathcal{M}^{-}_{4})^n], \tag{7.49}$$

$$(H^{2n+1})_{41} = (\delta/2)J_-\mathcal{J}_-\frac{(\mathcal{M}_1^+)^n-(\mathcal{M}_1^-)^n}{\sqrt{J_+J_-\mathcal{J}_+\mathcal{J}_-}}, \tag{7.50}$$

$$(H^{2n+1})_{42} = J_-\frac{\alpha/2}{\sqrt{NJ_+J_-}}[(\sqrt{\mathcal{J}_-\mathcal{J}_+}+\sqrt{J_+J_-})(\mathcal{M}_2^+)^n \tag{7.51}$$

$$+ (\sqrt{J_+J_-}-\sqrt{\mathcal{J}_-\mathcal{J}_+})(\mathcal{M}_2^-)^n], \tag{7.52}$$

$$(H^{2n+1})_{43} = \mathcal{J}_-\frac{\alpha/2}{\sqrt{N\mathcal{J}_+\mathcal{J}_-}}[(\sqrt{\mathcal{J}_+\mathcal{J}_-}+\sqrt{J_-J_+})(\mathcal{M}_3^+)^n \tag{7.53}$$

$$+ (\sqrt{\mathcal{J}_+\mathcal{J}_-}-\sqrt{J_-J_+})(\mathcal{M}_3^-)^n], \tag{7.54}$$

$$(H^{2n+1})_{44} = \frac{1}{2}\delta[(\mathcal{M}_4^+)^n+(\mathcal{M}_4^-)^n]. \tag{7.55}$$

Having in hand the explicit expressions of powers of the total Hamiltonian, it can easily be verified that the elements of the time evolution operator, obtained by inserting equations (7.25) and (7.32)-(7.55) into equation (7.8), are given by

$$U_{11}(t) = \frac{1}{2}\Big\{\cos\Big(t\sqrt{\mathcal{M}_1^+}\Big)+\cos\Big(t\sqrt{\mathcal{M}_1^-}\Big)-i\delta\Big[\frac{\sin\Big(t\sqrt{\mathcal{M}_1^+}\Big)}{\sqrt{\mathcal{M}_1^+}}+\frac{\sin\Big(t\sqrt{\mathcal{M}_1^-}\Big)}{\sqrt{\mathcal{M}_1^-}}\Big]\Big\}, \tag{7.56}$$

$$U_{21}(t) = -\mathcal{J}_-\frac{i\alpha/2}{\sqrt{N\mathcal{J}_+\mathcal{J}_-}}\Big\{\frac{\sqrt{J_+J_-}+\sqrt{\mathcal{J}_+\mathcal{J}_-}}{\sqrt{\mathcal{M}_1^+}}\sin\Big(t\sqrt{\mathcal{M}_1^+}\Big)$$
$$-\frac{\sqrt{J_+J_-}-\sqrt{\mathcal{J}_+\mathcal{J}_-}}{\sqrt{\mathcal{M}_1^-}}\sin\Big(t\sqrt{\mathcal{M}_1^-}\Big)\Big\}, \tag{7.57}$$

$$U_{31}(t) = -J_-\frac{i\alpha/2}{\sqrt{NJ_+J_-}}\Big\{\frac{\sqrt{J_+J_-}+\sqrt{\mathcal{J}_+\mathcal{J}_-}}{\sqrt{\mathcal{M}_1^+}}\sin\Big(t\sqrt{\mathcal{M}_1^+}\Big)$$
$$+\frac{\sqrt{J_+J_-}-\sqrt{\mathcal{J}_+\mathcal{J}_-}}{\sqrt{\mathcal{M}_1^-}}\sin\Big(t\sqrt{\mathcal{M}_1^-}\Big)\Big\}, \tag{7.58}$$

$$U_{41}(t) = J_-\mathcal{J}_-\frac{1}{2\sqrt{J_+J_-\mathcal{J}_+\mathcal{J}_-}}\Big\{\cos\Big(t\sqrt{\mathcal{M}_1^+}\Big)-\cos\Big(t\sqrt{\mathcal{M}_1^-}\Big)$$
$$-i\delta\Big[\frac{\sin\Big(t\sqrt{\mathcal{M}_1^+}\Big)}{\sqrt{\mathcal{M}_1^+}}-\frac{\sin\Big(t\sqrt{\mathcal{M}_1^-}\Big)}{\sqrt{\mathcal{M}_1^-}}\Big]\Big\}, \tag{7.59}$$

$$U_{22}(t) = \frac{1}{2}\Big\{\cos\Big(t\sqrt{\mathcal{M}_2^+}\Big)+\cos\Big(t\sqrt{\mathcal{M}_1^-}\Big)+i\delta\Big[\frac{\sin\Big(t\sqrt{\mathcal{M}_2^+}\Big)}{\sqrt{\mathcal{M}_2^+}}+\frac{\sin\Big(t\sqrt{\mathcal{M}_2^-}\Big)}{\sqrt{\mathcal{M}_2^-}}\Big]\Big\}, \tag{7.60}$$

$$U_{12}(t) = -\mathcal{J}_+\frac{i\alpha/2}{\sqrt{N\mathcal{J}_-\mathcal{J}_+}}\Big\{\frac{\sqrt{J_+J_-}+\sqrt{\mathcal{J}_-\mathcal{J}_+}}{\sqrt{\mathcal{M}_2^+}}\sin\Big(t\sqrt{\mathcal{M}_2^+}\Big)$$
$$-\frac{\sqrt{J_+J_-}-\sqrt{\mathcal{J}_-\mathcal{J}_+}}{\sqrt{\mathcal{M}_2^-}}\sin\Big(t\sqrt{\mathcal{M}_2^-}\Big)\Big\}, \tag{7.61}$$

$$U_{32}(t) = J_- \mathcal{J}_+ \frac{1}{2\sqrt{J_+ J_- \mathcal{J}_- \mathcal{J}_+}} \Big\{ \cos\Big(t\sqrt{\mathcal{M}_2^+}\Big) - \cos\Big(t\sqrt{\mathcal{M}_2^-}\Big) + i\delta \Big[\frac{\sin\Big(t\sqrt{\mathcal{M}_2^+}\Big)}{\sqrt{\mathcal{M}_2^+}} - \frac{\sin\Big(t\sqrt{\mathcal{M}_2^-}\Big)}{\sqrt{\mathcal{M}_2^-}} \Big] \Big\}, \tag{7.62}$$

$$U_{42}(t) = -J_- \frac{i\alpha/2}{\sqrt{N J_+ J_-}} \Big\{ \frac{\sqrt{J_+ J_-} + \sqrt{\mathcal{J}_- \mathcal{J}_+}}{\sqrt{\mathcal{M}_2^+}} \sin\Big(t\sqrt{\mathcal{M}_2^+}\Big) + \frac{\sqrt{J_+ J_-} - \sqrt{\mathcal{J}_- \mathcal{J}_+}}{\sqrt{\mathcal{M}_2^-}} \sin\Big(t\sqrt{\mathcal{M}_2^-}\Big) \Big\}, \tag{7.63}$$

$$U_{33}(t) = \frac{1}{2} \Big\{ \cos\Big(t\sqrt{\mathcal{M}_3^+}\Big) + \cos\Big(t\sqrt{\mathcal{M}_3^-}\Big) + i\delta \Big[\frac{\sin\Big(t\sqrt{\mathcal{M}_3^+}\Big)}{\sqrt{\mathcal{M}_3^+}} + \frac{\sin\Big(t\sqrt{\mathcal{M}_3^-}\Big)}{\sqrt{\mathcal{M}_3^-}} \Big] \Big\}, \tag{7.64}$$

$$U_{13}(t) = -J_+ \frac{i\alpha/2}{\sqrt{N J_- J_+}} \Big\{ \frac{\sqrt{\mathcal{J}_+ \mathcal{J}_-} + \sqrt{J_- J_+}}{\sqrt{\mathcal{M}_3^+}} \sin\Big(t\sqrt{\mathcal{M}_3^+}\Big) - \frac{\sqrt{\mathcal{J}_+ \mathcal{J}_-} - \sqrt{J_- J_+}}{\sqrt{\mathcal{M}_3^-}} \sin\Big(t\sqrt{\mathcal{M}_3^-}\Big) \Big\}, \tag{7.65}$$

$$U_{23}(t) = J_+ \mathcal{J}_- \frac{1}{2\sqrt{J_- J_+ \mathcal{J}_+ \mathcal{J}_-}} \Big\{ \cos\Big(t\sqrt{\mathcal{M}_3^+}\Big) - \cos\Big(t\sqrt{\mathcal{M}_3^-}\Big) + i\delta \Big[\frac{\sin\Big(t\sqrt{\mathcal{M}_3^+}\Big)}{\sqrt{\mathcal{M}_3^+}} - \frac{\sin\Big(t\sqrt{\mathcal{M}_3^-}\Big)}{\sqrt{\mathcal{M}_3^-}} \Big] \Big\}, \tag{7.66}$$

$$U_{43}(t) = -\mathcal{J}_- \frac{i\alpha/2}{\sqrt{N \mathcal{J}_+ \mathcal{J}_-}} \Big\{ \frac{\sqrt{\mathcal{J}_+ \mathcal{J}_-} + \sqrt{J_- J_+}}{\sqrt{\mathcal{M}_3^+}} \sin\Big(t\sqrt{\mathcal{M}_3^+}\Big) + \frac{\sqrt{\mathcal{J}_+ \mathcal{J}_-} - \sqrt{J_- J_+}}{\sqrt{\mathcal{M}_3^-}} \sin\Big(t\sqrt{\mathcal{M}_3^-}\Big) \Big\}, \tag{7.67}$$

$$U_{44}(t) = \frac{1}{2} \Big\{ \cos\Big(t\sqrt{\mathcal{M}_4^+}\Big) + \cos\Big(t\sqrt{\mathcal{M}_4^-}\Big) - i\delta \Big[\frac{\sin\Big(t\sqrt{\mathcal{M}_4^+}\Big)}{\sqrt{\mathcal{M}_4^+}} + \frac{\sin\Big(t\sqrt{\mathcal{M}_4^-}\Big)}{\sqrt{\mathcal{M}_4^-}} \Big] \Big\}, \tag{7.68}$$

$$U_{24}(t) = -J_+ \frac{i\alpha/2}{\sqrt{N J_- J_+}} \Big\{ \frac{\sqrt{\mathcal{J}_- \mathcal{J}_+} + \sqrt{J_- J_+}}{\sqrt{\mathcal{M}_4^+}} \sin\Big(t\sqrt{\mathcal{M}_4^+}\Big) - \frac{\sqrt{\mathcal{J}_- \mathcal{J}_+} - \sqrt{J_- J_+}}{\sqrt{\mathcal{M}_4^-}} \sin\Big(t\sqrt{\mathcal{M}_4^-}\Big) \Big\}, \tag{7.69}$$

$$U_{34}(t) = -\mathcal{J}_+\frac{i\alpha/2}{\sqrt{N\mathcal{J}_-\mathcal{J}_+}}\Big\{\frac{\sqrt{\mathcal{J}_-\mathcal{J}_+}+\sqrt{J_-J_+}}{\sqrt{\mathcal{M}_4^+}}\sin\Big(t\sqrt{\mathcal{M}_4^+}\Big) + \frac{\sqrt{\mathcal{J}_-\mathcal{J}_+}-\sqrt{J_-J_+}}{\sqrt{\mathcal{M}_4^-}}\sin\Big(t\sqrt{\mathcal{M}_4^-}\Big)\Big\}, \tag{7.70}$$

$$U_{14}(t) = J_+\mathcal{J}_+\frac{1}{2\sqrt{J_-J_+\mathcal{J}_-\mathcal{J}_+}}\Big\{\cos\Big(t\sqrt{\mathcal{M}_4^+}\Big)-\cos\Big(t\sqrt{\mathcal{M}_4^-}\Big) - i\delta\Big[\frac{\sin\Big(t\sqrt{\mathcal{M}_4^+}\Big)}{\sqrt{\mathcal{M}_4^+}}-\frac{\sin\Big(t\sqrt{\mathcal{M}_4^-}\Big)}{\sqrt{\mathcal{M}_4^-}}\Big]\Big\}. \tag{7.71}$$

It should be noted that the above components of the operator $\mathbf{U}(t)$ can also be derived by solving the Schrödinger equation [22]

$$i\frac{d\mathbf{U}(t)}{dt} = H\mathbf{U}(t). \tag{7.72}$$

For instance, we have

$$i\frac{dU_{11}(t)}{dt} = \delta U_{11}(t) + \frac{\alpha}{\sqrt{N}}\mathcal{J}_+U_{21}(t) + \frac{\alpha}{\sqrt{N}}J_+U_{31}(t), \tag{7.73}$$

$$i\frac{dU_{21}(t)}{dt} = \frac{\alpha}{\sqrt{N}}\mathcal{J}_-U_{11}(t) - \delta U_{21}(t) + \frac{\alpha}{\sqrt{N}}J_+U_{41}(t), \tag{7.74}$$

$$i\frac{dU_{31}(t)}{dt} = \frac{\alpha}{\sqrt{N}}J_-U_{11}(t) - \delta U_{31}(t) + \frac{\alpha}{\sqrt{N}}\mathcal{J}_+U_{41}(t), \tag{7.75}$$

$$i\frac{dU_{41}(t)}{dt} = \frac{\alpha}{\sqrt{N}}J_-U_{21}(t) + \frac{\alpha}{\sqrt{N}}\mathcal{J}_-U_{31}(t) + \delta U_{41}(t). \tag{7.76}$$

This set of differential equation can be solved by introducing the following transformations:

$$U_{11}(t) \to e^{-i\delta t}U_{11}(t), \tag{7.77}$$

$$U_{21}(t) \to e^{-i\delta t}\mathcal{J}_-U_{21}(t), \tag{7.78}$$

$$U_{31}(t) \to e^{-i\delta t}J_-U_{31}(t), \tag{7.79}$$

$$U_{41}(t) \to e^{-i\delta t}J_- \otimes \mathcal{J}_-U_{41}(t). \tag{7.80}$$

The resulting differential equations involve diagonal terms; they can be solved by taking into account the initial conditions:

$$U_{ij}(0) = \begin{cases} 1 & \text{for} \quad i = j, \\ 0 & \text{for} \quad i \neq j. \end{cases} \tag{7.81}$$

Following the same procedure, it is possible to derive the remaining matrix elements of the time evolution operator.

There exist many measures for entanglement. Here we shall use the concurrence, defined by [30]

$$C(\rho) = \max\{0, 2\max[\sqrt{\lambda_i}] - \sum_{i=1}^{4} \sqrt{\lambda_i}\}, \tag{7.82}$$

where the quantities λ_i are the eigenvalues of the operator $\rho(t)(\sigma_y \otimes \sigma_y)\rho(t)^*(\sigma_y \otimes \sigma_y)$. The above measure is equal to one for maximally entangled states, and is equal to zero for separable states. On the other hand, as is well known, due to the decoherence process, pure states evolve into mixed ones while the degree of mixing of mixed states increases. A suitable measure for decoherence is the purity $P(t)$, given by the trace of the square of the reduced density matrix of the central two-qubit system, that is:

$$P(t) = \mathrm{tr}\rho(t)^2. \tag{7.83}$$

The above measure is equal to $\frac{1}{4}$ for maximally mixed states, and is equal to 1 for pure states.

It turns out that the density matrices corresponding to the initial product states $|\epsilon_1\epsilon_2\rangle$, where $\epsilon_i \equiv \pm$, are always diagonal. The analysis of the dynamics in this case, reveals that if the qubits are prepared in one of the above states, they remain unentangled regardless of the values of N and δ, in contrast to the case of common bath where entanglement may be generated in the case of the initial product states $|\pm, \mp\rangle$. Furthermore, it is found that for finite values of α, the purity decreases slower with the increase of the interaction strength, δ. This decay is of Gaussian nature, as expected for non-Markovian spin dynamics [19](see section ??).

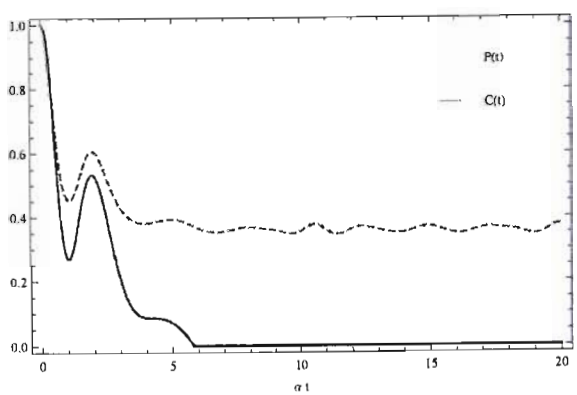

Fig. 7.1: The evolution in time of the concurrence (solid curve) and the purity (dashed curve) corresponding to the singlet state for $\delta = \alpha$ and $N = 10$.

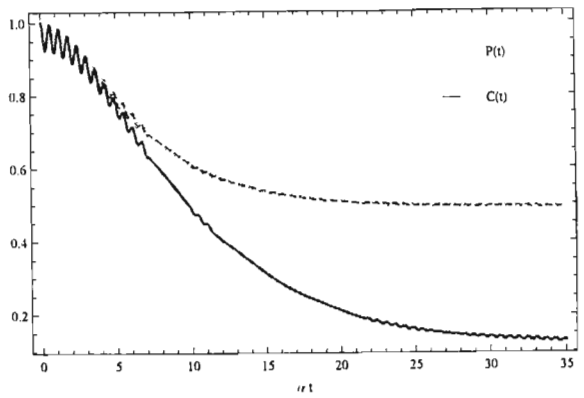

Fig. 7.2: The evolution in time of the concurrence (solid curve) and the purity (dashed curve) corresponding to the singlet state for $\delta = 4\alpha$ and $N = 10$.

The matrix elements of the reduced density matrices corresponding to the states $|e_\pm\rangle = \frac{1}{\sqrt{2}}(|-+\rangle \pm |+-\rangle)$ are explicitly given by:

$$\rho_{11}(t) = 2^{-(2N+1)}\mathrm{tr}_{B_1+B_2}\Big\{U_{12}(t)U_{12}^\dagger(t) + U_{13}(t)U_{13}^\dagger(t)\Big\}, \tag{7.84}$$

$$\rho_{22}(t) = 2^{-(2N+1)}\mathrm{tr}_{B_1+B_2}\Big\{U_{22}(t)U_{22}^\dagger(t) + U_{23}(t)U_{23}^\dagger(t)\Big\}, \tag{7.85}$$

$$\rho_{23}(t) = \pm 2^{-(2N+1)}\mathrm{tr}_{B_1+B_2}\Big\{U_{22}(t)U_{33}^\dagger(t)\Big\}, \tag{7.86}$$

$$\rho_{33}(t) = 2^{-(2N+1)}\mathrm{tr}_{B_1+B_2}\Big\{U_{32}(t)U_{32}^\dagger(t) + U_{33}(t)U_{33}^\dagger(t)\Big\}, \tag{7.87}$$

$$\rho_{44}(t) = 2^{-(2N+1)}\mathrm{tr}_{B_1+B_2}\Big\{U_{42}(t)U_{42}^\dagger(t) + U_{43}(t)U_{43}^\dagger(t)\Big\}. \tag{7.88}$$

Those associated with $|v_\pm\rangle = \frac{1}{\sqrt{2}}(|--\rangle \pm |++\rangle)$ read:

$$\rho_{11}(t) = 2^{-(2N+1)}\mathrm{tr}_{B_1+B_2}\Big\{U_{11}(t)U_{11}^\dagger(t) + U_{14}(t)U_{14}^\dagger(t)\Big\}, \tag{7.89}$$

$$\rho_{22}(t) = 2^{-(2N+1)}\mathrm{tr}_{B_1+B_2}\Big\{U_{21}(t)U_{21}^\dagger(t) + U_{24}(t)U_{24}^\dagger(t)\Big\}, \tag{7.90}$$

$$\rho_{14}(t) = \pm 2^{-(2N+1)}\mathrm{tr}_{B_1+B_2}\Big\{U_{11}(t)U_{44}^\dagger(t)\Big\}, \tag{7.91}$$

$$\rho_{33}(t) = 2^{-(2N+1)}\mathrm{tr}_{B_1+B_2}\Big\{U_{31}(t)U_{31}^\dagger(t) + U_{34}(t)U_{34}^\dagger(t)\Big\}, \tag{7.92}$$

$$\rho_{44}(t) = 2^{-(2N+1)}\mathrm{tr}_{B_1+B_2}\Big\{U_{41}(t)U_{41}^\dagger(t) + U_{44}(t)U_{44}^\dagger(t)\Big\}. \tag{7.93}$$

The evolution in time of the concurrence and the purity corresponding to the above maximally entangled states is practically the same. This is in clear agreement with [18] where, with a different model Hamiltonian, it is shown that all Bell's maximally entangled states display the same behaviour when the two qubits are located in different spin environments. The author also concluded that if the qubits interact with the same spin bath, then we can distinguish between the behaviour of the concurrence of the states $\frac{1}{\sqrt{2}}(|-+\rangle \pm |+-\rangle)$

on the one hand and that corresponding to the states $\frac{1}{\sqrt{2}}(|++\rangle \pm |--\rangle)$ on the other hand. In [27] we have shown that the singlet state is decoherence free whereas the concurrence of all the other Bell states decay in time. However, we found that the state $|e_+\rangle$ is less sensitive to the effect of the environment than the states $|v_\pm\rangle$. This implies a dependence of the behaviour of the concurrence on the relative orientation of the two qubits if they interact with the same bath. The above factor has no effect on the dynamics in the case of separate environments. In what follows, we only present the results obtained for the singlet state.

It is found that, for fixed δ, the concurrence and the purity saturate as the number of spins increases. This naturally suggests the investigation of the case $N \to \infty$ (see the next section). In figures 7.1 and 7.2 we have plotted the concurrence and the purity, obtained from the analytical solution for, respectively, $\delta = \alpha$ and $\delta = 4\alpha$ with $N = 10$ in both cases. We see that for small values of the coupling constant, the concurrence decays from its initial maximum value $C_{\max} = 1$, then vanishes at a certain moment of time (i.e. entanglement sudden death [31]). For sufficiently large δ, the purity and the concurrence decay less, displaying fast oscillations. At long times they converge to certain asymptotic values which increase with the increase of the strength of interaction. Notice that it may happen that the concurrence revives at later time which depends, of course, on the parameters of the model. It is also interesting to mention that at short times the concurrence and the purity are identical. The intervals at which this occurs are longer for large δ. The investigation of the short-time behaviour will be carried out in section ?? through the solutions of the second order master equation. Finally let us remark that, although we only have considered infinite temperature, we can ensure that for long-range antiferromagnetic Heisenberg interactions within the baths, low temperatures will have the same effect on decoherence and entanglement of the qubits as strong coupling constants.

7.4 Thermodynamic limit

In the thermodynamic limit, $N \to \infty$, the operators $\sqrt{J_\pm J_\mp / N}$ converge to the positive real random variable r whose probability density function is given by

$$r \mapsto f(r) = 4re^{-2r^2}, \quad r \geq 0. \tag{7.94}$$

Indeed, it has been shown in [25, 26] that the operator $J_+/\sqrt{N}$ converges to the complex normal random variable z with the probability density function

$$z \mapsto \frac{2}{\pi} e^{-2|z|^2}. \tag{7.95}$$

Expressing z in terms of the polar coordinates r and ϕ, i.e., $z = re^{i\phi}$, simply gives $|z|^2 = r^2$. Then integrating the corresponding probability density function over the variable ϕ from 0 to 2π yields

$$\begin{aligned} dP(r) = f(r)dr &= \frac{2}{\pi}\int_0^{2\pi} d\phi\ r\ dr e^{-2r^2} \\ &= 4re^{-2r^2}\ dr, \end{aligned} \tag{7.96}$$

from which (7.94) follows.

Hence we can ascertain that

$$\lim_{N\to\infty} 2^{-2N} \mathrm{tr}_{B_1+B_2}\Omega\Big(\sqrt{J_\pm J_\mp/N}, \sqrt{\mathcal{J}_\pm \mathcal{J}_\mp/N}\Big) = 16\int_0^\infty\int_0^\infty r\, s\, e^{-2(r^2+s^2)}\Omega(r,s)drds, \tag{7.97}$$

where $\Omega(r,s)$ is some complex-valued function for which the integrals in the right-hand side of equation (7.97) converge.

Using the above result, one can express the nonzero elements of the reduced density matrix corresponding to the initial state $\frac{1}{\sqrt{2}}(|-+\rangle - |+-\rangle)$, in the thermodynamic limit, as

$$\rho_{11}(t) = \rho_{44}(t) = \frac{1}{4}[\Lambda_+(t) + \Lambda_-(t)], \tag{7.98}$$

$$\rho_{22}(t) = \rho_{33}(t) = \frac{1}{4}[\Upsilon_+(t) + \Upsilon_-(t) + \Xi_+(t) + \Xi_-(t)], \tag{7.99}$$

$$\rho_{23}(t) = -\frac{1}{8}[\Upsilon_+(t) + \Upsilon_-(t) + \Xi_+(t) + \Xi_-(t) + 2\Psi(t)], \tag{7.100}$$

where (we set $\alpha = 1$ for the sake of shortness)

$$\Lambda_\pm(t) = 16\int_0^\infty\int_0^\infty rs\ e^{-2(r^2+s^2)}\frac{(r\pm s)^2}{\delta^2+(r\pm s)^2}\sin^2\Big(t\sqrt{\delta^2+(r\pm s)^2}\Big)drds, \tag{7.101}$$

$$\Upsilon_\pm(t) = 16\int_0^\infty\int_0^\infty rs\ e^{-2(r^2+s^2)}\cos^2\Big(t\sqrt{\delta^2+(r\pm s)^2}\Big)drds, \tag{7.102}$$

$$\Xi_\pm(t) = 16\int_0^\infty\int_0^\infty rs\ e^{-2(r^2+s^2)}\frac{\delta^2}{\delta^2+(r\pm s)^2}\sin^2\Big(t\sqrt{\delta^2+(r\pm s)^2}\Big)drds, \tag{7.103}$$

$$\begin{aligned} \Psi(t) = 16\int_0^\infty\int_0^\infty rs\ e^{-2(r^2+s^2)}\Big\{&\cos\Big(t\sqrt{\delta^2+(r+s)^2}\Big)\cos\Big(t\sqrt{\delta^2+(r-s)^2}\Big) \\ &+ \delta^2\frac{\sin\Big(t\sqrt{\delta^2+(r+s)^2}\Big)}{\delta^2+(r+s)^2}\frac{\sin\Big(t\sqrt{\delta^2+(r-s)^2}\Big)}{\delta^2+(r-s)^2}\Big\}drds. \end{aligned} \tag{7.104}$$

Unfortunately the above functions cannot be evaluated analytically; one should make recourse to numerical integration. This task can be significantly simplified by transforming the double integration into single one, which is much easier to carry out. To do that notice that the analysis of the expressions of the functions $\Lambda_{\pm}(t)$, $\Upsilon_{\pm}(t)$, and $\Xi_{\pm}(t)$ leads to the evaluation of the probability density functions $Q(\mu)$ and $R(\eta)$ corresponding, respectively, to the random variables $\mu = r + s$ and $\eta = r - s$ (see [32] for a similar situation).

Let us begin with the variable μ; its probability density function is simply given by the convolution of $f(r)$ with itself:

$$Q(\mu) = 16 \int_0^{\mu} (\mu - r) r e^{-2(\mu - r)^2 - 2r^2} dr. \tag{7.105}$$

Note that the upper limit of the integration over r is μ because the quantity $\mu - r$ should be positive. The evaluation of the integral is somewhat lengthy, but elementary; one finds that

$$Q(\mu) = [2\mu - \sqrt{\pi} e^{\mu^2} (1 - 2\mu^2) \mathrm{erf}(\mu)] e^{-2\mu^2}, \tag{7.106}$$

where $\mathrm{erf}(x)$ designates the error function [33].

Now consider the variable $\eta = r - s$. One should be careful when using the definition of the convolution, since, in this case, η belongs to the interval $]-\infty, \infty[$. We have to distinguish between two cases, namely, $\eta \geq 0$ and $\eta \leq 0$. In the first case $r \in [0, \infty[$, and hence

$$\begin{aligned} R(\eta \geq 0) &= 16 \int_0^{\infty} (\eta + r) r e^{-2(r+s)^2 - 2r^2} dr \\ &= \frac{1}{2} \{2\eta + \sqrt{\pi} e^{\eta^2} (1 - 2\eta^2)[1 - \mathrm{erf}(\eta)]\} e^{-2\eta^2}. \end{aligned} \tag{7.107}$$

When $\eta \leq 0$, then $r \in [-\eta, \infty[$, which implies that

$$\begin{aligned} R(\eta \leq 0) &= 16 \int_{-\eta}^{\infty} (\eta + r) r e^{-2(r+s)^2 - 2r^2} dr \\ &= \frac{1}{2} \{-2\eta + \sqrt{\pi} e^{\eta^2} (1 - 2\eta^2)[1 + \mathrm{erf}(\eta)]\} e^{-2\eta^2}. \end{aligned} \tag{7.108}$$

Combining (7.107) and (7.108), we obtain the following expression for the probability density function of η over the real line:

$$R(\eta) = \frac{1}{2} \{2|\eta| + \sqrt{\pi} e^{\eta^2} (1 - 2\eta^2)[1 - \mathrm{erf}(|\eta|)]\} e^{-2\eta^2}. \tag{7.109}$$

The above functions are depicted in figures 7.3 and 7.4. Clearly, $R(\eta)$ is an even function of its argument; it takes its maximum value at the origin, that is, $\max\{R(\eta)\} = R(0) =$

0.886227. The maximum value of $Q(\mu)$ occurs at $\mu_0 = 1.142088$, such that $\max\{Q(\mu)\} = Q(\mu_0) = 0.859664$.

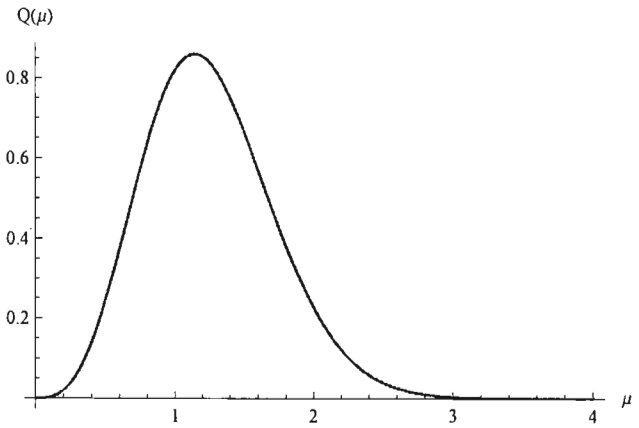

Fig. 7.3: The probability density function $Q(\mu)$.

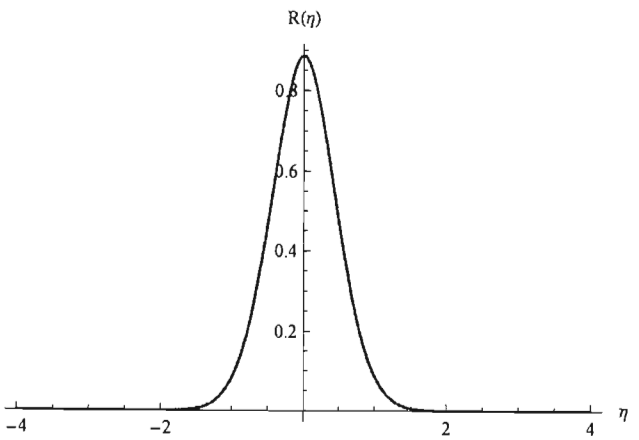

Fig. 7.4: The probability density function $R(\eta)$.

As a simple application let us prove the following:

Theorem 1: The moments around origin of the random variables μ and η are given by:

$$\langle \mu^{2n} \rangle = \frac{n!}{2^n}\Big[1 + 2^{n+1} n \; {}_2F_1\Big(1+n, \frac{1}{2}; \frac{3}{2}; -1\Big)\Big], \tag{7.110}$$

$$\langle \mu^{2n+1} \rangle = \frac{\Gamma(\frac{3}{2}+n)}{2^n}\Big[\frac{1}{\sqrt{2}} + 2^n(2n+1) \; {}_2F_1\Big(\frac{3}{2}+n, \frac{1}{2}; \frac{3}{2}; -1\Big)\Big], \tag{7.111}$$

$$\langle \eta^{2n} \rangle = \langle \mu^{2n} \rangle - n\sqrt{\pi}\Gamma\Big(\frac{1}{2}+n\Big), \tag{7.112}$$

$$\langle \eta^{2n+1} \rangle = 0, \tag{7.113}$$

where $\Gamma(x)$, and ${}_2F_1(a,b;c;d)$ denote the Gamma and the hypergeometric functions, respectively.

Proof. Relation (7.113) is obvious since the function $R(\eta)$ is even. Let us prove (7.110). We have that

$$\begin{aligned}\langle\mu^{2n}\rangle &= \int_0^\infty \mu^{2n}Q(\mu)\,d\mu \\ &= 2I_{n+1} - I_n + 2Y_n,\end{aligned} \tag{7.114}$$

where

$$I_n = \int_0^\infty \sqrt{\pi}\mu^{2n}\mathrm{e}^{-\mu^2}\mathrm{erf}(\mu)\,d\mu, \tag{7.115}$$

$$Y_n = \int_0^\infty \mu^{2n+1}\mathrm{e}^{-2\mu^2}\,d\mu. \tag{7.116}$$

To calculate Y_n and I_n, introduce the functions of the real variable $x > 0$:

$$Y_n(x) = \int_0^\infty \mu^{2n+1}\mathrm{e}^{-\mu^2(1+\frac{1}{x})}d\mu, \tag{7.117}$$

$$I_n(x) = \int_0^\infty \sqrt{\pi}\mu^{2n}\mathrm{e}^{-\mu^2/x}\mathrm{erf}(\mu)\,d\mu. \tag{7.118}$$

The first integral can be easily evaluated:

$$Y_n(x) = \frac{1}{2}\Big(\frac{x}{1+x}\Big)^{n+1}\int_0^\infty \chi^n\mathrm{e}^{-\chi}d\chi = \frac{n!}{2}\Big(\frac{x}{1+x}\Big)^{n+1}. \tag{7.119}$$

The second integral satisfies

$$\frac{dI_n(x)}{dx} = \frac{1}{x^2}I_{n+1}(x). \tag{7.120}$$

Integrating by parts the RHS of (7.118) with respect to μ, and using (7.119), yield

$$I_{n+1}(x) = \frac{x(2n+1)}{2}I_n(x) + \frac{xn!}{2}\Big(\frac{x}{x+1}\Big)^{n+1}. \tag{7.121}$$

Here we have used the fact that $\mathrm{erf}(x)' = 2\mathrm{e}^{-x^2}/\sqrt{\pi}$.

Let $I_n(x) = n!x^{n+1}g_n(x)$. Then from (7.121) we have

$$2(n+1)g_{n+1}(x) = (2n+1)g_n(x) + \frac{1}{(x+1)^{n+1}}. \tag{7.122}$$

On the other hand equation (7.120) implies that

$$x\frac{dg_n(x)}{dx} + (n+1)g_n(x) = (n+1)g_{n+1}(x). \tag{7.123}$$

Combining the last two equations yields the following first order differential equation for the function $g_n(x)$:

$$2x\frac{dg_n(x)}{dx} + g_n(x) - \frac{1}{(x+1)^{n+1}} = 0. \tag{7.124}$$

Differentiating both sides of (7.124), and again using (7.122), we obtain

$$\Big[\frac{d^2}{dx^2} + \Big(\frac{3}{2x} + \frac{n+1}{x+1}\Big)\frac{d}{dx} + \frac{n+1}{2x(x+1)}\Big]g_n(x) = 0. \tag{7.125}$$

By setting $y = -x$, and $h_n(y) = g_n(-x)$, we obtain

$$\Big[\frac{d^2}{dy^2} + \Big(\frac{3}{2y} + \frac{n+1}{y-1}\Big)\frac{d}{dy} + \frac{n+1}{2y(y-1)}\Big]h_n(y) = 0, \tag{7.126}$$

which should be compared with the hypergeometric equation

$$\Big[\frac{d^2}{dy^2} + \Big(\frac{c}{y} + \frac{1+a+b-c}{y-1}\Big)\frac{d}{dy} + \frac{ab}{y(y-1)}\Big]\ {}_2F_1(a,b;c;y) = 0. \tag{7.127}$$

Thus

$$a = n+1, \quad b = \tfrac{1}{2}, \quad c = \tfrac{3}{2}.$$

It follows that

$$I_n(x) = n!x^{n+1}\ {}_2F_1(n+1, \tfrac{1}{2}; \tfrac{3}{2}; -x). \tag{7.128}$$

Putting $x = 1$ yields

$$I_n = n!\ {}_2F_1(n+1, \tfrac{1}{2}; \tfrac{3}{2}; -1), \qquad Y_n = \frac{n!}{2^{n+2}}. \tag{7.129}$$

Also, using (7.121), we obtain

$$2I_{n+1} = (2n+1)n!\ {}_2F_1(n+1, \tfrac{1}{2}; \tfrac{3}{2}; -1) + \frac{n!}{2^{n+1}}, \tag{7.130}$$

from which (7.110) readily follows. The other moments can be evaluated with a similar method. ∎

The functions (7.101)-(7.103) can easily be expressed in terms of the functions $Q(\mu)$ and $R(\eta)$. For example, we have:

$$\Lambda_+(t) = \int_0^\infty Q(\mu)\frac{\mu^2}{\delta^2+\mu^2}\sin^2\Big(t\sqrt{\delta^2+\mu^2}\Big)d\mu, \tag{7.131}$$

$$\Lambda_-(t) = \int_{-\infty}^\infty R(\mu)\frac{\mu^2}{\delta^2+\mu^2}\sin^2\Big(t\sqrt{\delta^2+\mu^2}\Big)d\mu. \tag{7.132}$$

It should be noted that in contrast to r and s, the random variables η and μ are not independent. The function $\Psi(t)$ can not be further simplified, and should be evaluated using the double integration over the variables r and s. Nevertheless, using the Riemann-Lebesgue lemma, we can infer that

$$\lim_{t\to\infty} \Psi(t) = \Psi(\infty) = 0. \tag{7.133}$$

In a similar way, the remaining functions tend asymptotically to:

$$\Lambda_+(\infty) = \frac{1}{2}\int_0^\infty Q(\mu)\frac{\mu^2}{\delta^2+\mu^2}d\mu, \tag{7.134}$$

$$\Lambda_-(\infty) = \frac{1}{2}\int_{-\infty}^\infty R(\mu)\frac{\mu^2}{\delta^2+\mu^2}d\mu, \tag{7.135}$$

$$\Upsilon_\pm(\infty) = \frac{1}{2}, \tag{7.136}$$

$$\Xi_+(\infty) = \frac{1}{2}\int_0^\infty Q(\mu)\frac{\delta^2}{\delta^2+\mu^2}d\mu, \tag{7.137}$$

$$\Xi_-(\infty) = \frac{1}{2}\int_{-\infty}^\infty R(\mu)\frac{\delta^2}{\delta^2+\mu^2}d\mu. \tag{7.138}$$

Notice that

$$\Lambda_\pm(\infty) + \Xi_\pm(\infty) = \frac{1}{2}, \tag{7.139}$$

independent of the values of δ. It follows that the asymptotic density matrix can be expressed as

$$\rho(\infty) = \begin{pmatrix} \frac{\Pi}{4} & 0 & 0 & 0 \\ 0 & \frac{2-\Pi}{4} & -\frac{2-\Pi}{8} & 0 \\ 0 & -\frac{2-\Pi}{8} & \frac{2-\Pi}{4} & 0 \\ 0 & 0 & 0 & \frac{\Pi}{4} \end{pmatrix}, \tag{7.140}$$

where

$$\Pi = \Lambda_+(\infty) + \Lambda_-(\infty). \tag{7.141}$$

Before we study the general case let us have a look at the two extrem cases: $\delta = 0$ and $\delta = \infty$. It is easily seen that

$$\lim_{\delta\to 0} \Xi_\pm(\infty) = 0, \quad \lim_{\delta\to 0} \Lambda_\pm(\infty) = \frac{1}{2}. \tag{7.142}$$

The corresponding asymptotic reduced density matrix reads

$$\rho(\infty)_{\delta=0} = \begin{pmatrix} \frac{1}{4} & 0 & 0 & 0 \\ 0 & \frac{1}{4} & -\frac{1}{8} & 0 \\ 0 & -\frac{1}{8} & \frac{1}{4} & 0 \\ 0 & 0 & 0 & \frac{1}{4} \end{pmatrix}, \tag{7.143}$$

which has a concurrence and a purity identically equal to zero and 9/32, repectively.

On the contrary, in the limit of strong coupling between the central qubits,

$$\lim_{\delta\to\infty} \Xi_{\pm}(\infty) = \frac{1}{2}, \quad \lim_{\delta\to\infty} \Lambda_{\pm}(\infty) = 0. \tag{7.144}$$

Consequently,

$$\rho(\infty)_{\delta=\infty} = \begin{pmatrix} 0 & 0 & 0 & 0 \\ 0 & \frac{1}{2} & -\frac{1}{4} & 0 \\ 0 & -\frac{1}{4} & \frac{1}{2} & 0 \\ 0 & 0 & 0 & 0 \end{pmatrix}. \tag{7.145}$$

A straightforward calculation shows that

$$\lim_{\delta\to\infty} C(\rho(\infty)) = \frac{1}{2}. \tag{7.146}$$

We observe that the asymptotic concurrence and purity obtained here coincide, when $\delta \to \infty$, with those obtained for the states $|v_{\pm}\rangle$ in the case of common spin bath. They are however different from the asymptotic values corresponding to the state $|e_{+}\rangle$ which are identically equal to 1 (the state $|e_{-}\rangle$ is stationary).

In general, since $0 \leq \mu^2/(\mu^2+\delta^2) \leq 1$, then

$$\begin{aligned} 0 \leq \Pi &= \tfrac{1}{2}\int_0^\infty Q(\mu)\tfrac{\mu^2}{\delta^2+\mu^2}d\mu + \tfrac{1}{2}\int_{-\infty}^\infty R(\mu)\tfrac{\mu^2}{\delta^2+\mu^2}d\mu \\ &\leq \tfrac{1}{2}\int_0^\infty Q(\mu)d\mu + \tfrac{1}{2}\int_{-\infty}^\infty R(\mu)d\mu = 1. \end{aligned} \tag{7.147}$$

This allows us to find the following explicit form of the asymptotic value of the concurrence:

$$C(\infty) = \max\Big\{0, \frac{2-3\Pi}{4}\Big\}. \tag{7.148}$$

The latter can also be rewritten as:

$$C(\infty) = \begin{cases} \frac{2-3\Pi}{4} & \text{for} \quad 0 \leq \Pi \leq \frac{2}{3}, \\ 0 & \text{for} \quad \frac{2}{3} \leq \Pi \leq 1. \end{cases} \tag{7.149}$$

The variation of the asymptotic concurrence as a function of δ is shown in figure 7.5. It can be seen that $C(\infty)$ remains zero up to a critical value δ_c after which it increases, to tend asymptotically to $\frac{1}{2}$. The value of δ_c can be evaluated numerically:

$$\delta_c = 0.342842, \qquad \Pi|_{\delta=\delta_c} = 0.666666. \tag{7.150}$$

At the critical point, the density matrix reads

$$\rho_c(\infty) = \begin{pmatrix} \frac{1}{6} & 0 & 0 & 0 \\ 0 & \frac{1}{3} & -\frac{1}{6} & 0 \\ 0 & -\frac{1}{6} & \frac{1}{3} & 0 \\ 0 & 0 & 0 & \frac{1}{6} \end{pmatrix} \quad \text{with} \quad P(\rho_c(\infty)) = \tfrac{1}{3}. \tag{7.151}$$

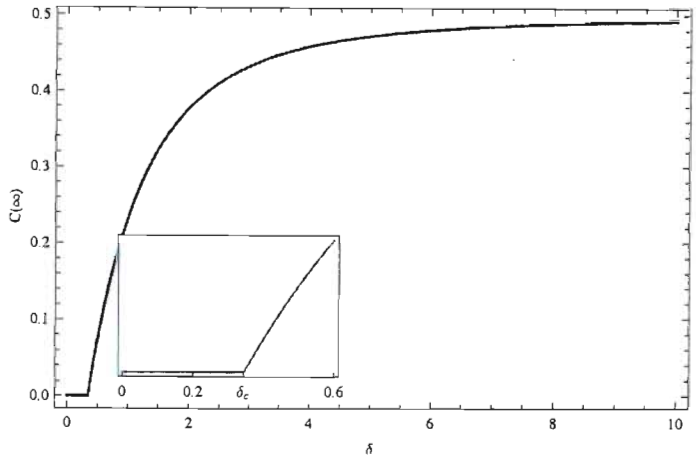

Fig. 7.5: The variation of $C(\infty)$ as a function of the coupling constant δ. The inset shows the critical point δ_c.

7.5 *Second-order master equation*

The aim of this section is to study the short-time behaviour of the dynamics. This will be achieved by investigating the second-order master equation under Born Approximation. In the interaction picture, the above yield the following set of integro-differential equations:

$$\dot{\tilde{\rho}}_{11}(t) = -\alpha^2 \int_0^t \Big(2\tilde{\rho}_{11}(s) - \tilde{\rho}_{22}(s) - \tilde{\rho}_{33}(s)\Big) \cos[2\delta(t-s)]\, ds, \tag{7.152}$$

$$\dot{\tilde{\rho}}_{12}(t) = -\alpha^2 \int_0^t \Big(2\tilde{\rho}_{12}(s)\mathrm{e}^{2i\delta(t-s)} - \tilde{\rho}_{34}(s)\mathrm{e}^{2i\delta(t+s)}\Big)\, ds, \tag{7.153}$$

$$\dot{\tilde{\rho}}_{13}(t) = -\alpha^2 \int_0^t \Big(2\tilde{\rho}_{13}(s)\mathrm{e}^{2i\delta(t-s)} - \tilde{\rho}_{24}(s)\mathrm{e}^{2i\delta(t+s)}\Big)\, ds, \tag{7.154}$$

$$\dot{\tilde{\rho}}_{14}(t) = -\alpha^2 \int_0^t 2\tilde{\rho}_{13}(s) \cos[2\delta(t-s)]\, ds, \tag{7.155}$$

$$\dot{\tilde{\rho}}_{22}(t) = -\alpha^2 \int_0^t \Big(2\tilde{\rho}_{22}(s) - \tilde{\rho}_{11}(s) - \tilde{\rho}_{44}(s)\Big) \cos[2\delta(t-s)]\, ds, \tag{7.156}$$

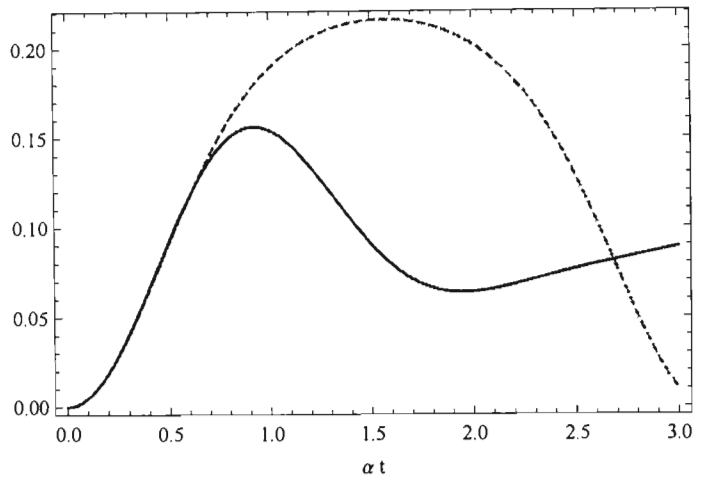

Fig. 7.6: The variation in time of the the matrix element $\rho_{11}(t)$ corresponding to the singlet state. The solid curve represents the exact solution, and the dashed curve represents the approximate solution (7.162). The parameters are $N = 10$ and $\delta = \alpha$.

$$\dot{\tilde{\rho}}_{23}(t) = -\alpha^2 \int_0^t 2\tilde{\rho}_{23}(s)\cos[2\delta(t-s)]\, ds, \tag{7.157}$$

$$\dot{\tilde{\rho}}_{24}(t) = -\alpha^2 \int_0^t \left(2\tilde{\rho}_{24}(s)\mathrm{e}^{2i\delta(s-t)} - \tilde{\rho}_{13}(s)\mathrm{e}^{-2i\delta(t+s)}\right) ds, \tag{7.158}$$

$$\dot{\tilde{\rho}}_{33}(t) = -\alpha^2 \int_0^t \left(2\tilde{\rho}_{33}(s) - \tilde{\rho}_{11}(s) - \tilde{\rho}_{44}(s)\right)\cos[2\delta(t-s)]\, ds, \tag{7.159}$$

$$\dot{\tilde{\rho}}_{34}(t) = -\alpha^2 \int_0^t \left(2\tilde{\rho}_{34}(s)\mathrm{e}^{2i\delta(s-t)} - \tilde{\rho}_{12}(s)\mathrm{e}^{-2i\delta(t+s)}\right) ds, \tag{7.160}$$

$$\dot{\tilde{\rho}}_{44}(t) = -\alpha^2 \int_0^t \left(2\tilde{\rho}_{44}(s) - \tilde{\rho}_{22}(s) - \tilde{\rho}_{33}(s)\right)\cos[2\delta(t-s)]\, ds, \tag{7.161}$$

Here the tilde designates the interaction picture, namely $\tilde{\rho}(t) = \mathrm{e}^{iH_0t}\rho(t)\mathrm{e}^{-iH_0t}$. It is worth mentioning that the integro-differential equations corresponding to the off-diagonal elements (except ρ_{13}) obtained from the second-order master equation in [27] are somewhat wrong; the matrix elements under the integral sign are, in fact, expressed in the Schrödinger picture.

Clearly, the above equations do not depend on the number of spins within the bath. In fact it is found that at short times, the exact solution discussed in the precedent sections, gives the same result with fixed δ no matter what the value of N. This explains the results

of [25, 26, 27]. Of course the solutions quickely diverge from each other as we increase the time.

Equations (7.152)-(7.161) can be solved under a time-local approximation in which the matrix elements $\tilde{\rho}_{ij}(s)$ are replaced by $\tilde{\rho}_{ij}(t)$. One can find that (α is set to one)

$$\tilde{\rho}_{11}(t) = \frac{1}{4}\Bigg\{1 + \Big[-1 + 2(\rho^0_{11} + \rho^0_{44})\Big]\exp\Big\{\frac{1}{\delta^2}[\cos(2\delta t) - 1]\Big\} + 2(\rho^0_{11} - \rho^0_{44})\exp\Big\{\frac{1}{2\delta^2}[\cos(2\delta t) - 1]\Big\}\Bigg\}, \tag{7.162}$$

$$\tilde{\rho}_{22}(t) = \frac{1}{4}\Bigg\{1 + \Big[-1 + 2(\rho^0_{22} + \rho^0_{33})\Big]\exp\Big\{\frac{1}{\delta^2}[\cos(2\delta t) - 1]\Big\} + 2(\rho^0_{22} - \rho^0_{33})\exp\Big\{\frac{1}{2\delta^2}[\cos(2\delta t) - 1]\Big\}\Bigg\}, \tag{7.163}$$

$$\tilde{\rho}_{33}(t) = \frac{1}{4}\Bigg\{1 + \Big[-1 + 2(\rho^0_{33} + \rho^0_{22})\Big]\exp\Big\{\frac{1}{\delta^2}[\cos(2\delta t) - 1]\Big\} + 2(\rho^0_{33} - \rho^0_{22})\exp\Big\{\frac{1}{2\delta^2}[\cos(2\delta t) - 1]\Big\}\Bigg\}, \tag{7.164}$$

$$\tilde{\rho}_{44}(t) = \frac{1}{4}\Bigg\{1 + \Big[-1 + 2(\rho^0_{44} + \rho^0_{11})\Big]\exp\Big\{\frac{1}{\delta^2}[\cos(2\delta t) - 1]\Big\} + 2(\rho^0_{44} - \rho^0_{11})\exp\Big\{\frac{1}{2\delta^2}[\cos(2\delta t) - 1]\Big\}\Bigg\}, \tag{7.165}$$

$$\tilde{\rho}_{14}(t) = \rho^0_{14}\exp\Big\{\frac{1}{\delta^2}[\cos(2\delta t) - 1]\Big\}, \tag{7.166}$$

$$\tilde{\rho}_{23}(t) = \rho^0_{23}\exp\Big\{\frac{1}{\delta^2}[\cos(2\delta t) - 1]\Big\}. \tag{7.167}$$

These solutions describe approximately the dynamics at short times (see figure 7.6). In fact, the smaller the coupling constant δ, the better these solutions are.

when $\delta = 0$ (i.e., nonlocal dynamics), then

$$\exp\Big\{\frac{1}{n\delta^2}[\cos(2\delta t) - 1]\Big\} \to \mathrm{e}^{-2t^2/n}, \qquad n = 1, 2. \tag{7.168}$$

Thus the second order time-local master equation shows that the nonlocal dynamics, or, in general, the short time behavior follow a Gaussian decay law. Note that the solutions corresponding to the diagonal elements reproduce the asymptotic values for $N \to \infty$, namely $\rho_{ii}(\infty) = \frac{1}{4}$. However, those corresponding to the off-diagonal elements fail to reproduce the steady state, since, for example, equation (7.167) implies that $\rho_{23}(t) \to 0$.

To end our discussion let us remark that equations (7.153), (7.154), (7.158) and (7.160) can be analytically solved only when $\delta = 0$. For instance (see figure 7.7),

$$\rho_{12}(t) = \frac{1}{2}\Big[(\rho_{12}^0 + \rho_{34}^0)\mathrm{e}^{-t^2/2} + (\rho_{12}^0 - \rho_{34}^0)\mathrm{e}^{-3t^2/2}\Big]. \tag{7.169}$$

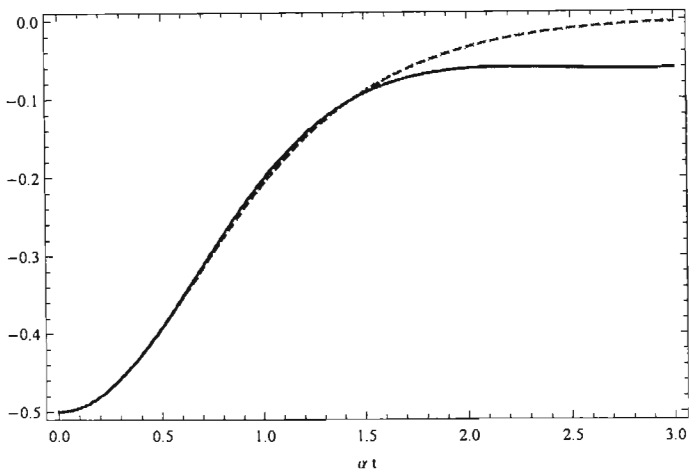

Fig. 7.7: The variation in time of the the matrix element $\rho_{12}(t)$ corresponding to the singlet state. The solid curve represents the exact solution, and the dashed curve represents the approximate solution (7.169). The parameters are $N = 10$ and $\delta = 0$.

7.6 Summary

In summary we have investigated the dynamics of two qubits coupled to separate spin star environment via Heisenberg XY interactions. We have derived the exact form of the time evolution operator and calculated the matrix elements of the reduced density operator. The analysis of the evolution in time of the concurrence and the purity shows that decoherence can be minimized by allowing the central qubits to strongly interact with each other. The short-time behavior, studied by deriving the second-order master equation, is found to be Gaussian. The next step may consist in considering more central qubits, and then investigate whether the above results still hold.

BIBLIOGRAPHY

[1] Baxter R J, 1982 *Exactly Solved Models in Statistical Mechanics* (Academic Press, London)

[2] Breuer H P and Petruccione F 2002 *The Theory of Open Quantum Systems* (Oxford University Press, Oxford)

[3] Zurek W H 1991 *Phys. Today* **44** No. 10 36

[4] DiVincenzo D P and Loss D 2000 *J. Magn. Magn. Matter.* **200** 202

[5] Zurek W H 2003 *Rev. Mod. Phys.* **75**, 715-775

[6] Nielsen M A and Chuang I L 2000 *Quantum Computation and Quantum Information* (Cambridge University Press, Cambridge)

[7] Bennett C H and Wiesner S J 1993*Phys. Rev. Lett.* **69** 2881

[8] Bennett C H and DiVincenzo D P 2000 *Nature* **404** 247

[9] Bennett C H, Brassard G, Crépeau C, Jozsa R, Peres A and Wootters W K 1993 *Phys. Rev. Lett.* **70** 1895

[10] Bennett C H, DiVincenzo D P, Smolin J A and Wootters W K 1996 *Phys. Rev.* A **54** 3824

[11] Lloyd S 1004 *Science* **261** 1569 (1993)

[12] Ekert A and Josza R 1998 *Philos. Trans. R. Soc. Lond.* A **356** 1769

[13] Loss D and DiVincenzo D P 1998 *Phys. Rev.* A **57** 120

[14] Burkard G Loss D and DiVincenzo D P 1999 *Phys. Rev.* B **59** 2070

[15] Prokof'ev N V and Stamp P C E 2000 *Rep. Prog. Phys.* **63** 669

[16] Zhang W, Dobrovitski V V, Al-Hassanieh K A, Dagotto E and Harmon B N 2006 *Phys. Rev.* B **74** 205313

[17] Amico L, Fazio R, Osterloh A and Vedral V 2008 *Rev. Mod. Phys.* **80**, 517

[18] Gedik Z 2006 *Solide State Communications* **138** 82.

[19] Coish W A and Loss D 2005 *Phys. Rev.* B **72** 125337

[20] Hutton A and Bose S 2004 *Phys. Rev.* A **69** 042312

[21] Breuer H P, Burgarth D and Petruccione F 2004 *Phys. Rev.* B **70** 045323

[22] Yuan X Z, Goan H J and Zhu K D 2007 *Phys. Rev.* B **75** 045331

[23] Jing J and LÜ Z 2007 *Phys. Rev.* B **75** 174425

[24] Jing J, LÜ Z and Yang G 2007 *Phys. Rev.* A **76** 032322

[25] Hamdouni Y and Petruccione F 2007 *Phys. Rev.* B **76** 174306

[26] Hamdouni Y, Fannes M and Petruccione F 2006 *Phys. Rev.* B **73** 245323

[27] Hamdouni Y 2007 *J. Phys. A: Math. Theor.* **40** 11569

[28] Bellomo B, Lo Franco R and Compagno G (2008) *Phys. Rev.* A **77** 032342

[29] Von Waldenfels W 1990 *Séminaire de probabilité (Starsburg)* tome 24 349-356 (Springer-Verlag, Berlin)

[30] Wootters W K 1998 *Phys. Rev. Lett.* **80** 2245

[31] Yu T and Eberly J H 2004 *Phys. Rev. Lett.* **93** 140404

[32] Hamdouni Y 2009 Phys. Lett. A 373 1233; *Preprint* arXiv:0807.3944v2

[33] Danos M and Rafelski J 1984 *Pocketbook of Mathematical Functions* (Verlag Harri Deutsch, Frankfurt)

8. CONCLUSION

In this work the focus was on the investigation of exact solutions for the dynamics of simple qubit systems which are coupled to their surrounding spin environments. We have mainly considered Heisenberg XY interactions with long-range uniform couplings. The coupling of the central qubits to the environment is equivalent to the interaction with a single giant spin, described by the collective spin operator of the spin bath. The nature of the interactions allowed us to use the underlying symmetries of the Hamiltonians of the compound systems, together with operator techniques and known commutation relations satisfied by the components of the total angular momentum, to derive the exact analytical forms of the reduced density matrices.

One of the main results of this work consists in providing a strong evidence and clear verification of the quantum central limit theorem for tracial states. Indeed, we have shown, both analytical and numerically, that the scaled components of the total angular momentum converge to classical, identically distributed, commuting normal random variables. The exact form of the corresponding probability density function is derived from simple analytical considerations. This result was successfully applied to the study of the thermodynamic limit, that is, the limit of an infinite number of environmental spin. Here the trace over the environmental spin degrees of freedom simplifies to an integration over Gaussian random variables having continuous probability functions with relatively small variances. As a consequence, the numerical investigation becomes easily accessible for very large sizes of the environments, breaking the constraints imposed by limited capacities offered by computers, for which the investigation of environments with sizes as small as 10^3 may need a huge amount of resources. This allowed us to compare the behavior of the qubits for finite and infinite numbers of spins within the environments. Moreover, using the above results, it was possible to find analytical expressions for the asymptotic reduced density matrices; the study of the second order master equation shows that the dynamics of qubits is non-Markovian in contrast to the case of bosonic environments, where the decay of the elements of the reduced density matrix is essentially exponential, i.e., Markovian.

It has been shown that in the case of a single central qubit, strong applied magnetic fields help reducing the effect of decoherence, which is also the case for low temperatures of the bath with antiferromagnetic interactions. The same result was obtained for the case of two central qubits, where strong coupling between the qubits plays the same role on the decoherence as low temperatures and strong magnetic field. The study of entanglement through the concurrence showed that the former can be preserved by allowing the qubits to strongly interact with each other. In the case of the Lipkin-Glick-Meshkov model, we showed that although the concurrence describing the pairwise entanglement detects the presence of the critical point, it does not give the expected value of the latter. This can be explained by the fact that in order to obtain a sharp characterization of the critical point, one has to consider the thermodynamic limit. However, we found that the concurrence vanishes as the number of spins increases.

It is well known that mathematics is the language of physics. This relation is, in fact, collateral, since many interesting mathematical results are originally the outcomes of physical investigations. In this work we were led, while studying the case of separate spin baths, to the derivation of analytical properties for both Wigner $3j$-symbols and the degeneracy entering the decomposition of the space $\mathbb{C}^{2\otimes n}$ into direct sum of the subspaces $\mathbb{C}^{2j+1}$, where j denotes the possible values of the total spin resulting from the addition of n spin-$\frac{1}{2}$ particles. We also derived the probability density functions of the sum of two independent variables each having the probability density function $4xe^{-2x^2}$. This enabled us to analytically calculate their moments around the origin at arbitrary order.

We feel that this subject is very interesting, and much work has still to be carried out. In particular, one has to check whether the effect of strong coupling between the qubits will persist as their number increases. Up to now the thermodynamic limit in the case of ferromagnetic interactions between the spins in the environment is not well understood. The difficulty resides in the fact that when the coupling constant is negative, the integration over the normal random variables diverges. Hence other techniques should be developed.

APPENDIX

A. DERIVATION OF THE ANALYTICAL FORM OF $\eta(T)$

This appendix is devoted to the derivation of the asymptotic behavior and the analytical form of the function $\eta(t)$ appearing in Eq. (2.81). Explicitly we have ($\Delta = 0$)

$$\eta(t) = \frac{8}{\bar{Z}} \int_0^\infty e^{-(g\beta+2)r^2} \frac{r^3}{\mu^2 + r^2} \sin^2\Big(t\sqrt{\mu^2 + r^2}\Big) dr. \tag{A.1}$$

By making the following change of variable $r^2 = s^2 - \mu^2$ and taking into account the trigonometric equality $\sin^2 x = \frac{1}{2}\Big[1 - \cos(2x)\Big]$, we can rewrite the above function as

$$\eta(t) = \frac{2}{\bar{Z}}\, e^{(2+g\beta)\mu^2} \Bigg(\int_{\mu^2}^\infty dv^2 \mathrm{e}^{-(2+g\beta)v^2} \Big[1 - \cos(2vt)\Big] - 2\mu^2 \Big\{ \int_\mu^\infty \frac{dv}{v} e^{-(2+g\beta)v^2} \Big[1 - \cos(2vt)\Big] \Big\} \Bigg). \tag{A.2}$$

The Riemann-Lebesgue lemma implies that the second and the fourth terms involving the cosine function in the above expression vanish when $t \to \infty$. The first term can be easily evaluated and we simply get

$$\int_{\mu^2}^\infty dv^2\, e^{-(2+g\beta)v^2} = \frac{1}{2+g\beta}\, e^{-(2+g\beta)\mu^2}. \tag{A.3}$$

The third term reads

$$2\int_\mu^\infty \frac{dv}{v}\, e^{-(2+g\beta)v^2} = \int_{\mu^2(2+g\beta)}^\infty \frac{dv^2}{v^2} \mathrm{e}^{-v^2} = \Gamma\Big[0, (2+g\beta)\mu^2\Big], \tag{A.4}$$

where we have made the change of variable $(2+g\beta)v^2 \to v^2$. Taking into account the expression of $\bar{Z}$ in Eq. (2.76) we obtain the asymptotic expression of $\eta(t)$ displayed in Eq. (2.90).

The second term simplifies to

$$\mathrm{Re}\left\{2\,e^{-\frac{t^2}{2+g\beta}}\int_{\mu}^{\infty} v\,dv\,\exp\Big[-(2+g\beta)\Big(v+\frac{it}{2+g\beta}\Big)^2\Big]\right\}$$

$$= e^{-\frac{t^2}{2+g\beta}}\mathrm{Re}\Big[\underbrace{\int_{\delta^2}^{\infty} dv\frac{\mathrm{e}^{-v}}{2+g\beta}}_{I_1} - \underbrace{\frac{2it}{(2+g\beta)^{\frac{3}{2}}}\int_{\delta}^{\infty} dv\;e^{-v^2}}_{I_2}\Big], \tag{A.5}$$

where $\delta = \sqrt{2+g\beta}(\mu + \frac{it}{2+g\beta})$. One can easily check that

$$\mathrm{Re}\;(I_1) = \frac{1}{2+g\beta}\exp\Big[-(2+g\beta)\mu^2 + \frac{t^2}{2+g\beta}\Big]\cos\Big(2\mu t\Big). \tag{A.6}$$

The second integral is given by the complementary error function, namely

$$I_2 = \frac{\sqrt{\pi}it}{(2+g\beta)^{\frac{3}{2}}}\mathrm{erfc}\Big[\Big(\mu+\frac{it}{2+g\beta}\Big)\sqrt{2+g\beta}\Big]. \tag{A.7}$$

It is then sufficient to use the property 2 Im $\mathrm{erfc}(a+it) = i\Big[\mathrm{erf}(a+it) - \mathrm{erf}(a-it)\Big]$, where a is real and $\mathrm{Im}(x)$ stands for the imaginary part of x, to get the first three terms appearing in the right-hand side of Eq. (2.81).

Similarly, we have

$$\mathrm{Re}\Big\{\;2\int_{\mu}^{\infty}\frac{dv}{v}\exp\Big[-(2+g\beta)\Big(v+\frac{it}{2+g\beta}\Big)^2\Big]\Big\} = \mathrm{Re}\Big\{\;2\int_{\delta}^{\infty}\frac{ds}{s-\frac{it}{\sqrt{2+g\beta}}}\;e^{-s^2}\Big\}, \tag{A.8}$$

where we have introduced the new variable $s = (v+\frac{it}{\sqrt{2+g\beta}})\sqrt{2+g\beta}$. By multiplying the numerator and the denominator of the quantity under the sign of integral by $s+\frac{it}{\sqrt{2+g\beta}}$ we get two new integrals. The first one is given by

$$\mathrm{Re}\Big\{2\int_{\delta}^{\infty} s\;ds\frac{e^{-s^2}}{s^2+\frac{t^2}{2+g\beta}}\Big\} = e^{\frac{t^2}{2+g\beta}}\mathrm{Re}\Big\{\int_{\delta_2}^{\infty}\frac{ds}{s}e^{-s}\Big\} = \exp\Big\{\frac{t^2}{2+g\beta}\Big\}\mathrm{Re}\Big\{\Gamma(0,\delta_2)\Big\}, \tag{A.9}$$

where $\delta_2 = (2+g\beta)\mu^2 + 2\mu it$. The remaining integral defines the function $\mathcal{M}$, namely,

$$\mathcal{M}(t;\mu,\beta) = \exp\Big\{-\Big[\frac{t^2}{2+g\beta} - (2+g\beta)\mu^2\Big]\Big\}\mathrm{Re}\Big\{2it\sqrt{2+g\beta}\int_{\delta}^{\infty}\frac{e^{-s^2}}{s^2+\frac{t^2}{2+g\beta}}\,ds\Big\}. \tag{A.10}$$

The analytical expressions of the functions $\xi(t)$ and $\zeta(t)$ can be determined with the same method. In the case $\gamma \neq 0$ we should replace μ by $\mu+\gamma m$ and then perform the integration with respect to m. For practical investigation, numerical integration is used.